Understanding papillomavirus-induced disease by means of a novel murine papillomavirus (MmuPV1) based *in vivo* infection model

By

Aayushi Uberoi

A dissertation submitted in partial fulfillment of

the requirements for the degree of

Doctor of Philosophy

(Cancer Biology)

at the

UNIVERSITY OF WISCONSIN-MADISON

2017

Date of final oral examination: 11/09/2017

This dissertation is approved by the following members of the Final Oral Committee
Paul F. Lambert, Howard M. Temin Professor and Chair, Oncology
Paul G. Ahlquist, Paul J. Kaesberg Professor, Molecular Virology and Oncology
Daniel D. Loeb, Professor, Oncology
William B. Sugden, James A. Miller Professor, Oncology
Nathan M. Sherer, Associate Professor, Molecular Virology and Oncology
John Yin, Vilas Distinguished Professor, Chemical and Biological engineering

© Copyright by Aayushi Uberoi 2017

All rights reserved

Abstract

Understanding papillomavirus-induced disease by means of a novel murine papillomavirus (MmuPV1) based *in vivo* infection model

Aayushi Uberoi

Under the supervision of Professor Paul F. Lambert

at the University of Wisconsin-Madison

Papillomaviruses (PVs) are species tropic double-stranded DNA viruses that have been implicated in causing several forms of cancer in humans and other animals. PVs can infect mucosal or cutaneous epithelium and their life cycle is dependent upon the epithelial differentiation program thus limiting our ability to monitor and study the progression of the disease in their natural hosts in depth. The recent discovery of the murine papillomavirus (MmuPV1) provides us, for the first time, a unique opportunity to define the role of PV genes in viral associated pathogenesis and life cycle in vivo, in the context of a genetically manipulatable host organism. We, and others have found that complete T-cell deficiency is required for MmuPV1 induced papillomatosis. While MmuPV1 failed to induce papillomatosis in immune competent strains of mice, we have made the novel discovery that ultraviolet radiation (UVR) assists MmuPV1 in causing wart formation and squamous cell carcinoma in such mice, by causing systemic immunosuppression. Using a genetic approach, UVR-induced susceptibility to MmuPV1-induced skin disease was abolished in mouse strains (specifically deficient for IL-10 and Aryl Hydrocabon Receptor) that were found to be resistant to UVR-induced systemic immunosuppression. These results demonstrate that UVR's ability to cause systemic

immunosuppression is necessary to make mice susceptible to MmuPV1-induced skin disease. We have also found that UVR-induced systemic effects are not just limited to MmuPV1-skin disease as MmuPV1 caused cancers in cervico-vaginal tract of UVB-irradiated female immunocompetent mice that were treated with estrogen. These data suggest that MmuPV1 can be used to study pathogenesis of high-risk cutaneous as well as mucosotropic papillomaviruses. That UVR assists in development of MmuPV1 dependent disease is valuable as epidemiological evidence suggests a correlation between exposure to UVR and prevalence of cutaneous HPVs in healthy and more predominantly immunocompromised patients rendering them susceptible to HPV-associated skin disease. In this context, MmuPV1-UV infection model provides valuable opportunities to understand papillomavirus pathogenesis and test immunotherapies in the context of papillomavirus-induced disease.

Approved by: _____

Date: _____

I. Dedication

This thesis is dedicated to my parents - Mr. Dinesh Uberoi and Mrs. Sunita Uberoi

II. Acknowledgement

Graduate School would not have been a possibility for me without the encouragement and support of my parents Mr. Dinesh Uberoi and Mrs. Sunita Uberoi. It is a courageous sacrifice to let your child go far from home to pursue their dreams and ambitions. I will be forever indebted to my parents for not only encouraging me to work hard, but also participating in this PhD as if it were their own. I may have been putting my heart and mind into this work, but the real effort was that of my parents. Thank you mom and dad!

One thing I can unequivocally say about my graduate school journey is that I have been able to experience the process of science. This has been, in large part, due to my advisor Dr. Paul Lambert. I take this opportunity to thank Paul for not only guiding me through the process of solving a scientific problem, but also guiding me to come up with questions of my own. Somewhere along my graduate school journey, our advisor-mentee relation transitioned into that of a scientific partnership. I started pursuing experiments that I wanted to conduct and was able to discover how much I enjoy being a scientist. Paul has been a great advisor to me and has provided me with excellent scientific training that makes me confident to pursue a scientific career. If I were to list just one thing that I have learnt from Paul, I'd say it to be able to admit fearlessly if I don't know something and then learn to seek help from experts. Whenever, I got stuck in my project due to a gap in knowledge, Paul encouraged me to seek help from other experts around campus. In fact, there are several chunks of my thesis work that made us, as a lab, at times step out of our comfort zones. Initially, I found it overwhelming, and often frustratingly

questioned why I was being forced to take this route. But this exercise has been, I believe, my most valuable experience.

In my time at UW-Madison, I have met so many wonderful people and been a part of such great organizations that I am overwhelmed and humbled that so many people have been a part of this journey with me. There is a saying that goes, “It takes a village to raise a child.” For me, it started in my own lab. I am thankful to all present and past members of the Lambert lab who have made this journey truly wonderful. Thank you: Denis Lee, Megan Spurgeon, Kathleen Makielski, Tao Wei, Myeong-Kyun Shin, Patrick Nyman, Alexandra Torres, Ruben Moreno, Andrea Bilger and Ella Ward. It has been a privilege to work with you all.

There are several past lab members who I would like to especially thank: Amy Liem (taught me to love animal work), Laurel Lorenz (being a friend and mentor), HaoShun Huang (helping me infect my first mouse!), Satoshi Yoshida (for introducing me to the UV model), Max Golden and Spencer Williams (my awesome students who taught me to teach!). Dr. Bill Sugden (also my committee member) once said to me that I should surround myself by people who are brutally honest to me and I have been fortunate to have such lab members who have only helped me excel.

I am especially thankful to Dr. Megan Spurgeon, who fondly calls/called me “the embryo”, for being a mentor, a friend and pretty much being my go-to person whenever I’ve needed any help during my graduate student life. Megan has been a great pillar of strength for me in my grad life right from reading my first ever paper to helping me prepare for my first talk and always guiding me to push the envelope further.

I thank Denis Lee, our lab manager. I started out as an undergraduate in Paul's lab with Denis as my mentor. I can say it that pretty much everything that I know about being in a lab and with bench-work, I have learnt from Denis.

It has been a pleasure to work with Kathleen Makielski all these years. Kathleen has been a wonderful friend and is truly one of the nicest people I have ever met. Thank you for looking at my presentations and papers every single time before I have gone to present them!

Thank you Tao Wei for being a fantastic colleague and friend and sitting through my worst rants. From teaching Tao how to navigate grad school, I've learnt valuable lessons from her too.

I have been extremely fortunate to have a very engaging thesis committee consisting of: Drs. Paul Ahlquist, Dan Loeb, Bill Sugden, Nate Sherer and John Yin. Through my committee meetings and in my one-on-one interactions, they have truly helped shape me as a well-rounded scientist. I would like to thank them for engaging with me frequently imparting several pearls of wisdom and taking time to know me.

Several times during my PhD, in particular when we were thinking of publishing my first manuscript, Dr. Ahlquist provided valuable advise on how to navigate the peer-review process and posed many challenging questions that have only strengthened my research.

I was fortunate to rotate in Dr. Dan Loeb's lab as a graduate student, and then having Dan's lab as a neighboring lab. Dan provided me with critical inputs on how to design my experiments. As a director of the cancer biology program Dan has given very

sound and impactful personal advice on how to improve constructively as a graduate student.

Besides Paul, if I were to think of someone who has played a significant role in shaping me as a scientist, it is Dr. Bill Sugden. Bill has given me life changing, more accurately, life-shaping advice at critical points of my PhD journey: when I started graduate school, my first McArdle seminar, preliminary examination, to when I started applying for postdoctoral positions. Thank you Bill for helping me clear my muddled mind and encouraging me to seek the best education that I deserve.

Dr. Nate Sherer started his lab around the same time as I began graduate school. From my first McArdle seminar, Nate has probably been as excited as Paul and myself about mouse papillomavirus! Nate's energy has been contagious and he has provided me with valuable advice, both professional and personal, all these years.

I am very thankful to Dr. John Yin for going out of his way in trying to understand my project and provide me with valuable advice, particularly in finding a new research area that I can venture into. At my 6-month committee meeting, John told me to be fearless and study whatever I wanted to. And I think, his encouragement over the years has given me the confidence to take risks in my PhD.

I would especially like to thank Dr. Karl Munger at Tufts University. Karl has been a collaborator on my thesis project since I started graduate school. I don't think we would have been able to increase the scope of my research without Karl's inputs and critical experiments by his student Jordan Meyers (my accomplice in MmuPV1 saga). Karl has been a fantastic influence during my PhD and I am very grateful to him.

Some of the experiments in this thesis would not have been possible without support of several individuals and collaborators. Thank you: Terry Fritter and Satya Kishore (Animal Care Staff), Jordan Meyers and Miranda Grace (Karl Munger's lab, Tufts University), Vladimir Majerciak (Thomas Zheng's lab, NCI), Dr. Ian Frazer (University of Queensland, Australia), Stephanie McGreggor (UW, Histopathology), Jeremiah Ye and Ed Glover (Chris Bradfield's lab for helping with the AhR studies), Zhang lab (for immunology based experiments), Lance Rodenkirch (UW Optical Imaging core),

I have been fortunate to be a part of UW's active teaching community. I would like to thank – Dr. Rich Halberg (for bearing through the changes I made every semester to Oncology 401, and letting me make them); Dr. Christopher Trimby (My advisor for teaching as research at WISCIENCE); Drs. Lilian Tong and Kristin Jenkins (HHMI teaching fellows program); Dr. Lindsy Boateng and Elaina Jones (my teaching partners) and Dr. Devin Wixon (Delta program) for letting me teach and making me better at it!

This PhD would not be possible without my friends, who actually participated in this process and bore my continuous discussions about viruses. Thank you: Yaman Singh Sangar, Harisha Rajanala, and Jayer Fernandes for getting excited about science with me as I powered on.

I would like to thank Gautam Prakriya for being my pillar of support and being my companion during this PhD journey. I am lucky that I walked this path with you. You have endured my craziness and have never let me lose sight of my goals and ambitions.

Finally, I would like to thank two people without whom this dream would not be a possibility - my aunt and uncle: Mrs. Punita Jolly and Mr. Arvind Jolly. They have been my support throughout this PhD and have helped me survive living far from home. Thank you!

III. Paul's poem

A virus I'm told, mice it seeks
warts it makes in merely weeks

Yet I find,when I infect
no warts arise, that I detect

No warts, no précis
no warts, no thesis

A skin virusI sit and ponder
what else skin my thoughts wonder

Then it dawns I see the light
for my mice I shine it bright.

Warts arise they spread galore
my thesis is here my way out the door

- Dr. Paul F. Lambert

IV. Contents

Abstract i

I. Dedication iii

II. Acknowledgement iv

III. Paul's poem x

IV. Contents xi

V. List of figures xvi

VI. List of tables xix

VII. List of abbreviations xx

VIII. Thesis 1

1. Overview 2

2. Rodent papillomaviruses 7

2.1. Introduction 8

2.2. Genomic analysis of rodent papillomaviruses 13

2.3. Pathogenesis by rodent papillomaviruses 20

2.3.1. Mastomys associated papillomaviruses 20

2.3.2. Mus Musculus associated papillomaviruses 23

2.3.3. Other rodent papillomaviruses 43

2.4. Insights into vaccine development 44

2.5. Transcript maps of rodent papillomaviruses 45

2.6. Roles of E6 and E7 of rodent PVs 52

2.7. Conclusion 55

3. Materials and methods 60

3.1. Materials 61

3.2. Methods 66

3.2.1. RCA to generate MmuPV1 clones 66

3.2.2. In vitro synthesis of MmuPV1 quasivirions 67

3.2.3. Quantification of MmuPV1 virions 68

3.2.4. Protocol for southern analysis of MmuPV1 68

3.2.5. MmuPV1-UV Skin Infection model 70

3.2.6. Harvesting of virus particles from papillomas 75

3.2.7. Harvesting papilloma tissue for histopathological analysis 76

3.2.8. MmuPV1 L1-K14 dual immunofluorescence by TSA 76

3.2.9. MmuPV1 DNA FISH 79

3.2.10. CHS assay for immunosuppression 80

3.2.11. Explant cultures and IL-10 ELISA 81

3.2.12. T-cell depletion using anti-CD4/CD8 82

3.2.13. Infection of animals with MmuPV1 DNA 84

3.2.14. Infection of female reproductive tract with MmuPV1 84

3.2.15. Estrogen treatment 85

3.2.16. Imaging 85

3.2.17. Statistical analysis 86

3.3. Considerations for MmuPV1 infection studies 86

4. Establishment and characterization of the MmuPV1 infection model in immunodeficient mice 92

4.1. Introduction 93

4.2. Results 94

4.2.1. Establishment of MmuPV1 infection *FoxN1*$^{nu/nu}$ mice 94

4.2.2. Spatial localization and expression dynamics of L1 and DNA replication 108

4.2.3. Dose dependent delay in onset of MmuPV1-papillomas 115

4.2.4. Disrupted epithelial differentiation papillomas 115

4.2.5. T-cell deficiency is required for MmuPV1-dependent disease 120

4.3. Discussion 124

5. UV irradiated immunocompetent mice are susceptible to MmuPV1 induced papillomas 132

5.1. Introduction 133

5.2. Results 135

5.2.1. MmuPV1 causes papillomas in UV irradiated immunocompetent FVB mice 135

5.2.2. Productive infection and neoplastic transformation is seen in papillomas arising in immunocompetent mice 148

5.2.3. UV-irradiation has a systemic effect on host biology 154

5.2.4. UVB-mediated immunosuppression correlates with development of MmuPV1-dependent cutaneous disease 157

5.2.5. Mice displaying UVB-induced immune suppression at three-months preferentially develop MmuPV1-induced warts 160

5.3.Discussion 163

6. UVB mediated immunosuppression is necessary for MmuPV1-dependent papillomatosis 170

6.1.Introduction 171

6.2.Results 174

6.2.1. UVB mediated immunosuppression via IL10 is necessary for MmuPV1-induced papillomatosis 174

6.2.1.1. UVB mediated immunosuppression in dependent on IL10 175

6.2.1.2.UVB irradiated IL10$^{-/-}$ mice are resistant to MmuPV1-induced papillomas 177

6.2.2. UVB mediated immunosuppression via AhR is necessary for MmuPV1-induced papillomatosis 181

6.2.2.1. UVB irradiated AhR-/- mice are impaired in production of IL10 and are resistant to UVB induced immunosuppression 181

6.2.2.2.UVB irradiated AhR$^{-/-}$ mice are resistant to MmuPV1-induced papillomas 182

6.2.2.3.T-cell depleted AhR$^{-/-}$ mice are permissive to MmuPV1_186

6.3.Discussion 190

6.4.

7. A novel *in vivo* infection model to study papillomavirus-mediated cancers of the female reproductive tract 197

7.1 Introduction 198

7.2 Results 200

7.3 Discussion 213

8. Discussion and Future Directions 218

8.1. Discussion 218

8.1.1. Role of T-cells in Papillomavirus infection 218

8.1.2. UVB mediated immunosuppression is necessary for MmuPV1-dependent disease 221

8.1.3. Implications of UVB-mediated immunosuppression in human disease 225

8.2. Future Directions 231

8.2.1. Is UVB-induced immunosuppression sufficient to cause susceptibility to MmuPV1 infections? 232

8.2.2. Effect of viral genes on host immunity 238

IX. References 250

V. List of Figures

Fig. No. Pg#

Chapter 2

2.1 Genome organization of rodent papillomavirus 14

2.2 Phylogenetic analysis 17

2.3 Progression of MmuPV1-induced papillomas in nude mice 28

2.4 Transcription map of MnPV1 48

2.5 Transcription map of MmuPV1 50

2.6 Amino acid analysis of E6 56

2.7 Amino acid analysis of E7 58

Chapter 3

3.1 UVB irradiator 64

3.2 Measuring papilloma size 73

3.3 General growth trends seen in MmuPV1-UV infection model 73

3.4 Principle of TSA staining 78

3.5 T-cell depletion regime 83

Chapter 4

4.1.Optimizing infection in *Balb/c FoxN1^{nu}* 96

4.2.Histopathology 100

4.3.Hallmarks of PV life cycle in nude mice 101

4.4. Characterization of MmuPV1 infection 102

4.5. Papillomas caused by lab generated vs synthetic MmuPV1 genomes 106

4.6. Time course analysis of MmuPV1 infected nude mice at base of tail 110

4.7. MmuPV1 DNA FISH 112

4.8. MmuPV1-induced papillomas growing asynchronously 113

4.9. Dose dependent delay in onset of MmuPV1-induced papillomas 117

4.10. Immunohistochemistry analysis of tail papillomas for differentiation markers 119

4.11. T-cell deficiency is required for MmuPV1 infection 122

Chapter 5

5.1. MmuPV1-induced papillomas in UVB-irradiated FVB/NJ mice 138

5.2. Papillomas in UVB-irradiated mice 140

5.3. Dose-dependent incidence in UVB-irradiated mice 146

5.4. Histopathology of papillomas in UVB-irradiated mice 149

5.5. Quantification of virus by southern blot 151

5.6. FISH to detect MmuPV1 in malignant regions 153

5.7. Systemic effect of UVB to cause MmuPV-disease 155

5.8. UVB causes systemic immunosuppression 159

5.9. Immune suppression correlates with papilloma incidence 162

Chapter 6

6.1. UVB mediated immunosuppression via IL-10 is necessary for MmuPV1-dependent papillomas 178

6.2. UVB mediated immunosuppression via AhR is necessary for MmuPV1-dependent papillomas 183

6.3. T-cell depleted AhR-/- mice are susceptible to MmuPV1 188

Chapter 7

8.1. MmuPV1 infection of female reproductive tract of nude mice _____202

8.2. MmuPV1 infection of female reproductive tract of immunocompetent mice _____207

8.3. Histopathological analysis of reproductive tracts _____208

8.4. L1 staining _____209

8.5. MmuPV1 causes cancers in mice treated with UVB and estrogen_____210

8.6. Infection junctions in infected mice_____211

8.7. Unusual histopathological features_____212

Chapter 8

8.1.Potential research avenues provided by MmuPV1 infection model_____231

8.2. Over-expression of IL-10 in epithelia is not sufficient for MmuPV1-induced papillomas _____235

8.3. Immune suppression in UVB irradiated mice 6-months post-infection__240

8.4. RNA-seq analysis of MmuPV1-induced papillomas_____243

8.5. K17-null mice are resistant to MmuPV1-induced papillomas _____248

VI. List of Tables

Table 2-1: List of Rodent papillomaviruses 11

Table 2-2: List of immunodeficient mice found to be susceptible to MmuPV1 skin infections 32

Table 2-3: List of immunodeficient mice found to be resistant to MmuPV1 skin infections 32

Table 2-4: List of immunocompetent mice found to be susceptible to MmuPV1 after treatment with immunosuppressants 34

Table 2-5: Key features of MnPV1 and MmuPV1 transcript maps 47

Table 3-1: Mouse strains used in this thesis work 61

Table 3-2: List of antibodies used 62

Table 3-3: Miscellaneous reagents used 62

Table 3-4: Description of morphological features post infection (PI) with MmuPV1s 74

Table 4.1: Strains resistant to MmuPV1 infection 125

Table 5-1: Papilloma incidence in UVB-irradiated FVB/NJ mice 136

Table 5-2: Papilloma incidence in FVB/NJ mice infected with MmuPV1 followed by treatment with UVB at different time points 142

Table 5-3: Papilloma incidence in FVB/NJ mice infected with MmuPV1 followed by treatment with UVB/UVA 142

Table 5-4: Papilloma incidence in immunocompetent mice infected with MmuPV1 followed by treatment with UVB 145

Table 7.1: Cervical disease scoring 206

VII. List of abbreviations

Ahr	Aryl Hydrocarbon Receptor
BPV1	Bovine Papillomavirus-Type 1
BrdU	5-bromo-2'-deoxyuridine
CHS	Contact Hypersensitivity Assay
COPV1	Canine oral Papillomavirus Type 1
CRPV1	Cottontail Rabbit Papillomavirus Type 1
Cyp1a	Cytochrome P450, family 1
DAPI	4',6-diamidino-2-phenylindole
DNCB	1-Chloro-2, 4-Di-Nitrobenzene
DOCK2	Dedicator Of Cytokinesis 2
DTH	Delayed type hypersensitivity assay
E2	Estrogen
ELISA	Enzyme Linked Immuno
FISH	Fluorescent in situ hybridization
FOXN1	Forkhead Box like-N1
FVB/NJ	Friendly Leukemia Virus B/New Jersey
HPV	Human Papillomavirus
HSV1	Herpes Simplex Virus Type 1
IL10	Interleukin 10
IL2rg	Interleukin 2 receptor gamma chain
K10	Keratin 10

K14	Keratin 14
K15	Keratin 15
K17	Keratin 17
Krt	Keratin
L1	Late Virus Capsid protein 1
L2	Late Virus Capsid protein 2
MCM7	Minichromosome Maintenance Complex Component 7
McPV	Mastomys Coucha Papillomavirus
mJ/cm2	Milijoules per square centimeter
MmuPV1	Mouse Papillomavirus Type 1
MnPV1	Mastomys Natalensis Papillomavirus Type 1
NMRI	Naval Medical Research Institute
NOD	Non-obese Diabetic
Nu	Nude
ORF	Open Reading Frame
PV	Papillomavirus
RCA	Rolling Circle Amplification
SCC	Squamous Cell Carcinoma
SCID	Severe Combined Immunodeficiency
SENCAR	Sensitivity to Carcinogenesis
SKH1	Short hair, Naked, Hairless
Th1	T-helper type responses 1
UV	Ultraviolet

UVB	Ultraviolet Radiation Spectra B
UVR	Ultraviolet Radiation
VGE	Viral Genome Equivalence
VLP	Virus Like Particle
XSCID	X-linked Severe Combined Immunodeficiency

VIII. Thesis:

Understanding papillomavirus-induced disease by means of a novel murine papillomavirus (MmuPV1) based *in vivo* infection model

Chapter 1: Overview

"If we knew what it was we were doing, it would not be called research, would it?"

– Albert Einstein

In my thesis work, I describe the development and application of the first ever in *vivo* infection model to study papillomavirus-associated disease in mice using the recently discovered Murine papillomavirus (MmuPV1). In 2011, MmuPV1 was reported to have been isolated from cutaneous papillomas arising spontaneously in a colony of *FoxN1*$^{nu/nu}$ mice (T-cell deficient nude mice) in a vivarium at Tata Memorial Hospital in India. This discovery is fascinating as it provides papillomavirus (PV) researchers the unique opportunity to study PV biology, for the first time in a genetically modifiable and tractable lab animal. I began my thesis work in the Lambert lab during the end of 2011. In this thesis work I have documented my findings and the novel insights provided by the MmuPV1-infection model and how it can be adapted to study PV biology. This chapter (i.e. **Chapter 1**) serves to provide an overview of the work that will be discussed in this thesis.

Besides MmuPV1, as of July (2017), 11 other rodent papillomaviruses have been discovered. These viruses that infect rodents species have provided interesting insights about papillomavirus biology. During our trysts with MmuPV1, I have spent a significant amount of time gathering information about all the rodent papillomaviruses. This has helped me become aware about what we learn about papillomavirus infections from other rodent species and what gaps can MmuPV1 address. Also, since 2011 several other groups have also made novel findings about MmuPV1. In **chapter 2: Rodent papillomaviruses** I have reviewed and carefully documented my findings from literature to provide information in a consolidated manner to present and future members of Lambert lab and the virology community. To the best of my knowledge, no such review of information was available and therefore I think it will be helpful.

Several methods that have been developed during the course of my thesis work (to study MmuPV1) are brand new and have been developed from scratch or modified from pre-existing methods from the papillomavirus field. In **Chapter 3** I have described the **materials required and the methods established** for studying MmuPV1 infection.

A large body of my thesis work is dedicated to understanding the contribution of ultraviolet radiation (UV) to understand cutaneous papillomavirus infections in immunocompetent animals. The motivation for even testing the role of UV comes from the research performed in the context of immunodeficient models during the initial phases of my graduate career (2012-2013). This preliminary work essentially laid the groundwork for my work in developing the MmuPV1-UV infection model. Therefore I have dedicated **Chapter 4** to describing the **knowledge gained from some of these immunodeficient strains**. In this chapter I describe the establishment and characterization of the MmuPV1 infection model in the *FoxN1*$^{nu/nu}$ immunodeficient strain and other immunodeficient mouse models selectively deficient for sub-populations of T-cells and B-cells respectively. These initial efforts, coupled with the observation that immunocompetent wild-type strains of mice are resistant to MmuPV1-dependent papillomatosis have led to the key observation that complete T-cell deficiency is required for MmuPV1-dependent disease.

Epidemiological studies have implicated that ultraviolet (UV) radiation from sunlight drive papillomavirus-induced disease in healthy and immunocompromised humans. Therefore, I tested whether immunocompetent wild-type animals, that were found to be resistant to papillomatosis by MmuPV1, became susceptible to MmuPV1-dependent disease following UVR. I found that indeed, UVB-irradiated wild-type

animals showed increased susceptibility to MmuPV1-associated papillomatosis and in some cases, squamous cell carcinoma. In this work, I made the seminal observation that UVB appears to have a systemic effect in causing animals to become susceptible to MmuPV1 papillomas. In characterizing this systemic effect, I observed a strong correlation between UV-induced immunosuppression and papillomavirus-based disease progression. I describe these findings in **Chapter 5.**

While I found there to be correlation between UV-induced immunosuppression and papillomatosis, we wanted to test whether **UV induced-immunosuppression is, in fact, necessary for MmuPV1-dependent disease**. I describe this work in **Chapter 6** of this thesis. Several mechanisms that drive UVB-induced immunosuppression have been reported in literature; for my studies, I have focused on IL10- and Aryl Hydrocarbon Receptor (Ahr)- mediated immunosuppression. I describe in this chapter the use of a genetic approach making use of IL10-/- and AhR-/- mice to address this question.

While initial efforts have focused on understanding cutaneous disease by MmuPV1, we and others have found that besides causing cutaneous disease MmuPV1 causes low-grade disease in the reproductive tracts of the T-cell deficient *FoxN1nu/nu* mice suggesting an expanded tropism of MmuPV1. Therefore, we sought to test the contribution of MmuPV1 in the reproductive tracts of wild-type mice. Surprisingly, we found that in contrast with the cutaneous disease where MmuPV1 does not cause any disease in wild-type animals, MmuPV1 does cause low-grade lesions in the reproductive tract of wild-type animals. Further we made the novel observation that **UVR coupled with estrogen, makes the reproductive tracts of female mice highly susceptible to cervical as well as vaginal cancers**. Preliminary data from this work is described in **Chapter 7** of this thesis.

In **Chapter 8**, I discuss the implications of the findings from Chapters 4-7. In this chapter I have also described some novel preliminary findings about MmuPV1 and possible future directions we can take to further understand papillomavirus mediated pathogenesis.

Chapter 2:

Rodent papillomaviruses

Besides murine papillomavirus (MmuPV1), 11 other papillomaviruses that can infect rodent species have discovered. Infection models for rodent papillomaviruses represent a fledgling area in PV research. In this chapter I present a review of literature that provides insights gained from studies using rodent papillomavirus-based infection models. I thank **Edward Evans** (graduate student, Cancer Biology, Dr. Nathan Sherer's lab) for teaching me how to perform phylogenetic analysis for this paper.

This review has been published in ***Viruses***[1] *(1)*.

1. Uberoi, A.; Lambert, P.F. Rodent papillomaviruses. *Viruses* **2017**, *9*.

2.1. Introduction

"Our attention was recently called to a disease occurring in wild cottontail rabbits in northwestern Iowa. Rabbits shot there by hunters were said to have numerous horn-like protuberances on the skin over various parts of their bodies. The animals were referred to popularly as "horned" or "warty" rabbits."

Shope and Hurst. *J Exp Med*; 1933; 58(5): 607–624.

In 1933, Dr. Richard Shope reported the discovery of a virus that could cause papillomas in cottontail rabbits (2). This virus, which we know as the Shope papillomavirus or cottontail rabbit papillomavirus, was the first to etiologically associate a DNA virus with malignant progression in a mammalian species. A half century later, Dr. Harald zur Hausen discovered that human papillomaviruses (HPV16 and HPV18) (3, 4) cause cervical cancer (reviewed in (5)). His Nobel Prize winning research provided momentum to the field of papillomavirus research, and since then many significant advances have been made in the field of papillomavirus tumor biology.

Papillomaviruses are non-enveloped, double-stranded DNA viruses that can infect mucosal and/or cutaneous epithelia and are largely species specific. As of today, 230 types of human papillomaviruses and 159 types of non-human papillomaviruses have been identified (https://pave.niaid.nih.gov/, (6)). Mucosotropic HPVs are the most common sexually transmitted pathogens, and a subset of these viruses cause 5% of human cancers, including cervical cancer, other anogenital cancers, and a growing fraction of head and neck cancers (reviewed in (7)). Other HPVs cause cutaneous warts, which are among the most common ailments treated by dermatologists (8-11). They arise most frequently in children (12, 13) and impose a significant burden to

immunocompromised patients, particularly amongst organ transplant recipients (14-16). They are ubiquitous in nature and can persist in the skin asymptomatically for years (14, 17). A subset of cutaneous HPVs also has been causally associated with skin cancer (reviewed in (14, 18, 19)).

Considering that papillomaviruses are species-specific, and their life cycle is dependent on epithelial differentiation, no animal model of human papillomavirus (HPV) infection exists. Although organotypic raft cultures have greatly aided our understanding the life cycles of high-risk mucosal HPVs (20), papillomavirus researchers have had to rely on animal papillomaviruses to study viral pathogenesis, virus-host interactions and immune responses to PVs. Initial studies using animal papillomaviruses tropic to cattle, rabbits or dogs led to significant advances in our basic understanding of papillomavirus biology. From these studies we gained fundamental knowledge about viral gene function, tissue tropism, cancer progression, vaccine efficacy and therapeutics. Recent reviews describe updates made in these classically used animal models (21-27). Among these, bovine papillomavirus type 1 (BPV1) was the first papillomavirus genome to be sequenced (28). BPV1 produces fibropapillomas on cattle, causes tumors in rodents and transforms fibroblasts in culture (2, 29, 30). BPV1 and other BPV genotypes have been used to study both cutaneous and mucosal infections and PV-associated cancers. The ability of BPV1 to establish a nonproductive infectious state in rodent cells in tissue culture, and to morphologically transform these cells, drove early studies in the 1980s that helped define the molecular genetics of papillomaviruses. Of particular note was the discovery of the E5 oncogene and elucidation of its ability to activate the platelet derived growth factor receptor [reviewed in (31-34)]. The revelation in the mid 1980s that

certain HPVs could cause human cancer and that these 'high-risk' HPVs have the ability to immortalize human keratinocytes led investigators largely to abandon BPV1 as a model system by the early 1990s.

Canine oral papillomavirus (CPV1) was the first canine PV to be studied [reviewed in (35, 36)] and is highly relevant to HPVs that cause anogenital and head and neck cancers due to the mucosotropic nature of this virus. This model was valuable in assessing efficiency of virus-like particle (VLP)-based and DNA-based prophylactic vaccines [reviewed in (37-40)]. As described earlier in this review, experiments with the cutaneous cottontail rabbit papillomavirus (CRPV1) that causes skin malignancy, began in the 1930s (2). Further studies demonstrated that various carcinogenic compounds could accelerate malignant progression rates (41) and provided an important preview into the subsequent connection between several high-risk HPV types and cervical cancer [reviewed in (23, 42-47)]. These classically studied preclinical models continue to offer valuable opportunities to study fundamental properties of papillomaviruses such as tissue restriction and function of viral genes in the context of intact hosts with functional immune systems.

As one can appreciate, while these models have been invaluable in educating us about PV biology, our understanding of papillomavirus biology remains limited, as these are not tractable laboratory animal models and the host species cannot be easily manipulated genetically, limiting mechanistic studies. A naturally occurring PV infection in rodent species, specifically laboratory mice, would provide not only a major new means to investigate the molecular pathogenesis of this group of viruses but also the means to study the biology of the host responses and to identify factors that influence

susceptibility to papillomavirus infections. In the last several decades, a dozen papillomaviruses that infect various rodent species have been isolated (Table 2.1), paving the way to such opportunities.

Table 2.1: List of Rodent papillomaviruses

	PV	Genome size bp	PAVE [1] name	Host common name	Genus	Reference
1.	AsPV1	7589	*Apodemus sylvaticus* Papillomavirus 1	Long-tailed field mouse	π	(48)
2.	CcanPV1	7435	*Castor canadensis* Papillomavirus 1	North-American beaver	*Dyosigma*	(49)
3.	EdPV1	7428	*Erethizon dorsatum* Papillomavirus 1	North-American porcupine	σ	(50)
4.	MaPV1	7647	*Mesocricetus auratus* Papillomavirus 1	Syrian golden hamster	π	(51)
5.	McPV2	7522	*Mastomys coucha* Papillomavirus 2	Southern multimammate rat	π	(52)
6.	MmiPV1	7393	*Micromys minutus* Papillomavirus 1	European harvest mouse	π	(53, 54)
7.	MmuPV1[2]	7501	*Mus musculus* papillomavirus type 1	House mouse	π	(55, 56)
8.	MnPV1	7687	*Mastomys natalensis* Papillomavirus 1	Southern multimammate rat	ι	(57, 58)
9.	PsuPV1	7630	*Phodopus sungorus* papillomavirus type 1	Siberian hamster	π	(59)
10.	RnPV1	7378	*Rattus norvegicus* Papillomavirus 1	Norwegian rat	π	(48)
11.	RnPV2	7724	*Rattus norvegicus* Papillomavirus 2	Norwegian rat	ι	
12.	RnPV3	7707	*Rattus norvegicus* Papillomavirus 3	Norwegian rat	ι	

[1] Papillomavirus Episteme: https://pave.niaid.nih.gov/

[2] Mouse papillomavirus was originally designated as MusPV1(55, 60)

Advances in cloning methods have facilitated the discovery of rodent papillomaviruses (61, 62). Some of these papillomaviruses were isolated from exophytic lesions that arose in animals in the wild such as the North American porcupine and beaver, Syrian golden hamster and most recently the Siberian hamster (49-51, 59). Others were cloned from skin swabs obtained from rodents including two novel species of rat papillomaviruses (RnPV2, 3) and one from the field mouse (AsPV1) (48). The most extensively studied rodent papillomaviruses are MnPV1, which was the first rodent PV to be discovered (in 1984) and infects the multimammate rat, and MmuPV1, which was discovered in 2011 and is the first papillomavirus identified to naturally infect the laboratory strain of mouse, *Mus musculus* (55). In the last six years, rapid progress has been made in understanding the biology of MmuPV1, which represents an attractive model to study papillomavirus pathogenesis due to the ubiquitous availability of laboratory mice and the fact that this mouse species is easily genetically modifiable (reviewed in (63)). Rodent PVs are a fledgling area of PV research and provide ample opportunities to understand PV biology. In this review, we have summarized the knowledge we have gained about PV biology from the study of rodent papillomaviruses.

2.2. Genomic analysis of rodent papillomaviruses

Papillomaviruses consist of a double-stranded, circular genome of around 8 kb containing one coding strand that is encapsidated in an icosahedral protein shell made up of a major (L1) and minor (L2) capsid protein (reviewed in (64)). Rodent PV DNA genomes follow the same general organization of genetic elements as seen in prototype papillomaviruses (e.g. HPV16 and BPV1) (65-67). Approximately half of the viral genome contains translational open reading frames (ORFs) that encode for the so-called "early" or E gene products. These early gene products are responsible for viral replication and maintenance, interact with multiple host factors to facilitate the viral life cycle, and contribute to the neoplastic properties of these DNA tumor viruses. The "late" or *L* ORFs encode for the proteins that form the viral capsid (Fig. 2.1). The long control region (LCR, also referred to as the upstream regulatory region (URR) or untranslated region (UTR)) carries cis elements required for DNA replication (i.e. the viral origin of DNA replication) as well as multiple transcriptional promoters and transcriptional enhancer elements.

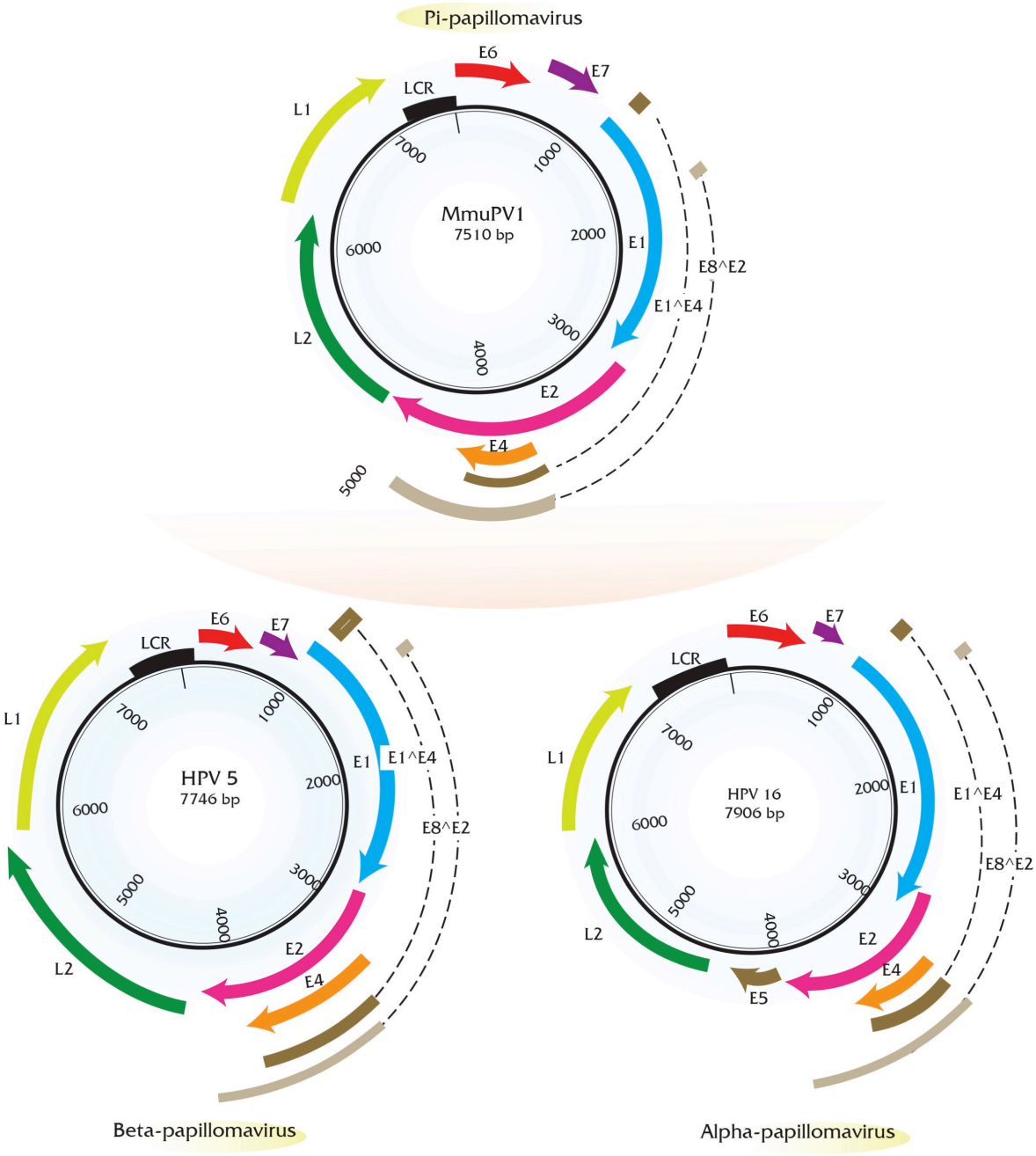

Fig. 2.1. Genome organization of rodent papillomaviruses compared to high-risk papillomaviruses.

Fig. 2.1. Genome organization of rodent papillomaviruses compared to high-risk papillomaviruses. Rodent PVs follow similar genome organization as prototype papillomaviruses and contain early and late ORFs. Shown here is the mouse papillomavirus (MmuPV1) genome (top) as an example of rodent papillomaviruses. For comparison, genomes of prototype high-risk HPVs i.e. HPV5 (bottom left, cutaneous HPV as an example of beta-papillomaviruses) and HPV16 (bottom right, mucosal HPV as an example of alpha papillomaviruses) have been shown. The early ORF of MmuPV1 and HPV5 consists of *E1* (blue), *E2* (pink), *E4* (orange), *E6* (red) and *E7* (purple) and the late ORF consists of *L2* (green), *L1* (lime). At the genomic level, the most notable change in rodent PV organization compared to HPV16 is the lack of *E5* oncogene (brown), which is present in HPV16. Genes *E5, E6, E7* have been shown to be oncogenic in the context of several papillomaviruses. The long control region (LCR) is shown in black. *E1^E4* (dark brown) and *E8^E2* (light brown) splice products are also indicated based on transcript maps of these viruses.

Phylogenetic analysis of rodent PVs based on *L1* nucleotide sequence by maximum likelihood estimation reveals that rodent PVs are not monophyletic (Fig. 2.2) consistent with previous reports (48, 60). They are found at disparate positions on the phylogenetic tree, in the Pi, Iota, Sigma or Dyo-sigma lineages (48). It has long been hypothesized that papillomaviruses co-evolved with their hosts (68). Were this hypothesis correct, then all PVs infecting the same host would appear close together on the phylogenetic tree because they would have shared a recent common ancestor (reviewed in (69, 70)). However, the existence of distantly related rodent PV lineages is inconsistent with the predictions of this hypothesis (48, 71). For instance, different PV types each isolated from *Rattus norvegicus* (RnPV1-3) and *Mastomys coucha* (MnPV1 and McPV2) do not constitute monophyletic groups. RnPV1 belongs to Pi-PVs whereas RnPV2 and RnPV3 belong to the distant iota-PVs. Likewise is true for *Mastomys*-associated PVs where McPV2 is a Pi-PV and MnPV1 is an iota-PV. Generally, viral tropism is conserved among the different PV lineages. For example, Alpha-PVs largely comprise of mucosotropic papillomaviruses with the exception of the cutaneotropic HPV2 and HPV4 (72). While the tropism of most rodent PVs remains under investigation, at least

Pi-PVs are comprised of both cutaneotropic and mucosotropic types of viruses. For example, MmiPV1 is associated with skin infections in *Micromys minutis,* whereas, McPV2 is associated with genital infections in *Mastomys coucha*. Mouse papillomavirus (MmuPV1) has been suggested to have an expanded tropism in its host species as *Mus musculus* is reported to induce disease in both cutaneous and mucosal epithelium (reviewed in (63)).

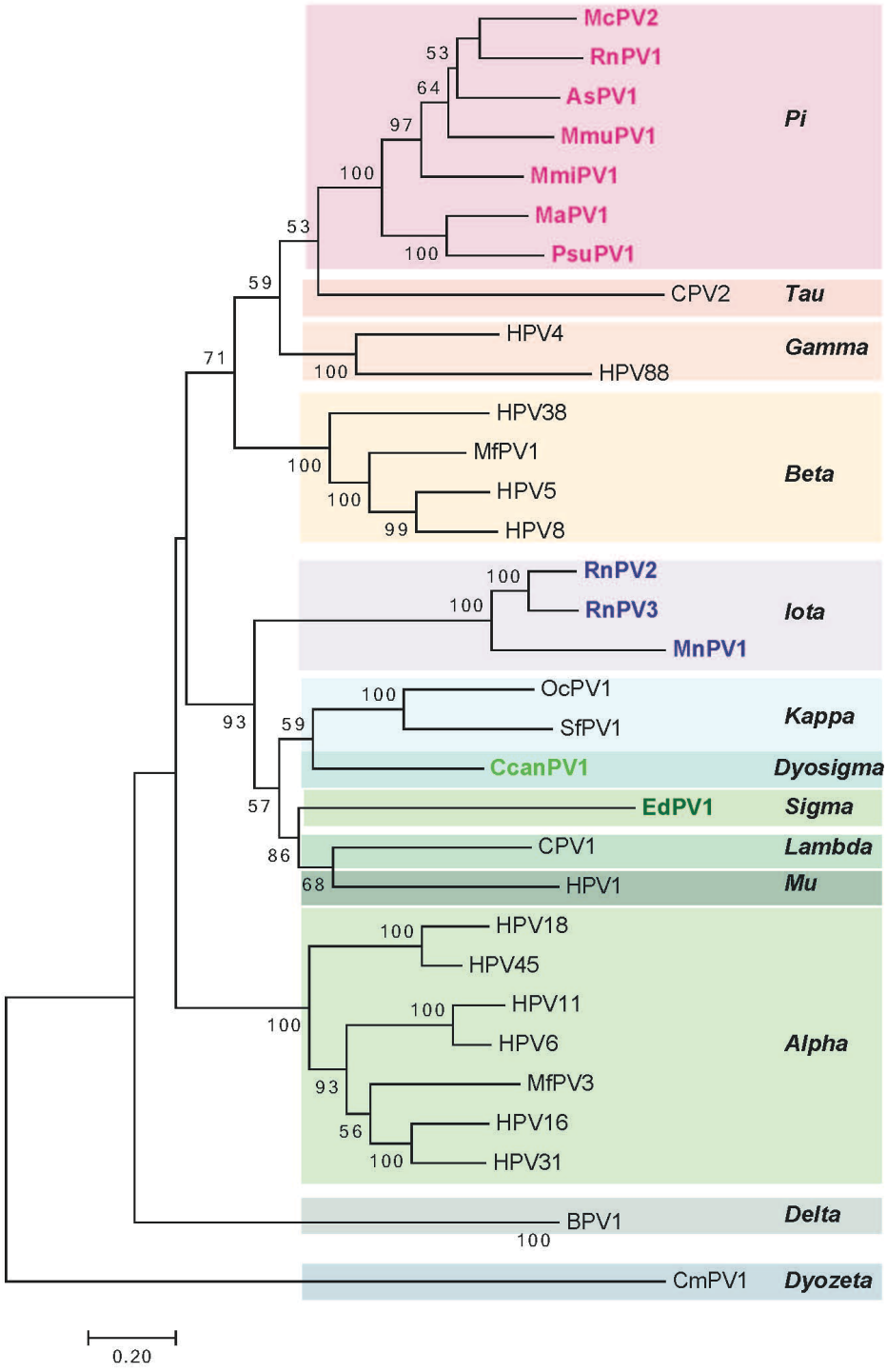

Fig. 2.2. Phylogenetic analysis of rodent PVs.

Fig. 2.2. Phylogenetic analysis of rodent PVs. Phylogenetic tree construction of rodent PVs was performed on the basis of L1 nucleotide sequences as per the standard criteria previously set for PV classification (73). The evolutionary history was inferred by using the Maximum Likelihood method based on the General Time Reversible model, and the tree with the highest log likelihood (-31759.0931) is shown. The percentage of trees in which the associated taxa clustered together is shown next to the branches. Values less than 50% are not shown. Initial tree for the heuristic search was obtained automatically by applying Neighbor-Join and BioNJ algorithms to a matrix of pairwise distances estimated using the Maximum Composite Likelihood (MCL) approach and then selecting the topology with superior log likelihood value. A discrete Gamma distribution was used to model evolutionary rate differences among sites (5 categories (+G, parameter = 0.9374)). The rate variation model allowed for some sites to be evolutionarily invariable (9.1152% sites). The tree is drawn to scale with branch lengths measured in the number of substitutions per site. All positions containing gaps and missing data were eliminated. There were a total of 1311 positions in the final dataset. Evolutionary analyses were conducted in MEGA7(74). In this small-scale phylogenetic analysis 33 papillomaviruses that represent prototype papillomaviruses in each clade were chosen for the analysis. For the most recent complete phylogenetic analysis of all papillomavirus species, the reader is referred to de Villiers, (2013) (75).

The early region of all rodent PVs consists of five translational open reading frames (ORFs): *E1, E2, E4, E6* and *E7* (Fig. 2.1). Among these, the *E1* and *E2* ORFs encode factors that are key for viral DNA replication and transcription similar to other papillomaviruses (reviewed in (76, 77)). Rodent papillomaviruses possess a clearly recognizable *E4* ORF that is present in most other papillomaviruses except for avian papillomaviruses (reviewed in (78)). Three papillomavirus early gene products, E5, E6 and E7, have been shown to stimulate cell proliferation and survival and modulate keratinocyte differentiation; therefore, these gene products are considered to be oncoproteins in the case of PVs associated with cancer. Beta papillomaviruses comprising largely of cutaneotropic HPVs lack an *E5* ORF, which is hypothesized to contribute to their inability to cause cancers. This is in contrast to the alpha-viruses including the high-risk mucosotropic papillomaviruses that do contain *E5* (79, 80). Similar to beta-HPVs, all rodent PVs lack an *E5* ORF, but possess the *E6* and *E7* ORFs. Great efforts have been made in the field to elucidate the oncogenic roles of E6 and E7 encoded by high-risk mucosotropic HPVs (reviewed in (81, 82)). The biological activities of rodent PV E6 and E7 gene products remain under investigation and are described in Section 2.5.

2.3. Pathogenesis by rodent papillomaviruses

2.3.1. Mastomys-associated papillomaviruses

Studies in multimammate mice belonging to the *Mastomys* genus of the rodent family *Muridae* have provided valuable insights into the biology of papillomaviruses. The first-discovered rodent papillomavirus was isolated from skin keratoacanthomas arising spontaneously in a colony of African multimammate rats, *Mastomys coucha* (83-87), originally misidentified as *Mastomys natalensis* (88), leading to its designation as the *Mastomys natalensis* papillomavirus (MnPV1). *M. natalensis* (common name: Natal multimammate mouse) and *M. coucha* (common name: Southern multimammate mouse) differ karyotypically, but are difficult to distinguish visually, leading to confusion in their identity.

Studies pertaining to these papillomaviruses have been performed in a *M. coucha* colony maintained at the German Cancer Research Center (DKFZ) in which animals were found to be naturally and persistently infected with two rodent papillomaviruses - the aforementioned *Mastomys natalensis* papillomavirus (MnPV1) and a second virus called *Mastomys coucha* papillomavirus-2 (McPV2) (52). Animals in this laboratory colony have been found to be latently infected with MnPV1 and to a lesser extent with McPV2 as determined by detection of viral DNA as well as by serological studies (89). Recently, a virus-free colony of the *M. coucha* was established at the DFKZ (90). Of the two *Mastomys*-associated papillomaviruses, McPV2 was only recently isolated from anogenital condylomas in aged *M. coucha* mice (52), and consequently, its biology is less well understood. However, substantial efforts have been made in understanding biology of MnPV1, which is associated predominantly with cutaneous lesions.

MnPV1-associated skin lesions develop spontaneously on exposed surfaces of *M.coucha*. These lesions present as exophytic papillomas, are highly keratinized, and do not regress (83). The MnPV1 DNA genome exists as extrachromosomal circular DNA in the skin lesions (58). While only 3% of young animals spontaneously develop overt MnPV1-associated lesions, the frequency increases to 30-40% of animals at one year of age (58). MnPV1-DNA based *in situ* hybridization analysis of skin papillomas from infected animals showed the presence of amplified viral DNA predominantly in subrabasal epithelial layers (91). MnPV1 genomes were also detected in the dermal papilla of the hair follicles (91) which is a known reservoir of stem cells [reviewed in(92)]. This is an intriguing observation as previous studies with CRPV in rabbits found viral gene expression in hair follicles raising the possibility that hair follicle stem cells might be a target for papillomavirus infections (93). The MnPV1 infection model also appears to represent an intriguing case of 'endogenous infection' as extrachromosomal DNA is found to occur in other internal tissues (e.g. liver, brain and lungs) in both tumor-free and tumor-bearing animals (58, 91). Nafz, *et al*. (2007) reported that fetuses or newborns from MnPV1-infected pregnant dams did not show any signs of MnPV1 infection suggesting that infection occurs after birth (91). In the same study the authors reported that 2 out of 6 tumor-free animals showed the presence of MnPV1 DNA in their blood. While analysis of more samples is required, this observation suggests that MnPV1 spread could occur via blood.

MnPV1 also has shed light on the concept of papillomaviral latency, which is described as a phase of the viral life cycle in which "no clinical signs of disease are apparent and new virus particles are not produced and released" (reviewed in (94)).

MnPV1 can be found to persist in young animals at low viral copy numbers without any overt sign of disease, consistent with latency. Upon chronic topical administration of the tumor promoter, 12-O-Tetradecanoylphorbol-13-acetate (TPA) to the skin of such mice, an earlier onset of MnPV1-induced papillomas was observed that contained higher viral DNA loads (58). Mechanical irritation of animals latently infected with MnPV1 also led to earlier onset of keratoacanthomas and increased viral DNA loads (95). These observations indicate that disruption of epidermal homeostasis triggers latent papillomavirus to establish a productive infection that results in overt clinical disease (95).

While MnPV1 mostly causes benign lesions, interesting insights have been gained about the role of MnPV1 in carcinogenesis in conjunction with chemical agents. Chronic administration of the chemical carcinogen, 7,12-dimethylbenz(a)anthracene (DMBA), led to both benign and malignant tumors in all animals. Furthermore, in a classical two-stage carcinogenesis study, MnPV1 led to squamous cell carcinomas (SCC) after a single topical application of DMBA followed by repeated challenge with TPA (96). To understand the biology of the MnPV1 putative oncogene, *E6*, transgenic mice expressing the MnPV1 *E6* gene in the skin under the control of the human cytokeratin-14 promoter were generated. MnPV1-E6 transgenic mice do not develop papillomas or keratoacanthomas spontaneously. However, squamous cell carcinomas were observed in MnPV1-E6 mice in conjunction with classical two-stage skin carcinogenesis studies as described earlier, indicating that MnPV1 E6 can cooperate with chemical carcinogens to cause cancer (97). To date, this is the only transgenic mouse model expressing a putative rodent papillomavirus oncogene in the epithelia. At present the biological interaction

partners of MnPV1 E6 remain largely unknown as a lack of reagent availability coupled with the lack of *in vitro* systems has impeded progress in this area. In this context the establishment of the first ever keratinocyte cell line from *M. coucha* provides a potential cell culture system to study the virus life cycle and interaction partners *in vitro* (98). Also, information derived from the recent transcriptome analysis of MnPV1 using high-throughput RNAseq analyses of productive lesions led to the assembly of a comprehensive transcript map with identification of several novel splicing patterns for MnPV1 (see Section 5). This knowledge will be valuable in moving forward the study of MnPV1 molecular biology (99).

2.3.2. Mus musculus- associated papillomaviruses

2.3.2.1. Discovery of the first papillomavirus to infect the standard laboratory mouse strain, *Mus musculus*.

MmuPV1 is the first cloned rodent papillomavirus to be isolated from the laboratory strain of mice, *Mus musculus* (55). Subsequently, a variant of the MmuPV-1 with very high sequence similarity (99%) was independently isolated from the skin of a house mouse (48). MmuPV1 is a valuable papillomavirus as it allows us the opportunity to study papillomavirus infections in a natural setting in a genetically modifiable organism. MmuPV1 was isolated from florid papillomas that arose spontaneously around the muzzle and nose regions in a colony of T-cell deficient NMRI-*FoxN1*$^{nu/nu}$ strain of mice at the Advanced Centre for Treatment and Research in Cancer (ACTREC) in India (55). Histopathological analysis of these lesions showed features consistent with papillomatosis i.e. papillary projections with koilocytes that were positive for PV group-

specific antigens. The viral extracts from these papillomas were found to be transmissible to other NMRI-*FoxN1*$^{nu/nu}$ mice. Lateral transmission of papillomavirus to uninfected sites was also observed in these animals (55, 100, 101) with naïve nude mice housed with infected nude mice developing MmuPV1-associated papillomas (101). Lateral transmission of virus resulting in papillomas at uninfected sites was attributed to general grooming behavior of mice, which can lead to microabrasions eventually promoting infection by MmuPV1. Analysis of MmuPV1-induced lesions arising on the NCR strain of *FoxN1*$^{nu/nu}$ suggests that this papillomavirus has an unusual pattern of late protein expression. In this study the authors generated polyclonal antisera specific for L1 and L2 and observed that L1 protein was expressed in all layers of the stratified epithelia of the papillomas whereas L2 protein was detected only in the subrabasal compartments (100). They also observed, unexpectedly, that the L1 expression was localized to the cytoplasm in lower layers of the epithelia prior to expression of L2. This is different from infections induced by high-risk HPVs where neither L1 nor L2 are detected in lower layers of the epithelia and L2 expression is turned on in layers prior to initiation of L1 expression (102). However, in cutaneous warts induced by HPV 1, L1 is expressed throughout the epithelium and in lower layers than is detected L2 (103), similar to that seen with MmuPV1.

In our lab, we performed a time-course analysis in which infected tissue was harvested 3 days, 10 days, and 21 days post-infection and from mature warts at 3 or 6 months post-infection from MmuPV1-infected BALB/c-*FoxN1*^{nu} mice (Fig. 2.3) (104). We observed that L1-positive cells are present throughout the epithelium in mature warts but restricted to more terminally differentiated cells at the earlier time points indicating

that the full manifestations of the viral life cycle are realized at times later than 4 weeks post-infection. In these studies we noted that L1 expression was predominantly nuclear though some cytoplasmic signal was observed as well. This is consistent with recent observations made in NU/J-*FoxN1*^{nu} mice (105). Differences in the pattern of detection of L1 may reflect the different genetic backgrounds of the mice used in these studies. We also observed amplification of MmuPV1 DNA in the basal layer of the epithelia. Basal cells have been seen to support viral DNA amplification in lesions caused by the cutaneous HPV1 and HPV63 and by canine oral papillomavirus (COPV1), which is a mucosal papillomavirus (25, 106). We also observed that in experimentally infected nude mice that have developed warts at the sites of infection, other uninfected areas of the epidermis show evidence of subclinical infections (i.e. no signs of overt papillomas). At the microscopic level, these subclinical infections showed evidence for productive infection based upon the detection of viral DNA amplification and L1 expression (104). This raises the intriguing possibility that subclinical PV infections may be common in immunodeficient or immunosuppressed contexts in humans as well. In this regard, organ transplant patients on immunosuppressants are known to have an increased abundance of HPV DNA in randomly sampled hair follicles from clinically normal skin (107).

L1 and L2 capsid proteins play key roles in in early events in PV infectious entry [reviewed in (108, 109)]. Studies attempting to tease apart early events in PV infectious entry have been performed using pseudoviruses (i.e. reporter plasmids encapsidated by PV L1 and L2) have produced different results, depending on the in vitro or in vivo model system utilized(108). It is worth considering that several of these in vivo studies have been performed in the context of a heterologous host. Recently, it has been reported

that murine skin as well genital tissues were similarly permissive to infection by pseudoviruses of multiples PV types that included HPV16 as well as MmuPV1(110). Despite this shared activity, pseudovirus infections performed in the context of cevicovaginal tract showed that HPV16 and MmuPV1 capsids interact with different host cell proteins (111). Heparin sulfate proteoglycans (HSPGs) have been shown to be an initial attachment receptor for multiple PV genotypes in vitro [reviewed in(108, 112)], and have been shown to contribute to infection via the binding of soluble complexes with growth factors(113). It has been shown that the interaction of PVs with basement membrane (BM) via HSPGs is critical for in vivo infection of mucosotropic HPV16 and HPV31 as well as the cutaneous HPV5. However, in the same study it was demonstrated that different heparin variants affected the alpha and beta types in dissimilar ways raising the possibility that cutaneous and mucosal HPVs may have evolved to recognize different forms of HSPGs. Day, *et al* (2015) demonstrated that unlike HPV16, MusPV1 bound BM in an HSPG-independent manner(111). Despite the differences in the initial interacting partners found for HPV16 and MusPV1, both viruses appear to use the same endocytic pathways as is consistent with other HPV types(114). It remains to be determined whether these interactions are identical for the cutaneous epithelia in the context of MmuPV1.

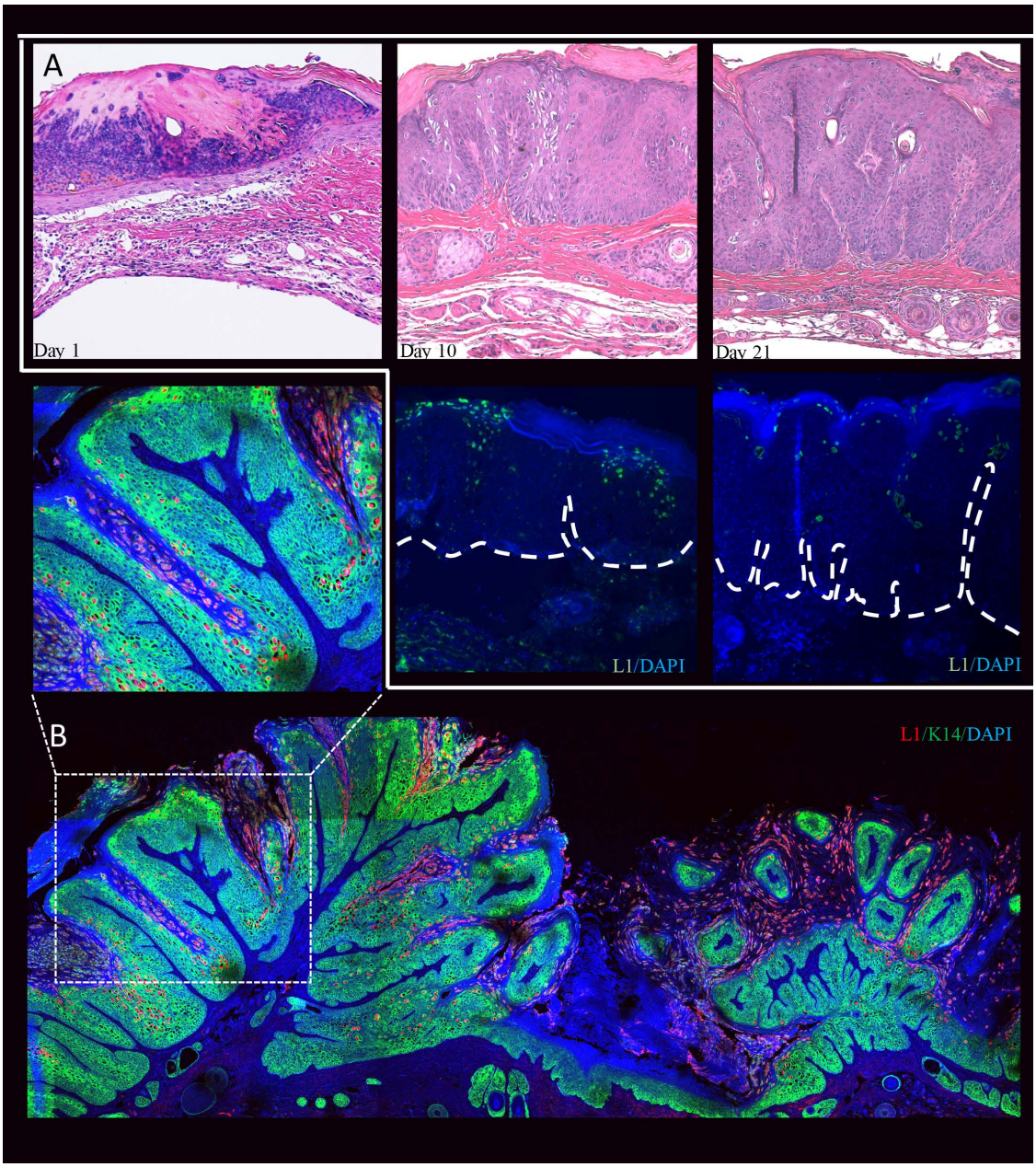

Fig. 2.3. Progression of MmuPV1-induced tail papillomas in BALB/C-*FoxN1*^{nu} nude mice.

Fig. 2.3. Progression of MmuPV1-induced tail papillomas in BALB/C-*FoxN1*^{nu} nude mice. This figure has been modified from Xue, *et al* (2017, in press) (104). Nude mice were infected with MmuPV1 virus extract following scarification and tissue was harvested at days 1, 10 and 21 post-infection. **Panel A** shows H&E staining of infected tissue at indicated time points post-infection with MmuPV1 and the corresponding L1 immunofluorescence (green) to show presence of MmuPV1 capsid proteins. At day 1 we see presence of a scab and immune infiltration but no L1 was detected (data not shown). At day 10 post-infection we can see hyperplasia, and formation of fibrillary projections begin to appear indicating formation of papilloma. At this time point we can detect L1 in the suprabasal layers. At day 21 we can see more pronounced papillomatosis, and L1 staining can be seen even in basal layers of the papilloma. The H&E images and fluorescent images were captured using a Zeiss AxioImager M2 microscope and AxioVision software version 4.8.2 (Jena, Germany). **Panel B** shows a high resolution wide-field image of an MmuPV1-induced tail wart at 6 months post-infection. In this image we have shown L1-K14 dual immunofluorescence. Extensive papilloma formation coupled with expansion of the K14 layer (green) is seen, and L1 expression (red) is seen throughout the epithelia (inset). The nuclei are stained with DAPI (blue). High resolution wide-field fluorescent images were acquired by means of a super-resolution Leica SP8 STED confocal microscope equipped with a motorized stage located in the UW optical core. This microscope is equipped with PMT and HyD lasers. All images were taken by means of a 20X objective lens (Specifications: HC PL APO 20x/0.75 CS2, Dry). The images were acquired by tile-scanning by marking positions around the region of interest on the LAS-X suite (version: 2.0.1). The merged wide-field image was obtained by automatic stitching of individual styles by means of an in-built auto-stitching algorithm that is part of the LAS-X suite.

2.3.2.2. T-cell deficient strains are susceptible to MmuPV1 infection**.**

Multiple other genetic backgrounds carrying the *FoxN1*$^{nu/nu}$ mutation are also susceptible to infection by naked, recircularized MmuPV1 DNA as well as quasivirions encapsidating synthesized MmuPV1 genomes (Summarized in Table 2.2). Mice carrying the *FoxN1*$^{nu/nu}$ mutation are null for the *FoxN1* (Forkhead Box N1) gene and are colloquially referred to as nude mice due to their characteristic hairless phenotype (115). These mice are immunodeficient by virtue of thymic aplasia that results in T-cell deficiency (116). MmuPV1 consistently causes exophytic papillomas in the muzzle and tail regions of nude mice but torso skin appears to be resistant to MmuPV1 papillomatosis (100, 101) except in the B6 and NMRI genetic backgrounds where locally invasive trichoblastomas are observed on the torso (101). This observation would suggest that the anatomical site of infection is a critical determinant of the nature of disease progression. Gene expression profiling studies performed recently on dorsal versus tail skin identified gene networks including Sonic Hedgehog (Shh), Wnt, Lgr family stem cell markers, and keratins that differed in expression at these tissue sites (117) providing a potential explanation for the differential susceptibility of dorsal and tail skin to the development of skin diseases and tumorigenesis. While titrating the virus dose to observe papilloma incidence in nude mice, we and others have found that the lowest dose of virus that can consistently cause papillomas at 100% of infected sites in nude mice is 10^7 virus particles containing viral DNA (100, 118). In our long-term monitoring of papillomas with 10^6 virus particles we observed that there was a delay in onset of papillomatosis in nude mice with papilloma incidence increasing over time (118). While MmuPV1 appears to be predominantly cutaneotropic, some groups have observed

extended tropism of the virus in these immunodeficient strains. This is evidenced by the ability of the virus to cause lesions in anogential and vaginal areas as well as in the oropharyngeal tract (119, 120). It has been shown that mice infected cutaneously display secondary infections at mucosal sites (120). Recently it has been reported that mice infected mucosally also display secondary infections at skin sites. Histopathological analysis of these skin lesions arising due to secondary infection in aged mice showed signs of micro-invasive squamous cell carcinoma (105).

Mice with a SCID mutation in the *Prkdc* gene (*Prkdc*^{scid}) on the SHO genetic background are susceptible to MmuPV1 infection (121, 122). These mice are generally characterized by the absence of functional T cells and B cells, however they have been known to have leaky production of B cells as they age (123-125). Interestingly, SCID mice on the NOD genetic background are resistant to MmuPV1-associated skin papillomas (101). This observation suggests that genetic background is probably a key factor in determining susceptibility to MmuPV1 infection. Lists of immunodeficient strains found to be susceptible or resistant to MmuPV1 infection are summarized in Tables 2 and 3, respectively.

Table 2.2: List of immunodeficient mice found to be susceptible to MmuPV1 skin infections

	Deficiency	Strain-*Mutation*	Reference
1.	Lack T cells	B6.Cg-*Foxn1^{nu}/J*	(56, 101)
2.		BALB/c-*Foxn1^{nu}*	(118)
3.		Hsd:NU-*Foxn1^{nu}*	(126)
4.		NCr nu/nu	(100)
5.		NMRI-*Foxn1^{nu}/Foxn1^{nu}*	(55)
6.		NU- *Foxn1^{nu}/Foxn1^{nu}*	(105)
7.	Lack T & B cells	B6.129S7-*Rag1^{tm1Mom}/J*	(101, 127)
8.		B6.CB17-*Prkdc^{scid}/SzJ*	(101)
9.		NCI SCID/Ncr	(127)
10.		SHO-*Prkdc^{scid}Hr^{hr}*	(120)

Table 2.3 : List of immunodeficient mice found to be resistant to MmuPV1 skin infections

Deficiency	Strain/Mutation	Reference
1. Lack T & B cells	NOD.CB17-*Prkdc^{scid}/SzJ*	(101)
2. Lack B cells	B6.129S2-Ighm^{tm1Cgn}/J	(101),(128)
3. Lack CD4+ T cells	B6.129S2-Cd4^{tm1Mak}/J	(101),(128),(127)
4. Lack CD8+ T cells	B6.129S2-Cd8^{tm1Mak}/J	(101),(128)
5. Lack T helper cells/CD40 ligand K	B6.129S2-Cd40lg^{tm1Imx}/J	(127)
6. Lack NK (CD1d) cells	B6.129S6-Del (3Cd1d2-Cd1d1) ^{1Sbp}/J	(128)
7. Decreased Anti-viral innate immunity, lack Type I Interferon	IFNAR KO	(127)

Multiple groups, including our lab, have reported that MmuPV1 does not cause papillomatosis in routinely used immunocompetent wild-type strains of mice such as BALB/c, FVB/NJ and C57/BL6 (55, 56, 100, 101, 118, 127, 128) although serological responses to MmuPV1 virus-like particles (VLPs) have been reported in C57/BL6 mice infected with MmuPV1 even 70 days post-infection (56). If a very high dose of virus was used (1012 virus particles), papillomas did arise in C57/BL6 and SENCAR strains of mice but these papillomas regressed within one or two weeks post appearance (128). Of these, the SENCAR strain of mice is a model classically used in skin tumorigenesis studies due to its high susceptibility to skin tumor induction by chemical carcinogens (129, 130). Continuous treatment with the immunosuppressant drug cyclosporine led to MmuPV1-induced papillomas in multiple immunocompetent mouse strains (127, 128). These observations have helped define what immune defects lead to susceptibility to MmuPV1 papillomas. Genetically modified strains selectively deficient for B-cells or subpopulations of T-cells (CD4+, CD8+, or CD40+) did not develop MmuPV1-associated papillomas (101, 127, 128). We have also observed the same in our hands (unpublished data) suggesting that complete T-cell deficiency is required for MmuPV1 susceptibility, at least on the C57BL/6 genetic background. This conclusion was confirmed by performing antibody-based depletion studies using a monoclonal antibody against the CD3 T-cell co-receptor, which led to MmuPV1-induced papillomas in multiple strains (127, 128). It is notable that while in the SENCAR strain administration of antibodies against either CD4+ or CD8+ led to susceptibility to MmuPV1, in C57/BL6 and BALB/c genetic backgrounds, elimination of both CD4+ and CD8+ cells was required. Studies that involved intervention with immunosuppressants have been

summarized in Table 4. Recently, it has been reported that when MmuPV1-induced tumors arising in T-cell deficient mice were transplanted onto immunocompetent congenic mice, the tumors completely regressed(131). Further, this elimination of MmuPV1-induced tumors was consistent with the induction of antitumor T cell immunity affirming the role of T-cell immunity in MmuPV1 infections.

Table 2.4: List of immunocompetent mice found to be susceptible to MmuPV1 after treatment with immunosuppressants

	Strain	Intervention	Reference
1. 2. 3. 4.	Cr:ORL SENCAR FVB/NCr BALB/cAnNCr A/JCr	Cyclosporine	(128)
5. 6. 7.	Cr:ORL SENCAR	Anti-CD3 Anti-CD4 Anti-CD8	(128)
8. 9.	C57BL/6	Anti-CD3 Anti-CD4+Anti-CD8*	(127, 128)
10.	BALB/c	Anti-CD3*	(127)

*Anti-CD4 or Anti-CD8 alone did not lead to warts

CD8+ T-cells, specifically effector cytotoxic T lymphocytes (CTLs), play a critical role in the clearance of virally infected epithelial cells as well as regression of epithelial neoplasia [reviewed in(132-134)]. In several well-characterized systems, CD4+ T-cells are necessary for induction of primary CD8+ T-cell responses as well as for their proliferation, activation, and differentiation into effector cytotoxic T lymphocytes. For example, in a murine model of herpes virus infection, CD4+ T cells were required for efficient local recruitment of herpes simplex virus-specific CD8+ T cells to the vaginal epithelium (135). Therefore, the observation that loss of CD4+ T-cells in C57/BL6 and BALB/c was not sufficient to increase susceptibility to MmuPV1-induced papillomas (101, 127, 128) is somewhat surprising. Furthermore, it was also observed that MmuPV1 infection sites in C57BL/6 mice had recruitment of CD8+ T-cells even in the absence of CD4+ T-cells (128). Recent studies have shown that CD4+ T helper-independent $CD8^+$ CTL responses can be elicited by several other viruses as well [e.g. ectromelia virus (136), influenza virus (137), and dengue virus (138)]. Although the details of immune recognition of MmuPV1 are yet to be determined, it seems likely that T-cells control MmuPV1 infection by having an effect on both innate and adaptive arms of the immune system. It is worth noting that increased incidence of HPV-associated papillomas is observed in T-cell-immunosuppressed patients further emphasizing the role of CD4+ and/or CD8+ T-cell responses in PV-mediated disease (139). T-cell infiltration is seen in both cutaneous and mucosal lesions during the spontaneous regression of papillomas (140-143). When T-cell responses to five HPV16 proteins (E6, E7, E4, L1 and L2) were analyzed in women with CIN or cervical carcinoma, CD4+ and CD8+ T-cell responses changed with severity of disease suggesting that there are differences in how viral

antigens are seen by the immune system during progressive disease of the cervix(144). Hence, there is a need to understand and define the role played by PV specific T-cells during the natural course of virus infection. While such a prospective study will be hard to conduct in humans, the MmuPV1-infection model provides us the opportunity to define the contribution of T-cells during the course of PV infections.

While most of the studies in MmuPV1 have been focused on the role of the adaptive arm of the immune system, specifically T-cell biology, there have been limited efforts in looking at the role of innate immunity in this infection model as well. In a previous study, no visible disease was seen in cutaneous sites of Interferon-alpha/beta receptor alpha chain-null (*Ifnar*^{KO}) mice that lack Type I interferons (127). However, in a recent review it was shared that MmuPV1 DNA persisted longer in the anogenital and vaginal tracts of *Ifnar*^{KO} mice compared to their wild-type counterparts (63). It is worth appreciating that the immune biology of mucosal epithelia is very different from cutaneous epithelia and can contribute to progression of disease differently (145, 146). In this context, a role of natural killer (NK) cells has been proposed (63); however, in earlier studies, NK-cell deficient mice were found to be resistant to MmuPV1 infection (128). Overall, the reported studies indicate that T-cells primarily control phenotypic disease caused by MmuPV1.

The MmuPV1-infection model affords us the opportunity to study the role of antiviral host-intrinsic immunity. Antiviral intrinsic immunity, a form of innate immunity that directly restricts viral replication and assembly, has been shown to an important host-restriction factor in the context of influenza and retroviruses [reviewed in (147)]. In the last decade, several host factors that restrict transcription (e.g. Sp100 (148), EVERs (149)) and early phases of viral replication (miR-145(150), p56(151) and IFI16(152)) of papillomaviruses have also been characterized [extensively reviewed in(153)]. In recent years, the apolipoprotein B messenger RNA-editing, enzyme-catalytic, polypeptide-like 3 (APOBEC3) family of cytidine deaminases has emerged as a critical player in governing intrinsic immunity [reviewed in(154)]. APOBEC3 enzyme APOBEC3A has been shown to cause mutations of HPV DNA(155) and inhibit HPV infectivity(156). Furthermore in a recent, large scale, case-control study of HPV16 associated cervical cancers and precancers it was shown that HPV16 rare variants were potentially induced by the antiviral activity of human APOBEC3 family of enzymes (157). It has been reported that *Apobec3*−/− mice (n=3) were not susceptible to MmuPV1-induced tumors(156). This preliminary study was performed in immunocompetent mice and suggests that perhaps loss of APOBEC3 is not sufficient to overcome host adaptive immune responses against MmuPV1 infection in immunocompetent mice. The role of APOBEC3 in disease progression is yet to be determined.

2.3.2.3. MmuPV1 infection in hairless strains.

In the original paper that described the discovery of MmuPV1, virus extracts from papillomas arising on nude mice were transmissible to other nude mice as well as to the immunocompetent but hairless strain of *S/RV/Cri*$^{ba/ba}$ mice (55). Interestingly, while papillomas persisted in the originally infected NMRI-*FoxN1*$^{nu/nu}$ strain they completely regressed in *S/RV/Cri*$^{ba/ba}$ mice 6-8 weeks post appearance. The *S/RV/Cri*$^{ba/ba}$ is an outbred strain endemic to India (158-161) and is at least phenotypically similar to the outbred SKH1-elite strain in the United States that has an autosomal mutation in the *Hr*^{Hr} allele resulting in a hairless phenotype. The SKH1-elite strain is a popular strain in the context of photocarcinogenesis studies(162), and subsequent studies by other groups have found that the SKH1-elite strain is also susceptible to MmuPV1-associated papillomas. In a recent, more comprehensive study it was found that only a subset (22.5% i.e. 9/40 mice) of infected SKH1-elite mice developed papillomas, some of which (5/9 mice) persisted while others regressed (4/9)(127). In a pilot study (16 total sites infected in 4 animals) we found that no papillomas developed in the SKH1-elite mice 6-months post-infection (unpublished data). This can be explained by our low number of mice and seems to be in conjunction with the speculation that only a subset of the outbred SKH1-elite mice are susceptible to MmuPV1-induced papillomatosis. It is worth noting that the immunobiology of SKH-1 elite strain is poorly understood.

2.3.2.4. Role of ultraviolet radiation (UVR) in MmuPV1-associated disease.

There are multiple lines of evidence that suggest UVR could play a role in infection by cutaneous PVs. One line of evidence comes from epidemiological data gathered from human studies; and the other line of evidence comes from studying UVR in other animal models of PV infection. Epidemiological studies indicate there is a correlation between exposure to ultraviolet radiation (UVR) from sunlight and the prevalence of cutaneous HPVs in healthy and immunosuppressed patients (163, 164). Cutaneous HPVs are more commonly found at anatomical sites exposed to sunlight, and a history of blistering sunburn is associated with prevalent and persistent cutaneous HPV infections (17, 163-165). In a case-control study, sunburn due to cutaneous sensitivity to sunlight exposure was associated with a higher seroprevalence for beta-HPV types (166). There is also limited prior evidence suggesting a role of UVR in other animal models for papillomavirus infection. Early studies investigating UVR-induced tumors in hairless HRA/Skh mice led to identification of novel a papillomavirus, which, based upon Southern hybridization, shared homology with MnPV1 DNA as well as with HPV11, -13, -16 and -18 DNA (167). The viral genome, however, was not isolated or sequenced. Further, studies showed that cell-free extracts containing this MnPV1-like viral DNA enhanced UVR-induced tumorigenesis (168) suggesting that perhaps there is some relation between UVR and PV pathogenesis. The most convincing evidence supporting the role of UVR in animal infection models comes from studies with the cottontail rabbit papillomavirus (CRPV) where it was found that papillomas were induced in a subset of cottontail rabbits latently infected with CRPV when the animals were exposed to UVR (169). Furthermore, UVR has been identified as a cofactor in causing skin cancers

in transgenic mouse models for several beta-HPVs (e.g. HPV8(170), HPV20(171), HPV27(171) and HPV38(172)).

In our studies, we made the novel observation that when FVB/NJ mice were infected with MmuPV1 and exposed to the UVB spectra of UVR, greater than 50% of infected sites developed papillomas, some of which persisted while the others completely regressed. UVB also induced MmuPV1-dependent papillomatosis in other strains of immunocompetent mice such as BALB/c and C57/BL6, but at higher doses of UVB. Histopathological analysis of the papillomas in the MmuPV1/UVB infection model also indicated progression to squamous cell carcinoma. While malignant potential of MmuPV1 had been suggested in nude mice, this was the first evidence demonstrating that MmuPV1 can cause cancer in immunocompetent strains of mice. The most significant observation of this study was the finding that there was a strong correlation between long-term immunosuppression induced by UVB and MmuPV1-dependent pathogenesis. This correlation supports the hypothesis that UVB-induced immunosuppression can help to drive papillomavirus-induced disease. Epidemiological data from human studies indicates that anatomical sites on individuals that are exposed to sunlight have increased susceptibility to HPV-induced warts. However, in this mouse study, the effects of UVB were found to be systemic i.e. sites of infection did not have to be exposed to UVB irradiation. Further studies are needed to assess whether a local effect of UVB on MmuPV1 can be identified in mice.

UVR has been shown to enhance pathogenesis of cutaneous (e.g. herpes simplex virus-type 1 or HSV-1) as well as non-cutaneous based viruses (e.g. murine leukemia virus, influenza virus, and reovirus) (reviewed in(173)). The effects of UVR on viral

pathogenesis can be indirect and/or direct. The indirect effects of UVR involve modulation of host immunity and have been extensively reviewed elsewhere (174-181). UVB plays a key role in initiating and mediating immunosuppression (182, 183), and its effects can be long lasting (184-186). UVR-dependent immunosuppression is initiated when chromophores (DNA, Urocanic acid) present in the skin first encounter UVR photons (187-189) and is largely T-cell mediated. UVB can inhibit development of memory T-cells as well as cause an overall reduction in T-cell subpopulations in the skin (190). UVR causes induction of immunosuppressive T-cell subpopulations (e.g. T_{regs}) (191, 192) and alters overall host cytokines from a pro-inflammatory Th1 to the immunosuppressive Th2 profile (193, 194). Recent studies have also implicated resident skin immune cells (e.g. langerhan cells, monocytes, macrophages) and keratinocytes in the process of UVB-induced immunosuppression (175, 181). While the effects of UVR on the host warrant further investigation, the observation that UVR can suppress immune responses to infectious microorganisms leads to the hypothesis that exposure to UVR can enhance susceptibility to microbial infections, particularly viruses, and/or worsen the state of infectious diseases (195, 196). Our data with MmuPV1 supports this hypothesis. Mechanisms underlying UVR induced-immunosuppression in the MmuPV1 pathogenesis model remain to be determined.

UVR can directly impact viruses and their host cells by causing mutations due to UVRs ability to form photo-adducts (197). Studies performed in the context of HSV-1 and parvovirus support this hypothesis (198, 199). UVR may also lead to the formation of DNA-protein cross-links, the impacts of which are unknown (200). In addition, UVR has been shown to enhance the frequency of viral recombination in both adenoviruses and

HSV (201, 202), which can potentially lead to more pathogenic variants of the viruses. UVR may directly induce viral transcription by acting on UVR response elements present in the promoters of certain viruses (e.g. HIV, HSV-1) (203, 204). Direct effects of UVR on papillomavirus biology remain to be understood. However, there is precedence to test roles of PV genes in modulating cellular responses to UVB. For example, beta HPVs (HPV5 and HPV8) E6 oncoproteins cause degradation of the pro-apoptotic protein Bak thereby inhibiting apoptosis (205, 206); on the other hand, HPV77 E6 oncoprotein has been shown to deregulate p53-dependent transactivation of proapoptotic genes upon UVB irradiation (207). The physiological relevance of these properties, if any, can be assessed by means of rodent models particularly, MmuPV1, as MmuPV1-E6 shares several properties in common with beta-HPVs (see below).

In the case of the HSV family of viruses, latent virus is reactivated by exposure to a variety of environmental or physiologic stimuli including UVR radiation exposure. In our MmuPV1-UVR infection model we observed that a single exposure to UVB as long as 14 days post-infection led to papillomatosis at sites infected with MmuPV1(118). This indicates either that the virus is stably retained at the site of infection or that latent infection arises that is then activated by UVB-induced immunosuppression. In support of the latter hypothesis, Doorbar and colleagues have observed that rabbit oral papillomavirus-induced lesions that regress can be reactivated upon drug-induced immunosuppression (208). It remains to be determined whether in the MmuPV1 infection model latency arises, and, if so, the nature of this latency.

2.3.3. Other rodent papillomaviruses

Besides MnPV1 and MmuPV1, MmiPV1 is another rodent papillomavirus that has been identified to infect the European harvest mouse belonging to the *Muridae* phyla of rodents. MmiPV1 was isolated from lesions arising in the European harvest mice housed in a regional zoo in Chicago. Initial efforts in characterizing MmiPV1 suggest that it is a cutaneous papillomavirus as no lesions were identified in any internal organs. The virus was found to be defective in transforming 3T3 and C127 cells (54, 209). The complete genome of MmiPV1 was sequenced fairly recently (53) making it possible to understand further the biology of this virus. Recently, three novel papillomaviruses that can infect rat species (RnPV1-RnPV3) have been isolated (48). These can be potentially useful models to study papillomavirus infections as rat models can also be studied in the laboratory setting.

2.4. Insights into vaccine development

There are few studies that have evaluated therapeutic approaches to treat MnPV1-induced papillomas. A modest response was seen in MnPV1-induced spontaneous papillomas in *M. coucha* treated with the immune response modifier imiquimod (210). Recently it has been shown that vaccinating *M. coucha* with an L1-based virus like particle (VLP)-based vaccine can prevent MnPV1-induced lesions (benign as well as malignant) in both naturally infected strains of *M. coucha* as well as experimentally infected naïve *M. coucha* animals. The authors also observed long-lasting humoral immune responses following vaccination in animals that had been chronically immunosuppressed via administration of cyclosporine A. The results of this study have valuable implications in the field of vaccine development as the authors demonstrated

that VLP-based vaccines could effectively prevent the appearance of skin tumors even in animals that are already infected or undergo systemic immunosuppression (90). Vaccination of immunosuppressed individuals with HPV-vaccines has produced modest results due to low seroconversion but recommendations for three doses of the vaccine have been made, which merit further research (211). Little is known about the similarities of the *M. coucha* immune system with the human immune system; therefore, the MmuPV1-infection model is potentially a more relevant animal model, given the extensive knowledge of the *Mus musculus* immune system and its relevance to humans. In this context, recently the Roden group has tested a naked-DNA vaccine expressing human calreticulin (hCRT) fused in frame to MmuPV1 E6 (mE6) and mE7 early proteins and residues 11 to 200 of the late protein L2 (hCRTmE6/mE7/mL2) in the MmuPV1-infection model established in SKH1-e (hairless mice) in which a low percentage of animals is susceptible to MmuPV1 infections (212). In this study the authors found that persistent papillomas arising due to MmuPV1 infections disappeared within 2 months after final vaccination, and the disease did not recur when CD3 T-cells of these animals were depleted.

2.5. Transcript maps of rodent papillomaviruses

Viral transcript maps have been analyzed for two rodent PVs, MnPV1 (99) and MmuPV1 (104) (Fig. 2.4, 2.5). Both of these transcript maps were generated using cutting edge RNA sequencing technologies in combination with classical techniques to determine mRNA coding regions leading to the generation of comprehensive transcription maps that will be very valuable to the field of papillomavirus biology. The MmuPV1 transcript map also made use of PacBio Iso-seq in combination with RNA seq to generate a very thorough transcript map. The salient features of the MnPV1 and MmuPV1 transcript maps are summarized in Table 5. Similar to other PVs, both MnPV1 and MmuPV1 have complex array of mono- and poly-cistronic transcripts arising from several promoters and multiple splice sites empowering these compact viral genomes to express multiple genes. In the case of MnPV1, similar to several high-risk HPVs (e.g. HPV 16, 18 and 31), the early promoter (P_{78}) is located upstream of E6 within the long control region (LCR)(213-215) leading to transcripts that can drive expression of both E6 and E7 gene products. A TATA box was identified upstream of the transcriptional start site (TSS) for this promoter. In contrast, similar to cutaneous HPVs and certain low-risk mucosotropic HPVs (216, 217), MmuPV1 makes use of two separate early promoters for expression of viral E6 (P_{7503}) and E7 (P_{360}) with P_{7503} being a stronger promoter. A third early promoter (P_{859}) was also identified for MmuPV1 and is most likely a weak promoter responsible for driving expression of E2 and/or E8^E2. High-risk HPVs usually express their late genes mainly from a differentiation-dependent TATA-less late promoter located within the E7 ORF. Similar to these HPVs, a strong late promoter was identified within the E7 ORF (P_{710}) of MnPV1 with a TATA-like sequence upstream of the TSS (99).

Interestingly, in the case of MmuPV1, two late promoters, P_{7107} (within the LCR region downstream of L1 ORF) and P_{533} (within the E7 ORF) were identified. Of these, P_{7107} has a TATA-like box upstream of its TSS, and the P_{533} bears a TATA box upstream of its TSS. Utilization of a late promoter in the LCR region for the expression of viral late genes L1 and L2 is a characteristic feature for BPV1, CRPV and some skin-tropic HPVs such as HPV1 and HPV5 (216, 218-220). By means of cutting edge technologies employed in constructing the MnPV1 and MmuPV1 transcript maps, several novel splice junctions as well as transcripts have been identified. In transcription maps of both MnPV1 and MmuPV1 the E8^E2 splice isoform was detected. The E8^E2 protein is encoded by a spliced message containing a short exon from the E8 ORF spliced to the major splice acceptor in the middle of the E2 ORF (reviewed in(77)). Transcripts encoding shorter E2 forms have been mapped in BPV1 and have been shown to repress E2-dependent transactivation of BPV1 E2-dependent enhancer (221) and to inhibit viral DNA replication (222). These E2 repressors have also been mapped in CRPV1, HPV11, HPV16 and HPV31 (223-226). Recently in monolayer keratinocytes stably harboring HPV16 it was shown that E8^E2 represses productive replication of HPV16 and knocking-out E8^E2 increased HPV16 copy numbers (227). Use of rodent models provides us the opportunity to understand the pathogenic relevance of this repressor protein in animal species. Besides E8^E2, in MnPV1 potential E2 repressors in the form of E2*I and E2*II were also identified. In the case of MmuPV1, splice isoforms E1^M1 and E1^M2 have been identified. These are predicted to be similar to E1Ma and E1M in HPV11 which encode fusion proteins that can strongly repress both E2-dependent and independent enhancer/promoter activities of HPV11, which is a low-risk genital HPV

(224). While the functional significance of these several isoforms remains to be elucidated for rodent PVs, broadly speaking we can say that, based on transcriptional analysis alone, MnPV1 appears to be more similar to high-risk mucosotropic HPVs and MmuPV1 appears to be more similar to high-risk cutaneous HPVs.

Table 2.5 : Key features of MnPV1 and MmuPV1 transcript maps

Feature	MnPV1	MmuPV1
Source	Skin papillomas from *M. Natalensis* colonized with MnPV1	Skin papillomas from immunodeficient mice infected with MmuPV1
Early Promoters	Single promoter (P_{78}) for E6 and E7	Three promoters: P_{7503} for E6, P_{360} for E7, P_{7503} for E2 and/or E8^E2
Late Promoters	Single late promoter (within E7 ORF)	Two late promoters (within LCR and E7 ORF)
Notable splice isoforms	E8^E2, E2*I, E2*II	E1^M1, E1^M2, E8^E2

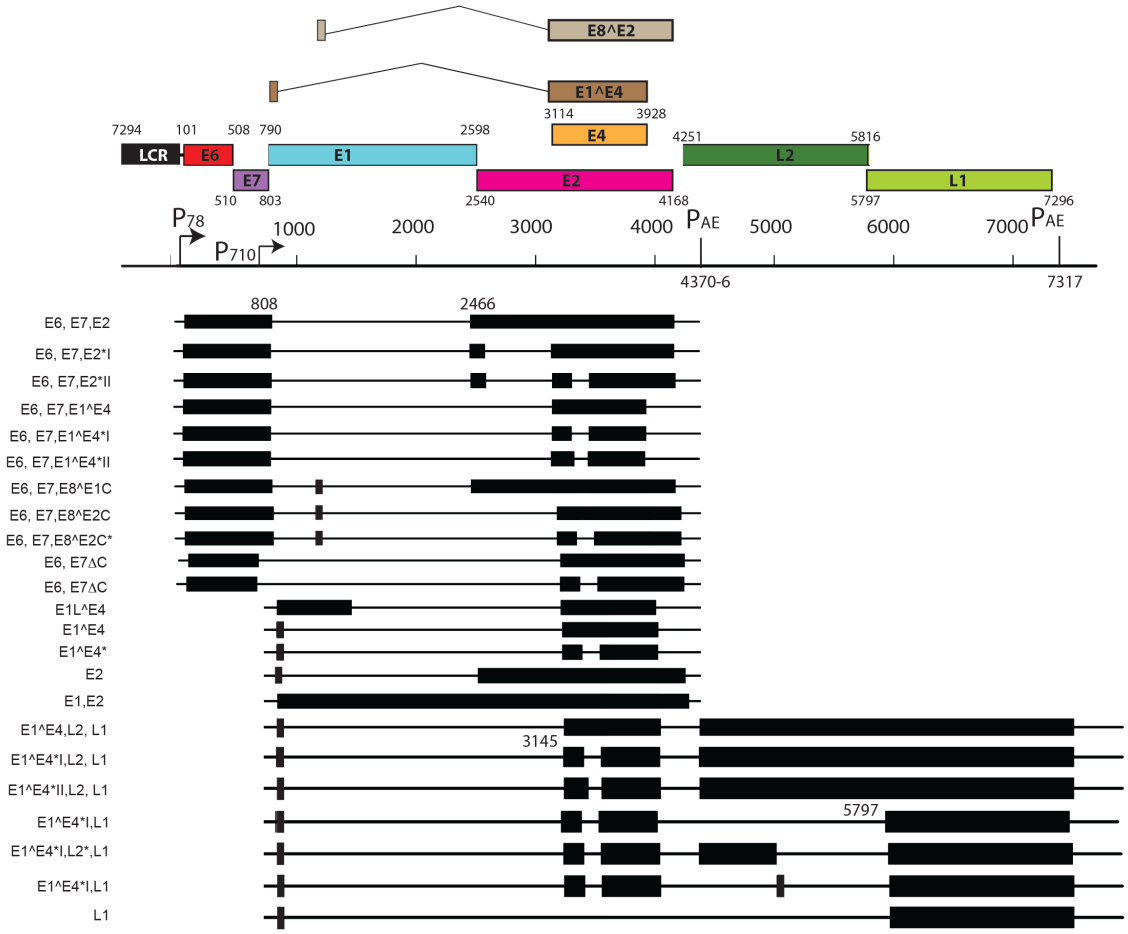

Fig. 2.4. Transcription map of MnPV1.

Fig. 2.4. Transcription map of MnPV1. This figure has been modified from (99). The full transcription map for MnPV in productive lesions was assembled from PCR, RACE and RNA-seq data. At the top, the genome organization of MnPV is presented for better understanding; numbers indicate the position of ORF starts and ends. Mapped TSSs 78 and 710 and pA cleavage sites 4370–6 and 7317 are depicted. For transcripts, exons are represented by black boxes (when coding for a particular ORF) while introns are marked as thin solid lines. Positions of the splice junctions in each transcript are given by numbers at the top.

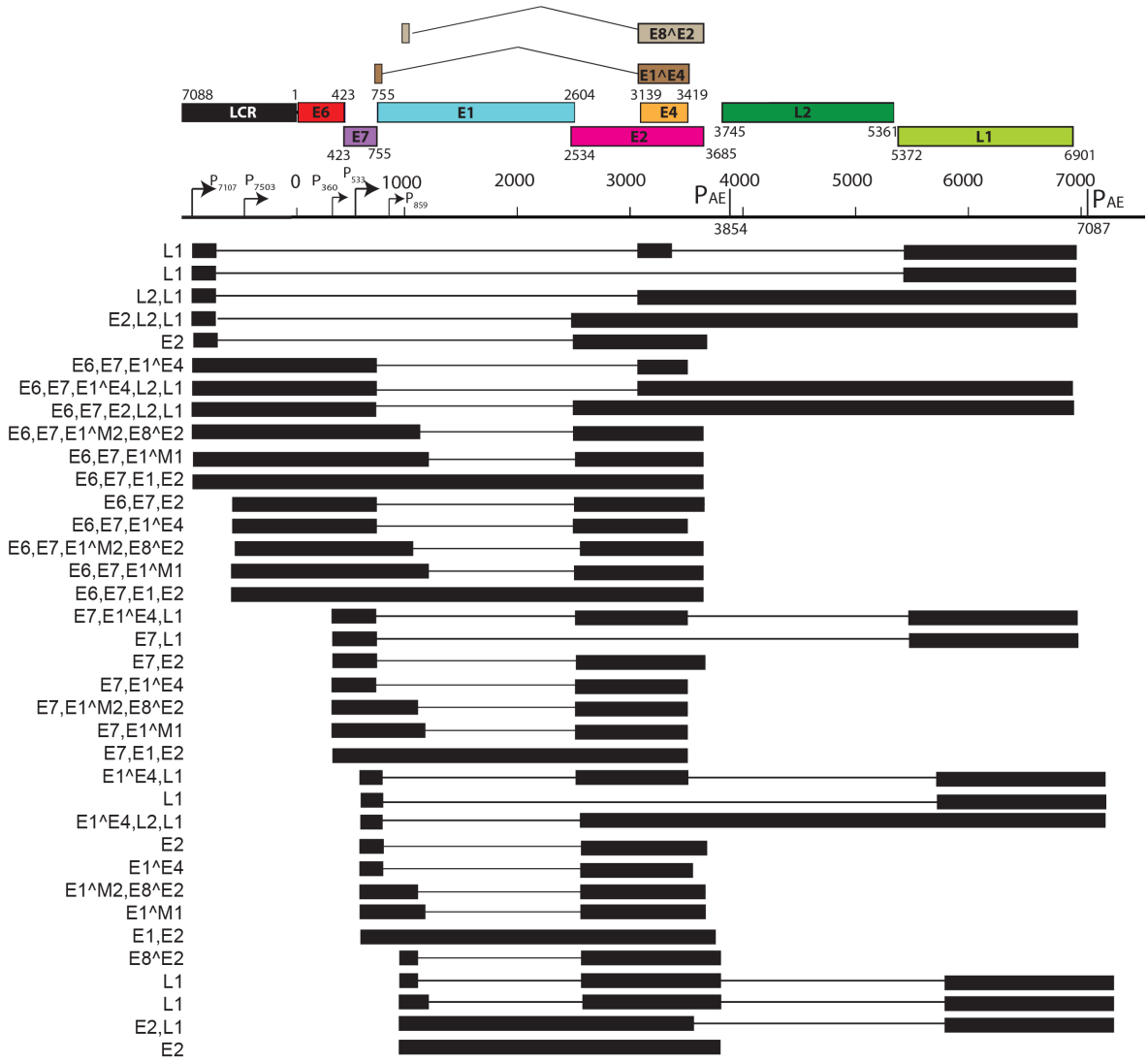

Fig. 2.5. Transcription map of MmuPV1.

Fig. 2.5. Transcription map of MmuPV1. This figure has been modified from Xue, *et al*. (2017) (Manuscript accepted (104)) The bracket line in the middle of the panel represents a linear form of the virus genome for better presentation of head-to-tail junction, promoters (arrows), and polyadenylation cleavage sites, early pA CS 3864 and late pA CS7063. The open reading frames (ORFs) are diagramed above the bracket line as colored boxes, and the numbers above each ORF are nucleotide positions of the first nucleotide of the start codon and the last nucleotide of the stop codons in the MmuPV1 genome. LCR indicates a long control region. Below the bracket line are the RNA species derived from alternative promoter usage and alternative RNA splicing. Exons (black boxes) and introns (thin lines) are illustrated for each species of the RNA, with the mapped splice site positions numbered by nucleotide position in the virus genome and coding potentials are shown on the left.

2.6. Roles of rodent PV's E6 and E7 proteins

Preliminary studies using MnPV1 E6 transgenic mice suggest an oncogenic role in MnPV1(97). In the context of MmuPV1, E6 is necessary for virus-induced papillomas in nude mice (228). This suggests that E6 is potentially critical in viral pathogenesis for rodent PVs, and its function merits further investigation. E6 proteins are approximately 150 amino acids in length containing two CX2C-X29-CX2C zinc-like fingers flanked by short amino (N) and carboxy (C) terminal domains of variable lengths [reviewed in (82)]. Like most PVs, rodent PV E6 proteins also have these zinc-like finger domains (Supplementary Fig. S1). Multiple cellular proteins have been identified to associate with E6 proteins. The primary interaction seen with mucosal and cutaneous HPV's E6 and BPV1 E6 is their binding to an alpha-helical acidic LXXLL peptide motif present in multiple cellular target proteins. This interaction has been validated by solving the crystal structures of HPV16 E6 bound to E6AP peptide and BPV1 E6 bound to paxillin peptide (229). Some well-known binding partners of papillomaviruses containing the LXXLL domain include paxillin, E6AP, MAML-1, and IRF3 (230-236). Among these, the interaction of HPV16 E6 and HPV18 E6 with E6AP is perhaps the most widely studied interaction due to the ability of these E6 proteins, together with E6AP, a ubiquitin ligase, to form a complex with the tumor suppressor p53 (231) targeting the latter for proteasome-mediated degradation (reviewed in (237)). Two groups identified Mastermind-like 1 (MAML1) of the Notch transcription complex as a cellular interacting protein of the E6 proteins encoded by BPV1 and the beta-HPVs (238, 239). MAML1 is a core component of the transcriptional activation complex that mediates the effects of the canonical Notch signaling pathway (240). More recent studies of HPV8 E6 (a β-HPV)

demonstrated that Notch activation was subverted by suppressing the function of MAML1 during keratinocyte differentiation (241). MmuPV1 E6 shares with the skin cancer-associated HPV8 E6 protein the capacity to inhibit Notch signaling by binding to MAML1, and MmuPV1-E6 mutants defective in MAML1 binding are defective in causing MmuPV1-induced papillomas (228). Interestingly, most high-risk mucosotropic HPV E6s bind to E6AP whereas most high-risk cutaneous HPV E6s bind to MAML1 (232). The significance of this difference in preference of different E6 proteins to bind different LXXLL motif-containing cellular proteins is yet to be determined, however, rodent PV models, specifically MmuPV1, can now be used to understand the significance of this association in pathogenesis.

Amino acid sequence comparisons of rodent PV E6s suggest other potentially interesting putative roles as well. For example, MmuPV1 E6 contains an LXCXE motif implicated in RB binding. This motif is more commonly found in the E7 proteins in other papillomaviruses (60). In the case of MnPV1, the LXCXE domain is present in both E6 as well as E7 (Supplemental Fig. S1, S2). LXCXE motifs in E6 proteins were also observed in *Phocoena spinipinnis* papillomavirus type 1 (PsPV1) and bottlenose dolphin PV types 1, 2 and 3 (TtPV1–3), which do not have identifiable E7 ORFs. While LXCXE-independent interactions of E7 with RB have been reported for canine papillomaviruses (242), deeper analysis of such interactions, if any, is required in the context of rodent PVs. A unique characteristic of the high-risk HPV E6 oncoproteins is the presence of a PDZ (PSD-95 / DLG /ZO-1) binding site motif designated by the amino-acid sequence XS/TXV on the extreme C-terminus. This motif is absent from all the so-called low-risk HPV E6 oncoproteins [reviewed in (243)]. None of the rodent papillomaviruses possess

PDZ binding motifs on the extreme C-terminus of either E6 or E7 genes; however, putative PDZ binding site motifs can be found elsewhere in both E6 and E7s of several rodent PVs (Supplemental Fig. 2.6, 2.7).

The other well-studied HPV oncogene is E7. The ability of E7 in high-risk mucosal papillomaviruses to cause cancer is often attributed to the ability of E7 to interact with UBR4 and cullin family ubiquitin ligases and to bind to the RB family of proteins (p105, p107, and p130) that regulate E2F family transcription factors (reviewed in (244). While high-risk E7s are oncogenic, E7 from low-risk viruses (HPV 6, 11) are weakly oncogenic and have cooperative activity when co-expressed with additional oncogenes from the high-risk viruses (245). A hallmark feature of high risk HPV E7 proteins is their ability to bind the tumor suppressor RB through their LXCXE motif, (246); however, this is not the case for E7 proteins encoded by other papillomaviruses.. For example, BPV1 E7 does not contain a LXCXE motif. In fact, the E7 proteins encoded by all animal papillomaviruses that cause fibropapillomas lack this motif. This is also true for avian papillomaviruses (247). Interestingly, some papillomaviruses have no E7 gene at all (isolates from domestic pigs, SsPV, polar bear UmPV, and porpoises) (248-250). Furthermore, many RB-independent biological activities of E7 have also been reported (reviewed in (251)). One such activity is the ability of high-risk E7s to bind and degrade the cellular non-receptor protein tyrosine phosphatase PTPN14. Recently, it has been demonstrated that PTPN14 degradation correlates with the retinoblastoma-independent transforming activity of high-risk HPV E7. Interestingly, immunoprecipitation-tandem mass spectrometry (IP-MS/MS) experiments have determined that the MmuPV1 E7 does bind to PTPN14 suggesting that this rodent model

is a valuable model for PV carcinogenesis (252). Interaction partners of E6 and E7 of other rodent PVs are yet to be determined and provide a plethora of opportunities.

2.7. Conclusion

In conclusion, rodent models of papillomavirus infection are a fledgling area of research that merit further investigation. The progress made in rodent PV research, particularly the MmuPV1 infection model, provides us with great opportunities to understand the biology of papillomavirus. These models can help us understand multiple unanswered questions about papillomaviruses particularly in the context of virus tropism and host immunity, as these are easily tractable infection models. For MmuPV1, we have a wide array of genetic tools available to answer several of these questions.

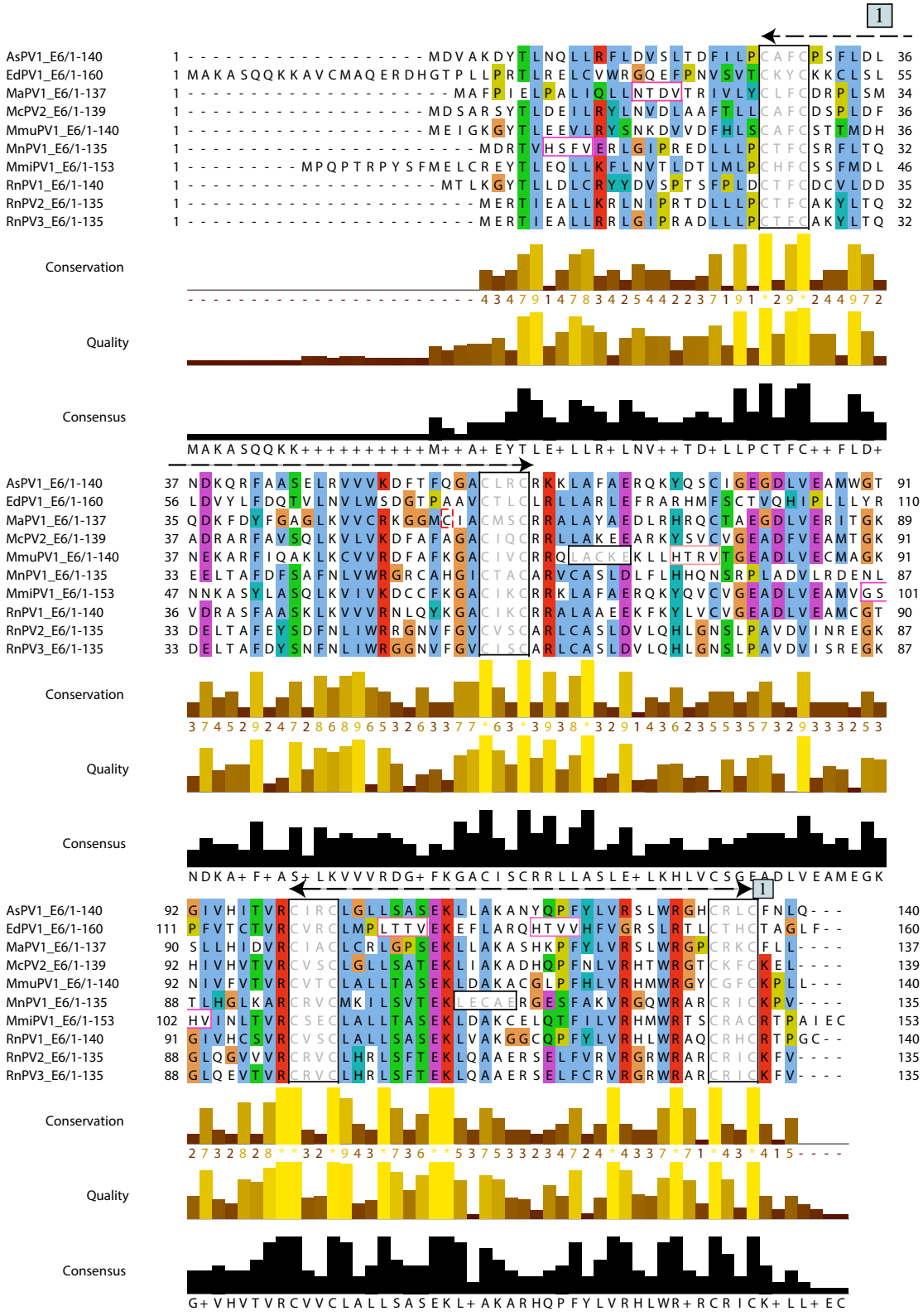

Fig. 2-6. Amino acid analysis of E6

Fig. 2-6. Amino acid analysis of E6

E6 amino acids of Rodent Papillomaviruses from Table 2-1 were aligned in JalView using ClustalX algorithm. Two zinc-like finger domains with consensus sequence CX2C-X29-CX2C are highlighted in 1. Numerous PDZ domains (XS/TXV, magenta box) were seen throughout the E6 sequence. Rb binding motif (LXCXE, white box) was seen in MmuPV1 and MnPV1.

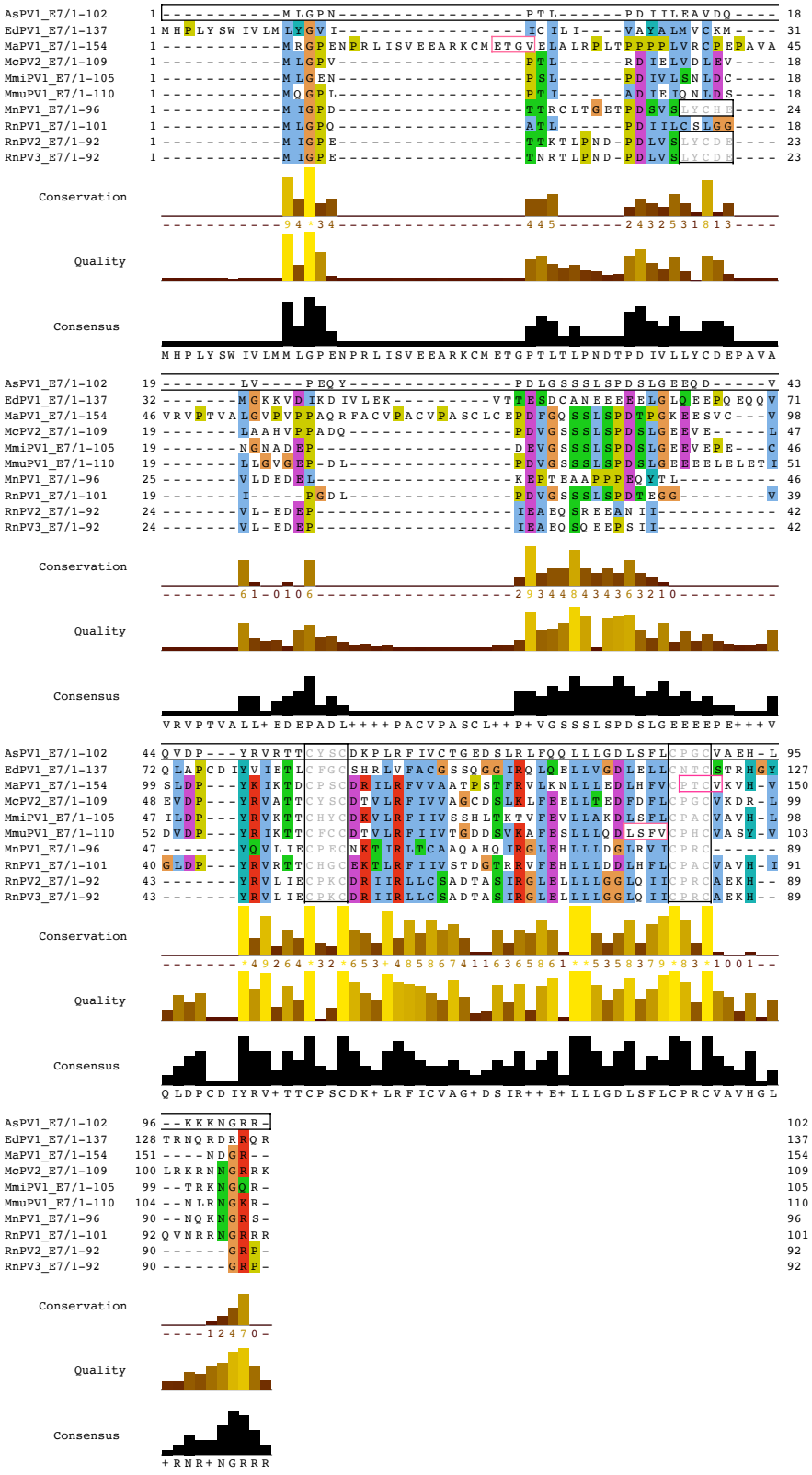

Fig. 2-7. Amino acid analysis of E7

Fig. 2-7. Amino acid analysis of E7

E7 amino acids of Rodent Papillomaviruses from Table 2-1 were aligned in JalView using ClustalX algorithm. One zinc-like finger domains with consensus sequence CX2C-X29-CX2C was seen near the C-terminus. Numerous PDZ domains (XS/TXV, magenta box) were seen throughout the E7 amino acid sequence of rodent PVs. Rb binding motif (LXCXE, white box) was seen in MnPV1, RnPV2 and RnPV3.

Chapter 3: Materials and Methods

Parts of this chapter have been submitted to ***Journal of Virological methods*** (253).

1. Uberoi A, Yoshida S, Lambert PF. Development of an in vivo infection model to study Mouse papillomavirus-1 (MmuPV1) skin infection. *J Virolo Meth. Accepted*. 2017.

3.1. Materials

3.1.1. Mouse strains

Table 3-1. Mouse strains used in this thesis work

S.No.	Strain Name	Source	Reference
1.	BALB/cOlaHsd-*Foxn1^{nu}*	Envigo	(115)
2.	B6.Cg-*Foxn1^{nu}*/J	Jax Lab	(254)
3.	*NOD.Cg-Prkdc^{scid} Il2rg^{tm1Wjl}/SzJ*	Jax Lab	Reviewed in (255)
4.	*NOD.Cg-Prkdc^{scid}/SzJ*	Jax Lab	(125)
5.	B6.129S4-*Il2rg^{tm1Wjl}*/J	Jax Lab	(256)
6.	B10.129S2(B6)-*Ighm^{tm1Cgn}/J*	Jax Lab	(257)
7.	B6.129S2-*Cd4^{tm1Mak}/J*	Jax Lab	(258)
8.	B6.129S2-*Cd8^{tm1Mak}/J*	Jax Lab	(259)
9.	C57Bl/6J*	Jax Lab	(260)
10.	BALB/c	Charles River	(261)
11.	FVB/N	Taconic	(262)
12.	Ahr null	Dr. Christopher Bradfield (McArdle Lab)	(263)
13.	IL10 null	Jax Lab	(264)
14.	K17 null	Dr. Pierre Coulombe (Johns Hopkins)	(265)
15.	K14vIL10 (also known as vIL-10Tg)	Dr. Richard Granstein (Cornell)	(266)

*Please use C57BL/6J mice from Jax lab as they do not have DOCK2 mutations(267)

3.1.2. Antibodies used

Table 3-2. List of antibodies used

S.No.	Antibody	Purpose	Source/Catalog#
1.	K14	IF/IHC	Covance #PRB-159P
2.	K10	IF/IHC	Covance #PRB-155P
3.	Involucrin	IF	Covance #PRB-140C
4.	MCM7	IHC	NeoMarkers #MS862
5.	L1	IHC	Dr. Chris Buck
6.	CD4 (clone GK1.5)	T-cell depletion	BioXCell #BE0003-1
7.	CD8 (clone 2.43)	T-cell depletion	BioXCell #BE0061
8.	K17	IF	Dr. Pierre Coulombe
9.	K15	IF	Santa Cruz #SC47697
10.	BrdU	IHC	Oncogene #NA20

3.1.3. Other reagents used

Table 3-3. List of miscelleneous reagents used

S.No.	Reagent/Equipment	Purpose	Source/Catalog#
1.	Illustra-TempliPhi 100 Amplification Kit	Rolling Circle Amplification	GE Healthcare #25640010
2.	Micrometer screw gauge	Sizing of warts	iGaging, #205630
15.	Siliconized eppendorf tubes	Virus collection	Fisher Scientific, #02-681-320
16.	Siliconized pipette tips	Virus Collection	VWR, #83007-380
17.	Slide staining system	TSA staining	IHC world #M905-12DGY
18.	TSA Blocking buffer		Perkin Elmer #FP1012
19.	Antigen Retrieval Buffer		Abcam #ab93684
20.	Biotin-NHS		Sigma #H1759
21.	N,N-Dimethylformamide (DMF)		Acros Organics,#327171000
22.	Tyramine hydrochloride		Thermo Fisher Scientific #25108
23.	Imidazole		Sigma, #I5513
24.	IL-10 ELISA kit	ELISA	R&D Systems #M1000B,
25.	Conceptrol (4% Nonoxynol-9)	Vaginal tract infections	Options, #247149

3.1.4. UVB-irradiator

A custom-designed "Spectra" research irradiation unit (48'' unit, S. No. R2017-AXBX-0606, 110-120V, 60 Hz) manufactured by Daavlin (Bryan, Ohio) was used for these studies [also described in (268, 269)]. The irradiator consists of an exposure unit (52'' X 27 ¼'' X 25'') mounted on fixed legs (Fig. 3-1A). The height of the irradiating surface to the lamps can be adjusted. Within the exposure unit there are six UVA lamps (F40T12BL/HO) and six UVB lamps (FS40T12HO-BB) lamps (Fig. 3-1B). These lamps are controlled using a Flex Control Integrating Dosimeters that automatically compensates for variations in energy output in order to deliver the desired UV dose with consistency and accuracy. Desired dosage is entered in milli-Joules per Centimeter Square for UVB (mJ/cm^2) and Joules per Centimeter Square for UVA (J/cm^2). The

experiments performed in the thesis were performed with the instrument being calibrated to deliver UVB output at 2-4-2.9 mW/cm^2. This output was measured using a UV meter provided by the manufacturer. To prevent exposure of user to UV, a UV blocking curtain is attached to the irradiator. The usable radiation area is approximately 40'' X 26'', allowing one to irradiate up to 3 mouse cages at a time.

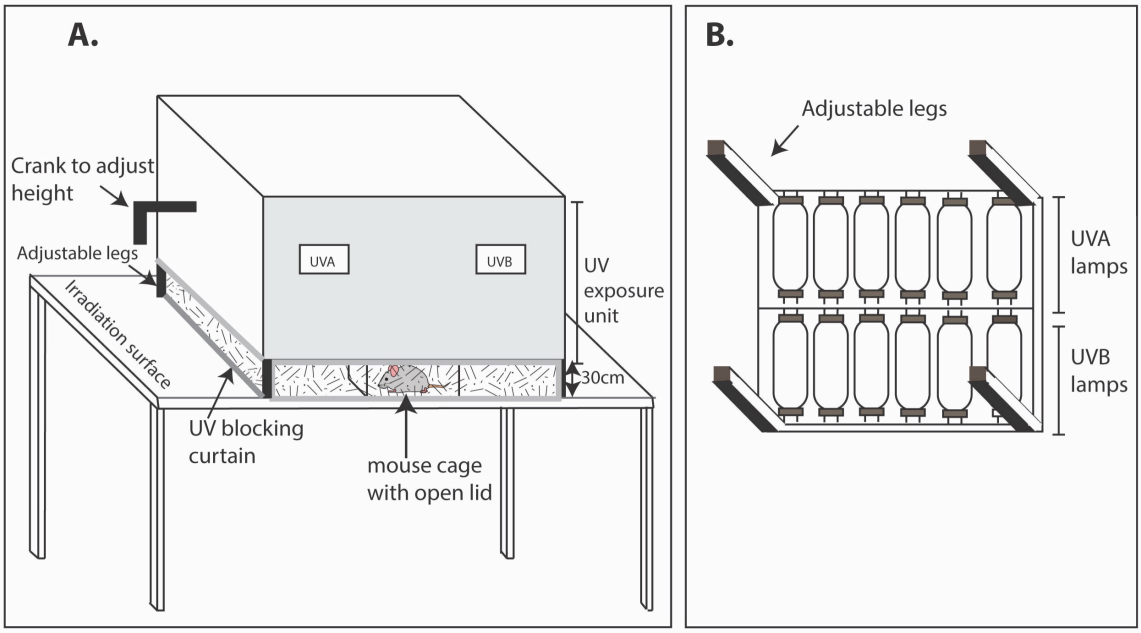

Fig. 3-1: UVB-irradiator

3.1.5. Virus socks

Several kinds of MmuPV1 stocks have been used in this thesis. The original colony of nude mice in the lab was infected with MmuPV1 quasivirions generated (as described in Section 3.2.2.) using the MmuPV1 genome present in the plasmid pSynMusPV. This plasmid contains a synthesized viral genome based on the original published sequence of MmuPV1. It was encapsidated using pMusSHELL, a mammalian expression plasmid carrying codon-optimized copies of the MmuPV1 major (L1) and minor (L2) capsid genes (110). These plasmids were generously provided by Dr. Chris Buck (NIH, Bethesda, MD). We also generated our own clone of MmuPV1 (pAU505.4) by performing rolling circle amplification on DNA isolated from warts arising on nude mice in the original colony of nude mice infected with MmuPV1 (generously provided by Dr. Aravind Ingle, ACTREC, India) followed by cloning into the pUC19 vector. Unless otherwise indicated, studies were performed using virus containing this genome generated from MmuPV1-induced papillomas that arose in nude mice as described in section 3.2.4. Virus extracts were either as “crude extract" or purified over an optiprep gradient, referred to as “purified virus”.

3.2. Methods

3.2.1. Rolling circle amplification to generate MmuPV1 clones

Dr. Aravind Ingle (ACTREC, India) sent us total genomic DNA isolates prepared from MmuPV1 warts that arose in a colony of nude mice in India from which MmuPV1 was originally isolated (55). These samples were thawed on ice and 5μl of DNA solution was predigested in a total volume of 50μl containing PSafe enzyme (10U/μl), high-fidelity *Not1* (20U/μl), PSafe buffer (1.5X) and rATP (1.5mM) at 37ºC for 30 min. DNA was precipitated using Ammonium Acetate (4.5mM) in 95% Ethanol following overnight incubation at -20ºC. Rolling Circle Amplification (RCA) was performed using IllustracTempliPhi 100 Amplification Kit (GE healthcare) as per the manufacturer's instructions. Briefly, the DNA pellet was resuspended in 5μl sample buffer and incubated at 95ºC. RCA enzyme mix was added to the samples and incubated overnight at 30ºC. After inactivating the RCA reaction by incubating samples at 65ºC for 15 minutes, samples were digested with Xba1 to linearize amplified MmuPV1 genomes, the viral genome gel purified and ligated to Xba1-digested pUC19 that had been treated with alkaline phosphatase to reduce monomeric vector ligation.

3.2.2. *In vitro* synthesis of MmuPV1 quasivirions for *in vivo* infection

MmuPV1 quasivirions were generated following the method of papillomavirus particle generation described by Dr. Chris Buck (100, 110). This protocol is described in great depth on the following website: https://home.ccr.cancer.gov/lco/pseudovirusproduction.htm. 293FT cells (5.6 x10^6 cells per 85mm-plate/ 36 plates) were transfected with 15 μg each of pMusPVSheLL and recircularized MmuPV1 genome using lipefectamine. 48 hours after transfection, cells were collected in a 1.5ml siliconized eppendorf tube and 600μl DPBS supplemented with 9.5mM $MgCl_2$ was added to 5.6 x10^6 and transferred to a siliconized eppendorf tube and Triton-X-100 (0.4%), Ammonium Sulfate (pH=9, 25mM), Benzonase (10U) were added to lyse the cells and allow the virus particles to 'mature' (i.e. allow disulfide bonds to form between capsomeres) at 37ºC overnight. The lysate was chilled at 4ºC for 10 minutes, and centrifuged at 7800 RPM for 10 minutes. The supernatant was collected and represents the "crude extract" sometimes used in subsequent infections. To generate "purified virus", the crude extract was further enriched for virus over a 27%-33%-39% (1.5ml each step) Optiprep gradient by spinning at 16ºC, 50,000 RPM for 3.5 hours using an SW55 rotor. Fractions were collected drop-wise by piercing the bottom of centrifuge tube as follows: 750 μl as one fraction, then 250 μl fractions up to fraction 10 and discarding top 2ml of the gradient. Fractions were screened for the presence of virus particles by extracting DNA and electrophoresing the DNA in a 0.6% agarose gel that was then stained with SYBR Green to visualize the viral DNA.

3.2.3. Quantification of MmuPV1 virions

MmuPV1 virions were treated with 1% SDS, Proteinase K and 0.5mM EDTA and denatured by heating at 55ºC to release virus DNA that was electrophoresed on an agarose gel. Viral genome equivalents (VGE) were determined by comparing the amount of encapsidated viral DNA in the viral stock to known amounts of cloned MmuPV-1 genome by Southern analysis using MmuPV1-specific probes followed by quantification using ImageJ software.

3.2.4. Protocol for Southern analysis of MmuPV1.

MmuPV1 plasmid DNA and viral DNA (extracted by denaturation of virions clarified over an optiprep gradient) was separated on a 1X TBE (90 mM Tris, 90 mM boric acid, 2.5 mM EDTA) 0.6% agarose gel (Seakem LE Agarose Lonza Allendale, NJ) at 1 volt/cm for 18-24 hours. The gel was depurinated in 0.25 M HCl for 10 minutes, denatured in two changes of denaturing solution (1.5 M NaCl, 0.5 M NaOH) for 15 minutes each and neutralized in two changes of neutralizing solution (1.5 M NaCl, 1M Tris pH 7.4) for 15 minutes each. DNA was transferred to a positively charged nylon membrane (Hybond N+ Amersham Pittsburgh, PA) using the upward capillary transfer method with 10x SSC (1.5 M NaCl, 150 mM sodium citrate) for 24 hours. The nylon membrane was briefly rinsed in ddH_20 and dried on 3 MM blotting paper (MidSci St. Louis, Mo) for ten minutes before cross-linking using a UV Stratalinker 2400 (Stratagene). After pre-hybridization of the membrane for 15 minutes at 55°C in Church hybridization buffer (250 mM Na_2HPO_4, 1% BSA, 245 mM SDS and 5 mM EDTA pH 8.0), radiolabeled MmuPV1 probe was added and hybridization carried out overnight at 55°C. The membrane was washed five times, five minutes each, in Church wash buffer (140 mM SDS, 80 mM Na_2HPO_4) at 37°C. The hybridized membrane was exposed to

phosphor screen (Amersham Pittsburgh, PA) overnight and scanned in a Typhoon 8610 (Amersham). Brightness and contrast were adjusted using ImageJ version 1.46r to visualize radiolabeled probe. Radiolabeled probes were generated by labeling 10 pmoles of oligonucleotides specific for MmuPV1 (synthesized by Integrated DNA Technologies, see sequences below) in the presence of T4 polynucleotide kinase (PNK (New England Biolabs)), 1X T4 PNK buffer (New England Biolabs), 5 mM DTT and 75 μCi of ATP (γ-^{32}P) 6000 Ci/mmol EasyTide (PerkinElmer) at 37°C for 1-2 hours. Unincorporated nucleotides were removed using a micro bio-spin P-30 chromatography column (Bio-Rad Hercules, CA) per the manufacturer's instructions.

Sequences of MmuPV1 oligonucleotides (5'-3'):

1. AACATCGGGTAGGTCAGGCTCAC
2. AGCCCCAAACACAGCTACGACCC
3. AGGCTGCAGCCAGAACTGACTCC
4. ACTTATGCCAGTTGCCGTTCTCA
5. TTGACGCGCCTGCTTCTGTC
6. TCTGTGTTGGAGATTGTGGTGCC
7. TTGCCCCAACCTGCTCACTC
8. ACCCCTTAACCTCCACACTAACCG
9. TGGTGTGTTGGTTTGCTGGGAGATAG
10. ACGAATACGGTTATGGGGGCAC
11. TGGAAATCGGCAAAGGCTACACTC
12. TGAGGCTGAATGTGTGGATGATG
13. AGCACGCTCGCCGCACTTTATT
14. TGCAGGCCTTTGAGTTTCATAAGC
15. TCCCACCGACACCACTGACACA
16. TAAACTCTGCTGGTGGAAGGGTAAC
17. ACACCTGAAGGCCCGTTGC
18. TGCCAGCTGCGGATCTATTCC
19. TGGAGCTCTGGAGAAGGGTGAC
20. TCCCCCACAGCAGTCCATCTC

3.2.5. MmuPV1 UV skin-infection model

A. Infection of mice with MmuPV1 virus

This procedure can be used to infect any cutaneous site. Animals were anesthetized using 5% isoflurane in 100% oxygen (flow rate 2 L/min). All cutaneous sites (tail, ear, torso skin) were scarified by gently scraping the epithelia using a sterile razor blade lightly 4-5 times over an area approximately 2 X 2 mm^2. Using a sterile 27-gauge syringe needle a "brush-burn" was created by scraping the scarified surface at least 10-15 times with the needle. This resulted in a superficial wound that allows enough wounding for the virus to reach the basal layer (pink-red in color). Care was taken to not cause profuse bleeding. Virus solution (less than 3μl) was administered to the sites of scarification using a siliconized pipette tip. The animal was kept under anesthesia for at least 5 additional minutes to allow the virus solution to dry, at which point the animal was returned to the cage.

B. UVB irradiation of infected animals

UVB irradiation of animals was most commonly performed 24 hours post infection, but other timings of UVB irradiation were also tested as described in subsequent chapters. UVB dose was set to desired dosage in mJ/cm^2 according to machine operating instructions. The plastic lid of the microisolator cage was removed but the cage wire was left on to contain the mice, and the cage placed under the UVB lamps in the UV irradiation unit to expose the mice to UVB for the indicated dosage (usually taking 5-6 minutes). For ear shielding experiments, ear sites were shielded from UV exposure by covering the head of anesthetized mice with tin foil during UV exposure.

C. Scoring of papillomas

Animals were monitored for PV-associated disease at least once a week until reaching the end-point of the study. To aid the scoring process, animals were anesthetized using isoflurane and hand-held magnifying glass and forceps were used to expose the infected sites. Papilloma size was measured 1-2 weeks after onset of papillomas by measuring the length, width and thickness of the papilloma using a micrometer screw gauge. To measure the length and width of the papilloma micrometer was placed along Y-axis and X-axis as indicated in Fig. 3-2. The thickness of the papilloma was obtained by subtracting the measurement of the papilloma-free edge of the pinna from the measurement of the thickest part of the papilloma. The size of the papilloma was determined by calculating the geometric mean diameter (GMD; cubic root of the product of length X width X thickness. We found that papilloma incidence can be determined with accuracy once papilloma GMD is at least 2 mm. Papilloma incidence (expressed as a percentage) is the (# sites with overt papillomas/ # of sites infected) X 100. Morphological features of ears observed in mice post-infection and UVB irradiation are described in Table 3-2 and illustrated in Fig. 3-3. Under standard conditions in which we infect scarified pinna of FVB/NTac mice with 10^8 VGEs of MmuPV1 and irradiate with 300 mJ/cm^2 UVB, papillomas arise at approximately 50% of infected sites 6-8 weeks post-infection and continue to arise up to 3-4 months post-infection. The 3-4 month time-frame is the peak incidence of papillomatosis. These data are described in detail in Chapter 5. In animals where papillomas do not arise, skin returns to its normal appearance within 2-3 weeks post-infection.

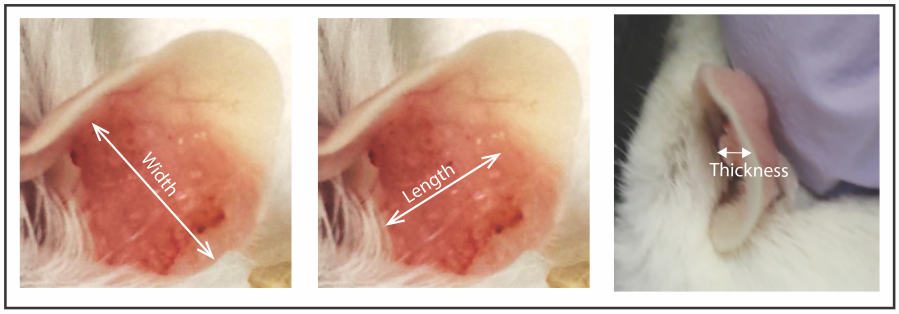

Fig. 3-2. Measuring papilloma size

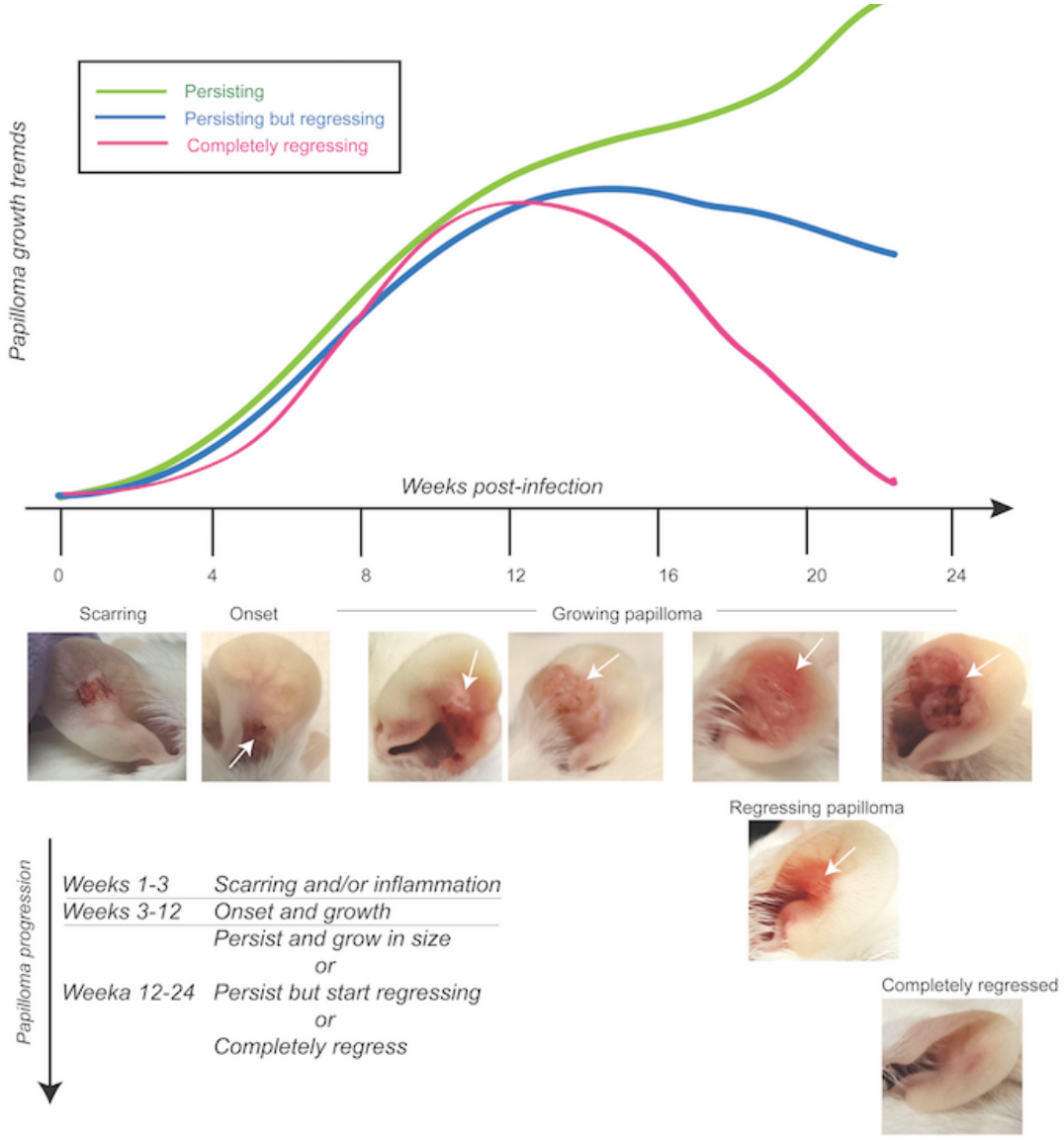

Fig. 3-3. General growth trends seen in MmuPV1-UV infection model

Table 3-4: Description of morphological features post infection (PI) with MmuPV1

Time	Morphology	Description
Week 1	Wounding	• Partial thickness wound (4mm^2) • Some wounds may have accompanying swelling • Some reddening of ears can be seen post UVB irradiation up to 48 hours post treatment. • Several wounds show signs of healing 3-4 days PI
Weeks 1-3	Scarring and/or edema	• Scabs are apparent 4-7 days PI • Some scars may be hypertrophic or give appearance of raised scars • In some cases swelling may be seen up to 2 weeks PI
Weeks 3-5	Skin healing without papilloma development (In a subset of mice)	• Scars flatten • Normal looking skin is restored
Weeks 3-12	Papilloma onset and growth (In another subset of mice)	• Clusters of white-brown bumpy papillary projections start appearing that are crusty to touch • Papillomas usually continue to grow at least 2-3 weeks post onset
Weeks 12-24	Papilloma growth/regression	• Subset of papillomas continue to persist and grow in size • Subset of papillomas continue to persist but start regressing • Subset of papillomas completely regress between 18-24 weeks PI

3.2.6. Harvesting of virus particles from papillomas

In our studies we have used both crude virus extracts or purified virus. Crude virus extract refers to virus present in supernatants obtained by clarifying papillomatous tissue extracts from nude mice. Our method for generating crude virus extract is a modified version of a protocol used to isolate merkel cell polyomavirus from human skin swabs (270). Purified virus refers to crude extract that has been enriched for virus using an Optiprep gradient. Animals were euthanized and a scalpel used to excise the papilloma taking care not to collect the surrounding, non-papilloma epithelia. The papilloma was weighed and, for every 10mg of wart tissue, 700μl DPBS was added to the tube and the papilloma homogenized for less than one minute using a homogenizer. The suspension was immediately transferred to a siliconized 1.5 ml sterile eppendorf tube. Triton-X-100 solution was added (1% Triton-X-100), followed by addition of 2μl Benzonase endonuclease and the tube was incubated at 37ºC for 20 minutes. Subsequently, 2-3 mgs of Collagenase H was added, the sample vortexed, and incubated at 4ºC overnight. NaCl concentration of suspension was adjusted to 0.8M, the suspension centrifuged for 5 mins at 5000 x g and the supernatant was transferred to fresh siliconized tube. At this point virus extract was either aliquoted and stored at -80ºC or purified over an optiprep gradient.

3.2.7. Harvesting papilloma tissue for histopathological analysis

Papillomas were harvested from euthanized animal by cutting pinna off at base using surgical scissors and excess non-papillomatosis tissue trimmed off. Tissue was flattened on a piece of Whattmann paper and placed in the tissue cassette in a Whattman paper-tissue-sponge sandwich. Tissue was fixed in 4% paraformaldehyde (PFA) for 10-12 hours at 4ºC and embedded on edge in a paraffin block following dehydration. Five micron sections were cut and H&E staining was performed on every 10th section for histopathological analysis.

3.2.8. MmuPV1 L1- cytokeratin dual immunofluorescence using Tyramide signal amplification

To accomplish MmuPV L1-K14 double fluorescent staining, we made use of tyramide-based signal amplification (TSA) technique. This technique allowed for easy multiplexing of immunofluorescent staining, but perhaps its biggest advantage is that it permits double immunofluorescent staining using two unconjugated primary antisera raised in the same species (271-274). We adopted a home-based method of TSA staining using reagents as described previously (275) for performing L1-K14 dual fluorescent staining. The general principle of TSA staining is described in Fig. 3-4. Tissue was deparaffinized and then rehydrated in an ethanol gradient series as follows: Twice in 100% ethanol, then once in 95%, 70%, 50%, 25%, 12.5% and final rehydration in double distilled water. Sections were washed twice in 1X PBS and endogenous biotin was blocked by incubating sections in 0.3% Hydrogen peroxide in Methanol for 10 mins. After washing slides twice in 1X PBS, antigen retrieval was performed using citrate

buffer at pH=6 by boiling in a microwave. Slides were cooled to room temperature by placing the entire slide chamber on the lab bench for at least 1.5 hours, washed twice in 1X PBS and then tissue was circled with hydrophobic pen. Tissue was then washed in 1X PBST (2liter PBS+1gm Tween-20) 3 times for 3 minutes each. TSA blocking buffer was applied to tissue and incubated at room temperature for 1 hour in a humidifier chamber. Tissue was rinsed in 1X PBST, primary antibody (rabbit-anti-L1) was applied at 1:5000 dilution and incubated overnight in a humidified chamber at 4°C. Slides were washed with 1X PBST 3 times for 3 minutes and Goat-anti-rabbit- HRP secondary antibody (1:500 dilution) applied in blocking buffer for 1 hour at room temperature in a humidified chamber. While washing tissue in 1X PBST 3 times for 3 minutes each, TSA reaction buffer was prepared (1μl 30% Hydrogen peroxide solution in 30ml 0.1M Imidazole). Biotin-tyramide stock solution (1mg/ml) prepared as described previously (275), was brought to room temperature, diluted 1:100 in reaction buffer, added to the slide and incubated for 10 minutes at room temperature. Tissue was washed with 1X PBST and rabbit anti-K14 (1:1000) applied at room temperature for 1 hour. Detection was performed using anti-rabbit conjugated to Alexafluor-488 (for K14) and anti-streptavidin conjugated to Alexafluor594 (for biotinylated L1) for 1 hour at room temperature. Tissue was counterstained with Hoechst stain.

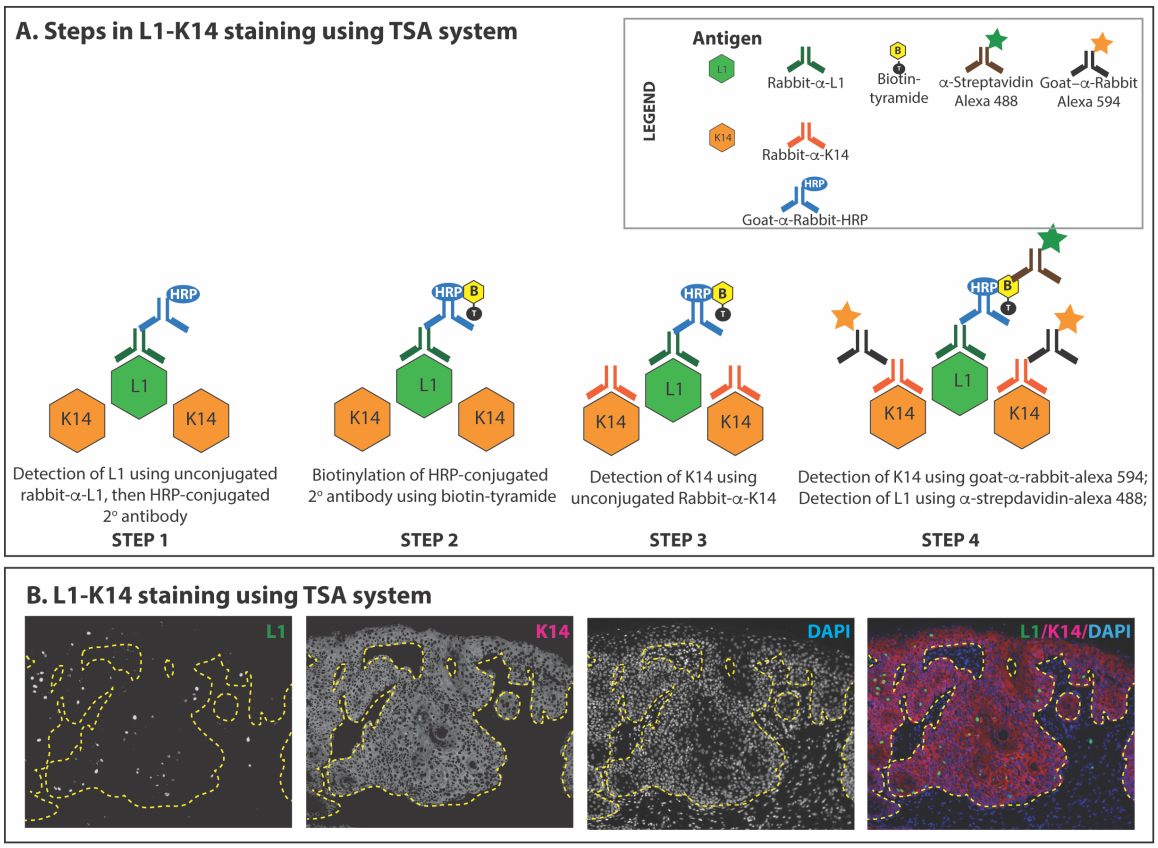

Fig. 3-4. Principle of TSA staining

The general principle of TSA staining is described above. The first step involves staining of viral capsid using rabbit sera raised against L1 (100, 128) followed by HRP conjugated secondary antibody. The HRP-conjugated 2° antibody is then biotinylated using biotin conjugated with tyramide. We can then proceed to stain with antibody against cytokeratin-14 (raised in same species as L1 antibody, i.e. rabbit). Both antibodies can now be detected easily – i.e. L1 can be detected with anti-Streptavidin and K14 can be detected with an anti-rabbit 2° antibody.

3.2.9. MmuPV DNA FISH

MmuPV1 DNA FISH was performed as described previously [56,69]. This protocol has been adapted from a DNA FISH protocol used to detect Epstein Barr Virus (EBV) DNA in monolayer cells and is described in detail at: https://mcardle.oncology.wisc.edu/sugden/protocols.html. Briefly, formalin-fixed paraffin-embedded slides were baked at 65°C overnight and deparaffinized using xylene followed by treatment with 100% ethanol. Slides were then boiled in 10 mM sodium citrate buffer (pH=6.0) for 30 minutes in a microwave. Slides were rinsed with PBS and completely dried before pre-hybridizing with 2 x SCC containing 0.5% IPECAL (pH=7.0) for 30 min at 37°C containing RNase A (1μg/ml). Slides were dehydrated using a series of ice cold ethanol (70%, 80%, 95%) for 2 min each. Slides were dried by placing them in an empty container at 50°C for 5 minutes and then placed in denaturation solution (28 ml formamide, 4 ml 20 x SSC (pH=5.3) and 8 ml water) at 72 °C for 2 minutes. The ethanol series was repeated again, and after drying the sections, denatured, biotin-16-dUTP (Sigma-Aldrich, #11093070910) labeled probe was hybridized to the tissue overnight at 37°C in a humidified chamber. To make the probe, nick translation was used to label the entire MmuPV1 plasmid DNA (pMusPV [6]) with biotin-16-dUTP. Slides were then washed twice for 30 min with 2 x SSC in 50% formamide at 50°C followed by two washes for 30 min with 2 x SSC at 50°C. Signals were detected with streptavidin conjugated to Cyanine-3 (Sigma, #S6402) at 1% by volume in STM solution (4 x SSC, 5% non-fat dried milk, 0.05% Tween-20, 0.002% sodium azide) for 30 min at 37°C. Nuclei were counterstained with Hoechst coverslips

and the tissue section mounted using ProLong gold antifade (Thermo Fisher Scientific, #P36930).

3.2.10. Use of Contact Hypersensitvity (CHS) assay to assess immunosuppression

CHS assays were performed by topically applying 1-Chloro-2,4-Di-Nitrobenzene (DNCB) (Sigma) using a modification of a method described previously (276). For short-term immunosuppression studies, mice irradiated with 300mJ/cm^2 UVB. Ten days post UVB-irradiation mice were shaved on their backs and sensitized by topically applying 0.5 mg DNCB in 50μl vehicle (4:1 acetone:olive oil). Five days post-sensitization mice were challenged with DNCB in the left ear and ear thickness was measured. To assess correlation between wart incidence and long-term immunosuppression mice were either infected with MmuPV1 or mock infected in the right ear followed by treatment with 300mJ/cm^2 UVB. Mice were sensitized with DNCB (0.5mg in 50μl vehicle) 10 days post UVB exposure on their backs. Three months post-sensitization, mice were challenged with DNCB in the left ear and ear thickness was measured. Ear thickness was measured by means of micrometer screw gauge up to 96 hrs. The average of three readings taken at different points across the ear swelling was considered as a single measurement. Ear thickness was reported as the average of the difference between challenged and control ears 24-96 hours post challenge. The readings reported are those taken at 48 hrs post-challenge. The control (right) ear was the ear that was challenged with the vehicle only. The standard error was computed by determining the standard deviation.

3.2.11. Explant cultures and IL10 ELISA

Skin explant cultures were performed as described by Gosmann, *et al*. (2014) with slight modifications (277). Mice were UVB irradiated and ears were harvested 5 or 24 hours later. Ears were split in half, weighed and cultured, dermis side down, in DMEM supplemented with penicillin/streptomycin (1 mM) and sodium pyruvate (1 mM), and incubated in 24-well plates (37°C, 5% CO2). To remove any cytokine released as a result of tissue preparation, medium was exchanged after 1 hour and 2 hours after placement in tissue culture. Supernatants were collected 20 hours after the last medium exchange for analysis using a mouse IL-10 ELISA kit (Catalog #M1000B, R&D Systems) following manufacturers instructions. IL-10 levels were quantified following generation of a standard curve and were normalized to the weight of the explant.

3.2.12. T-cell depletion using anti CD4/Anti CD8

Anti-mouse CD4 (clone GK1.5) and Anti-mouse CD8-alpha (clone 2.43) diluted in *InVivo* Pure pH7.0 dilution buffer were administered at 100μg per antibody per mouse via IP injection using the regimen shown in the chart illustrated in Fig. 3-5. In parallel control mice were treated with Rat IgG2b isotype control. Briefly, mice were treated with booster doses of antibodies for three days daily; allowed to recover for one day, infected with MmuPV1 and thereafter treated every three days with antibodies. To ensure that antibody depletion was working, CD4+ and CD8+ T-cell populations were analyzed by performing flow cytometry analysis on fresh blood (100μl) collected by submandibular bleeding using a 5 mm Lancet needle in K2-EDTA coated blood collection tubes that prevent coagulation of blood. 1ml of cold ACK lysis buffer (NH_4Cl 150mM, $KHCO_3$

10mM, EDTA 0.1mM; pH 7.2-7.4) was added and samples incubated on ice for 15 minutes. Samples were transferred to library tubes and centrifuged for 3 mins at 800rpm. Supernatant was discarded and the cell pellet washed with 1ml 1X PBS, resuspended in 50μl volume of Fc block (1:200 dilution CD16/CD32 in 2% FBS), incubated for 15 minutes on ice and then stained with 50μl of solution containing diluted antibodies (1:200 dilution, PE conjugated anti-CD4 and APC conjugated anti-CD8a) by keeping suspension on ice for 15 minutes. Sample cells were washed with PBS , counterstained with propidium iodide and analyzed by flow cytometry using a FACScaliber instrument.

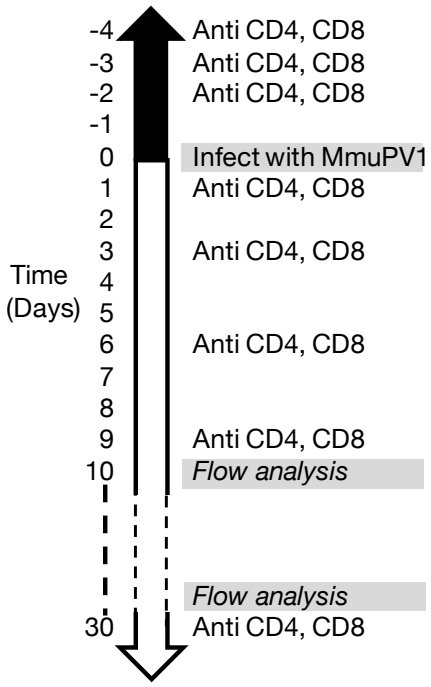

Fig. 3-5. T-cell depletion regime

3.2.13. Infection of animals with MmuPV1 DNA

In vivo infection with wild type or mutant MmuPV1 DNA was performed using a protocol modified from previously published reports (100, 110, 120, 128). Animals were scarified as described above for virus infection. Four days post-scarification the scarified site was inoculated with 10 μg recircularized viral DNA (in a 10μl volume) by injecting the DNA under the scab using a 30-gauge needle. The viral genomes were recovered by excision from the plasmid backbone using the restriction enzyme XbaI, followed by intramolecular religation using T4 DNA ligase, as detailed on the website of the Laboratory of Cellular Oncology (http://home.ccr.cancer.gov/Lco).

3.2.14. Infection of female reproductive tract using MmuPV1 virions

Mice were injected subcutaneously with 1 mg medroxyprogesterone acetate (Depo-Provera) at least 4 days prior to MmuPV1 infection to induce diestrus. On the day of the infection, mice were pre-treated vaginally with Contraceptrol (Options, #247149), an over the counter spermicide product containing 4% nonoxynol-9. Administration of nonoxynol-9 has previously been shown to potentiate HPV psueodovirus infection due to chemical injury of the vaginal/cervical epithelium (278, 279). At least 6 hours post-treatment with contraceptrol, 10^8 VGE MmuPV1 virions were delivered intravaginally in 4% carboxyl methylcellulose (Sigma, #C4888). All intravaginal treatments were performed on mice anesthetized with 5% isoflurane.

3.2.15. Estrogen treatment

Hormonal treatment with estrogen was performed as described previously(280, 281). Female mice were anesthetized with 5% isoflurane, and a continuous-release estrogen (E2) tablet (17β-estradiol; 0.05 mg/60 days; Innovative Research of America, Sarasota, FL) was inserted subcutaneously in the shoulder fat pads of the dorsal skin. A new tablet was inserted every 2 months as needed.

3.2.16. Microscope Imaging

H&E images and fluorescent images were captured using a Zeiss AxioImager M2 microscope and AxioVision software version 4.8.2 (Jena, Germany). High resolution, wide-field fluorescent images were acquired using a super-resolution Leica SP8 STED confocal microscope equipped with a motorized stage. This microscope is equipped with PMT and HyD lasers. All images were taken by means of a 20X objective lens (Specifications: HC PL APO 20x/0.75 CS2, Dry). The images were acquired by tile-scanning by marking positions around the region of interest using the LAS-X suite software package (version: 2.0.1). The merged wide-field image was obtained by automatic stitching of individual styles by means of in-built auto stitching algorithm part of the LAS-X suite software package.

3.2.17. Statistical analysis

All statistical analyses were performed using MSTAT statistical software version 6.1.4 (http://www.mcardle.wisc.edu/mstat).

3.3. Considerations to keep in mind while performing MmuPV1-infection studies

i. Preventing contamination with MmuPV1 in the animal facility

MmuPV1 naturally infects laboratory strains of mice. We recommend personnel to diligently follow necessary precautions in handling animals infected with the virus to prevent spread to uninfected mice housed in the same room and mice located elsewhere in the vivarium.

ii. If there is lack of papillomas in mice 16 weeks post-infection

a. In our experience, the incidence of MmuPV1-induced papillomas arising in immunocompetent strains of mice is dependent upon 4 main variables: the dose of virus, the strain of mouse, the method of scarification, and the UVB dose. Therefore, we recommend using a significantly large sample size. In our statistical determination via power analysis we have found this number to be greater than 12 sites of infection.

b. In this thesis, we described incidence of 50% when infecting the pinna of UVB-treated FVB/NTac mice with 10^8 VGE of MmuPV1. Papillomas can also arise in C57/BL6 and BALB/c mice with higher doses of UVB (118). While UVB causes immunosuppression in both FVB and C57/BL6, the FVB strain is classically used for skin cancer studies (282); and, therefore, is the strain we have preferred to use

in studying neoplastic disease induced by MmuPV1. If using a different genetic background we recommend titrating the dose of UVB to achieve the desired incidence. For example, we have found UVB doses between 600-1000mJ/cm^2 to induce MmuPV1-associated papillomatosis in 30-50% of sites on the pinna of C57/BL6 mice infected with 10^8 MmuPV1 VGE per site(118).

c. We do not recommend freeze thawing stocks of virus, especially when working with crude viral extracts as this reduces the infectivity of the virus stock. Also see point (iii) for virus dose considerations.

d. It is important that the manufacturer calibrate the UVB irradiator equipment periodically so that the correct dose of UVB is delivered to the animals. It may be recommended to anesthetize or singly house animals during UVB irradiation so that the animals receive similar exposure of UVB. If using a different source of UVB, it may be necessary to optimize the UVB dose in experimenters' hand.

iii. Amount of virus to use

We have consistently seen papillomatosis arising on the ears of UVB-treated mice on different genetic backgrounds infected with 10^8 MmuPV1 VGE per site. In FVB/NTac mice, a minimum of 10^7 MmuPV1 VGE is required to see papilloma induction in this model. In contrast, in immunodeficient nude mice we have seen papillomatosis arise with 10^6 MmuPV1 VGE (118). The reasons for this observation remain to be investigated but we can conclude that a higher threshold of virus is required to see papilloma induction in immunocompetent mice treated with UVB. If using a virus amount less than 10^7 VGE, it is possible that one may not see papillomas develop up to 6-months post-infection. It has been reported that some immunocompetent strains of mice not exposed to UVB are

susceptible to MmuPV1 infection if using greater that 10^{11} MmuPV1 VGE, however these papillomas completely regressed within a month of appearing (100). In our hands 10^{8} VGE dose virus particles does not cause papillomas in non-UVB-irradiated, immunocompetent strains of mice.

iv. Control groups

For every experiment we recommend having the following control groups:

1. Athymic group of mice (n=3) to test whether the virus stock is infectious.
2. Non UVB-irradiated immunecompetent mice (n>4) as a negative control
3. UVB-irradiated mock-infected mice (n>4) as a negative control

v. Scoring papillomas

It is recommended to monitor animals daily for at least one week post-infection. If animals do not look healthy or appear in any discomfort, we recommend treating the animals with analgesics by injection or in drinking water. Following this period, we recommend scoring of papillomas weekly. It is possible to mistake swelling, edema and scabs for papillomas in the initial weeks following infection. For this reason, we recommend observing the animal carefully under anesthesia and using a hand-held magnifying glass if necessary. It may be beneficial to wait for a few days, as the papillomas are usually harder to diagnose at onset earlier than 3 months post-infection at which time they continue to grow in size. Re-evaluation of the same site can provide further confidence that there is a progressive increase in size of the emerging wart. If measuring papilloma size, we strongly recommend that one person perform all size measurements to ensure consistency. For each measurement, we take three independent

reads and then use the average. In addition to scoring size of papillomas over time, photo-documentation of each site can provide a useful temporal record of disease. If tracking animals longitudinally, we recommend identifying animals by tattooing the tail or notching the edge of the ear. We do not recommend ear tagging for these studies as ear tagging has itself been reported to promote inflammation and skin cancer in mice (283, 284). Papillomatosis should be confirmed via histopathology by consulting a pathologist.

vi. Timing for UVB irradiation

Most studies described in this thesis involve UVB irradiation 24 hours post-infection. However, we have seen no difference in papilloma onset at the following time points: (i) 24-hours prior to infection (118), (ii) 5 days post-infection, or (iii) 5 days prior to infection.

vii. Variability in wounding and delivering of virus particles at infection site

Perhaps the greatest variability that can arise in this infection model is performing wounding of the infection site. This has been reported to be an important factor during characterization of the infection model for cottontail rabbit papillomavirus (CRPV) as well (285). When infecting tail sites in immunosuppressed mice, other groups have reported wounding animals and then injecting virus particles 3 days post-wounding under the scab using a needle (120, 286). Our preferred site of infection is the ear, in which case it is difficult to inject under the scab due to ear thickness and curvature of the ear. Therefore we pipetted the virus solution directly onto the wounded site immediately after scarification. To adopt this approach, it is essential to have the virus in a minimal volume (e.g. 1-3μl) so that the virus solution dries quickly post-application before returning the

animal to its cage. Another way to deliver the virus is via intraderm injections. In our hands we found that intraderm injection at ear following scarification caused papillomas in athymic nude mice (unpublished data), but we have not tested this approach in the context of the UVB-infection model. It is worth noting that, in the context of CRPV-based infection studies, intradermal injection was found to be inconsistent in causing papillomas. The authors noted that this might be due to the depth of delivery by intraderm injection, which could result in the virus only being delivered to the dermis (287).

As we have reported in the detailed protocol of *in vivo* infection, the goal of the wounding is to create a "brush-burn" like lesion while taking care to not cause profuse bleeding. Since the mouse pinna is delicate, it is important to take care to not pierce or cut the ear while causing the wound. It is worth noting that the depth of wounding may differ from one person to the other, so we strongly recommend that one person perform all the wounding in a single experiment to reduce the concern of intra-experimental variation. We found it easiest to wound using a 27-gauge syringe needle but it might be useful to test other methods of wounding as described by other investigators (110). For all of these reasons, we recommend optimizing ear infection technique using nude mice first, and using nude mice as a positive control in parallel for each experiment.

Chapter 4:

Establishment and characterization of the MmuPV1 infection model in immunodeficient mice

In this short chapter I have described the establishment of MmuPV1 infection model in immunodeficient mice. Majority of this work was performed during the initial parts of my PhD (2012-2013) and essentially laid the groundwork for the work presented in this thesis. Parts of this chapter have been published as parts of manuscripts:

1. Virus dose curves have been published in Uberoi, *et al*. (2016), PLoS Pathog 12:e1005664 (118)
2. Immunohistochemistry analysis has been published in Uberoi, *et al*. (2017), PLoS Pathog 13:e1006171 (228).
3. Time course analysis of spatial distribution of L1 and amplified viral DNA in Xue, *et al*.(2017), PLoS Pathog 13(11): e1006715.(288)

Dr. Chris Buck (NIH) provided the synthetic clone of MmuPV1 and pSheLL. Dr. Hao Shun Huang generated the first stock of MmuPV1 quasivirus used to establish the MmuPV1 infection model. Denis Lee helped clone pAU505, which is the lab-generated clone of MmuPV1. Amy Liem and assisted with monitoring of mice and performing grafting of IL2rg null mice. All experiments and analyses were performed by me.

4.1. Introduction

MmuPV1 is the first rodent papillomavirus identified to infect the laboratory strain of mice, *Mus musculus*. It was isolated from papillomas arising spontaneously in NMRI strain of mice carrying the *FoxN1*^{nu} mutation that renders these mice T-cell deficient (55). The MmuPV1-infection model presents a great opportunity to papillomavirus biologists to study a naturally arising infection in a genetically modifiable and tractable laboratory animal. In order to be able to study MmuPV1 we first needed to establish an infection model in the laboratory. In this chapter, I describe the establishment of MmuPV1 infection model in lab mice in Madison, which laid the groundwork for future work performed in the context of my thesis. In this chapter I describe the establishment and characterization of the MmuPV1 infection model in the *FoxN1*$^{nu/nu}$ immunodeficient strain and other immunodeficient mouse models selectively deficient for sub-populations of T-cells and B-cells respectively. These initial efforts, coupled with the observation that immunocompetent wild-type strains of mice are resistant to MmuPV1-dependent papillomatosis have led to the understanding that complete T-cell deficiency is required for MmuPV1-dependent disease.

4.2. Results

4.2.1. Establishment of MmuPV1 infection model in *FoxN1^{nu}* (nude) mice

To establish the MmuPV1 infection model in our lab, we initially used a synthetically constructed genome of MmuPV1 (pMusPV, gift from Dr. Chris Buck) (110) to generate MmuPV1 quasivirions generated as described previously (279, 289, 290). Viral genome equivalence (VGE) was assessed by quantification by means of southern hybridization by comparing with known amounts of viral plasmid. As MmuPV1 was originally isolated from the T-cell deficient *FoxN1^{nu}* strain, we established our infection model by infecting immune-deficient *FoxN1^{nu}* strain of mice on the BALB/c genetic background. It has been shown in the cottontail rabbit papillomavirus (CRPV) infection model that wounding prior to infection improves overall infectivity and allows for more consistent infection. Therefore we attempted different forms of wounding using - (i) hand-held drill equipped with a rotary sanding disk, (ii) 27 gauge needle and (iii) intraderm injection via a 30 gauge Hamilton syringe. Four wounds were made on the tail separated approximately 1cm apart from each other starting at base of tail by indicated method (n=4 mice/group) as shown in Fig. 4.1A panel. This was followed by immediate application of 10^8 viral genome equivalents (VGE) of MmuPV1 virions per site and onset of papillomas was monitored daily up to one month post-infection. The wounds healed within one week and within 2-3 weeks post-infection we observed raised bumps on the tail (Fig. 4.1A). These lesions appeared wart-like in appearance and were from pinkish to brown in color. On touching they felt like heavily wrinkled and keratinized tissue and were distinct in their appearance from the rest of the tail. These papillomas grew in size over time and over time the warts became more cornified and harder to the touch. These

features were consistent with those described first by Dr. Shope in his studies performed using CRPV(2). These lesions or papillomas arose in nude mice by all the three methods of wounding. Since papillomas arose only at individual sites of wounding, we considered wound as an individual infection site and documented onset of papillomas at each site as represented in a Kaplan-Meier plot (Fig. 4-1B). There was no significant difference between either of the wounding methods in terms of onset of tail papillomas in nude mice (Log-rank analysis, $P>0.05$) and papillomas arose with similar multiplicities as well. As an example, we have shown papilloma multiplicity at 18th day post-infection (Fig. 4-1C). We proceeded with needle scarification for all future studies due to ease of use. We continued to keep and monitor the infected animals after this time point and observed that papillomas continued to grow in size. At three months post-infection we started observing that papillomas started arising at sites that had not been experimentally infected with MmuPV1 e.g. muzzle/outer cheek region, eyelids, limbs and even ears (Fig. 4-1D) suggesting that the virus can be laterally transmitted on the same mouse to many sites on the body.

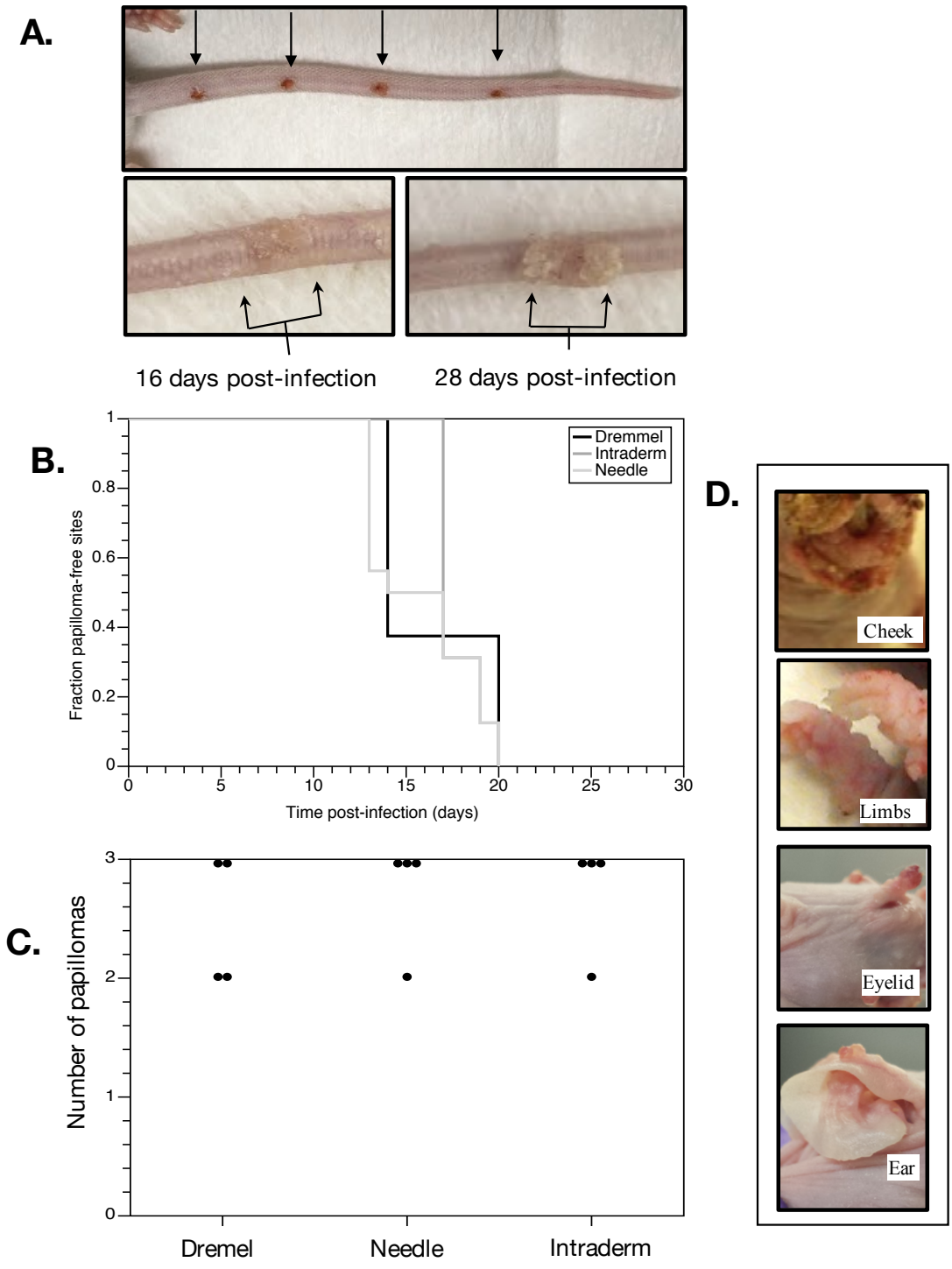

Fig. 4-1. Optimizing infection of BALB/c-*Foxn1*^{nu} mice.

Fig. 4-1. Optimizing infection of BALB/c-*Foxn1*^{nu} mice.

(A) Top- Needle-based scarification of 4 tail spots in nude mice. Bottom left- Onset of papilloma as seen 16 days post-infection. Bottom right- a growing papilloma 28 days post-infection.

(B) Different modes of wounding to deliver MmuPV1. Mice were anesthetized and wounded as follows: (i) hand-held drill equipped with a rotary needle (black line, dremel), (ii) 27 gauge needle (light gray, needle) and (iii) intraderm injection via a 30 gauge Hamilton syringe (dark gray, intraderm) at 4 spots on tail as shown in A. Following wounding 10^8 VGE MmuPV1 was applied to infected sites using pipette tips and papilloma onset was documented by scoring mice daily up-to 30 days post-infection. We found there to be no significant difference between papilloma onset by either methods of wounding.

(C) Papilloma multiplicity. Four nude mice were infected following different methods of wounding (as shown in B). Papillomas arose with similar multiplicity by all methods. As an example we provide a dot plot showing number of sites per animal at which papillomas had arisen at 18th day post-infection, depending on wounding method used.

(D) Laterally transmitted MmuPV1 results in papillomas at other uninfected sites. At about 3 months post-infection of tail sites with MmuPV1 we observed that papillomas started arising at other sites that had not been infected with MmuPV1.

Histopathological analysis of overt tail papillomas 6 months post-infection from immunodeficient *Foxn1*^{nu} mice confirmed the presence of exophytic papillomas at the infected sites (Fig.4-2). We observed hyperkeratinized epithelia and presence of papillary projections in the epithelia. Further we saw presence of koilocytes whose presence is consistent with papillomatosis. Expression of the major viral capsid protein, L1, was detected using sera against MmuPV1 L1, providing evidence that the warts were supportiing the late stages of the viral life cycle in which progeny virus is made (Fig.4-3). We observed that L1 was present in all the epithelial layers of the papillomas but in greater abundance in the upper layers of the epithelia, consistent with observations made by others (100). Presence of amplified viral DNA was confirmed by fluorescent in *situ* hybridization (FISH) analysis. On the these same mice we had experimentally infected on their tails, we also detected MmuPV1 L1 protein and amplified viral DNA in the epidermis of experimentally uninfected ears that appeared normal by visual scoring (Fig. 4- 4A) demonstrating spread of virus and presence of subclinical infections.

Southern hybridization using MmuPV1-specific probes performed on virus extracted from the tail papillomas confirmed presence of MmuPV1 (Fig.4-4B). This virus was transmissible to other mice and different sites e.g. muzzle and ears were susceptible to MmuPV1-induced disease in addition to tail (data not shown) but the back skin of Balb/c- *Foxn1*^{nu} mice was resistant to infection by virus as reported previously (100). In testing these freshly prepared viral extracts for performing serial infections we observed consistent patterns of papilloma incidence in nude mice, i.e. papillomas arose within 2-3 weeks post-infection (data not shown). When the extracts were recovered from storage after freeze thawing prior to infection there was a slight delay in the onset of papillomas

(Fig. 4-4C), though this delay was not statistically significant (Log-rank, *P=0.084*). While we did not test in our hands the effect of multiple freeze-thaws on infectivity of MmuPV1 virus in nude mice, we have anecdotal evidence based on our experience with HPV16 pseudovirus (encapsidating reporter plasmid) that viral titer decreases upon multiple freeze thaws. For this reason virus was stored in aliquots at -80ºC and virus aliquots thawed only one single time were used in all subsequent experiments.

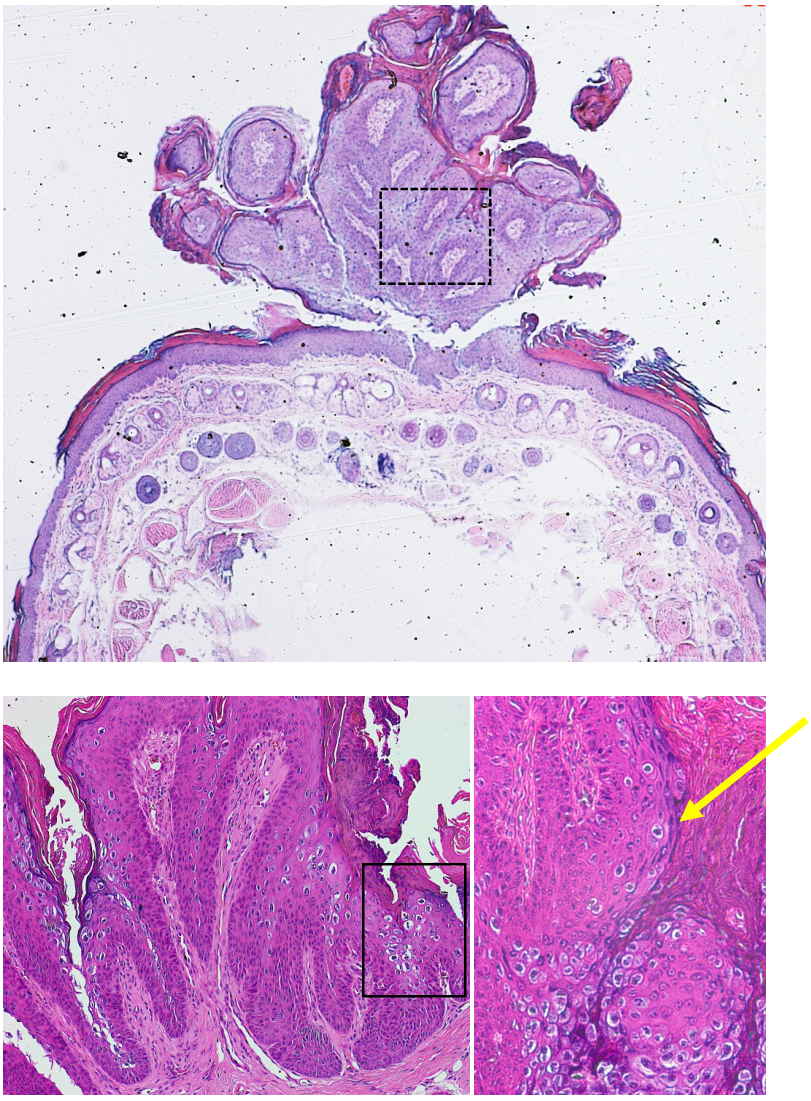

Fig. 4-2. Histopathology

H&E staining was performed on the cross-section of tail papilloma (arising 6 month post-infection). A large exophytic papilloma (2.5X magnification) can be seen on top of the tail (top) with finger-like projections confirming papillomatosis 10X magnification (top-right). At higher magnification presence of koilocytes (inset, bottom right) consistent with papillomavirus infection.

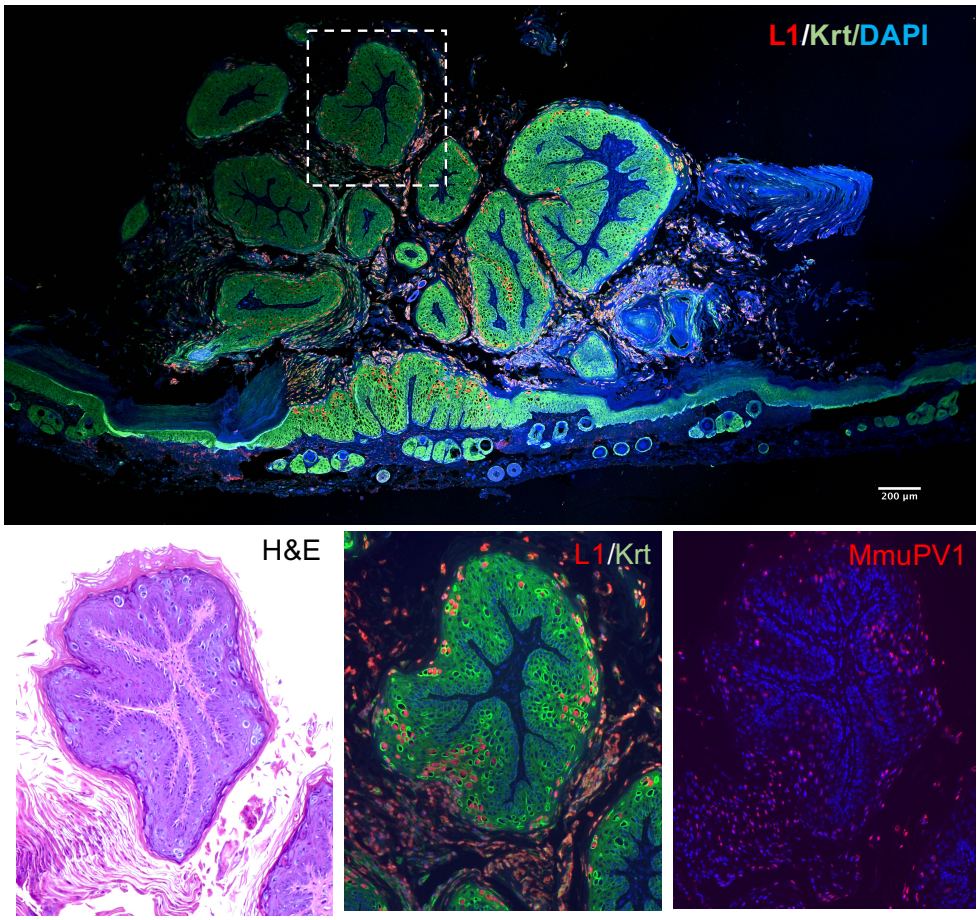

Fig. 4-3. Hallmarks of the papillomavirus life cycle in MmuPV1 induced papillomas in BALB/c-*Foxn1*^{nu} mice.

Top image: Wide-field immunofluorescence of tail warts indicating L1 (red)-Keratins 10 and 14 (Krt, green) immunofluorescence. Bottom images: Higher magnification images of a region of same papilloma (see boxed region in top image) stained with H&E (left image), abs to L1, in red, and Krt, in green (middle image) or subjected to fluorescence in situ hybridization (FISH) to detect MmuPV1 DNA, in red with DAPI (blue) counterstain (right panel).

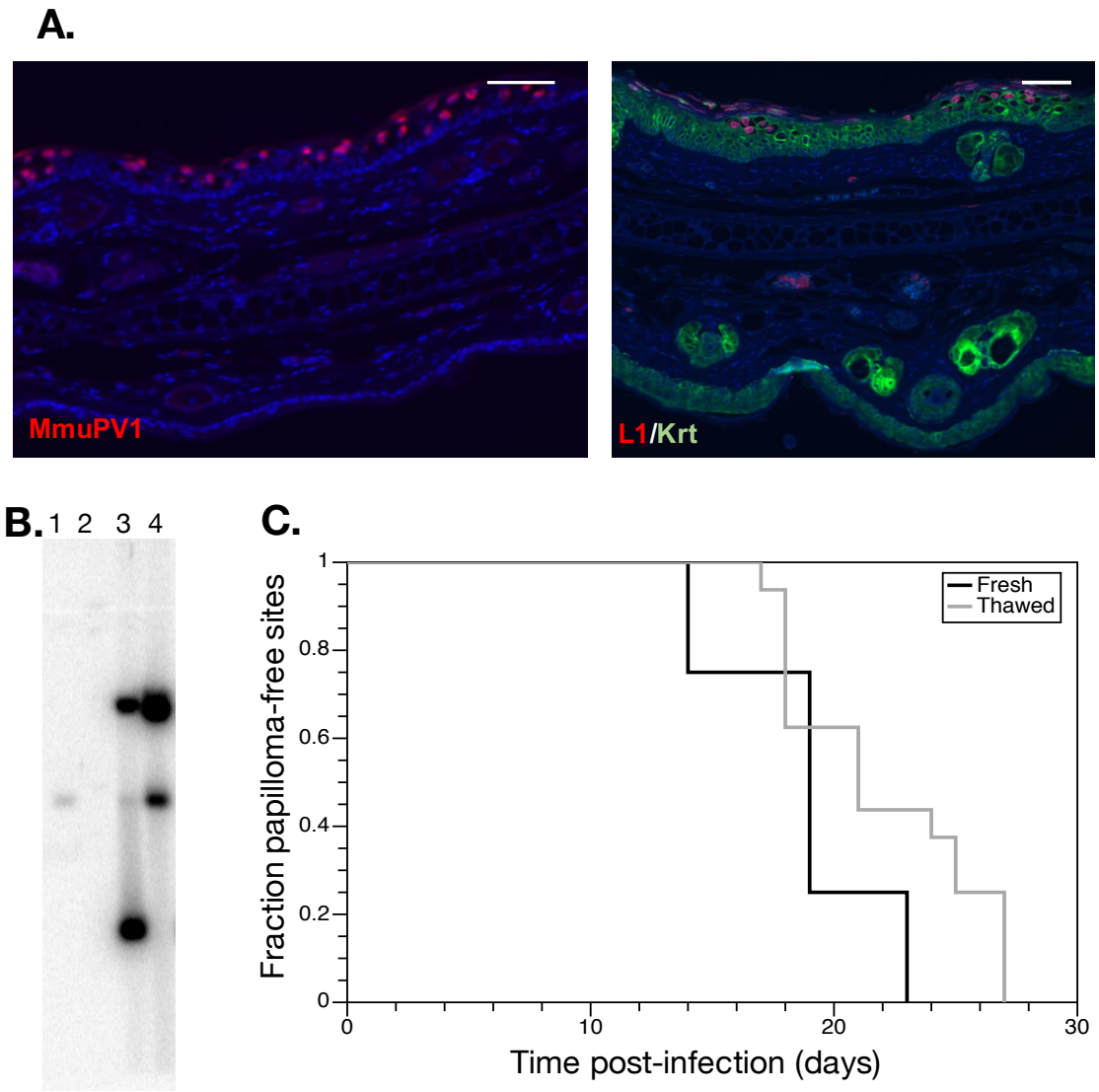

Fig. 4-4. Characterization of MmuPV1-induced disease

Fig. 4-4. Characterization of MmuPV1-induced disease

A. Left ear harvested from a nude mouse that was infected on the tail and right ear. This ear appeared normal looking but we can detect amplified MmuPV1-DNA (Red) as detected by FISH (left) and MmuPV1-L1 capsid protein (Right).

B. Southern hybridization using MmuPV1 specific probes was performed on viral extracts harvested from MmuPV1-induced papillomas. Lane 1 depicts linearized MmuPV1 genome (positive control); Lane 2 contained HPV-16 plasmid that was not detected by Southern showing specificity of probes (negative control); Lane 3 contained 2μl of viral extract harvested from MmuPV1-induced warts showing extrachromosomal (top), linearized (middle) and supercoiled (bottom) forms of DNA; Lane 4 is a partial digest of MmuPV1 virus extract where the extract was digested with Xba1 and shows extrachromosomal and linearized forms of MmuPV1.

C. Kaplan-Meier analysis of MmuPV1-induced warts when freshly prepared virus extract (10^8 VGE dose MmuPV1) was used to infect mice (black line) compared to singly thawed virus extract (10^8 VGE dose MmuPV1) that was used to infect mice (gray line). While there was a slight delay in onset of papillomatosis using the thawed virus extract, the efficiency of papilloma formation was not compromised. n=16 sites were infected for each condition.

While the initial characterization of the MmuPV1 infection model, was done using the artificially synthesized MmuPV1 genome (100) we independently cloned MmuPV1 by performing Rolling Circle Amplification on DNA extracted from the warts that originally arose in the colony of NCR-FoxN1nu mice in India, from which MmuPV1 was first isolated (55, 60). This clone, pAU505, was sequenced. We found three nucleotide differences compared to the original reported sequence of MmuPV1: a silent (synonomous) change in E1 and two missense (nonsynonymous) mutations in L2. The missense mutations in L2 were observed at aa253 (Vè E) and at aa443 (LèR). BLAST analysis showed that the V253E polymorphism is seen in several papillomavirus species (data not shown) but more clones of MmuPV1 need to be sequenced to understand the significance. To test whether there is any difference between infectivity of virus particles generated using the lab-generated (pAU505) versus synthetic clone (pMusPV_Syn) of MmuPV1 in nude mice we generated stocks of virus in 293FT cells using a method previously described (citation) using each of the two cloned viral genomes and infected mice (n=3/group) on their tails at 4 sites and scored for onset of papillomas daily up to 30 days (Fig. 4-5A). There was no significant difference in time of onset of papillomas induced by the two the virus stocks (Log-rank analysis, *P=0.74*). At 4-weeks post-infection, when 100% of infected sites had papillomas, we measured geometric mean diameters (weekly) of the papillomas on these mice up to 10 weeks post-infection. We found there to be no significant difference between the average size of the papillomas produced by either virus nor their rate of growth (Fig. 4-5B, Kruskal-Wallis test, *P=0.27*). It is worth noting however, that, for both virus stocks, the papillomas arising closer to the base of the tail grew larger than those closer to the distal tip of the tail (Fig.

4-5C). This is an observation consistently made by us over any experimental cohorts. We proceeded to use virus extracts obtained from papillomas generated using the lab-generated clone of MmuPV1 (pAU505) for the rest of our studies unless otherwise indicated.

A.

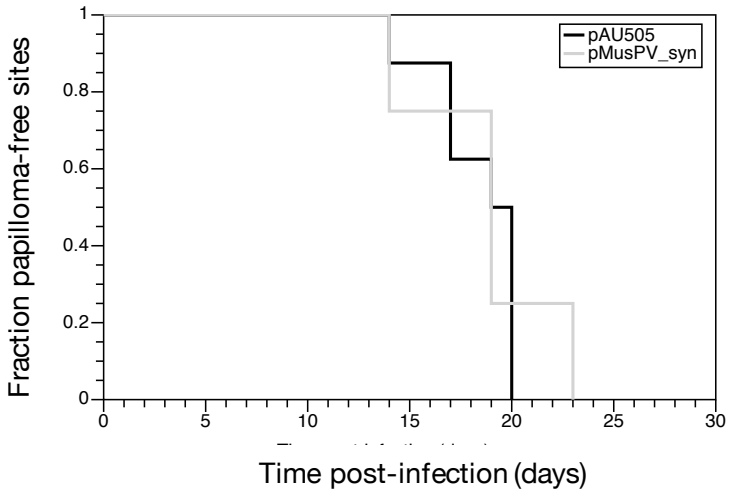
pAU505
pMusPV_syn
Fraction papilloma-free sites
Time post-infection (days)

B.

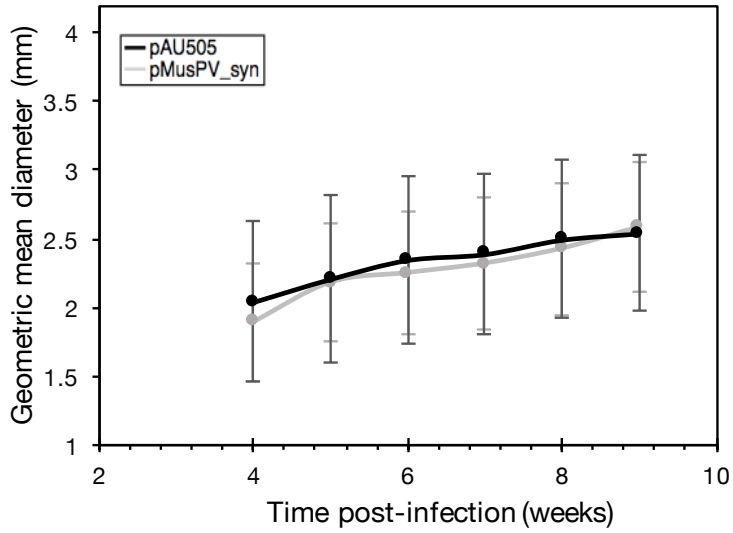
pAU505
pMusPV_syn
Geometric mean diameter (mm)
Time post-infection (weeks)

C.

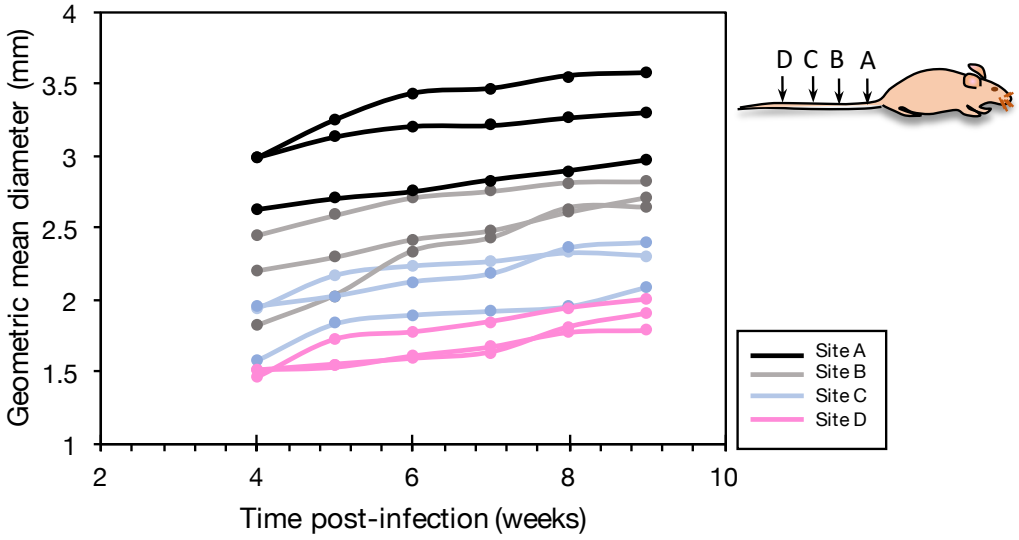
D C B A
Site A
Site B
Site C
Site D
Geometric mean diameter (mm)
Time post-infection (weeks)

Fig. 4-5. Papillomas caused by lab-generated versus synthetically synthesized MmuPV1

Fig. 4-5. Papillomas caused by lab-generated versus synthetically synthesized MmuPV1

A. Kaplan-Meier analysis of MmuPV1-induced warts when Synthetic MmuPV1 quasivirus (pMusPV_Syn at 10^8 VGE dose) used to infect mice (gray line) was compared to quasivirus generated using lab generated clone of MmuPV1 (pAU505 at 10^8 VGE dose) was used to infect mice (black line). n=16 sites were infected for each condition. There was no significant difference between onset of papillomas using either virus.

B. Sizes of papillomas (generated by either viruses described in A) were measured weekly starting week 4 when 100% of infected sites (n=12 sites/virus) had papillomas and geometric mean diameter was calculated. Average size of papillomas at each time point are represented by a line graph (black for pAU505 and gray for pMusPV_Syn). We found there to be no significant difference between size of papillomas generated by either virus.

C. All infected sites had papillomas at the end of 4 weeks but papillomas grew asynchronously. As an example sizes of individual papillomas generated by infection with pAU505 are shown. Papillomas growing closest to base of tail (Site A) were much larger than the ones arising close to tip of tail (Site D). Geometric mean diameter of each papilloma is shown at each time point.

4.2.2. Spatial localization and expression dynamics of late viral gene expression and viral DNA replication in MmuPV1 infected tissues

To understand the expression dynamics of viral L1 and MmuPV1 DNA over time, nude mice were infected (three spots on the tail) with equivalent amounts of MmuPV1 per site (10^8 VGE) and tissue was harvested by sacrificing animals at different time points until papillomas were overtly seen (28 days post-infection). These tissues collected at each time point were analyzed for appearance of L1 viral protein and amplified viral DNA, hallmarks of the productive phase of the viral life cycle. As shown in Fig. 4-6 and Fig. 4-7, no obvious L1 expression or viral DNA was detected in any of the infected sites (0/3 infected sites) at 4 days post-infection. Hypertrophic scarring of terminal epithelia with intact basement membrane was observed. At day 10, both L1 and MmuPV1 DNA were detected in one of the infected sites (that closest to base of tail - shown in Fig 4-4). L1 expression was found in the suprabasal layers along with terminally differentiating epithelia whereas MmuPV1 DNA appeared to be present only in suprabasal layers. Microscopically, this site had evidence for hyperplasia, koilocytes and some fibrillary projections; however, the overt appearance was that of a raised scar. At day 21, one site of infection, that is closest to the tail, showed evidence of productive infection with an abundance of L1-positive and viral DNA-positive cells and more prominent fibrillary projections. The remaining 2 infected sites appeared mostly normal and no L1 or FISH positive nuclei were detected. At 28 days post infection, all three infected sites showed overt appearance of warts with L1 positivity (Fig. 4-8). While sites were infected at the same time, papillomas grew asynchronously as is evident by variation in size of the papillomas, which we had also noted previously (Fig. 4-5C). We consistently observe

that papillomas near the base of the tail grow fastest and show the most robust features of a productive viral infection. The pattern of L1 expression and viral DNA amplification at day 28 was similar to that observed at day 21.

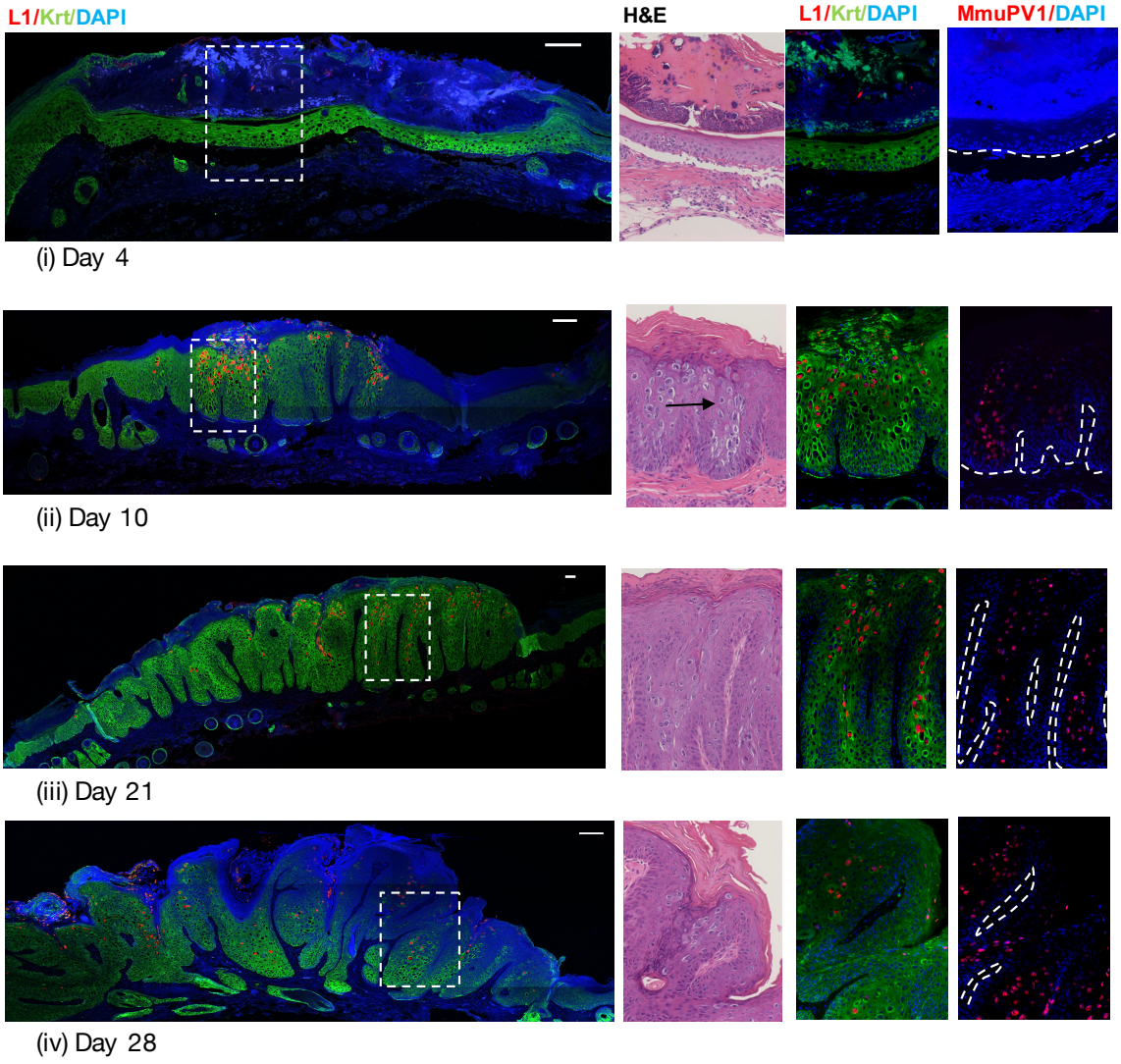

Fig 4-6. Time-course analysis of MmuPV1 infected tail site near base of tail of *FoxN1*$^{nu/nu}$ mice.

Fig 4-6. Time-course analysis of MmuPV1 infected tail site near base of tail of *FoxN1*$^{nu/nu}$ mice.

Each panel consists of a high-resolution wide-field image representing immunofluorescence detection of L1 (red) and Keratins (Krt10 & Krt14, green) of the infected site accompanied by an inset consisting of H&E staining (left), L1-Krt immunofluorescence (middle) and MmuPV1 DNA FISH (right). H&E staining and FISH were performed on adjacent sections. For both IF and FISH nuclei were counter-stained with Hoechst. Accompanying wide-field images for FISH staining are provided in Fig. 4-7. The scale bar for 100μm is indicated by means of a white bar. The white dashed line indicates basement membrane.

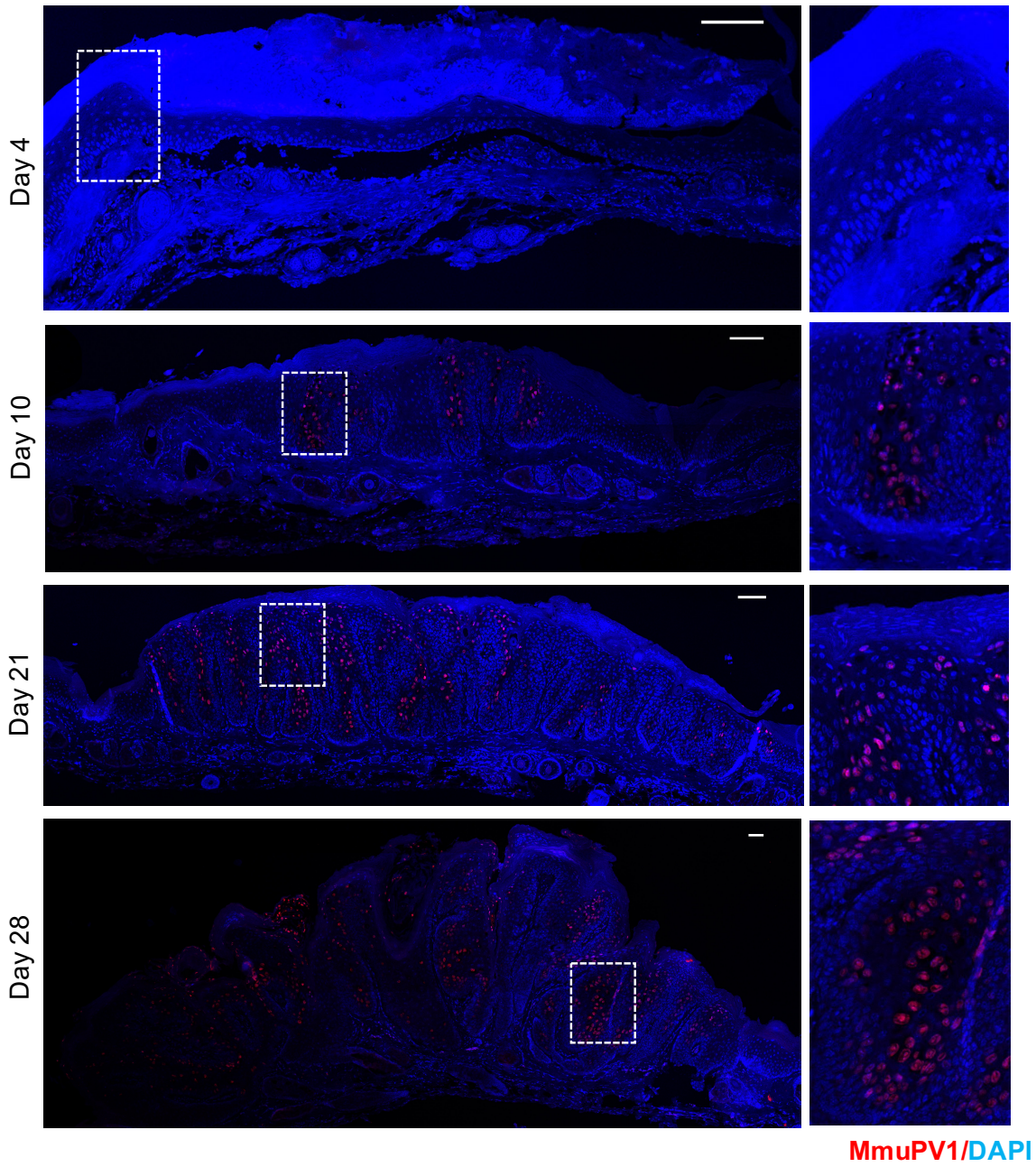

Fig 4-7. MmuPV1 DNA FISH

Accompanying MmuPV1 DNA FISH image of samples from time-course analysis of MmuPV1 infected tail site near base of tail of *FoxN1*$^{nu/nu}$ mice. The scale bar for 100μm is indicated by means of a white bar. The white dashed line indicates basement membrane.

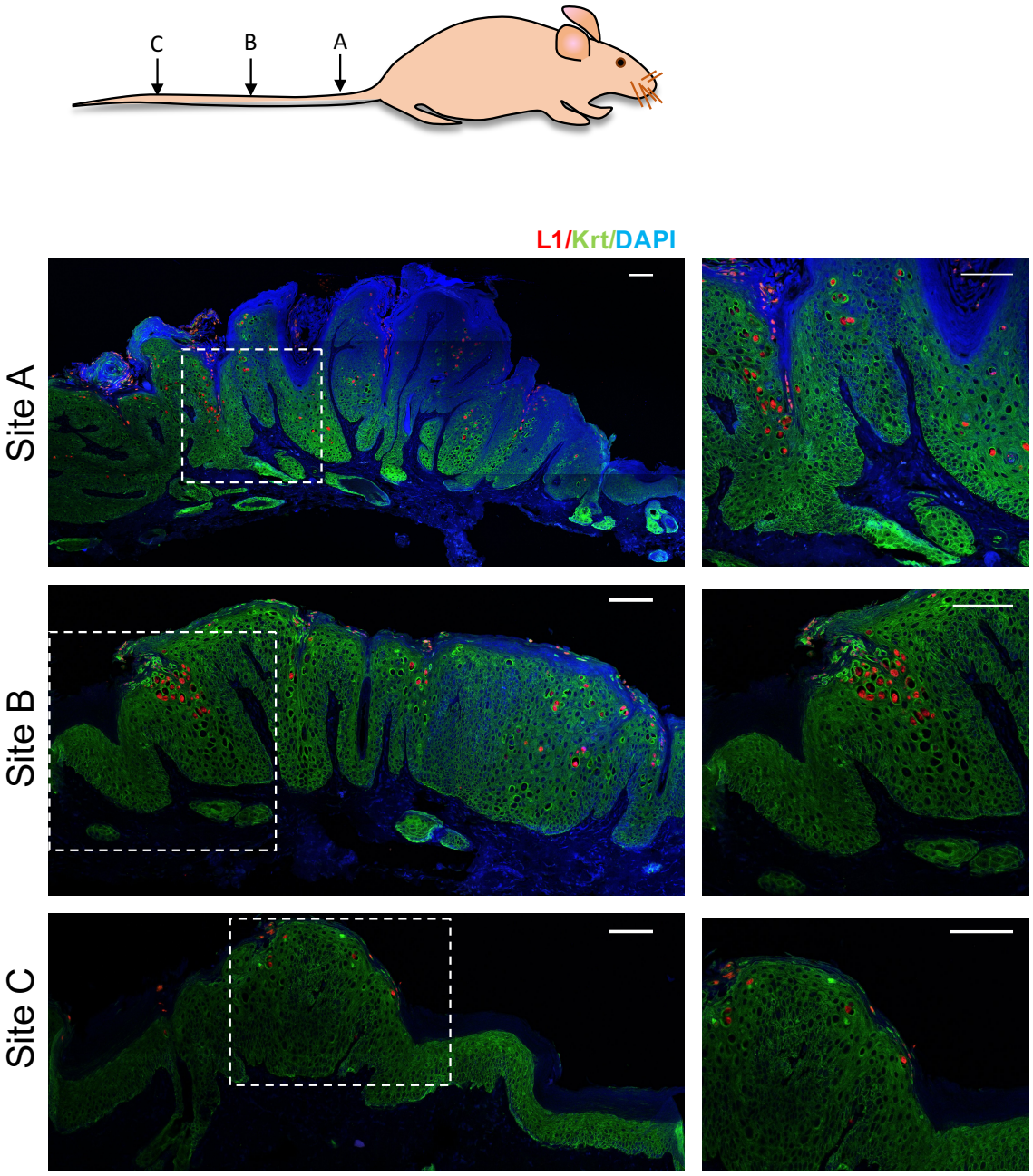

Fig. 4-8. MmuPV1-induced papillomas growing asynchronously

Fig. 4-8. MmuPV1-induced papillomas growing asynchronously

Each panel consists of a high-resolution wide-field image representing immunofluorescence detection of L1 (red) and Keratins (Krt10 & Krt14, green) of the infected site accompanied by an inset consisting of a higher magnification of L1-Krt immunofluorescence. The panels depict L1-Krt dual IF staining of papillomas arising at all three sites at 28th day post-infection showing that papillomas are growing asynchronously. While all sites show presence of a papilloma and are L1 positive, size of papillomas is not uniform across the three sites.

4.2.3. There is a dose dependent delay in onset of MmuPV1-induced papillomas

In order to characterize relationship between viral dose and papilloma incidence, various concentrations of MmuPV1 virus were used to infect BALB/c-*Foxn1*^{nu} mice at ear (Fig 4-9A) and tail (Fig 4-9B) sites. When 10^9, 10^8, and 10^7 VGE/site were used for infection, papillomas developed as early as 2-3 weeks post-infection and resulted in greater than 90% papillomatosis incidence. However at lower doses (e.g. 10^6 VGE/site), papillomas did not appear until 2 months post-infection and developed with much lower frequency. At the lowest dose tested (10^5 VGE/site), mice remained papilloma-free until approximately 4 months post infection. At the end of six months some sites (less than 10%) infected with 10^5 VGE/site did develop papillomas, albeit at low frequency, suggesting the presence of a subclinical infection at these low doses.

4.2.4. MmuPV1 induced papillomas show evidence of disrupted epithelial differentiation

Immunohistochemical analysis of cytokeratin markers K14, K10 and involucrin (Fig 4-10) was used to assess the differentiation state of papillomas in comparison with normal uninfected skin. The papillomas showed expansion of basal-like epithelia indicated by IHC analysis of cytokeratin-14 (K14), which is a marker for basal layers of the epidermis. Cytokeratin-10 (K10) expression is found in the suprabasal compartment of normal, uninfected murine skin. MmuPV1-induced papillomas showed diffuse pattern of K10 throughout the papilloma with irregular intense staining in the suprabasal epidermis of the papillomas. In normal skin, involucrin - a terminal differentiation marker is usually detected in the cell periphery of high stratum spinosum cells (291).

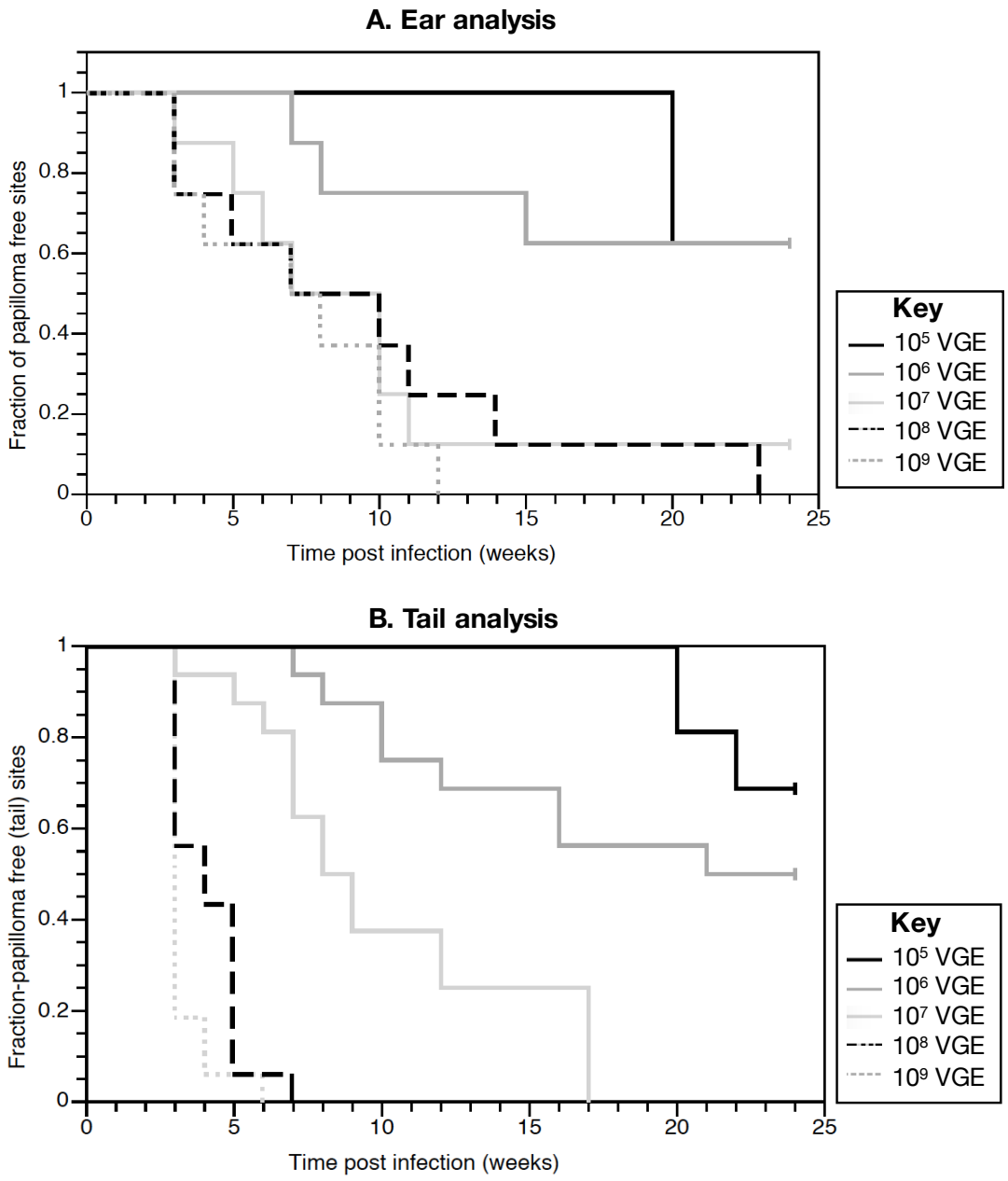

Fig. 4-9. Dose-dependent delay in onset of MmuPV1-induced papillomas.

Fig. 4-9. Dose-dependent delay in onset of MmuPV1-induced papillomas.

Graphs representing fraction of papilloma free infected ear sites (A) and tail sites (B) with respect to time. (A) Groups containing four mice were infected at ear sites (2 sites per mouse) post scarification with 10^9, 10^8, 10^7, 10^6 and 10^5 VGE amounts of MmuPV1 virions. Mice were scored weekly for presence of ear papillomas up to 6 months and results have been plotted as a Kaplan-Meier curve. No animals were censored during the course of the experiment. (B) Groups containing four mice were infected on the tail (4 tail sites per mouse) post scarixfication with 10^9, 10^8, 10^7, 10^6 and 10^5 VGE amounts of MmuPV1 virions. Mice were scored weekly for presence of ear papillomas up to 6 months and results have been plotted as a Kaplan-Meier curve. No animals were censored during the course of the experiment.

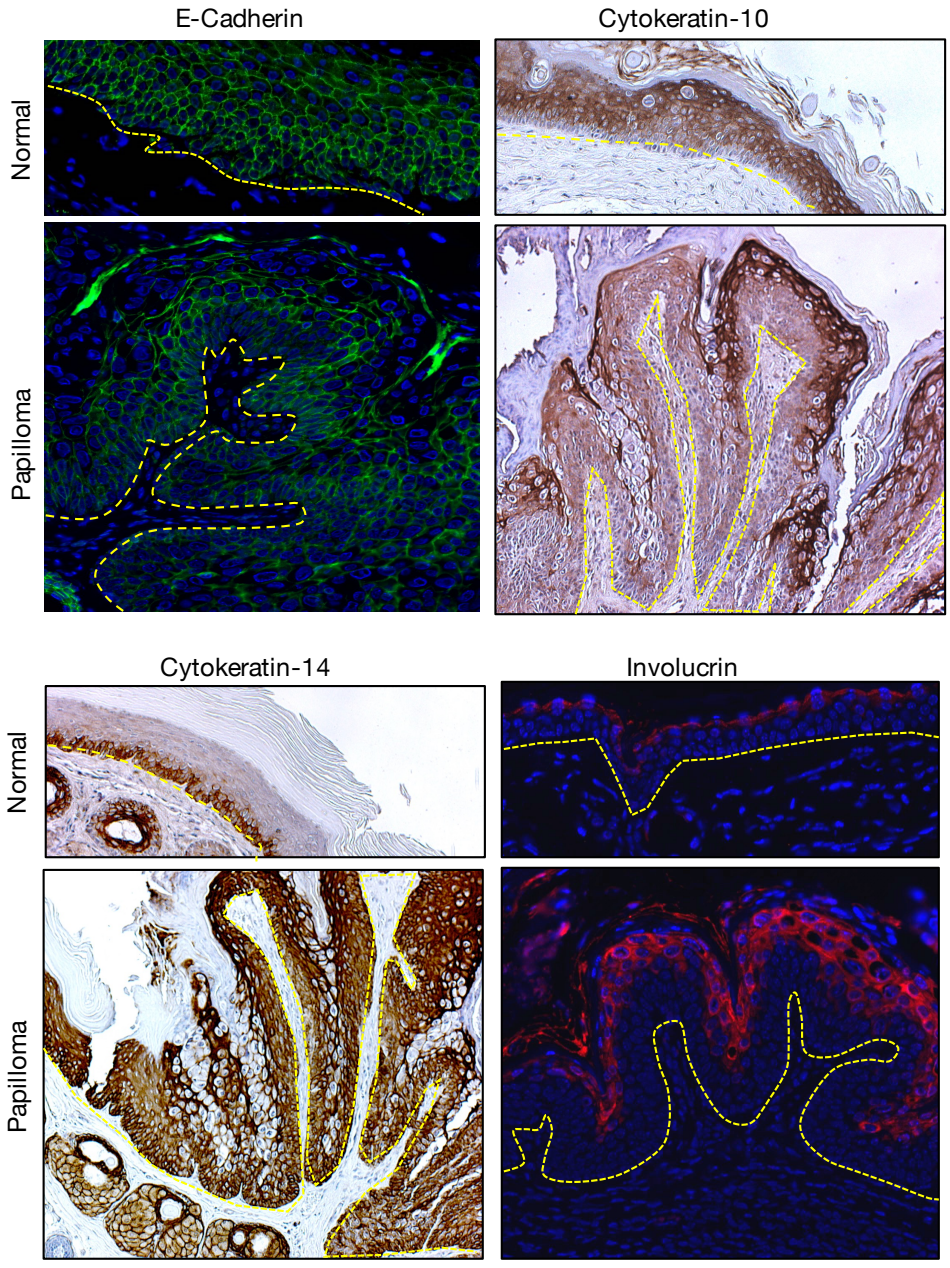

Fig. 4-10. Immunohistochemistry analysis tail papillomas for differentiation markers.

IHC for epithelial differentiation markers of normal uninfected skin compared to MmuPV1 induced skin papillomas is shown. Immunohistochemistry analysis for Cytokeratin14 (bottom left), Cytokeratin10 (top right) and Involucrin (bottom right) indicates delay in terminal differentiation program of epithelia in the papillomas.

4.2.5. T-cell deficiency is required for MmuPV1 dependent disease

Besides *Foxn1*^{nu} mice on Balb/c genetic background, we also infected *Foxn1*^{nu} mice on the BL/6 genetic background at tail sites and scored for papilloma formation (Fig. 4-11A). There was no statistical difference between the timing of onset of papilloma formation on these two strains (Log-rank analysis, P=0.732). Contrary to *Foxn1*^{nu}-Balb/c mice, infection of torso skin of *Foxn1*^{nu}-BL/6 mice did result in papillomas (Fig. 4-11B) suggesting that genetic background could potentially be playing a role in MmuPV1 infection. Besides nude mice, which are primarily T-cell deficient, we also tested susceptibility of other popularly used immunodeficient strains as shown in Fig. 4-11A and compared papilloma onset to *Foxn1*^{nu}-Balb/c mice. We found that the commonly used *NOD.Cg-Prkdc*^{scid} *Il2rg*^{tm1Wjl}*/SzJ* (hereafter referred to as NSG mice) strain is susceptible to MmuPV1 infection as well (Fig. 4-11, Green line). NSG mice are characterized by presence of two mutations - the *scid* mutation in the *Prkdc* (Protein Kinase, DNA-Activated, Catalytic Polypeptide) gene that renders the mice T and B-cell deficient; and *IL2rg*^{null} mutation in the IL2-receptor gamma (IL-2Rγ) chain that leads to deficiency in functional natural killer cells. There was no statistical difference between timing of onset of papillomas between NSG mice and *Foxn1*^{nu}-Balb/c mice (Log rank, P=0.0625). Interestingly, *NOD.Cg-Prkdc*^{scid}*/SzJ* (NOD-SCID) mice, that lack the *IL2rg*^{null} mutation and are also extensively used model were found to be resistant to MmuPV1 infection (Fig. 4-11, Navy blue line). This is consistent with studies by other groups as well (101). Therefore we tested the contribution of the IL-2Rγ to MmuPV1-dependent disease by making use of B6.129S4-*Il2rg*^{tm1Wjl}/J mice (hereafter referred to as IL2rg^{null} mice) that are used to study X-linked severe combined immunodeficiency

(XSCID) which is characterized by mutations in the IL-2Rγ chain (292). These mice lack natural killer (NK) cells and a subset of dendritic cells (DCs) producing IFN-γ (256, 293-295) and also show defects in development of the T-cells (296). We found that IL2rg^{null} mice are susceptible to MmuPV1 induced papillomas (Fig. 4-11A, Magenta line) similar to *Foxn1*^{nu}-Balb/c mice (Log-rank analysis, *P=0.1208)*. These observations together suggested that at immunodeficient strains are susceptible to MmuPV1 infection. During the course of these studies animals were kept under observation for a total period of at least 6 months. We observed that lateral transmission of virus to uninfected sites that resulted in overt papillomas was observed only in the nude mouse strains and none of the other strains tested (data not shown).

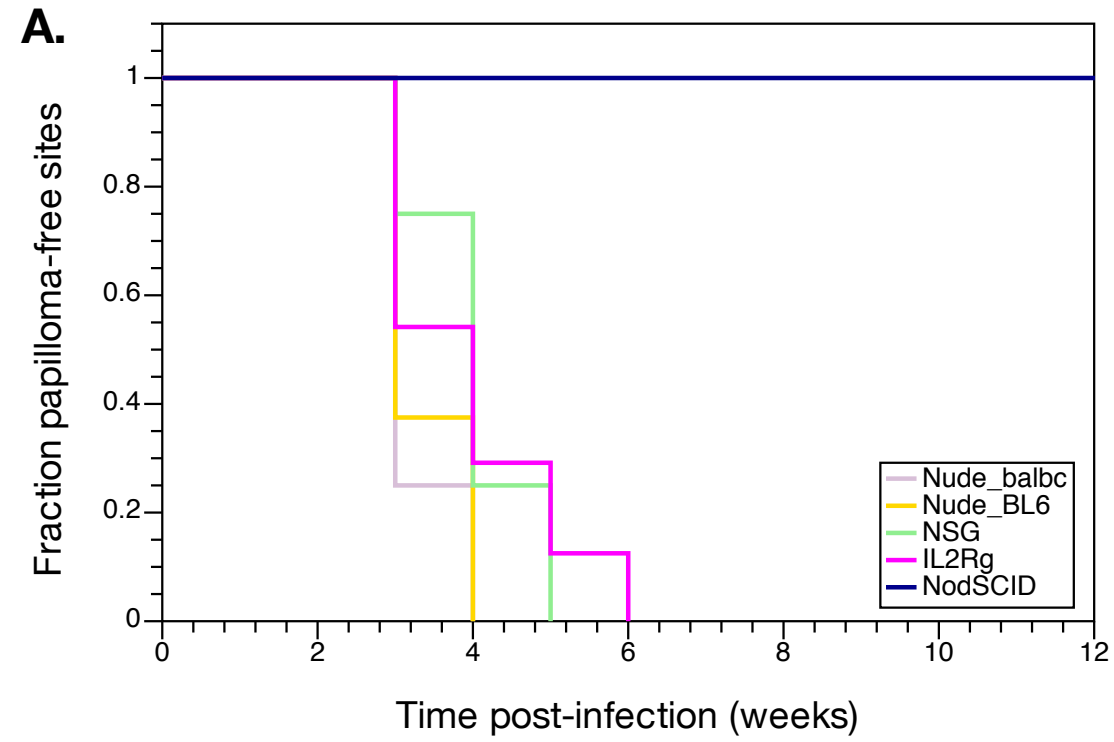



Fig. 4-11. T-cell deficiency is required for MmuPV1-induced infection

Fig. 4-11. T-cell deficiency is required for MmuPV1-induced infection

A. Different immunodeficient strains were infected (16 sites/condition) with 10^8 VGE dose MmuPV1 at tails and papilloma onset was monitored up to 12 weeks post-infection. Papillomas arose in all strains except NOD-SCID mice. Results have been plotted as a Kaplan-Meier curve. No animals were censored during the course of the experiment.

B. *FoxN1*$^{nu/nu}$ mutation on C57/BL6 mice did result in formation of papillomas on dorsal skin whereas all other strains were found to be resistant to MmuPV1-induced papillomas on dorsal skin.

To delineate which arm of the immune system is required for MmuPV1 infection we tested whether strains of mice selectively deficient for B-cells (B10.129S2(B6)-*Ighm*^{tm1Cgn}/*J*, Table 4.1-Group 1) or sub-populations of T-cells i.e. CD4 deficient (B6.129S2-*Cd4*^{tm1Mak}/*J*, Table 4.1-Group 2) or CD8 deficient (B6.129S2-*Cd8*^{tm1Mak}/*J*, Table 4.1-Group 3) are susceptible to MmuPV1-induced papillomas. Finally, we tested several popularly used immunocompetent strains commonly used for animal research in lab settings - C57/BL6 (Table 4.1, Group 4), BALB/c (Table 4.1, Group 5) and FVB/NJ (Table 4.1, Group 6) for susceptibility to MmuPV1 infection. We infected these mice on tails (as shown in Table 4.1) and ear as well as back sites (data not shown) and observe no papillomas arise up-to six months post infection. This observation is consistent with reports from other groups (56, 100, 101, 128). Recently, in studies where rabbits were infected with vaccinia virus, it was observed lethal disease was seen in rabbits when vaccinia virus was introduced by means of an intradermal injection whereas disease severity was reduced when animals were infected by scarification. On characterizing this observation, it was found that the process of scarification itself is a major contributor to immunoprotection (297). For this reason we tested whether different modes of infection led to disease in immunocompetent mice. We found that while nude mice were susceptible to MmuPV1 infection via multiple modes of infection (Fig. 4-1B), FVB mice were resistant to disease even when virus was introduced via intraderm injection (data not shown). Together, these observations suggest that T-cell deficiency is, in fact, required for MmuPV1 dependent papillomas.

Table 4.1: Strains resistant to MmuPV1 infection

Group No.	Strain	Immune deficiency	# Tail Sites infected*	# Sites w/papillomas (%)**	
1.	B10.129S2(B6)-*Ighm*^{tm1Cgn}/*J*	B cell	16	0	(0)
2.	B6.129S2-*Cd4*^{tm1Mak}/*J*	CD4 T cell	16	0	(0)
3.	B6.129S2-*Cd8*^{tm1Mak}/*J*	CD8 T cell	16	0	(0)
4.	C57/Bl6	None	36	0	(0)
5.	BALB/c	None	48	0	(0)
6.	FVB/NJ	None	48	0	(0)

* Each site infected with 2-4 x 10^8 VGE. **Sites scored at the end of 6 months

4.3. Discussion

Murine papillomavirus, MmuPV1, isolated from cutaneous warts arising on immune deficient *NCR-FoxN1*$^{nu/nu}$ laboratory mice (55, 60) is a valuable animal papillomavirus that provides us, for the first time the opportunity to study papillomavirus infections in the context of a genetically manipulatable host. Using a lab generated clone of MmuPV1 we established the infection model in BALB/c-*FoxN1*$^{nu/nu}$ mice (Fig. 4-5), which are deficient for T-cells, and saw development of papillomatosis at different sites in these animals. This is consistent with observations made by others in characterizing the MmuPV1 infection model in *FoxN1*$^{nu/nu}$ mice (on NCR and NMRI genetic backgrounds) as well as SHO-SCID mice (55, 100, 120). Like previous reports, we also observed that there was lateral transmission of the virus to uninfected sites (Fig. 4-1 D).

To characterize relationship between viral dose and papilloma incidence, we infected BALB/c-*Foxn1*^{nu} with different doses of MmuPV1 virions and found that there is a dose dependent delay in onset of virus-induced papillomas (Fig. 4-9). We found that higher doses of MmuPV1 (10^9, 10^8, and 10^7 VGE respectively) produced consistent MmuPV1 infection with lesions being observed in 100% of the infected sites. In an earlier study it was reported that 10^6 VGE dose did not cause papillomas consistently within 2 months of infection in the athymic mice (100). Our data is consistent with this

observation, but in our longer term monitoring protocol (six months) of infected animals, we found that a number of sites that were infected with low doses of MmuPV1 (i.e. 10^6 and 10^5 VGE) went on to develop papillomas. For example, at the end of three months post infection sites infected with 10^5 VGE MmuPV1 virions did not show any signs of papillomas, but at the end of six months 20% of the infected sites had developed papillomas. Studies with other animal papillomaviruses (ROPV and CRPV) have shown that at low doses papillomaviruses can persist in the animals for a long period of time asymptomatically but exposure to exogenous factors can lead to appearance of papillomavirus associated lesions presumably due to activation of the virus (169, 208, 298, 299). Therefore, it may not be surprising that we saw no lesions for about four months in mice infected with 10^5 VGE MmuPV1 virions prior to some sites then developing warts. Given that these mice were not exposed to any specific exogenous factor over this period of observation,,we conclude that MmuPV1 can establish asymptomatic infections from which clinical disease can arise spontaneously. Indeed, in other studies, we could detect L1 protein and amplified viral DNA at clinically normal, experimentally uninfected sites on the ears of animals that had been experimentally infected with MmuPV1 on their tails (Fig. 4-4A).

That the virus can be laterally transmitted to other uninfected sites is worth noting. While we have documented transmission to other cutaneous sites, others have observed virus being harbored in the oral cavity as well (126). It has also been observed that when an uninfected nude mouse was placed in the same cage with infected littermates the uninfected mouse also developed papillomas (101) demonstrating that the virus can be transmitted horizontally. These observations are potentially valuable as they

can shed light on possible routes of transmission of HPV, particularly in immunodeficient patients who are highly susceptible to HPV infections. One simple reason for transmission of virus to other infected sites is that high titers of virus are produced in nude mice, which can then be easily transmitted to other sites and even other animals, presumably facilitated by the grooming behaviors of mice that may result in microwounds. Upon quantifying the amount of virus produced in viral extracts harvested from nude mice (Fig. 4-4 B), we found that 1mg of wart tissue can produce up to 10^{12} viral genome equivalents (VGE) of MmuPV1, which is an extremely high yield of virus. Studies with Hantaviruses have shown that immunodeficient rats produced much higher amounts of virus upon infection resulting in intracage transfer of virus as opposed to immunocompetent animals(300).

In order to characterize relationship between viral dose and papilloma incidence, we infected BALB/c-*Foxn1*^{nu} with different doses of MmuPV1 virions and found that there is a dose dependent delay in onset of virus-induced papillomas (Fig. 4-9). We found that higher doses of MmuPV1 (10^9, 10^8, and 10^7 VGE respectively) produced consistent MmuPV1 infection with lesions being observed in 100% of the infected sites. In an earlier study it was reported that 10^6 VGE dose did not cause papillomas consistently within 2 months of infection in the athymic mice (100). Our data is consistent with this observation, but in our long term monitoring (six months) of infected animals, we found that a number of sites that were infected with low doses of MmuPV1 (i.e. 10^6 and 10^5 VGE) went on to develop papillomas. Surprisingly at the end of three months post infection sites infected 10^5 VGE MmuPV1 virions did not show any signs of papillomas, but at the end of six months 20% of infected sites developed papillomas. Given that these

mice were not exposed to any exogenous factor to stimulate an emergence of active infection from some latent state of infection, the observation that at the end of 6 months post infection some sites gave rise to papillomas raises the possibility that most likely even at low doses the virus can establishes it's life cycle asymptomatically. As more and more and more virions are produced during the course of the viral life cycle, they continue to re-infect the tissue. Another factor maybe at play is the hypothesized importance of the virus having to infect an epithelial progenitor cell in order to produce a wart. With higher initial doses of virus, the likelihood of infecting the rare progenitor cell is greater. At lower doses of virus, the chance of initially infecting a progenitor cell is much less; but over time, an asymptomatic but active infection would increase the odds that a subsequent infection event ultimately results in a progenitor cell being hit, and thereby a wart emerges. Follicular stem cells have been speculated to be reservoirs of PV infections(93).

It is worth noting that nude mice are hairless due to mutation in FOXN1 gene. This observation may be significant as we did not see papillomas occur as a result of lateral transmission in other immunodeficient strains that have fur and intact FOXN1 (Fig. 4-11A). It has been shown that FOXN1 mutation in nude mice leads to severe keratinization defects and therefore a compromised epithelial barrier. In fact FOXN1 is a major activator of several keratin genes and is generally thought to be a pro-differentiation gene [Reviewed in (301)]. Further, it has been shown that nude mouse skin has a large population of OCT4-positive dermal cells supporting a highly proliferative epithelial stem-cell niche (302). These properties of nude mice coupled with the hypothesis that stem cells are reservoirs for PV infections, suggests that nude mice

maybe more susceptible to skin infection by MmuPV1 than other T-cell deficient mice due to their unique epithelial properties as well.

It is apparent from our observations, as well as other reports that the genetic background is an important factor in MmuPV1-dependent disease. We found that in T-cell deficient immunodeficient nude mice (*FoxN1*^{nu}) genetic background influences site and size of papilloma incidence (S1 Fig 1). For example, BL6-*Foxn1*^{nu} mice were susceptible to MmuPV1 induced papillomas on the torso whereas BALB/c-*Foxn1*^{nu} mice were not. It is interesting to note that nude mice on some genetic backgrounds have inherent resistance to MmuPV1 dependent disease(101). In our studies we found that mice lacking the interleukin-2 receptor common gamma chain (IL-2Rγ-/-), which represent X-SCID, were susceptible to MmuPV1 infection. The IL-2Rγ-/- mice lack NK cells and peyer's patches (responsible for innate immunity) and have limited number of mature T and B cells(256). Further, NSG mice that do lack IL-2Rγ chain were susceptible to MmuPV1; whereas NOD-SCID mice that lack this mutation are resistant to MmuPV1 infection. Given that loss of IL-2Rγ chain contributes to NK-cell deficiency, it remains to be learnt whether innate immune factors play a role in the infection process.

In this study we also performed a careful assessment of the timing of onset of viral gene expression and productive amplification of viral DNA in the context of emerging warts (Fig. 4-6. 4-7 and 4-8). These studies used a fixed amount of virus (10^8 VGE per infection site) applied to three scarified sites on the tail of each nude mouse. We found that both viral late gene expression (L1 capsid) and viral DNA amplification could be observed in differentiated cell compartment as early as 10 days post infection, well before overt warts can be observed, which starts at 4 weeks with this dose of virus

and this strain of mouse. We observed variability in the onset of detectable infection, be it at a microscopic or overt levels, with the some infection sites not showing any microscopic evidence of infection until the 4-week time point when overt warts first appeared. Interestingly, we observed a reproducible spatial pattern in which sites of infection at the base of the tail gave rise to faster growing warts than sites infected at the tip of the tail. The reason for this is unknown, but some possibilities may include blood flow, temperature, and grooming behavior.

Another feature of the time course study is that, whereas in mature warts harvested at 3 (data not shown) or 6 months (Fig. 4-3) post-infection, we observe L1 positive cells throughout the epithelium, including basal cells, an uncommon feature of MmuPV1 observed by others (128), L1-positive cells were restricted to differentiated cells in the early time points, out to day 28 post-infection (Fig. 4-3), suggesting that the complete nature of the viral life cycle is realized at times later than 4 weeks post-infection. Interestingly, canine oral papillomavirus (COPV) is also found to be amplified in basal epithelial cells, though the timing at which this first appears is slightly different(106). COPV, while a mucosal papillomavirus, is closely related to cutaneous HPVs, HPV1 and HPV63, that cause plantar warts (303). Basal cells have been seen to support viral DNA amplification in lesions caused by HPV1 and HPV 63 (25).

In conclusion we think that the MmuPV1 infection model can be a valuable model to study papillomavirus pathogenesis. Based on our limited studies performed in immunodeficient strains, we think this model can be used to study papillomavirus pathogenesis particularly in immunodeficient patients who are highly susceptible to PV infections.

Chapter 5:

UV irradiated immunocompetent mice are susceptible to MmuPV1 induced papillomas

The work described in chapter 4 showed that wild-type immunocompetent mice are resistant to MmuPV1-induced disease. However, we made the novel observation that UVB-irradiated wild-type animals showed increased susceptibility to MmuPV1-associated papillomatosis and in some cases, squamous cell carcinoma. Further we saw a correlation between UVB-induced immunosuppression and onset of papillomas. This work is described in the current chapter. Parts of this chapter have been modified from the following manuscripts:

1. Uberoi A, Yoshida S, Frazer IH, Pitot HC, Lambert PF. 2016. **Role of Ultraviolet Radiation in Papillomavirus-Induced Disease**. PLoS Pathog 12:e1005664.
2. Uberoi A and Lambert PF. **Development of an in vivo infection model to study Mouse papillomavirus-1 (MmuPV1) skin infection.** JVirological Methods (Manuscript submitted).

Dr. Satoshi Yoshida helped in performing UV irradiation using a custom designed UV irradiator that is located in Dr. Hasan Mukhtar's lab in UW-Madison (Medical Sciences Center). Dr. Henry Pitot provided histopathological diagnosis of the tissue. All experiments described in this chapter were performed by me with assistance from Amy Liem and animal care staff when needed. All analyses of the data described in this chapter were performed by me.

5.1. Introduction

Papillomaviruses are species-specific, epitheliotropic, double-stranded DNA viruses. There are over 200 strains or genotypes of human papillomaviruses (HPVs) (73). Mucosotropic HPVs are the most common sexually transmitted pathogens, and a subset of these viruses cause 5% of human cancers, including cervical cancer, other anogenital cancers, and a growing fraction of head and neck cancers (reviewed in (7)). Other HPVs cause cutaneous warts, which are among the most common ailments treated by dermatologists (8-11). They arise most frequently among children (12, 13), and impose a significant burden in immunocompromised patients, particularly amongst organ transplant recipients (14-16). They are ubiquitous in nature and can persist in the skin asymptomatically for years most clearly in context of immunosuppressed patients (14, 17). A subset of cutaneous HPVs also has been causally associated with skin cancer (reviewed in (14, 18, 19)).

The study of papillomavirus-induced disease has long been hindered by the absence of any identified strains of virus that infect laboratory mice. This limitation was overcome with the recent identification of the murine papillomavirus, MmuPV1, isolated from cutaneous warts arising on the T-cell deficient *NMRI-FoxN1*$^{nu/nu}$ strain of laboratory mice (55). MmuPV1 belongs to the *pi*-papillomaviridae genus and is phylogenetically related to cutaneous HPVs and other animal PVs that cause cutaneous disease in exotic rodent species (60). MmuPV1 causes warts in cutaneous epithelium as well as in mucosal epithelium lining the female reproductive tract and oral cavity (55, 100, 101, 120, 128), and in some cases these lesions show signs of neoplastic progression (101, 119).

Multiple studies have shown that the ability of MmuPV1 to cause overt disease is largely restricted to immunodeficient strains of mice (101, 128).

Epidemiological studies have suggested that there is a correlation between exposure to ultraviolet radiation (UVR) and the prevalence of cutaneous HPVs in healthy and immunosuppressed patients, respectively (163, 164). Cutaneous HPVs are more commonly found at anatomical sites exposed to sunlight, and a history of blistering sunburn is associated with prevalent and persistent cutaneous HPV infections (17, 163-165). UVR has also been shown to play a role in papillomavirus-associated disease caused by animal papillomaviruses that infect the African multimammate rat (MnPV) or the cottontail rabbit (CRPV) (58, 167, 169).

In this chapter we demonstrate that UVR, specifically UVB (280 to 315 nm) assists in development of MmuPV1 dependent papillomas and associated malignant progression to squamous cell carcinomas, in immunocompetent strains of mice. We further show that there is a correlation between UVR-induced susceptibility to MmuPV-1 associated disease and UVR-induced immunosuppression. These findings provide a potential explanation for the role of UVR-mediated immunosuppression in papillomavirus-associated disease in humans.

5.2.Results

5.2.1. MmuPV1 causes papillomas in immunocompetent FVB mice following exposure to UV irradiation

Several lines of evidence support a link between UVR exposure and papillomavirus infection (163, 164, 167). We sought to determine if UVR facilitates MmuPV1-induced papillomatosis in immunocompetent strains of mice. We used the inbred FVB/NJ strain of mice for our initial studies because it has been used extensively to study chemically induced skin tumorigenesis (282). Ears and tails of 8-10 week old FVB/NJ mice were infected with 10^8 viral genome equivalents (VGE, a measure of the amount of encapsidated genomes in a stock of virus) of MmuPV1 virions following topical scarification of the epidermis. Twenty-four hours post-infection (h.p.i.), mice were or were not exposed to varying doses of UVB whole body irradiation (280-320nm range UVR). Mice were then observed weekly for papillomatosis (Fig. 5-1A). By 3 months post-infection greater than 50% of infected ear sites developed papillomas in FVB/NJ mice treated with 300 mJ/cm^2 UVB (Fig. 5-1B, Table 5-1, Fig. 5-2 -Panel A). Sites on the tails of the same mice infected with an equal dose of virus failed to develop papillomas. We did not see any papillomas develop at infected sites on non-irradiated mice or mice treated with a lower dose (150 mJ/cm^2) of UVB (Table 5-1). Mock-infected mice exposed to the same doses of UVB did not develop warts (Table 5-1). Lateral transmission of MmuPV1 has been observed in immunodeficient strains of mice experimentally infected with MmuPV1 (55, 101); however, we did not see any warts arise at uninfected sites on the UVB-treated, MmuPV1-infected FVB/NJ mice.

Table 5-1. Papilloma incidence in UVB-irradiated FVB/NJ mice

Group	UVB Dose mJ/cm^2	MmuPV1 infection	# Sites infected*	# Sites w/papilloma**	(%)
1.	0	Infected	8	0	(0)
		Mock-infected	6	0	(0)
2.	150	Infected	16	0	(0)
		Mock-infected	6	0	(0)
3.	300	Infected	24	14	(58.3)
		Mock-infected	8	0	(0)

* Each ear site infected with 10^8 VGE.

** Sites scored at the end of 3 months

The presence and size of warts arising on the MmuPV1-infected ears sites of UVB-treated FVB/NJ mice were monitored for 6 months. In this time frame 17% of the sites developed papillomas that completely regressed (Fig. 5-1D, E: red lines in 1E). 25% of sites developed papillomas that partially regressed (Fig. 5-1D, E-blue lines). Another 17% of sites developed papillomas that continued to grow over the 6 month period (Fig. 5-1D, 5-1E - green lines). 41% of the sites did not develop papillomas. To address whether UVB is exerting its effect directly on the virus, we tested whether UVB treatment at 300 mJ/cm^2 24 hours before infection (h.b.i.) had the same impact on papilloma incidence. Over the initial 4-month period post-infection, papillomas arose with similar frequency as in groups of mice exposed to UVB 24 hpi (Fig. 5-1B, P= 0.814, log-rank, *two-sided*). Again, we saw complete regression of a similar fraction of papillomas when mice were observed up to 6 months post-infection (Fig. 5-1C). We also found that a subset of animals infected with MmuPV1 and treated with a UVB fourteen days post-infection also developed papillomas at a similar frequency (Table 5-2). To learn if the UVA spectra (315-400nm range UVR) also caused immunocompetent mice to become susceptible to MmuPV1-induced papillomatosis, we infected FVB/NJ mice with 10^8 VGE of MmuPV1 at sites on the ears and exposed them to 300 mJ/cm^2 of UVA 24 hours post-infection. We failed to observe papillomas arise at any sites on these mice (Table 5-3). Combining UVA (300 mJ/cm^2) and UVB (300 mJ/cm^2) treatment gave a similar incidence of papillomas as seen with UVB alone (Table 5-3).

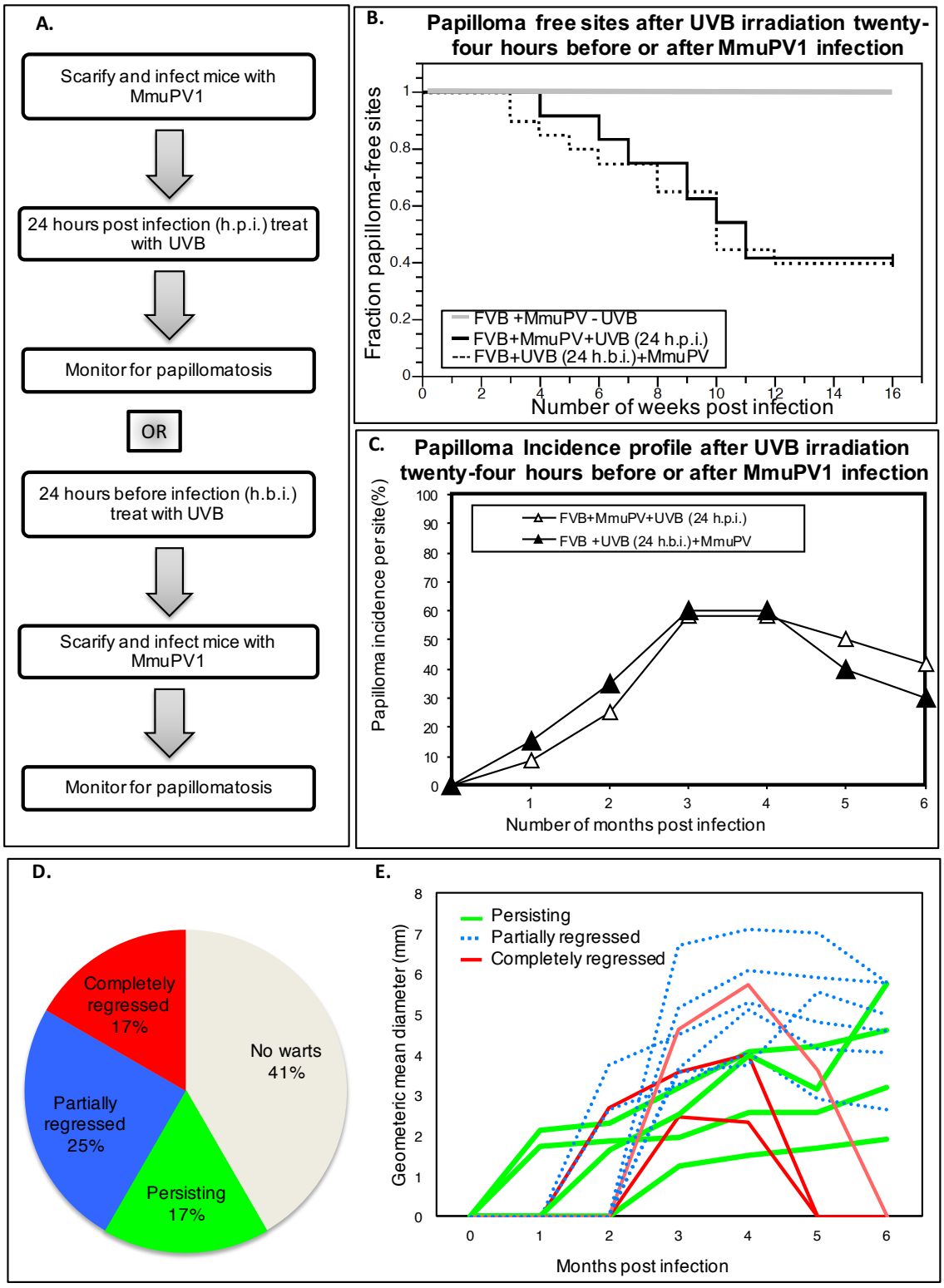

Fig 5-1. MmuPV1-induced papillomas in UVB-irradiated FVB/NJ mice.

Fig 5-1. MmuPV1-induced papillomas in UVB-irradiated FVB/NJ mice. **(A)** Sequence of manipulations to FVB/NJ mice in the MmuPV1-UVB infection model system. Ear sites were scarified and exposed to 10^8 VGE of MmuPV1 either 24 hours before (FVB+UVB 24 h.b.i.+MmuPV) or 24 hours after (FVB+MmuPV1+UVB 24 h.p.i.) 300mJ/cm^2 UVB whole-body irradiation. Sites were then scored weekly for presence of papillomas.

(B) Kaplan-Meyer plots of the fraction of papilloma-free infected ear sites with respect to time. There is no significant difference in the temporal onset of disease between the two experimental groups (FVB+UVB 24 h.p.i.+MmuPV1 vs FVB+MmuPV1+UVB 24 h.b.i.; P= 0.814, Wilcoxon log-rank test, *two-sided*).

(C) Percentage of sites with overt papillomas over a 6-month observation period. In both the cohorts of mice, a subset of papillomas completely regressed by 6 months post-infection.

(D) Distribution of ear sites of UVB-treated FVBN/J mice (FVB+UVB 24 h.p.i.+MmuPV1 group) infected that developed papillomas that completely regressed (red), partially regressed (blue) or continued to grow (green) over the 6 month monitoring period. In grey is the fraction of sites that did not develop papillomas.

(E) Growth profiles of individual papillomas arising in the FVB+UVB 24 h.p.i. +MmuPV1 group during the 6-month monitoring period. Individual lines represent the geometric mean diameter of each papilloma as a function of time. Red lines are papillomas that completed regressed. Blue lines are papillomas that partially regressed. Green lines are papillomas that continued to grow.

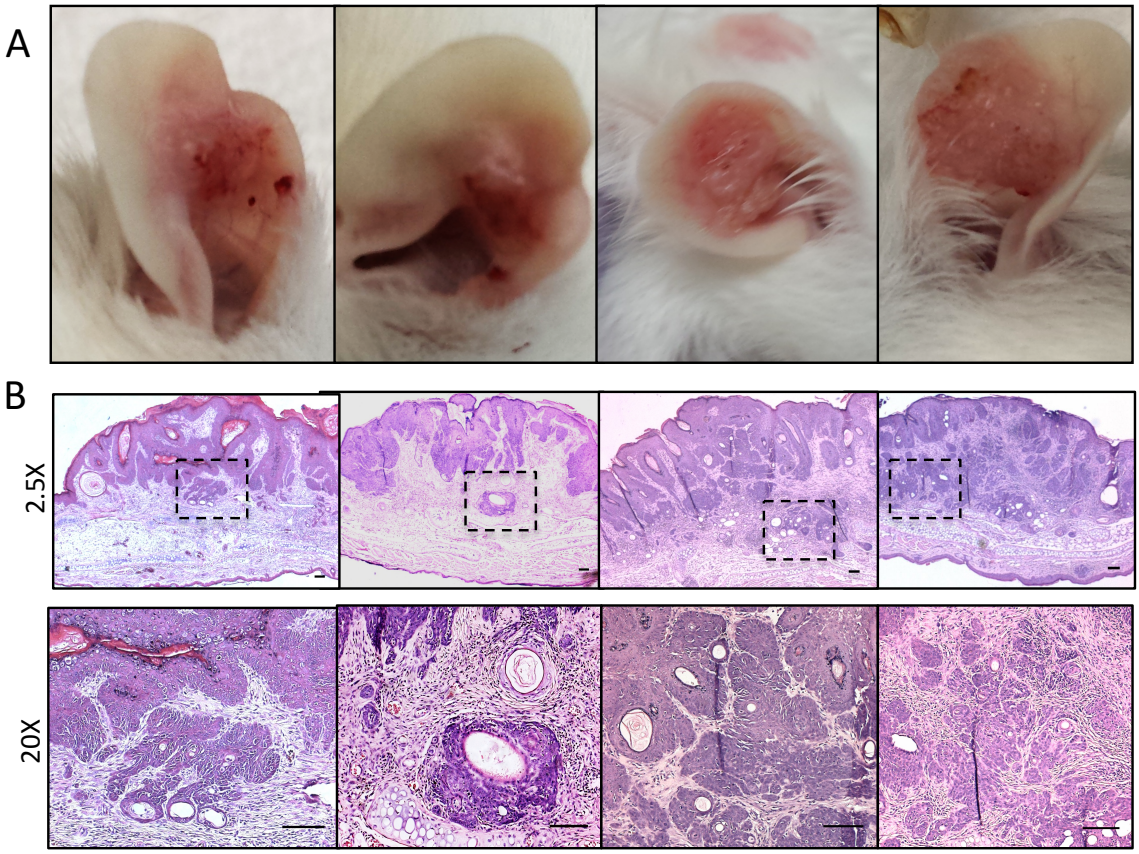

Fig 5-2. Papillomas on ears of immunocompetent FVB/NJ mice.

Fig 5-2. (A) Papillomas on ears of immunocompetent FVB/NJ mice. Examples of papillomas that arose on ears of FVB/NJ mice infected with 10^8 VGE MmuPV1 followed by irradiation with 300mJ/cm^2 UVB. These images represent papillomas at 6 months post infection. **(B) Histopathology of MmuPV1-induced ear papillomas in UVB irradiated FVB/NJ mice.** Top panel shows H&E images (taken using a 2.5X objective) of lesions. Bottom panel with insets (taken using a 20X objective) indicate corresponding areas of lesions showing focal regions invasivity within the underlying dermis. Scale bars denote 100μm.

Table 5-2. Papilloma incidence in FVB/NJ mice infected with MmuPV1 followed by treatment with UVB at different time points

Group	UVB Dose mJ/cm^2	UVB-Time post infection*	MmuPV1 infection	# Sites infected**	# Sites w/papillomas*** (%)
1.	300	24 hrs before	Infected	24	14 (58.33)
			Mock-infected	8	0 (0)
2.	300	24 hrs after	Infected	8	3 (37.50)
			Mock-infected	6	0 (0)
3.	300	14 days after	Infected	16	8 (50.00)
			Mock-infected	8	0 (0)

* Indicates when the UVB treatment was performed

** Each ear site infected with 10^8 VGE.

*** Sites scored at the end of 3 months

Table 5-3. Papilloma incidence in FVB/NJ mice infected with MmuPV1 followed by treatment with UVB/UVA

Group	UVB Dose mJ/cm^2	UVA Dose J/cm^2	MmuPV1 infection	# Sites infected*	# Sites w/papillomas** (%)
1.	0	300	Infected	12	0 (0)
			Mock-infected	6	0 (0)
2.	300	0	Infected	16	7 (43.75)
			Mock-infected	6	0 (0)
3.	300	300	Infected	16	8 (50)
			Mock-infected	6	0 (0)

* Each ear site infected with 10^8 VGE.

** Sites scored at the end of 3 months

We also tested the susceptibility of other commonly used, wild-type, inbred strains of mice to MmuPV1-induced disease with varying doses of UVB (Table 5-4): 30% of infected ear sites on C57/BL6 mice developed papillomas at the three-month time point when treated with UVB at a higher dose of 600mJ/cm^2. Only one infected site on a BALB/c mouse developed a papilloma when exposed to 1200mJ/cm^2 UVB (Table 5-4). These results indicate that there are strain differences in susceptibility of mice to MmuPV1-induced disease following UVB irradiation. Overall, we found that FVB/NJ mice were most susceptible to MmuPV1 disease at the lowest dose of UVB. Therefore, we pursued all further studies of the role of UVB in inducing MmuPV1 infection using the FVB/NJ strain of mice.

To investigate the relationship between viral dose and papilloma incidence in FVB/NJ mice treated with UVB, we infected mice on their ears with 10^8, 10^7 or 10^6 VGE of MmuPV1 and exposed the mice to 300mJ/cm^2 of UVB 24 hours post-infection (Fig. 5-3). In parallel, T-cell deficient FoxN1$^{nu/nu}$ mice were also infected at ear sites with the same stock of virus at designated doses in the absence of UVB-treatment (Fig. 5-3). By 3 months post-infection, 90% of ear sites in FoxN1$^{nu/nu}$ mice infected with 10^8 and 10^7 VGE MmuPV1 developed papillomas (Fig. 5-3A,B – Right). At this time-point, papillomas developed in UVB-irradiated FVB/NJ mice infected with 10^8 and 10^7 VGE MmuPV1, but at lower penetrance (Fig. 5-3A,B - Left) and no papillomas formed on UVB-treated FVB/NJ mice infected with 10^6 VGE of MmuPV1 up to 6 months post-infection (Fig. 5-3B- Right). In contrast, 37.5% of FoxN1$^{nu/nu}$ mice ear sites infected with 10^6 VGE of MmuPV1 develop papillomas (Fig. 5-3B-Left). Non-irradiated FVB/NJ mice infected with 10^8, 10^7 or 10^6 VGE of MmuPV1 did not develop any papillomas (data not shown).

These results indicate that a higher threshold in the amount of virus is required to see papilloma induction in immunocompetent animals after UVB irradiation. Furthermore, there was complete regression of a subset of papillomas in FVB/NJ mice infected with 10^7 and 10^8 VGE of MmuPV1 when monitored up to 6 months post-infection (Fig. 5-3B). There was no regression of papillomas in immunodeficient FoxN1$^{nu/nu}$ mice.

Table 5-4: Papilloma incidence in immunocompetent mice infected with MmuPV1 followed by treatment with UVB

S. No.	Genetic background	UVB Dose mJ/cm^2	Infection	# Sites infected*	# Sites w/papillomas (%)
1.	FVB/NJ	0	MmuPV1 infected	8	0 (0)
			Mock infected	6	0 (0)
2.	FVB/NJ	150	MmuPV1 infected	16	0 (0)
			Mock infected	6	0 (0)
3.	FVB/NJ	300	MmuPV1 infected	24	14 (58.3)
			Mock infected	8	0 (0)
4.	C57/BL6	0	MmuPV1 infected	6	0 (0)
			Mock infected	6	0 (0)
5.	C57/BL6	150	MmuPV1 infected	6	0 (0)
			Mock infected	6	0 (0)
6.	C57/BL6	300	MmuPV1 infected	8	1 (12.5)
			Mock infected	8	0 (0)
7.	C57/BL6	600	MmuPV1 infected	10	3 (30.0)
			Mock infected	10	0 (0)
8.	BALB/c	0	MmuPV1 infected	6	0 (0)
			Mock infected	6	0 (0)
9.	BALB/c	150	MmuPV1 infected	6	0 (0)
			Mock infected	6	0 (0)
10	BALB/c	300	MmuPV1 infected	8	0 (0)
			Mock infected	8	0 (0)
11	BALB/c	600	MmuPV1 infected	8	0 (0)
			Mock infected	8	0 (0)
12	BALB/c	1200	MmuPV1 infected	8	1 (12.5)
			Mock infected	8	0 (0)

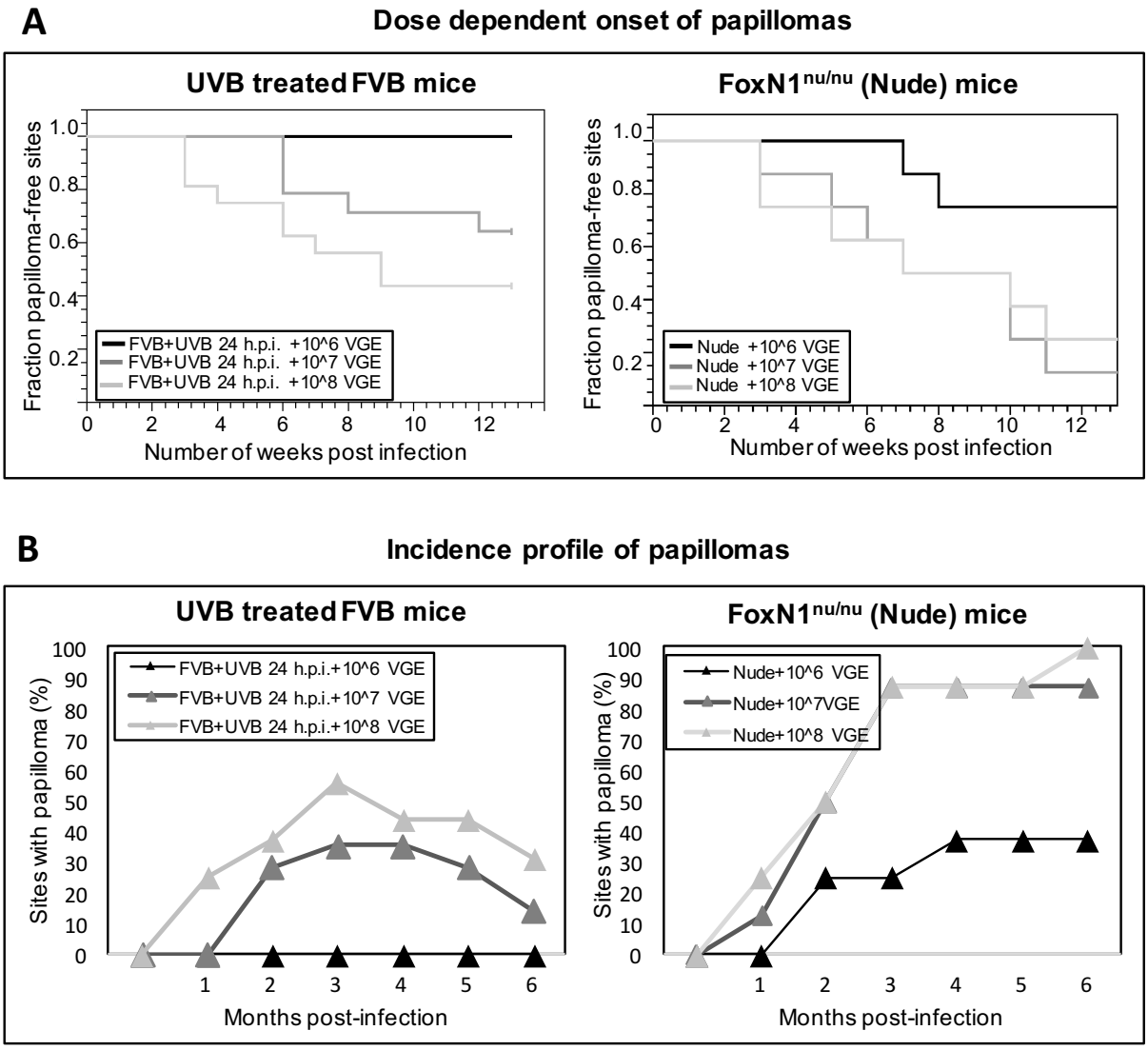

Fig 5-3. Viral dose-dependent incidence of papillomas in UVB-treated FVB/NJ mice and in *FoxN1*$^{nu/nu}$ mice.

Fig 5-3. Viral dose-dependent incidence of papillomas in UVB-treated FVB/NJ mice and in FoxN1$^{nu/nu}$ mice. Immunocompetent FVB/NJ mice were infected at ear sites with 10^8, 10^7 or 10^6 VGE of MmuPV1 virions following scarification. Twenty-four hours post-infection (h.p.i.), mice were irradiated with 300mJ/cm^2 UVB and scored weekly for presence of ear papillomas up to 6 months. In parallel, T-cell deficient FoxN1$^{nu/nu}$ mice not treated with UVB were infected at ear sites with the same stock of virus at designated doses. Graphs for each strain are shown separately.

(A) Kaplan-Meyer plot of the fraction of papilloma-free infected sites over the initial four-month period following infection. There was no significant difference between incidences of disease between UVB-irradiated FVB mice treated with 10^7 versus 10^8 VGE of MmuPV1 (P= 0.21, Wilcoxon log-rank test, *two-sided*). FVB/NJ mice infected with 10^6 VGE of MmuPV1 did not develop any papillomas.

(B) Percentage of sites with overt papillomas over a 6-month observation period. Note that in both groups, UVB-irradiated FVB mice infected with 10^7 and 10^8 VGE of MmuPV1, a subset of papillomas completely regressed by 6 months post-infection (left). There was no regression of papillomas in FoxN1$^{nu/nu}$ mice (right).

5.2.2. MmuPV1-induced papillomas in UVB-irradiated immunocompetent mice show productive infection and signs of neoplastic transformation

Lesions arising on the ear sites of MmuPV1-infected FVB mice treated with UVB were harvested at 6 months post-infection and analyzed histopathologically. They showed sessile papilloma-like morphology with hyperkeratosis (Fig. 5-4A, left; Fig. 5-2-Panel B). Cells within the stratum granulosum showed presence of koilocytes consistent with productive papillomavirus infection (Fig. 5-4A, middle). The MmuPV1 major viral capsid protein was expressed in these papillomas as indicated by L1-specific immunofluorescence (Fig. 5-4A, right). Viral capsid protein was mostly detected in the koilocytes and other cells within the upper layers of the epithelia (suprabasal and terminally differentiated) with some L1-positive cells occasionally observed in the basal layer consistent with prior findings in immunodeficient mice (100). The sessile papillomas were accompanied by multiple areas of atypical squamous cell hyperplasia, several of which were suggestive of early neoplastic transformation, consistent with other reports (100, 101, 120). In our case, however, we also found focal areas of malignant progression consistent with squamous cell carcinoma with invasion extending into follicular structures deep within the dermis as evident from cytokeratin-14 staining (Fig 5-4B). These areas of malignant progression were observed in several histopathologically scored lesions (e.g. see Fig. 5-2 - Panel B). Foci of chronic inflammation were also noted in the lesions, some of which extended into the atypical dermis (Fig 5-4B).

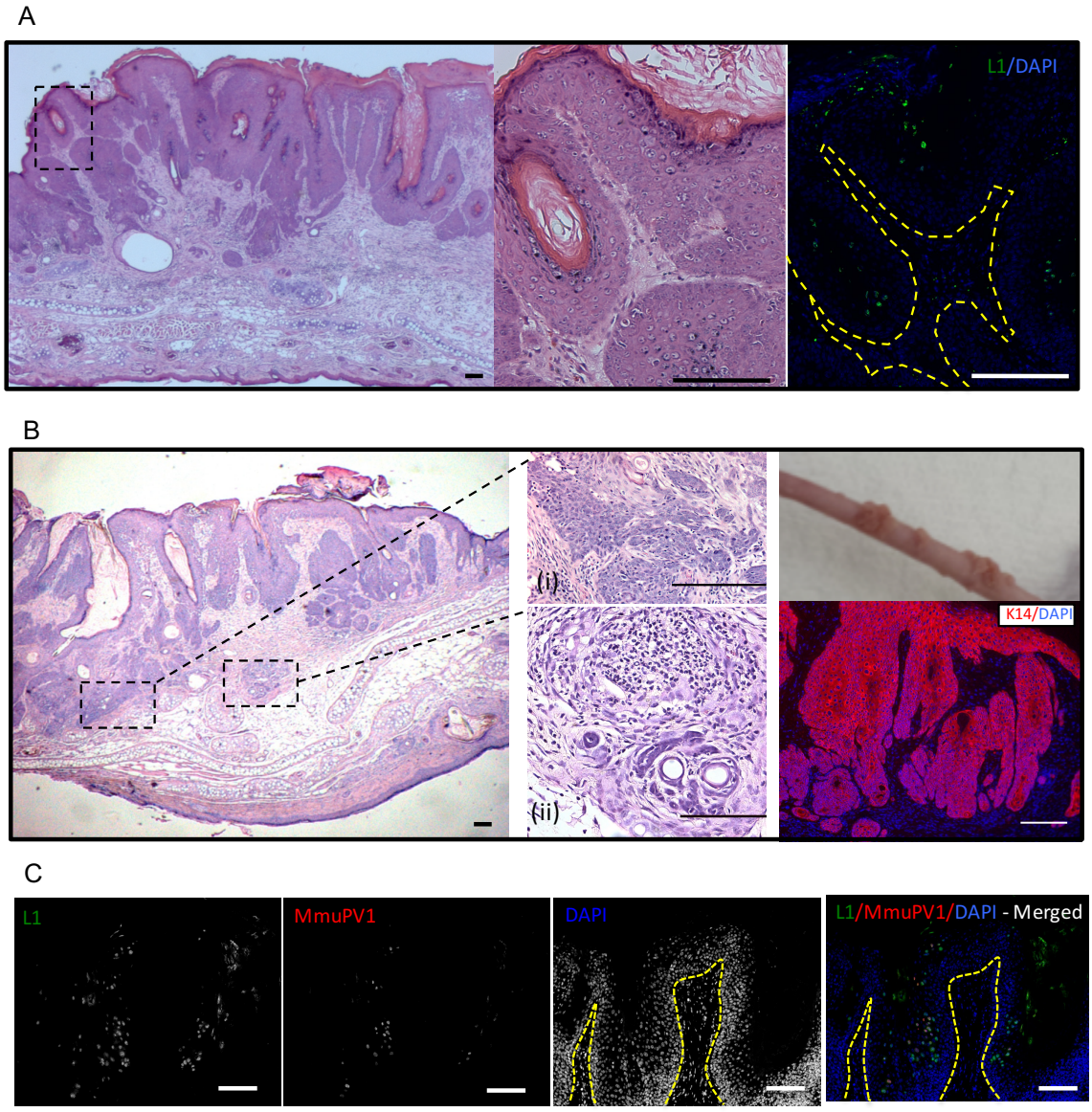

Fig 5-4. Histopathological analysis of MmuPV1-induced papillomas in UVB – irradiated mice.

Fig 5-4. Histopathological analysis of MmuPV1-induced papillomas in UVB – irradiated mice.

(A) H&E staining of ear tissue indicating presence of a sessile ear papilloma caused by MmuPV1 in FVB mice following UVB irradiation (left). Presence of koilocytes is indicated (middle). L1-immunofluorescent staining of papillomas (right).

(B) Sessile papilloma with areas indicating frank malignant transformation (inset;i) and foci of inflammation (inset;ii). K14 staining of papilloma showing epithelial invasion into dermis. Papillomas on the tail of an immunodeficient BALB/c *FoxN1*^{nu} mice (right, top). These papillomas were formed as a result of infection with viral extracts prepared from papillomas that arose in immunocompetent FVB mice infected with MmuPV1 followed by UVB irradiation.

(C) L1 (green)-MmuPV1 FISH (red) co-staining of MmuPV1-induced ear papillomas in UVB irradiated FVB/NJ mice. The nuclei were counterstained with DAPI (blue). Scale bars represent 100μm.

Southern blot quantification showed that viral extracts harvested from papillomas from immunocompetent mice had a 1000-fold reduction in the amount of VGE/mg of wart harvested compared to that quantified from papillomas arising in immunocompromised *FoxN1*^{nu} mice (Fig 5-5). Regardless, the viral extracts from immunocompetent mice were infectious and caused papillomas in *FoxN1*^{nu} mice (Fig 5-4B). MmuPV1 DNA-specific *in situ* hybridization coupled with L1 immunohistochemistry analysis of MmuPV1-induced ear papillomas in UVB irradiated FVB/NJ mice (Fig. 5-4C) showed presence of amplified viral DNA and L1 capsid. Robust L1 expression was seen throughout the papilloma most frequently in the suprabasal layers of the epithelia. The FISH positive cells were comparatively less frequent and predominantly seen in the spinous epithelium occasionally showing co-localization with L1 positive nuclei. We observed that, while regions of papillomatosis showed presence of amplified MmuPV1 DNA, areas of malignancy showed little to no presence of MmuPV1 amplified DNA (Fig. 5-6). Presence of the viral major capsid protein (L1) and amplified viral DNA, which are markers for the productive stage of the viral life cycle [reviewed in (72)], coupled with findings from the transmission experiments (Fig. 5-4B), confirm that MmuPV1 establishes a productive infection in immunocompetent mice following UVB treatment.

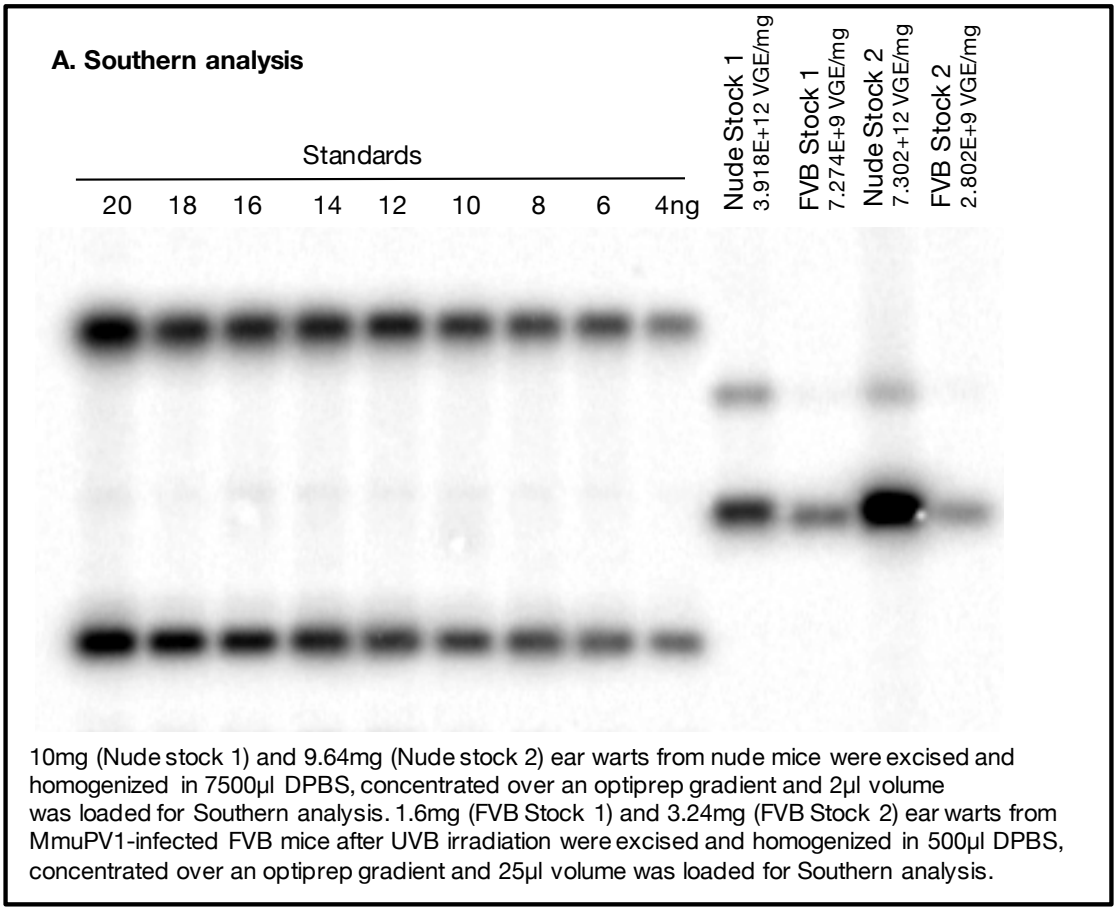

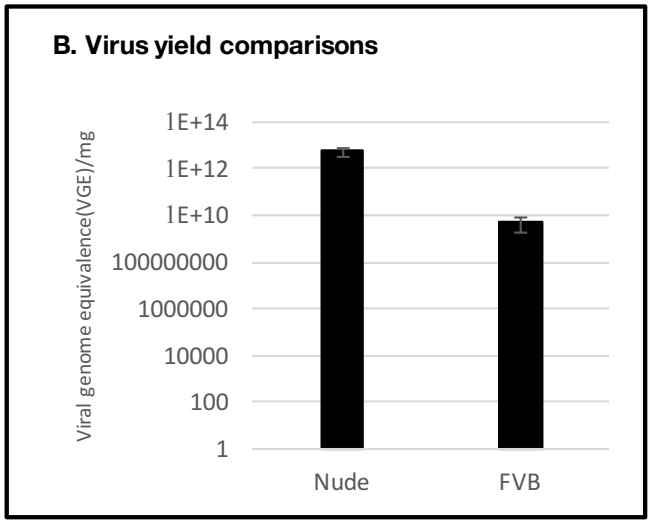

Fig. 5-5. Quantification of Viral Genome Equivalence by Southern Hybridization.

Southern analysis used to quantify virus stocks obtained from MmuPV1 induced ear warts in immunodeficient nude mice and UVB-irradiated FVB/NJ mice.

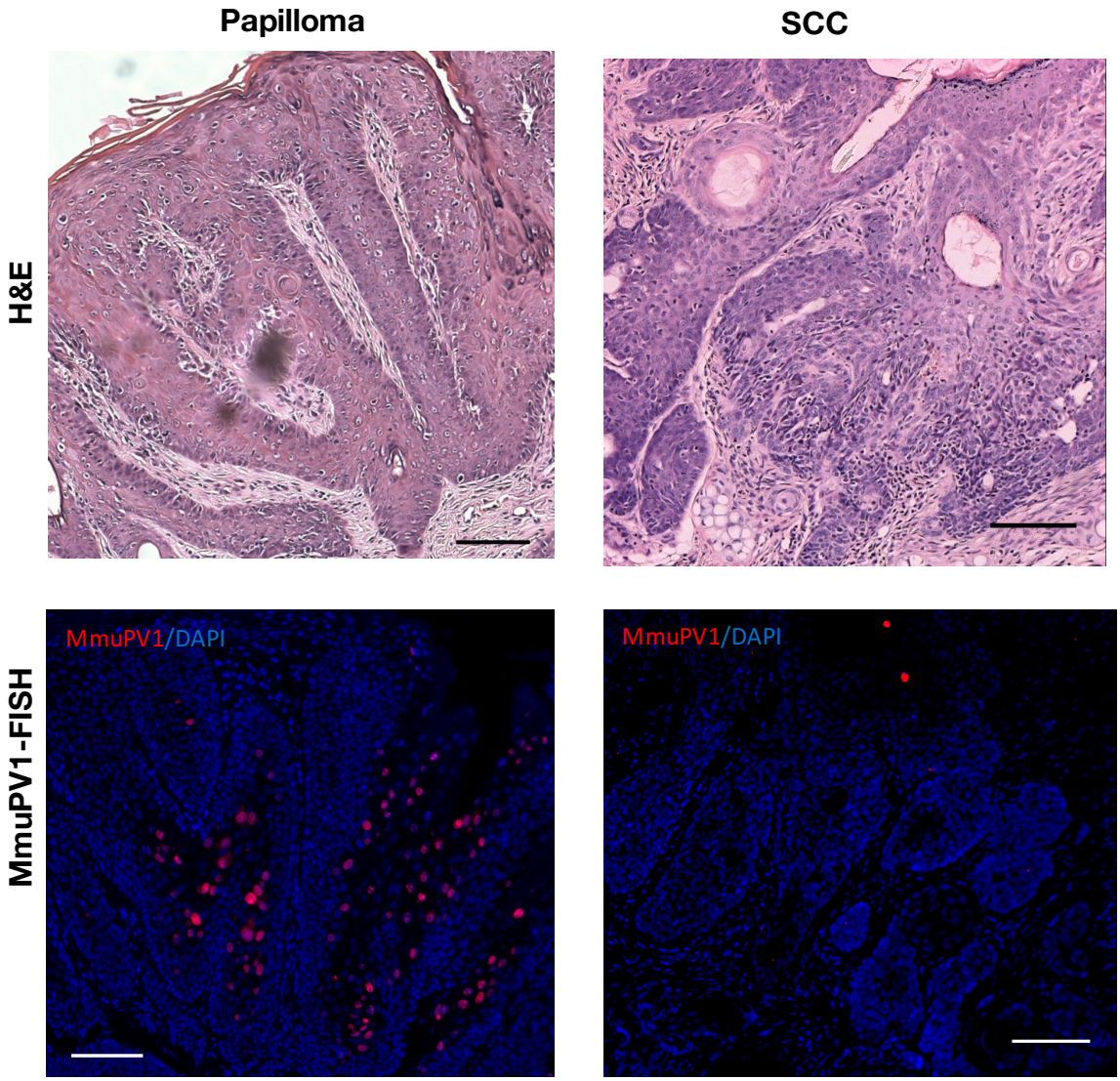

Fig. 5-6. Fluorescent in *situ* hybridization to detect MmuPV1 in papilloma and malignant regions.

MmuPV1-FISH was performed on papillomas that arose on ears of FVB/NJ mice infected with 10^8 VGE MmuPV1 followed by irradiation with 300mJ/cm^2 UVB. Areas of papillomatosis show presence of amplified viral DNA (red) whereas cancerous regions show little to no presence of amplified viral DNA. Nuclei were counterstained with DAPI (blue). Scale bars denote 100μm.

5.2.3. UVB irradiation has a systemic effect on host biology

There are several lines of evidence in the field of photoimmunology indicating that UVB impairs a variety of immune responses in humans and laboratory animals both locally, within UV-irradiated skin, and systemically, at distant sites (174, 304, 305)**.** To test whether UVB-assisted pathogenesis in MmuPV1-infected FVB/NJ mice is due to a systemic or a local effect of UVB-irradiation, we infected FVB/NJ mice at ear sites as described previously. Twenty-four hours after infection, mice were anesthetized and the infected ear sites were shielded with tin foil leaving the rest of the mouse exposed to 300 mJ/cm^2 of UVB irradiation (Fig. 5-7A). Mice were then observed weekly to score for papillomatosis up to six months post-infection. At the end of 16 weeks, approximately 55% of infected mice developed papillomas on ear sites (Fig. 5-7B). There was no significant difference in the temporal onset of papillomas between shielded and unshielded mice (P= 0.938, log-rank, *two sided*). The animals were kept under observation for 6 months and scored weekly for papilloma incidence. We found that by six months post-infection 27% of the papillomas completely regressed in the mouse cohort whose infection sites were shielded, similar to that seen in the unshielded cohort, where 28.5% of the papillomas had completely regressed. These results indicate that systemic effects of UVB on host biology must contribute to the ability of UVB to induce MmuPV1-dependent disease.

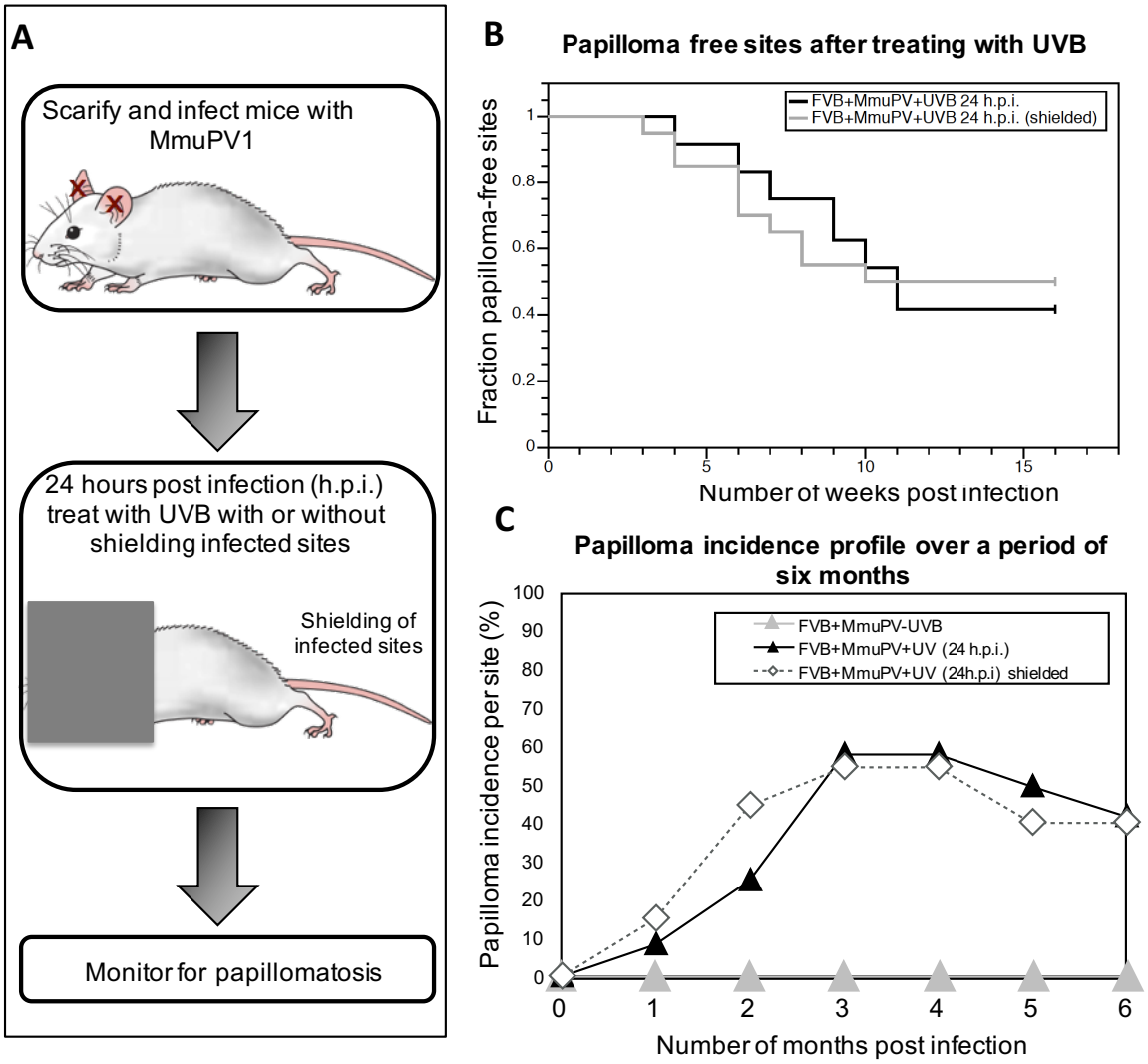

Fig 5-7. Systemic effect of UVB assists in MmuPV-dependent papillomatosis.

Fig 5-7. Systemic effect of UVB assists in MmuPV-dependent papillomatosis.

(A) Schematic illustrating the experimental design. Twenty-four hours post infection with 10^8 VGE, groups of mice were either whole body UVB irradiated (FVB+MmuPV+UVB 24h.p.i.) or infected sites were shielded from UVB (FVB+MmuPV+UVB 24h.p.i. shielded) and scored weekly for presence of ear papillomas up to 6 months. UVB dose was 300mJ/cm^2. Scoring data is compared to the FVB+MmuPV+UVB 24h.p.i. group also shown in Figure 2, as both experiments were performed at the same time.

(B) Kaplan-Meyer plots of the fraction of papilloma-free infected sites over the first 12 weeks post-infection. There was no significant difference between the two experimental groups (shielded versus unshielded ears) (P= 0.938) as assessed by Wilcoxon log-rank analysis.

(C) Percentage of sites with overt papillomas over a 6-month observation period. Some papillomas completely regressed in both groups. Control animals i.e. non-UVB irradiated FVB mice infected with MmuPV1 (FVB+MmuPV-UVB) did not develop any papillomas over the 6 month observation period.

5.2.4. UVB-mediated immunosuppression correlates with development of MmuPV1- dependent cutaneous disease

Through the study of different strains of immunodeficient mice, it has been found that T-cell deficiency is necessary for the development of MmuPV1-dependent papillomas (101, 128). Several studies have demonstrated that UVB causes cell-mediated immunosuppression in mice (306, 307), reviewed in (174, 184, 304, 308). Cell-mediated immunosuppression by UVB has traditionally been measured by monitoring contact hypersensitvity (CHS) responses (174, 184, 186, 304, 309). A single exposure to UVB irradiation is sufficient to inhibit CHS responses in some strains of mice (185, 310). To determine if the single dose of UVB irradiation (300mJ/cm^2) that makes FVB/NJ mice susceptible to MmuPV1-induced papillomatosis (Table 5-1) is sufficient to cause immunosuppression in this strain of mice, we measured DTH responses in these and control mice not treated with UVB (276, 311). Ten days post-UVB treatment, FVB/NJ mice were sensitized to an antigen by topically applying 0.5 mg 1-Chloro-2, 4-Di-Nitrobenzene (DNCB) on the shaved backs of the mice. Five days later we determined the level of immune response to this antigen by applying 0.2 mg DNCB to a distant site (the ears) and monitoring CHS responses (Fig. 5-8). CHS was assessed by measuring ear swelling every 24 hours for four days. A single exposure to UVB (300mJ/cm^2) was capable of causing immunosuppression in FVB/NJ mice as evidenced by a marked decrease in swelling in response to DNCB challenge in the UVB treated mice compared to non-UVB treated mice (Fig. 5-8). This difference was statistically significant ($p<0.005$, T-test).

To assess whether this immunosuppression was systemic or local, we repeated the CHS assay on mice in which we shielded their ears from UVB as described previously. These mice also displayed reduced swelling in response to challenge with DNCB on their ears, indicating that UVB-induced immunosuppression in these mice is systemic (Fig. 5-8). This observation suggests that UVB causes systemic immunosuppression that may assist MmuPV1-dependent disease (Figs. 5-1- 5-4).

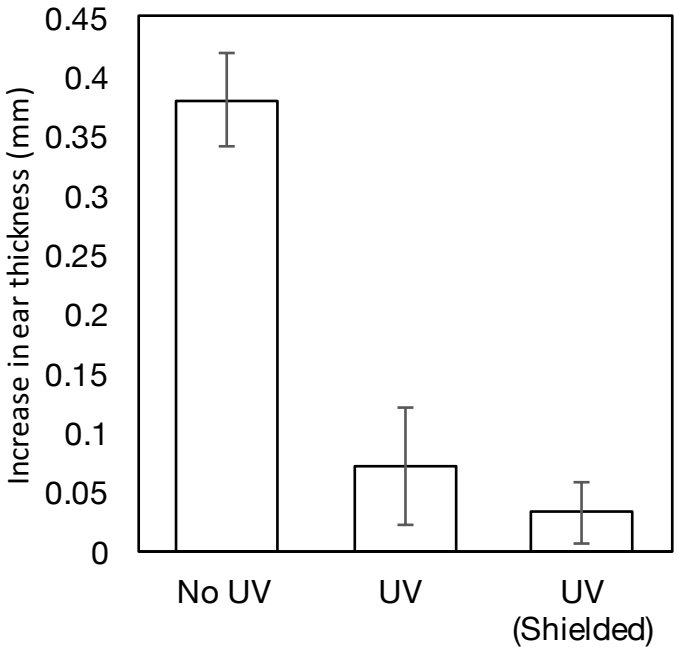

Fig 5-8. UVB causes systemic immunosuppression of host.

Three groups of mice were treated as follows: a control group that was not UVB irradiated (FVB-UVB, White bars, n=3), UVB-irradiated group (FVB+UVB, n=6) and UVB-irradiated group in which ears were shielded from UVB exposure (FVB+UVB (ears shielded)). Ear thickness reported as the average of the difference between DNCB-challenged (left) and unchallenged (right) ears 72 hours post challenge. SEM refers to standard error in measurement computed by measuring standard deviation. CHS measured by the change in thickness of the ear was found to be statistically significant between UVB-treated mice and non-irradiated control mice (student t-test, $p<0.005$, *two-sided)* for both UVB-treated groups.

5.2.5. Mice displaying UVB-induced immune suppression at three-months preferentially develop MmuPV1-induced warts.

To determine if UVB-mediated immune suppression correlates with papilloma incidence we performed long-term CHS assays in FVB/NJ mice following infection with MmuPV1 and UVB-treatment. Mice were infected with MmuPV1 in their right ear and exposed to a single dose of UVB (300 mJ/cm^2) 24 hrs post-infection as described previously (Fig. 5-1A). Ten days post UVB-treatment animals were sensitized to antigen by painting 0.5 mg of DNCB on their shaved backs. Mice were monitored for papilloma formation. Three months post infection, animals were challenged with 0.2 mg DNCB on the uninfected, left ear. We chose the three-month time period because this is the time by which FVB/NJ mice treated with UVB develop the maximal number of MmuPV1-induced warts (Fig. 5-1C). Post-challenge we measured ear swelling up to 96 hrs (Fig. 5-9). We found that in the control group (animals not treated with UVB) a long-lived CHS response was established as evidenced by swelling of the ears. UVB-treated, uninfected control mice displayed a range in levels of CHS response, indicative of variable levels of long-term immune suppression. This was also seen in UVB-treated, MmuPV1-infected mice. Of specific note, the mice in this latter group that retained immune-suppression at the end of 3 months were the same ones that had developed MmuPV1-induced warts. The difference in ear swelling between the UVB-irradiated animals infected with MmuPV1 that developed warts and those that did not develop warts was statistically significant (P=0.016, Wilcoxon rank-sum, *two-sided*). These data demonstrate a strong correlation between, UVB-induced immmunosuppression and MmuPV1-dependent pathogenesis.

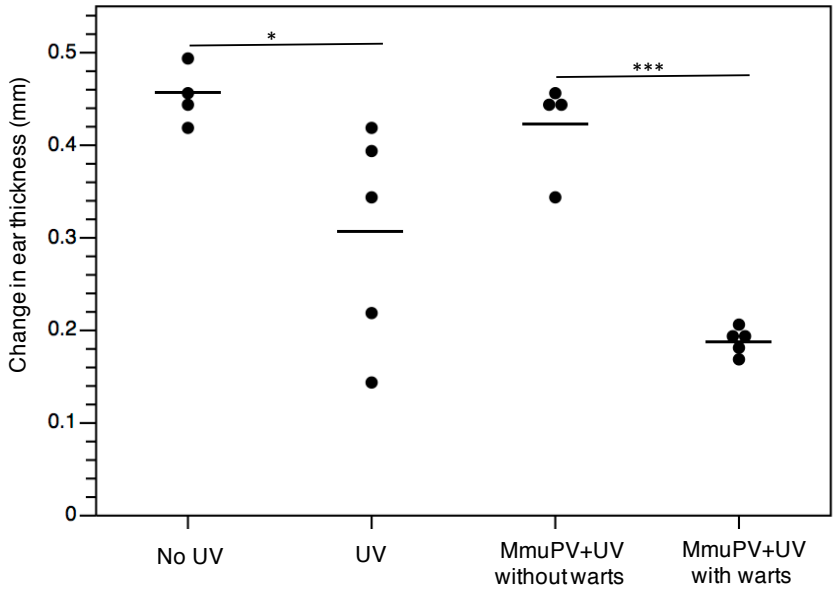

Fig 5-9. Immune suppression in UVB-irradiated mice correlates with papilloma incidence.

Mice were either infected with MmuPV1 or vehicle followed by UVB irradiation (300mJ/cm^2) in the right ear. Mice were sensitized with DNCB 10 days post UVB exposure and were challenged DNCB in the left ear 3 months following infection. Ear swelling was measured by means of a Vernier calipers. Ear thickness is reported as the average of the difference between ear thickness 0 hrs post challenge and 72 hrs post challenge. Ear thickness for each mouse is shown as a dot plot. The black lines represent the mean reading for each group. Wilcoxon rank-sum test was used to analyze difference between several groups. There was significant difference between UVB-irradiated (UV) and control (no UV) groups (*p=0.021, *two-sided*). There was significant difference between the UVB irradiated animals infected with MmuPV1 that developed warts and those that did not develop warts (**p=0.016, *two-sided*). There was no significant difference between control (no UV) and UVB-irradiated

mice infected with MmuPV1 that did not develop warts (MmuPV1+ UV without warts).

5.3.Discussion

The lack of infection models in a tractable laboratory animal has limited our ability to study the pathogenesis of papillomaviruses in their natural hosts. The murine papillomavirus, MmuPV1, isolated from cutaneous warts arising on immunodeficient *NCR-FoxN1*$^{nu/nu}$ laboratory mice (55, 60) is a valuable animal papillomavirus because it provides us, for the first time, the opportunity to study papillomavirus infections in the context of a genetically manipulatable host.

Prior to this study, MmuPV1-associated papillomatosis has been described primarily in the context of immunodeficient strains of mice (101, 119, 120, 128), though there have been reports that MmuPV1 can cause warts on hairless strains of mice, which are thought to be immunocompetent (55, 127). Consistent with a role of the host immune system in limiting MmuPV1-induced disease, Handisurya, *et al*. (2014) found that Cyclosporin A treatment is required for induction and maintenance of MmuPV1-induced papillomas in immunocompetent mice (128). These authors did find that, at very high doses of virus (10^{12} VGEs), the SENCAR strain of mice, selectively bred for high susceptibility to skin tumor induction by chemical carcinogens (129), developed papillomas, but these papillomas regressed within two weeks of appearing.

In this study we investigated whether the UVB spectra impacts susceptibility of immunocompetent mice to MmuPV1. There was limited prior evidence suggesting the role of UV radiation in other animal models for papillomavirus infection. *Mastomys*

natalensis Papillomavirus (MnPV) is a rodent papillomavirus that is shown to cause papillomatosis in the African multimammate rat (58). MnPV DNA was found in UV induced tumors in HRA/Skh mice that are hairless but immunocompetent (167). Further, studies showed that cell-free extracts containing MnPV enhanced UV-induced tumorigenesis (168). We found that when FVB/NJ mice were exposed to high doses of UVB (Table 5-1) greater than 50% of infected sites developed papillomas by 3 months, some of which persisted for 6 months (Figs. 5-1 – 5-4). UVB also induced MmuPV1-dependent papillomatosis in other strains of immunocompetent mice (Table 5-4).

Histopathological analysis of the papillomas in the MmuPV1/UVB infection model also indicated progression to squamous cell carcinoma (Fig. 5-4). Interestingly, we observed that while regions of papillomatosis showed many cells that had amplified viral DNA, we only observed a few cells harboring amplified viral DNA in papilloma-associated malignant regions (Fig. 5-6). More sensitive *in situ* hybridization techniques will be required to determine whether MmuPV1 viral genomes are lost as malignant progression arises, as is thought to occur in beta-HPV associated non-melanoma skin cancers (312).

Several lines of evidence supports the hypothesis that UVB is having an indirect effect on increasing the susceptibility to MmuPV-1 induced papillomatosis by inducing systemic immunosuppression. First, we did not find any significant difference in susceptibility to wart formation in mice that were treated with UVB 24 hours before or 24 hours after infection with MmuPV1 (Fig. 5-1). Second, UVB's ability to increase susceptibility to MmuPV1-induced papillomatosis was equally efficient whether or not

the site of infection was exposed to UVB (Fig. 5-6). And third, immunosuppression at three months post-infection correlated with wart formation (Fig. 5-9).

A second but not mutually exclusive hypothesis is that UVB also directly influences MmuPV1-induced pathogenesis. Supportive of this hypothesis, expression of the viral genes in K14HPV8 transgenic mice were increased following exposure to UVR (313). The physiological relevance of this observation remains unclear, however, because the HPV8 genes are under the control of a heterologous, keratin 14 promoter in the context of this transgenic mouse model. The MmuPV1 infection model should provide a valuable experimental platform for further testing this second hypothesis.

The ability of papillomaviruses to persist in their host in the absence of causing overt disease, i.e. latency, has long been suspected. Compelling evidence for latency comes from the observation that cyclosporine-induced immunosuppression led to elevation of the viral DNA copy number at sites of wart regression in cottontail rabbits infected with rabbit oral papillomavirus, consistent with reactivation of virus from latency (208). In the MmuPV1-infection model, ELISA analysis of serum from C57BL/6 mice infected with MmuPV1 showed seroreactivity to MmuPV1 virus particles at 70 days post-infection even though they did not develop warts (56). Likewise, seroconversion was seen in all mice (n=20) in a group of SKH-1 mice infected with MmuPV1, of which 3 mice actually developed papillomas (127). Together, these observations indicate that the virus is presented to the immune system even in the absence of causing overt disease. Whether this results from the original exposure of the animals to the virus or the consequence of a latent infection remains unclear. Our own observation that a single exposure to UVB 14 days post-infection led to papillomatosis at

sites infected with MmuPV1 (Table 5-2) indicates either that infectious virus is stably retained at the site of infection for that period of time and then initiates infection post UVB exposure or that latent infections arose that were then activated by UVB-induced immunosuppression. It remains to be determined whether latency arises in the MmuPV1 infection model, and, if so, the nature of this latency.

In this study we observed an unexpected tissue specificity in terms of susceptibility to MmuPV1-induced papillomatosis; while infection of the ear led to efficient formation of papillomas in UVB-treated FVB/NJ mice, papillomas did not arise at tail sites that were infected in the same mice. Others have reported that there is some site specificity for MmuPV1-induced disease in immunodeficient mice (100, 101). For example, while tail and muzzle of immunodeficient mice are susceptible to MmuPV1-induced papillomatosis, the torso skin is not. There are limited studies that have been directed towards looking at difference in susceptibility of different cutaneous sites of mice to cancer. Therefore the molecular differences between the sites are not very clear. In our studies with HPV 16 transgenic (K14E6, K14E7) mice we have consistently observed epithelial hyperplasia most extensively in the ear skin (281, 314, 315). Likewise, ear skin of HPV 38 E6/E7 transgenic mice display patches of hyperproliferation (316). Recently, there has been one report that suggests that difference in miR-155 expression of ear versus chest/torso skin of K14HPV16 mice could explain the difference in susceptibility of different tissues to develop HPV-mediated carcinogenesis (317). It is also possible that grooming behaviors of mice, such as scratching of ear, promotes wounding (318) thereby allowing virus to access lower layers of epithelia better.

In our studies we observed a clear viral-dose dependence in causing disease. Interestingly, we found that a viral dose of 10^7 VGE or greater was required to see papillomas in UVB-irradiated FVB/NJ mice whereas 10^6 VGE of MmuPV1 were sufficient to induce papillomas on BALB/c-*Foxn1*$^{nu/nu}$ mice, albeit at low incidence over the same 6-month observation period (Fig 5-3). This suggests that there is a higher threshold of virus required to see MmuPV1-dependent disease in UVB treated immunocompetent animals. We posit that this observation reflects, at least in part, the fact that immnosuppression induced by UVB in FVB/NJ mice only occurs in a subset of the UVB-treated mice (Fig. 5-9).

In our testing of different genetic backgrounds, only FVB/NJ was susceptible to MmuPV1-associated pathogenesis at 300mJ/cm^2, whereas C57/BL6 and BALB/c mice were susceptible to MmuPV1-associated pathogenesis at higher doses of UVB (Table 5-4). This observation is consistent with a previous study that suggests that different genetic backgrounds respond differently to UVB in terms of levels of immmunosuppression based upon DTH assays (319). While that study did not test FVB/NJ mice, they found that C57/BL6 mice were more sensitive to UVB-induced immunosuppression than BALB/c mice. This correlates with the level of MmuPV1-dependent papillomatosis observed in our studies (Table 5-4).

In our study we observed that UVB, but not UVA alone makes immunocompetent mice susceptible to MmuPV1-dependent papillomatosis (Table 5-3). UVB has been shown to play a key role in initiating and mediating immunosuppression, whereas the mechanisms and roles of UVA in immunosuppression are not well understood (182, 183). UVB can cause both short-term as well as long-term defects in cell-mediated CHS

responses (184-186), at least in part by inhibiting development of memory T-cells and by causing an overall reduction in T-cell subpopulations in the skin (190). We observed that at three months post-irradiation, UVB caused variable levels of long-term immunosuppression in FVB/NJ animals and that MmuPV1-induced papillomas developed preferentially in those animals retaining immunosuppression (Fig 5-9). This can explain the observation that papillomas arise in approximately 50% of animals. Based upon these findings we also posit that the observed regression of papillomas (Figs. 5-1) correlates with a loss of immunosuppression.

The observation that there is a strong correlation between immunosuppression induced by UVB and MmuPV1-dependent pathogenesis is perhaps the most notable finding of this study. This correlation supports the hypothesis that UVB-induced immunosuppression can help drive papillomavirus-induced disease. There is correlative epidemiological data from human studies in which anatomical sites on individuals that are exposed to sunlight, or at which sunburn has occurred are increased in their susceptibility to HPV-induced warts. One difference however, is that in our studies with FVB/NJ mice, the effect of UVB was found to be systemic; UVB irradiation did not have to be applied to the infection site. This raises the interesting question: is there a difference in the role of UVB in HPV-driven pathogenesis compared to MmupV1-driven pathogenesis? Further studies are needed to assess whether a local effect of UVB on MmuPV1 can be identified in mice. Recently, it has been shown that MmuPV1 also infects the mucosal epithelium of the female reproductive tract and oral cavity (119). In this regards MmuPV1 infection model is truly unique and the systemic immunosuppression by UVB can further be tested in the context of mucosal disease.

In conclusion, we have reported the novel finding that UVR makes immunocompetent mice susceptible to development of MmuPV1-induced cutaneous papillomas, and this correlates with UVB-induced systemic immunosuppression. This observation opens the door to pursuing studies using genetically engineered mice to study molecular pathways that mediate the role of UVB in making mice susceptible to papillomavirus-induced pathogenesis, as well as identifying cellular targets of MmuPV-1 encoded factors that mediate their role in pathogenesis.

Chapter 6:

UVB mediated immunosuppression is necessary for MmuPV1-dependent papillomatosis

The work described in the current chapter is a part of a manuscript in preparation:

Uberoi A, Spurgeon ME, Glover E, Bradfield C, Lambert PF. **UVB-mediated immunosuppression is necessary for MmuPV1-dependent papillomatosis.** (Manuscript in preparation)

Dr. Megan Spurgeon assisted in performing explant analysis experiments. Ed Glover (Dr. Christopher Bradfield's lab) provided AhR null mice for the study. Dr. Jing Zhang's lab trained me in performing flow cytometery analysis for assessing CD4+/CD8+ T-cell depletion.

6.1. Introduction

The study of papillomavirus-induced disease has long been hindered by the absence of any identified strains of virus that infect laboratory mice. This limitation was overcome with the recent identification of the murine papillomavirus, MmuPV1, isolated from cutaneous warts arising on an immunodeficient NMRI-FoxN1$^{nu/nu}$ strain of laboratory mice (55). Multiple studies have shown that the ability of MmuPV1 to cause disease is largely restricted to immunodeficient strains of mice (101, 128). Recently, we made the novel observation that UVR causes immunocompetent strains of mice to become susceptible to MmuPV1-dependent disease, including the development of papillomas and associated malignant progression to squamous cell carcinomas (118). Specifically, we found that when MmuPV1-infected FVB/NJ mice were exposed to a single dose of UVB (300mJ/cm^2) twenty-four hours before or after infection, papillomas arose at approximately 50% of the infected sites. In contrast, non-UVB-irradiated animals were resistant to MmuPV1 induced papillomatosis. When just the sites of infection on the ears were shielded from UVB exposure, papillomas still arose with equal penetrance to that seen with mice whose infections sites were not shielded, demonstrating that UVB has a systemic effect in increasing susceptibility to MmuPV1-induced disease. We found by means of contact hypersensitivity assays that there was a correlation between UVB-induced susceptibility to MmuPV-1 associated disease and UVB-induced immunosuppression. The focus of the present study is to test the hypothesis that UVB mediated immunosuppression is necessary for UVB to increase susceptibility of mice to MmuPV1-induced papillomatosis.

Studies in the photoimmunology field have illuminated how UVB induces systemic immunosuppression in mice. UVB-mediated immunosuppression of host is a highly complex process that can be achieved by several mechanisms (174, 176, 192, 304, 320, 321). One of these pathways is the IL-10 signaling cascade. UVB causes induction of Th2 immune response by inducing production of the cytokine IL-10 which in turn activates regulatory-T cells (T_{regs}) leading to sustained immunosuppression (322-327). Several kinds of cells in the skin have been demonstrated to produce IL-10 in response to UVB exposure including keratinocytes, skin-resident T-cells and their subpopulations, macrophages and Langerhans cells (327-330). A clear role of IL10 in mediating UVB-induced immunosuppression was established using IL10-null mice (325).

The aryl hydrocarbon receptor (AhR) was identified as a cytoplasmic target for UVB radiation (331, 332). AhR is a conserved member of the Per-Arnt-Sim, basic helix-loop-helix family of heterodimeric transcription factors, which are thought to mediate most of the toxic and carcinogenic effects of many environmental xenobiotics, via cytochrome p450 (333). AhR binds several exogenous ligands such as natural plant flavonoids, polyphenolics and indoles, as well as dioxin-like compounds such as polycyclic aromatic hydrocarbons (334). AhR has emerged as a significant player in immunity as it can affect T-cell function and T-cell helper differentiation (335). Recently, it has also been shown that AhR activation induces T cells that produce IL-10 thus - suggesting a link between AhR and IL-10 pathways (336). In the context of UVB, it has been shown that UVB causes induction of AhR responsive gene Cyp1A in human skin (337, 338). Importantly, UVB-induced immunosuppression is abrogated in AhR-null mice (339).

Given the established roles of IL10 and AhR in mediating UVB induced immunosuppression, we utilized IL10-null and AhR-null mice to test the hypothesis that UVB-induced immunosuppression is necessary for UVB to make mice susceptible to MmuPV1-induced papillomas. We first confirmed that UVB induces production of IL10 and the activation of AhR in the skin of mice exposed to the same dose of UVB used to induce susceptibility to MmuPV1-associated disease. We also confirmed that using the same dose of UVB used in our MmuPV1 infection challenge studies, IL10-null and AhR-null mice are resistant to UVB-induce systemic immunosuppression. We then carried out infection studies and learnt that the ability of UVB to increase susceptibility of mice to MmuPV1-induced skin disease was lost in both the IL10-null and AhR-null mice. These results prove correct the hypothesis that UVR's ability to cause immunosuppression is necessary for UVB to increase the susceptibility of mice to MmuPV1-induced skin disease. Implications of these findings on ski disease caused by HPVs are discussed.

6.2. Results

6.2.1. UVB mediated immunosuppression via IL10 is necessary for MmuPV1-dependent papillomatosis

It has been shown that UV-irradiated mice show increased IL10 levels in blood sera and murine skin (340, 341). UV-irradiated mice treated with antibodies against IL-10 are resistant to induction of immune suppression as measured by delayed type hypersensitivity (DTH) and contact hypersensitivity (CHS) assays (342). Subsequently, IL-10 was shown to be involved in production of T_{reg} cells that are immunosuppressive in function. By means of adoptive T-cell transfer experiments, Loser, *et al*. (2007) demonstrated that splenic T_{reg} cells from UV-irradiated $IL10^{-/-}$ mice are unable to confer

immunosuppression upon transfer into naive recipients (325). These data demonstrate that IL-10 is a critical player in UV-induced immunosuppression. Therefore, we sought to test whether UVB mediated immunosuppression mediated via IL-10 was necessary for development of MmuPV1-induced papillomatosis.

6.2.1.1. UVB mediated immunosuppression is dependent on IL10

We previously demonstrated that C57/BL6 mice are susceptible to MmuPV1-induced papillomatosis at ear sites following UVB-irradiation (118). To test whether UVB causes induction of IL-10 in ear skin of C57/BL6 mice we measured IL-10 levels via ELISA on ear explants harvested from UVB-irradiated mice. C57/BL6 mice were exposed to 1 J/cm^2 dose UVB and twenty-four hours post UVB whole ears were harvested, split and placed dermis side down in serum-free cell culture media. Media was collected up to twenty-four hours post harvest and IL10 levels were measured by means of an IL-10 ELISA. Cumulative IL-10 levels were determined and normalized to weight of the ear tissues as measured following harvest and compared to IL-10 levels elicited from skin explants of non-UVB irradiated, age-matched, control mice (Fig. 6.1A). We found that UVB irradiated mouse ears produced significantly higher levels of IL-10 (P= 0.0029, *T-test*, two-sided) compared to the non-UVB irradiated control animals. This finding confirms that UVB causes induction of IL-10 in our hands.

Previous reports have shown that *IL10*$^{-/-}$ mice are impaired in immune response to UVB. To test whether *IL10*$^{-/-}$ mice are impaired in UVB-induced immunosuppression we performed contact hypersensitivity assay (CHS) on UVB irradiated *IL10*$^{-/-}$ mice and compared them to non-UVB irradiated *IL10*$^{-/-}$ mice (Fig. 6.1B). Cell-mediated immunosuppression by UVB has traditionally been measured by monitoring contact

hypersensitivity (CHS) responses (174, 184, 186, 304, 309) and we have previously also demonstrated that UVB irradiated causes significant reduction in of CHS response (118). In this assay mice were sensitized to an antigen by topically applying 0.5 mg 1-Chloro-2, 4-Di-Nitrobenzene (DNCB) on the shaved backs of the mice. Five days post-sensitization, mice were UVB irradiated, using the same dose as indicated above, and five days post-irradiation we determined the level of immune response to this antigen by applying 0.2 mg DNCB to a distant site (the ears) and monitoring CHS responses by measuring ear swelling every 24 hours for four days. As a positive control for immunosuppression by UVB we treated *IL10*$^{+/+}$ mice on C57/BL6 genetic background with UVB. We found that upon UVB irradiation, *IL10*$^{+/+}$ mice showed immunosuppression as indicated by decrease in ear swelling (Fig. 6.1B). In contrast, *IL10*$^{-/-}$ mice did not show any significant change in ear swelling upon UVB irradiation suggesting that *IL10*$^{-/-}$ mice are impaired in immune responses to UVB.

6.2.1.2. UVB-irradiated IL10$^{-/-}$ mice are resistant to MmuPV1-induced papillomas

As described above, we learnt that, while *IL10*$^{+/+}$ mice are systemically immunosuppressed by UVB irradiation, *IL10*$^{-/-}$ mice were resistant to UVB-induced immunosuppression. We had previously demonstrated that there is a correlation between UVB induced immunosuppression and MmuPV1 dependent papillomatosis. To test whether UVB-induced immunosuppression is necessary for UVB to increase the susceptibility of mice to MmuPV1-associated skin disease, we infected *IL10*$^{+/+}$ mice (n=24 infection sites) and *IL10*$^{-/-}$ mice (n=48 infection sites) with 10^8 VGE MmuPV1 at each scarified site on their ears. Five days post-infection mice were UVB-irradiated at 1

J/cm^2 and monitored for papillomatosis over a 4 month period of time, because, in our prior studies (118) we found that papillomas arise over the first three months. We found that, while one third of infected ear sites (8/24 sites) in *IL10*$^{+/+}$ mice developed MmuPV1-induced warts by 10 weeks post-infection, no infected ear sites on the *IL10*$^{-/-}$ mice developed papillomas (Fig. 6.1C). This difference was statistically significant (p= 0.008, Two-sided Fisher's exact test). A subset of the UVB-irradiated *IL10*$^{-/-}$ mice (n=24 infection sites) were monitored up to 1 year post-infection; no papillomas were observed to arise during this extended period. Based upon these studies using *IL10*$^{-/-}$ mice, we conclude that UVB's ability to induce systemic immunosuppression is necessary for UVB to make mice susceptible to MmuPV1-induced skin disease.

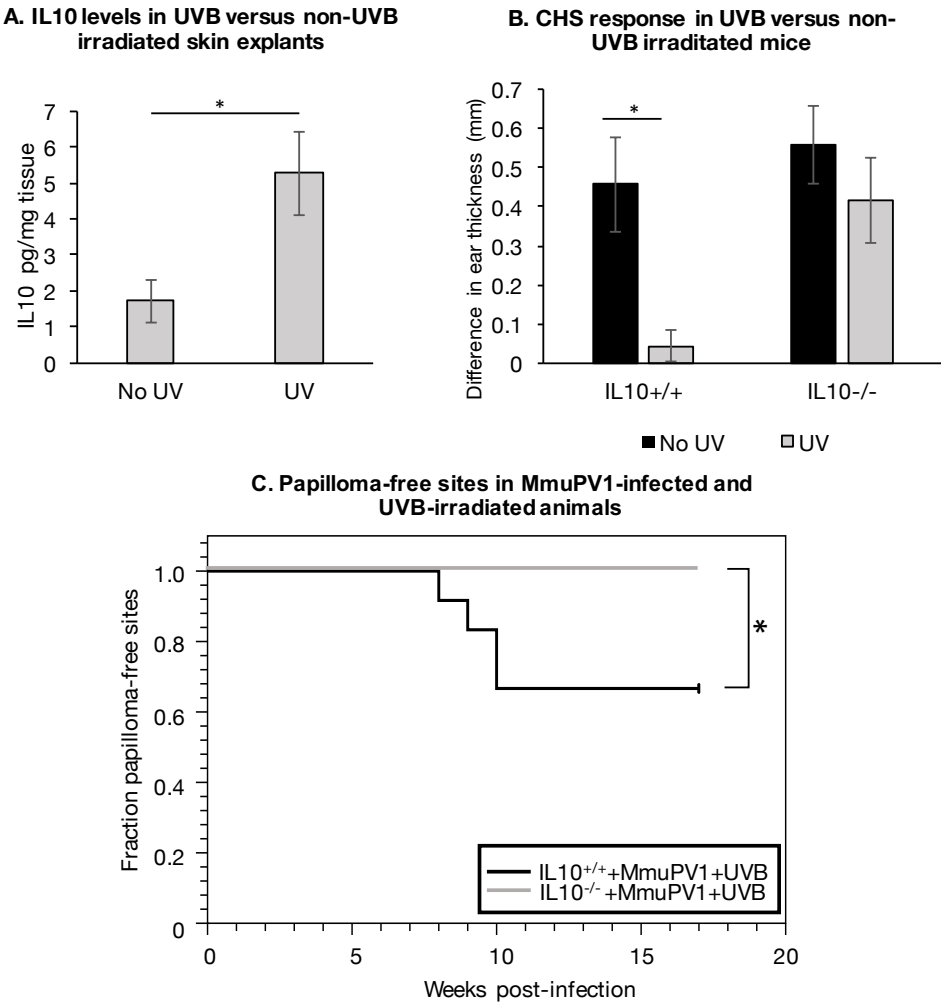

Fig. 6.1. UVB mediated immunosuppression via IL10 is necessary for MmuPV1-dependent papillomatosis

Fig. 6.1. UVB mediated immunosuppression via IL10 is necessary for MmuPV1-dependent papillomatosis

A. IL10 levels in explant cultures. Both ears were harvested twenty-four hour post UVB irradiation from $IL10^{+/+}$ i.e. C57/BL6 mice (n=4 mice per group) and explant cultures were established. Media was collected up to twenty-four hours post harvest and IL10 levels were determined by ELISA. The total IL10 produced over 24 hours has been calculated and normalized the weight of the ears harvested at the time of tissue harvest. UV irradiated mice produced significantly higher amount of IL10 as compared to non-UV irradiated animals.

B. CHS responses in $IL10^{-/-}$ and $IL10^{+/+}$ mice following UVB irradiation. Cohorts of mice (n=6 mice per group) were sensitized with DNCB on shaved backs and UVB irradiated 5 days post sensitization. 5 days post UVB irradiation, mice were challenged on their right ears with DNCB and ear swelling was determined by measuring ear thickness by means of a micrometer 24 hrs post challenge to measure immunosuppression. UVB irradiated $IL10^{+/+}$ mice showed significant decrease in ear thickness compared to non-UVB irradiated group. In case of $IL10^{-/-}$ mice immunosuppression following UVB was abolished as there was no significant difference in ear thickness of UVB-irradiated $IL10^{-/-}$ vs non-UVB irradiated mice. Difference in ear thickness was computed by measuring the difference in thickness of challenged (right) ear vs the unchallenged (left) ear.

C. *IL10*$^{+/+}$ i.e. C57/BL6 mice (n=24 infection sites) and *IL10*$^{-/-}$ mice (n=48 infection sites) were infected with 10^8 VGE MmuPV1. Five days post-infection mice were UVB irradiated and monitored for papillomatosis. Kaplan-Meyer plots of the fraction of papilloma-free infected sites over the first 17 weeks post-infection. Over this time none of the *IL10*$^{-/-}$ mice (black line) developed MmuPV1-induced papillomas post UVB irradiation. In contrast, *IL10*$^{+/+}$ mice (grey line) did develop MmuPV1-induced papillomas and the difference between the two experimental groups was significant (p= 0.008) as assessed by Fisher's exact test.

6.2.2. UVB mediated immunosuppression via AhR is necessary for MmuPV1-dependent papillomatosis

To validate further the conclusions drawn from the above-described studies using *IL10*-null mice, we pursued parallel studies with *AhR*-null mice.

6.2.2.1. UVB-irradiated AhR null mice are impaired in production of IL-10 and are resistant to UVB-induced immunosuppression

Independent of its well-characterized role in activation of cytochrome P450, AhR pathways has emerged as a key regulator of immune responses and has been shown to be important for production of IL-10 in T-cells (343). Furthermore, $AhR^{-/-}$ mice are impaired in CHS responses in response to UVB irradiation, demonstrating that AhR mediates UV-mediated immunosuppression, as does IL-10 (339). To confirm a link between AhR and IL-10 in UVB-induced immunosuppression in our hands, we first asked whether the ability of UVB irradiation to elicit production of IL-10 in skin of mice is dependent upon AhR. $AhR^{+/+}$ and $AhR^{-/-}$ mice were UVB-irradiated (1 J/cm^2), ear explant cultures established and IL-10 levels measured via ELISA as described earlier (Fig. 6.1A). We found that while $Ahr^{+/+}$ mice produced significantly high amounts of IL-10 protein levels (Fig. 6.2A), as seen earlier (Fig. 6.1A), $Ahr^{-/-}$ mice were impaired in the production of IL-10 (Fig. 6.2A). This observation indicates that UVB-induction of IL-10 in the skin, under the conditions used in our infection studies, is dependent on AhR. Further, when we performed contact hypersensitivity assay (CHS) on UVB irradiated $AhR^{-/-}$ mice and compared them to non-UVB irradiated $AhR^{-/-}$ mice we found there to be no significant difference between swelling responses as measured by ear thickness (Fig. 6.2B) showing that $AhR^{-/-}$ mice are resistant to UVB-induced immunosuppression. In contrast the control

group, i.e. *AhR*$^{+/-}$ mice, were immunosuppressed by UVB as evidenced by their impaired CHS response (Fig. 6.2B), consistent with our observations with *AhR*$^{+/+}$ mice (Fig. 6.1B). The results of the CHS assay were consistent with previous reports (339) and confirm that AhR plays a critical role in UVB-mediated immunosuppression under the conditions used in our infection studies.

6.2.2.2. UVB-irradiated AhR$^{-/-}$ mice are resistant to MmuPV1-induced papillomas

To test whether UVB-induced immunosuppression is necessary for MmuPV1-dependent disease we infected *AhR*$^{+/-}$ mice (n=20 infection sites) and AhR$^{-/-}$ mice (n=20 infection sites) with 10^8 VGE MmuPV1 at each scarified sites on their ears. Five days post-infection mice were UVB irradiated at 1 J/cm^2 and monitored for papillomatosis (Fig. 6.2C). We found that while 30% of infected ear sites (6/20 sites) in *AhR*$^{+/-}$ mice were susceptible to MmuPV1-induced warts, *AhR*$^{-/-}$ mice were resistant to MmuPV1-induced warts (Fig. 6.2C). This difference was statistically significant (p= 0.021, Two-sided Fisher's exact test). The incidence of papillomas in *AhR*$^{+/-}$ mice is similar to that seen in wild type C57/BL6 mice (6.1C), indicating that complete loss of AhR is required for onset of disease.

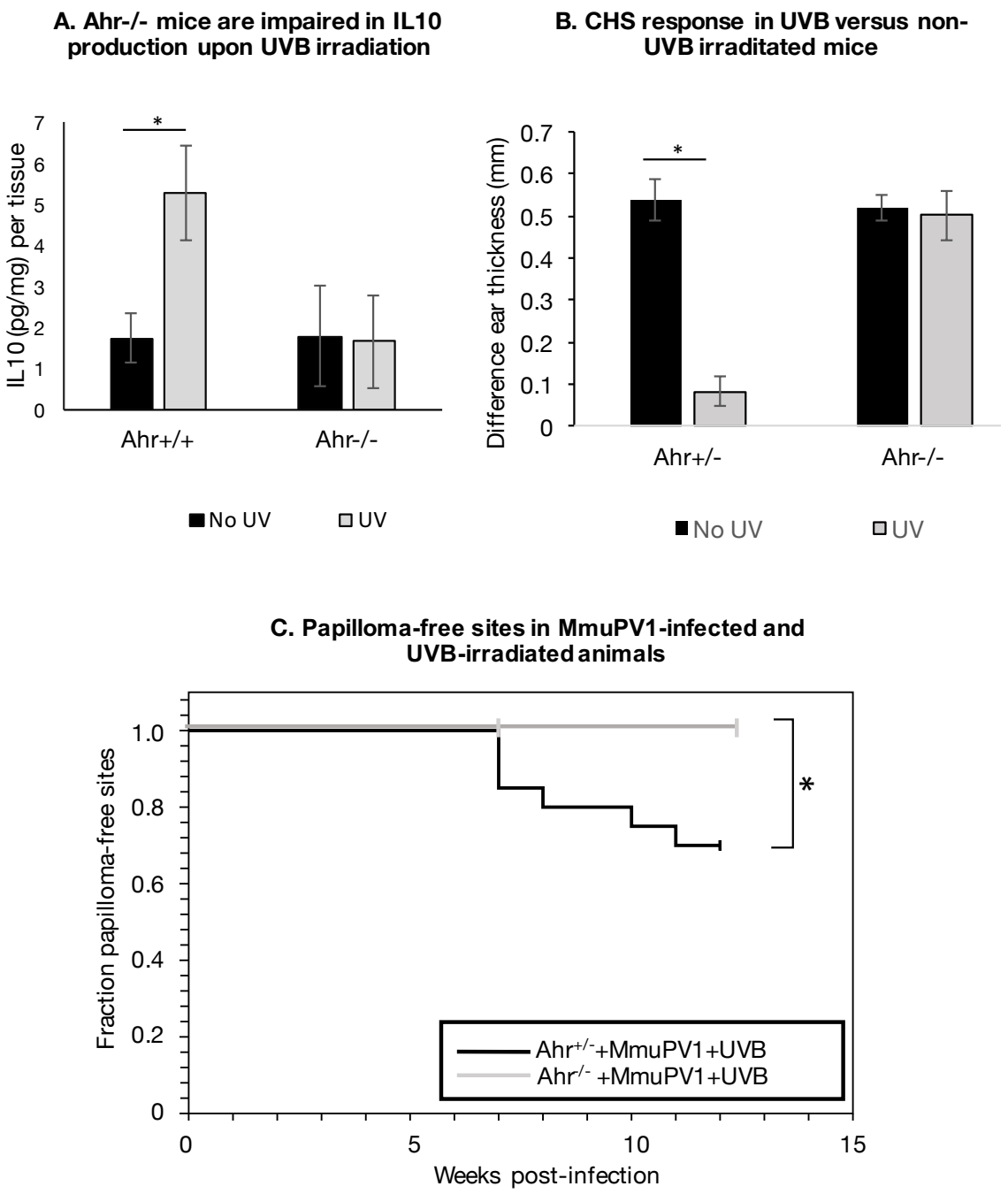

Fig. 6.2. UVB mediated immunosuppression via AhR is necessary for MmuPV1-dependent papillomatosis

Fig. 6.2. UVB mediated immunosuppression via AhR is necessary for MmuPV1-dependent papillomatosis

A. IL10 levels in explant cultures. Both ears were harvested twenty-four hour post UVB irradiation from $AhR^{+/+}$ i.e. C57/BL6 mice (n=6 mice per group) and $AhR^{-/-}$ (n=6 mice per group) and explant cultures were established. Media was collected up to twenty-four hours post harvest and IL10 levels were determined by ELISA. The total IL10 produced over 24 hours has been calculated and normalized the weight of the ears harvested at the time of tissue harvest. UV irradiated $AhR^{+/+}$ mice produced significantly higher amount of IL10 as compared to non-UV irradiated $AhR^{+/+}$ mice (*p<<0.0001, T-test*). There was no statistical difference between IL10 levels produced between UV irradiated versus non UV-irradiated $AhR^{-/-}$ mice.

B. CHS responses in $AhR^{-/-}$ and $AhR^{+/-}$ mice following UVB irradiation. Cohorts of mice (n=6 mice per group) were sensitized with DNCB on shaved backs and UVB irradiated 5 days post sensitization. 5 days post UVB irradiation, mice were challenged on their right ears with DNCB and ear swelling was determined by measuring ear thickness by means of a micrometer 24 hrs post challenge to measure immunosuppression. UVB irradiated $AhR^{+/-}$ mice showed significant decrease in ear thickness compared to non-UVB irradiated group indicating systemic immunosuppression. In case of $AhR^{-/-}$ mice, UVB failed to induce immunosuppression because there was no significant difference in ear thickness of UVB-irradiated vs non-UVB irradiated $AhR^{-/-}$ mice. Difference in ear thickness was computed by measuring the difference in thickness of challenged (right) ear vs the unchallenged (left) ear.

C. *AhR*$^{+/-}$ mice (n=20 infection sites) and *AhR*$^{-/-}$ mice (n=20 infection sites) were infected with 10^8 VGE MmuPV1. Five days post-infection mice were UVB irradiated and monitored for papillomatosis. Kaplan-Meyer plots of the fraction of papilloma-free infected sites over the first 16 weeks post-infection. Over this time none of the *AhR*$^{-/-}$ mice (black line) developed MmuPV1-induced papillomas post UVB irradiation. In contrast, *AhR*$^{+/-}$ mice (grey line) did develop MmuPV1-induced papillomas. The difference between the two experimental groups was significant (p= 0.021) as assessed by Fisher's exact test.

6.2.2.3. T-cell depleted AhR-/- mice are permissive for MmuPV1 infection

Stimulation of AhR by xenobiotics has been shown to affect epidermal differentiation and skin barrier formation (344). Also, in older *Ahr*$^{-/-}$ mice (6-8 months), there is observed some degeneration of hair follicles and the mice exhibit alopecia along with ulceration and regenerative hyperplasia (345). Recent transcriptome analysis of *Ahr*$^{-/-}$ and *Ahr*$^{+/+}$ murine keratinocytes, led to the revelation that primary *Ahr*$^{-/-}$ keratinocytes are significantly reduced in expression of terminal differentiation genes (e.g. filaggrin and involucrin) (346). Together, these data suggest that *AhR*$^{-/-}$ mice may be compromised in their skin differentiation program. We wondered whether this feature of these mice could be contributing to the failure of *Ahr*$^{-/-}$ mice to develop MmuPV1-indced warts, independently of the requirements for Ahr in UVB-induced immunosuppression. To address this potential caveat, we asked whether *AhR*$^{-/-}$ mice become susceptible to MmuPV1 induced skin disease when they are immunosuppressed by a different means, using antibody-mediated T cell depletion. Several groups have shown that complete T-cell deficiency is required in C57/BL6 mice to see MmuPV1-induced papilloma formation, and that antibody-mediated T cell depletion is an effective means for making mice susceptible to MmuPV1-induced papilloma formation (127, 128). Therefore we depleted both CD4+ and CD8+ T-cell subtypes using antibody-mediated depletion. Six weeks old mice were injected in their intraperitoneal cavity with Anti CD4 and Anti CD8 antibodies twice a week up to 4-weeks post-infection. T-cell depletion was assessed by measuring the number of CD4+ and CD8+ T-cells in peripheral blood (collected by submandibular bleeding) by performing flow cytometery analysis at 2-week (data not shown) and 4-week time points compared to the respective isotype control (Fig. 6.3A). In

parallel CD4+ and CD8+ T-cell depletion was also performed in *AhR*$^{+/+}$ mice as a positive control. We found that T-cell depleted *AhR*$^{-/-}$ as well as *AhR*$^{+/+}$ mice were susceptible to MmuPV1 infection (Fig. 6.3B) and there was no significant difference between onsets of papillomas between the two groups of mice (Log-Rank analysis, $P>0.05$). This data indicates that, while *AhR*$^{-/-}$ mice may be impaired for certain differentiation processes, T-cell depleted *AhR*$^{-/-}$ mice are equally susceptible to MmuPV1 infection as are T-cell depleted *Ahr*$^{+/+}$ mice. This data then confirms that the underlying reason why *AhR*-null mice are not increased in their susceptibility to MmuPV1-induced skin disease upon UVB treatment is because they are resistant to becoming immunosuppressed by UVB, not because of some inability of the epidermis of these mice to support the MmuPV1 infectious life cycle.

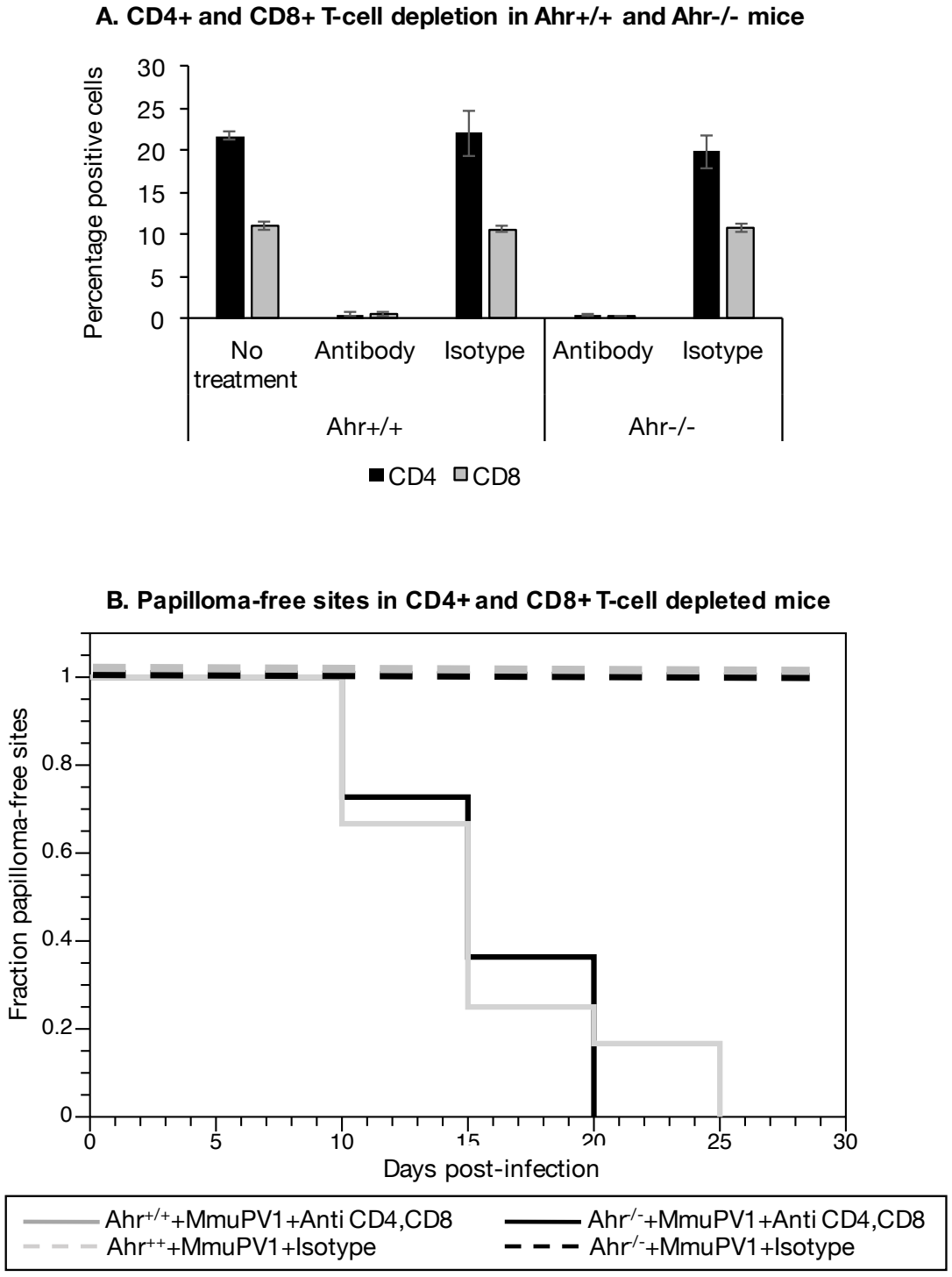

Fig. 6.3. T-cell depleted *AhR*$^{-/-}$ mice are permissive for MmuPV1 infection

Fig. 6.3. T-cell depleted *AhR*$^{-/-}$ mice are susceptible to MmuPV1 infection

6 weeks old *AhR*$^{-/-}$ and *AhR*$^{+/+}$ mice were injected intraperitoneally with 0.5mg anti-CD4 and anti-CD8 antibodies (n=3 mice per group) twice a week for a total of 5 weeks. One-week post antibody depletion, mice were infected in their ears (n=2/mouse) and tails (n=3 sites/mouse) with 10^8 VGE MmuPV1. As negative controls groups of mice were treated with the relevant antibody isotype controls.

A. To assess whether CD4+ and CD8+ T-cells were getting depleted 200μl of blood was collected from the mice via submandibular bleeding at 4-weeks post-treatment and FACS analysis was performed to assess the percentage of CD4+ (black bars) and CD8+ (grey bars) T-cells per mouse. The average percentages across the mice are reported.

B. Following infection, papilloma onset was monitored up to 4 weeks post-infection. Papillomas arose at all infected sites in T-cell depleted *AhR*$^{-/-}$ and *AhR*$^{+/+}$ mice. However no papillomas arose in the negative control group.

6.3. Discussion

UVR is the most common environmental carcinogen that we encounter on daily basis that causes majority of skin cancers worldwide (347, 348). UVR spectra is divided into ultraviolet C (UVC; 200 – 280 nm), ultraviolet B (UVB; 280 – 320 nm) and ultraviolet A (UVA; 320 – 400 nm) (349). Of these, UVB has been reported to be most carcinogenic and its effects have been studied more extensively than others(350). Besides its role as a mutagen, UV has been shown to cause local as well as systemic immunosuppression(304). In recent years, there is increasing epidemiological evidence in support of effects of UV and exacerbation of virus-associated health conditions(173, 351-355). The effect of UV in this scenario can be two pronged wherein UV can directly impact activity of viruses or it's effects can be more indirect in which it causes immunomodulation of host leading to altered susceptibility to disease. While there is precedence for both these mechanisms, this field is largely unexplored and merits consideration.

Decades of work in the field of photoimmunology have shown UVB plays a key role in initiating and mediating immunosuppression (182, 183). UVB can cause both short-term as well as long-term defects in cell-mediated delayed type hypersensitivity responses (184-186), at least in part by inhibiting development of memory T-cells and by causing an overall reduction in T-cell subpopulations in the skin (190). Over the years, extensive efforts have been made to understand the effects of UVR, particularly UVB, on the host skin immunity. The effects of UV on the host immune system are highly complex and there are several excellent reviews detailing these mechanisms (174-181). The exact sequence in the events leading to immunosuppression by UV has not been

determined but there is consensus that the process is initiated when chromophores (DNA, Urocanic acid) present in the skin first encounter UV photons (187-189). UVB mediated immunosuppression is thought to be largely T-cell mediated and several immunosuppressive populations of T-cells (e.g. Tregs) have also been identified in response to UVR (191, 192). UVR has been shown to result in altered cytokine profiles from pro-inflammatory Th1 to the immunosuppressive Th2 profile that involves upregulation of TNF-alpha, IL10, IL-4 and prostaglandin E2 (193, 194). At the same time, it is worth appreciating that the skin, by itself is a complex organ system composed of multitude of immune cells (langerhan cells, monocytes, macrophages) and keratinocytes that are directly impacted by UVR (175, 181). While the effects of UVR on host warrant further investigation, the observation that UVR can suppress immune responses to infectious microorganisms, leads to the hypothesis that exposure to UVR can enhance susceptibility to microbial infections particularly viruses and/or it could worsen infectious diseases (195, 196). Our data with MmuPV1 supports this hypothesis. Several groups had previously shown that T-cell deficiency is required for MmuPV1-induced disease [Reviewed in (63)]. However, we made the novel observation that approximately 50% of immunocompetent mice that are exposed to UVB irradiation are susceptible to MmuPV1-dependent papillomas and accompanying squamous cell carcinomas. We found that the animals that were immunosuppressed were those that preferentially developed MmuPV1-dependent papillomas showing that there is a strong correlation between UV-induced immunosuppression and virus-induced papillomatosis (118) but the mechanisms underlying UV-induced immunosuppression in this context are largely unexplored. In this report we have explored two pathways that have been found to

be important for UV-induced immunosuppression i.e. IL-10 pathway and AhR pathway and their contribution to MmuPV1-induced disease.

UV-irradiated mice show increased IL-10 levels in blood sera and murine skin(340, 341). When UV-irradiated mice are treated with anti-IL-10 they have been found to be resistant to induction of immune suppression as measured by delayed type hypersensitivity (DTH) and contact hypersensitivity (CHS) assays (342). Recently, it has been demonstrated that splenic T_{reg} cells from UV-irradiated $IL10^{-/-}$ mice are unable to confer immunosuppression upon transfer into naive recipients(325). These observations have cemented the role of IL-10 as critical player in UV-induced immunosuppression. In support of these observations we found that in our hands too we saw that there is induction of IL-10 in mouse skin (Fig. 6.1A). To test whether IL-10 is involved in UVB-induced immune suppression we adopted a genetic approach in which we found that IL10-/- mice were resistant to UV-induced immunosuppression (Fig. 6.1B). We first sensitized the animals with DNCB on their backs (allergen), then exposed the animals to UVB irradiation five days post-sensitization and 5 days post UV, proceeded with the effector phase in which animals were re-treated with DNCB at their ear sites. This sequence of CHS assay can be used to assess whether UVB has an effect on the effector phase of CHS assay. Our data is consistent with earlier studies where IL10 was reported to suppress the effector phase of CHS. In these prior studies it was found that injection of murine recombinant IL-10 into naive mice prior to sensitization with did not affect ear swelling when ears were challenged 5 days later. However, injection of IL-10 into mice already sensitized with antigen prior to challenge resulted in a significant suppression of the ear swelling response, suggesting that employed IL-10 is able to block the effector

phase, but not the induction phase of CHS in vivo (342). These data confirm that IL-10 is necessary for UVB-mediated immunosuppression and we tested whether UVB-mediated immunosuppression via IL-10 is necessary for MmuPV1-dependent papillomatosis by infecting IL10-/- mice with MmuPV1 followed by UVB-irradiation (Fig. 6.1C). We found that while UVB-irradiated IL10+/+ mice were susceptible to MmuPV1-induced papillomatosis, UVB-irradiated IL10-/- mice were resistant to MmuPV1-induced papillomas over long-term monitoring. This observation supports the hypothesis that IL-10 is required by UVB to increase susceptibility to MmuPV1-associated disease. Interestingly, IL-10-like open reading frames (ORFs) have been identified in multiple members of the Herpes and Poxvirus families [Reviewed in (356)] several of which possess immunosuppressive properties. It is possible that existence of these IL-10 like ORFs have helped these viruses (e.g. Epstein Barr Virus, Human Cytomegalovirus) to infect immunocompetent hosts providing these viruses with an arsenal to avoid immune surveillance. In the context of papillomaviruses no such IL-10 like ORFs have been identified. That IL-10 appears to play an important role in MmuPV1-UVB infection model can lead us to speculate that upregulation of IL-10 in the host by UVB most-likely provides an immune suppressive environment for the virus to cause disease. In the context of HPV16-mediated cervical cancers there has been one report where there was correlation between high levels of IL-10 and disease grade but these merit further investigation(357).

While IL-10 has been studied extensively in the context of UVB mediated immunosuppression, recently AhR has been identified as another pathway that can modulate UVB induced immunosuppression in the skin (331). The AhR pathway has

been studied extensively in the context of toxic responses in response to several environmental pollutants that lead to activation of Cytochrome p450. There are limited studies which have assessed the contribution of the AhR pathway in UVB mediated immunosuppression. It has been seen that exposure of rat and human skin to UVB induces AhR-dependent CYP1a activity and protein expression(337, 338). Further, $AhR^{-/-}$ mice have been found to be resistant to UVB mediated immunosuppression (339) and that these mice are impaired in UVB-responsiveness as they do not produce CYP1a1(331) upon UVB radiation. While the role of AhR specifically in the context of UVB-mediated immunosuppression is less studied, AhR has been shown to be a modulator of several immunological pathways [Reviewed in (358)]. In particular, it has been shown that activation of AhR causes induction of a specific population of T-cells, which produce IL-10 (336). Subsequent studies have shown that AhR does so by interacting with transcriptional factor c-Maf (343). Interestingly, we found that the skin of AhR-/- mice was impaired in the production of IL-10 in response to UVB (Fig. 6.2A) suggesting that AhR controls production of IL-10 in the context of UVB mediated immunosuppression. Consistent with prior reports we found that UVB-irradiated AhR-/- mice are resistant to UVB-induced immunosuppression (Fig. 6.2B) and that they were resistant to MmuPV1-induced papillomas as well (Fig. 6.2C). The papillomavirus life cycle is intimately tied to the differentiation program of the epithelia and there have been recent reports that suggest that loss of AhR can impair the epithelial differentiation program (346). To out rule the possibility that the impairment of the epithelial differentiation program by AhR can influence susceptibility to papillomavirus infection, we performed T-cell depletion of AhR-/- mice (Fig. 6.3A). We found that upon T-cell

depletion AhR-/- mice were susceptible to MmuPV1-associated papillomas (Fig. 6.3B). This observation is significant as it shows that while T-cell deficient AhR-/- mice are susceptible to MmuPV1 infection, UVB-irradiated AhR-/- mice that are resistant to UVB-induced immunosuppression are not susceptible to MmuPV1-induced papillomas. These data together show that UVB-mediated immunosuppression mediated by AhR is necessary for MmuPV1-induced papillomatosis.

To summarize, in this report we have shown by two independent approaches that UVB-induced immunosuppression is necessary for MmuPV1-induced disease. This study provides evidence that modulation of host immune responses via IL-10 and AhR contribute towards papillomavirus-induced skin disease by making use of a novel papillomavirus infection model. It is worth appreciating that besides AhR and IL-10 several other pathways have also been implicated in UVB-mediated immunosuppression – PGE_2, cis-urocanic acid, histamine, IL-4, and TNF-α [Reviewed in(174, 327)]. Recently, platelet-activating factor (PAF), a potent phospholipid mediator, has also been identified as a modulator of UV induced systemic immune responses and has been shown to be upstream of IL-10 (359). While testing all possible immune modulators of UV responses is beyond the scope of this study, the MmuPV1-UV infection model provides us with the opportunity to test how UV modulation of host-responses can lead to papillomavirus-induced disease.

Chapter 7:

A novel *in vivo* infection model to study papillomavirus-mediated cancers of the female reproductive tract

In this chapter I describe the preliminary finding that MmuPV1 can cause cancer in the female reproductive tract of immunocompetent mice in conjunction with UVB and estrogen. We are currently in the process of performing studies to understand the mechanisms responsible for this observation. I carried out all the animal studies along with L1 and FISH analysis described in this chapter. Dr. Megan Spurgeon performed the histopathological analysis. Dr. Stephanie McGreggor was the consultant histopathologist for this study.

The work described in the current chapter is a part of a manuscript in preparation:

Uberoi A, Spurgeon ME, Wei T, McGreggor S, Lambert PF.**A novel *in vivo* infection model to study papillomavirus-mediated cancers of the female reproductive tract.** (Manuscript in preparation)

7.1. Introduction

About 20% of all human cancers arising globally are caused by infectious agents, of these 15% of cancers are caused by viruses. Human papillomaviruses (HPVs) are an established etiological agent of human cancer and virtually all cervical cancers arising in women are caused by "high-risk" oncogenic HPVs (e.g. HPV16, 18, 31). Most HPV infections in young women are transient, but persistent infection with high-risk genotypes can lead to the progression of precancerous lesions to invasive cancer. HPV vaccines can protect against new infections by high-risk HPVs implicated in cervical cancer, however they do not have any effect on pre-existing infections, and their utilization remains low worldwide, particularly in developing natons where HPV-associated cervical cancer is often the leading cause of death by cancer in women. Hence there remains the need to explore more effective and more accessible therapeutic interventions. Meeting this need would be greatly facilitated by the availability of a preclinical model in which papillomavirus infection results in cervical cancer. .

Recently, a murine papillomavirus (MmuPV1) was isolated for the first time from skin papillomas arising in T-cell deficient, hairless *FoxN1*$^{nu/nu}$ (nude) mouse (55). This is the first papillomavirus that can naturally infect the laboratory strain of mice providing an attractive opportunity to study species-specific papillomavirus infections in a tractable, *in vivo* laboratory model. While MmuPV1 has been largely studied thus far in the context of cutaneous disease (55, 101, 118, 127, 128, 212), one group found that MmuPV1 is capable of exhibiting expanded tissue tropism as it is capable of causing low-grade disease in the female reproductive tracts of *FoxN1*$^{nu/nu}$ mouse mice (119). We recently reported that ultraviolet radiation (UVR) makes wild-type immunocompetent mice highly

susceptible to MmuPV1-induced cutaneous disease by causing systemic immunosuppression (118). In this chapter, I sought to learn if MmuPV1 can cause disease in the female reproductive tracts of immunocompetent *FVB/N* (wild-type) mice. In prior studies using K14-HPV16 E6/E7 transgenic mice in which the expression of HPV16 oncogenes is directed to basal epithelia, the Lambert lab found that estrogen and its nuclear receptor, estrogen receptor alpha (ERa), are necessary cofactors required for the genesis and maintenance of cervical carcinogenesis (280, 281, 360). Therefore, in this chapter, I tested whether administration of estrogen and UVR, alone or together, contributes to papillomavirus infection and neoplastic progresssion in the female reproductive tracts of immunocompetent strains of laboratory mice infected with MmuPV1. In contrast to prior observations regarding cutaneous disease in immunocompetent strains of mice, wherein infection with MmuPV1 was found not to cause disease in the absence of suppressing host immunity (55, 101, 118, 127), herein, I found that infection with MmuPV1 induces formation of low-grade precancerous lesions in the cervix and the vagina of wild-type animals. Treatment with either UVR or estrogen led to high-grade precancerous lesions. Treatment with both UVR and estrogen led to high incidence of cervical and vaginal cancers in addition to a greater burden of precancerous lesions. This first report of *in vivo* cervical carcinogenesis induced by a natural papillomavirus infection in immunocompetent mice provides a novel preclinical model system for basic and translational studies on papillomavirus-induced cervical/vaginal disease.

7.2. Results

In Chapter 3, I described the establishment of the MmuPV1 infection model to study cutaneous disease in our laboratory in T-cell deficient *FoxN1*$^{nu/nu}$ mice. In parallel, I optimized a method to infect the lower female reproductive tract of nude mice with MmuPV1. This method was adapted from a method used previously in our lab to infect the lower female reproductive tract of micewith HPV pseudovirus for studies on factors that mediate virus entry into epithelial cells *in vivo* (279). Briefly, six week old nude female mice were treated with 1mg medroxyprogesterone acetate (DEPO Provera) to induce diestrous. Four days post-treatment with DEPO Provera, the epithelial lining of the lower female reproductive tracts were chemically injured by topical application of an over the counter spermicide, Contraceptol, that contains 4% nonoxynol-9. Nonoxynol-9 is a detergent that had been previously reported to induce sufficient chemical injury to the epithelial lining of the vagina and cervix to increase greatly the ability of HPV pseudovirus to infect the tissue (278). Mice (n=6) were infected in the lower female reproductive by application of 10^8 VGE MmuPV1 4-6 hours after treatment with Contraceptol. Four months post-infection, the cervicovaginal tract was harvested and subjected to histopathological analyses. We observed that 3/6 mice infected in the reproductive tract showed signs of CIN1/2 MmuPV1 infection was established in the vaginal epithelia (Fig. 7.1). The tissue was characterized by presence of koilocytes, hyperplasia and papillomatous undulations of the epithelia. L1 staining indicated that the productive phase of the virus life cycle was established in the cervico-vaginal tract.

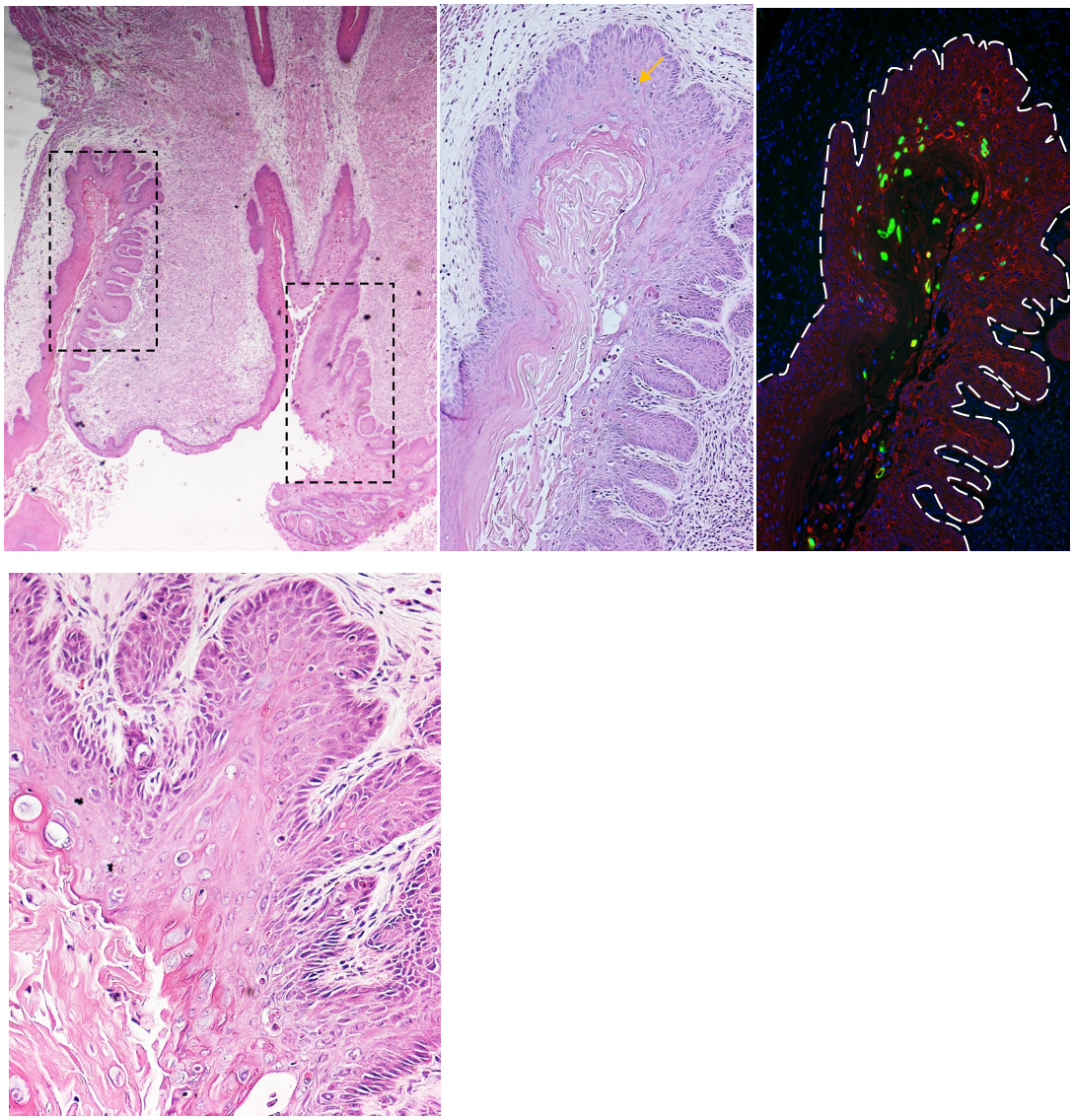

Fig. 7.1: MmuPV1 infection of female reproductive tract of nude mice

Fig. 7.1: MmuPV1 infection of female reproductive tract of nude mice.

MmuPV1 infection of cervico-vaginal tract was optimized by infecting *FoxN1*$^{nu/nu}$ mice with 10^8 VGE dose MmuPV1. Reproductive tracts were harvested 4-months post-infection and H&E analysis was performed. Insets show presence of koilocytes (yellow arrow, top panel), hyperplasia and papillomatous undulations of the epithelia Productive viral infection was seen as indicated by L1 (green) immunofluorescence (right) in the vaginal epithelia (Krt:red).

These observations were consistent with those reported by others who infected the lower female reproductive tract of nude mice with MmuPV1 using an alternative methodology, and provided me a basis for pursuing studies in immunocompetnet strains of mice (119).

To test whether MmuPV1 can cause disease in the female reproductive tracts immunocompetent mice, I used the above-described method to infect female *FVB/N* mice. In the context of the cutaneous MmuPV1-infection model, we reported that ultraviolet radiation (UVR) makes wild-type immunocompetent mice highly susceptible to MmuPV1-induced cutaneous disease (118). We and others previously identified estrogen and its receptor ERa as necessary cofactors for cervical carcinogenesis in *K14-HPV16* mice (280, 281, 360, 361). Therefore I sought to test the role of these two co-factors in contributing towards reproductive tract disease as well. Using our optimized infection methodology described in Section 7.2.1, we infected immunocompetent female *FVB/N* mice and divided them into 4 cohorts - Group 1:mice infected with MmuPV1 only; Group 2: MmuPV1-infected mice that were UVB-irradiated following infection; Group 3: MmuPV1-infected mice treated exogenously with estrogen; Group 4: MmuPV1-infected mice that were both UVB-irradiated and treated with estrogen. The sequence of manipulations in these studies is described in Fig. 7.2A. Reproductive tracts were harvested four months post-infection, histopathologically scored and and cervical and vaginal disease grades were reported (Fig. 7.2B, Table 7.1) as described previously (281).

In our experience with the cutaneous infection model of MmuPV1, we have observed that male and female FVB/N mice infected with 10^8 VGE MmuPV1 show no

signs of skin disease. However, 4 of 5 of female *FVB/N* mice infected with MmuPV1 in their lower reproductive tract showed signs of low to moderate grade cervical and vaginal disease (Group 1, Table 7.1; Figs. 7.2, & 7.3). This observation indicates that MmuPV1 can cause low-grade reproductive tract disease in immunocompetent mice. In our analysis of mice infected with MmuPV1 and subsequently treated with estrogen or UVB, we observed there to be high-grade disease in both groups at the 4-month time point (Groups 2&3; Table 7.1; Figs. 7.2, & 7.3,) The severity of cervical (*P=0.016,* Wilcoxon rank-sum, two sided) and vaginal disease (*P=0.015*) in mice infected with MmuPV1 followed by estrogen treatment was significantly higher than that of mice infected with virus only (Fig. 7.2B). This data indicates that estrogen exacerbates the progressive neoplastic disease caused by MmuPV1. Differences in severity of disease between infected versus infected and UVB-treated did not reach statistical significance.

Interestingly, mice treated with both UVB and estrogen post-infection with MmuPV1 frequently developed cancers in the cervical (55.5%) and vaginal (44.4%) tracts (Group 4; Table 7.1.). The severity of disease was significantly higher in these mice compared to those infected with virus only (cervix: *P= 0.008*, vagina: *P=0.022;* Wilcoxon rank-sum, two sided). The cervical cancers were characterized by invasion into the epithelia and presence of keratin pearls (Figs. 7.3, & 7.5).

To assess productive stage of viral life cycle we performed L1 immunofluorescence staining of the female reproductive tracts. While we did not detect any L1 positive cells in the lesions seen in mice infected with MmuPV1 only (Fig. 7.4, Top panel) we were able to see L1 positive cells in the remaining groups of mice that had been treated with either UVB or estrogen, respectively after MmuPV1 infection (Fig. 7.4,

middle and lower panels, respectively). We also observed L1 positive cells in the mice that developed cancers after treatment with UVB and estrogen (Fig. 7.5).

In our analysis of MmuPV1-induced disease we observed several interesting histopathological features that were consistent with the cytopathic effects of the virus. We observed stark transition zones between normal epithelium and infected epithelium (Fig. 7.6), where we could see clear boundaries between epithelium with normal histopathology juxtaposed to epithelium with histological hallmarks of virus infection such as the presence of many koilocytes (Fig. 7.6A), amplified viral DNA (Fig. 7.6B, middle panels) and expression of the viral major capsid protein L1 (Fig. 7.6B, right panels). In some samples we saw presence of papillomas exhibiting exophytic morphology (Fig. 7.7A) which have been reported to have been seen previously in genital warts caused by low-risk mucosotropic HPVs (HPV6, 11) (362). In several samples we observed hyperkeratinization in the luminal space (Fig. 7.7B, middle panel) This appears to be an effect of virus infection, as it is associated with robust L1 expression indicative of productive virus replication (Fig. 7.7B, right panel).

Table 7.1. Disease scoring

Treatment Group			No Disease	Dysplasia			Cancer
		N	Cervix (Vagina)	CIN1 (VAIN1)	CIN2 (VAIN2)	CIN3 (VAIN3)	Cervix (vagina)
1	MmuPV1	5	1(1)	3(0)	1(4)	0(0)	0(0)
2	MmuPV1+Estrogen	5	0(0)	0(0)	3(1)	2(4)	0(0)
3	MmuPV1+UVB	7	1(1)	1(0)	4(3)	1(3)	0(0)
4	MmuPV1+UVB+Estrogen	9	0(0)	1(1)	3(1)	0(3)	5(4)

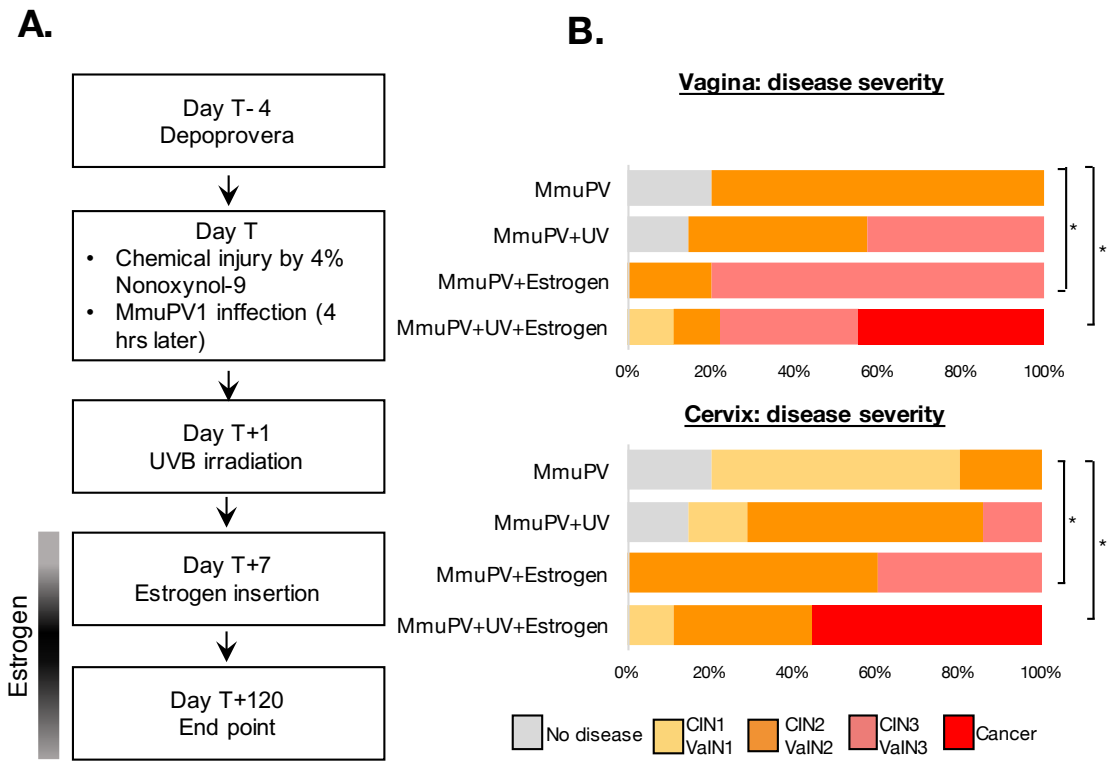

Fig. 7.2 : MmuPV1 infection of female reproductive tract of immunocompetent mice

A. Flowchart depicting sequence of manipulations in the MmuPV1 infection methodology to infect female reproductive tract.

B. Severity of disease in vaginal (top graph) and cervical (bottom graph) tract.

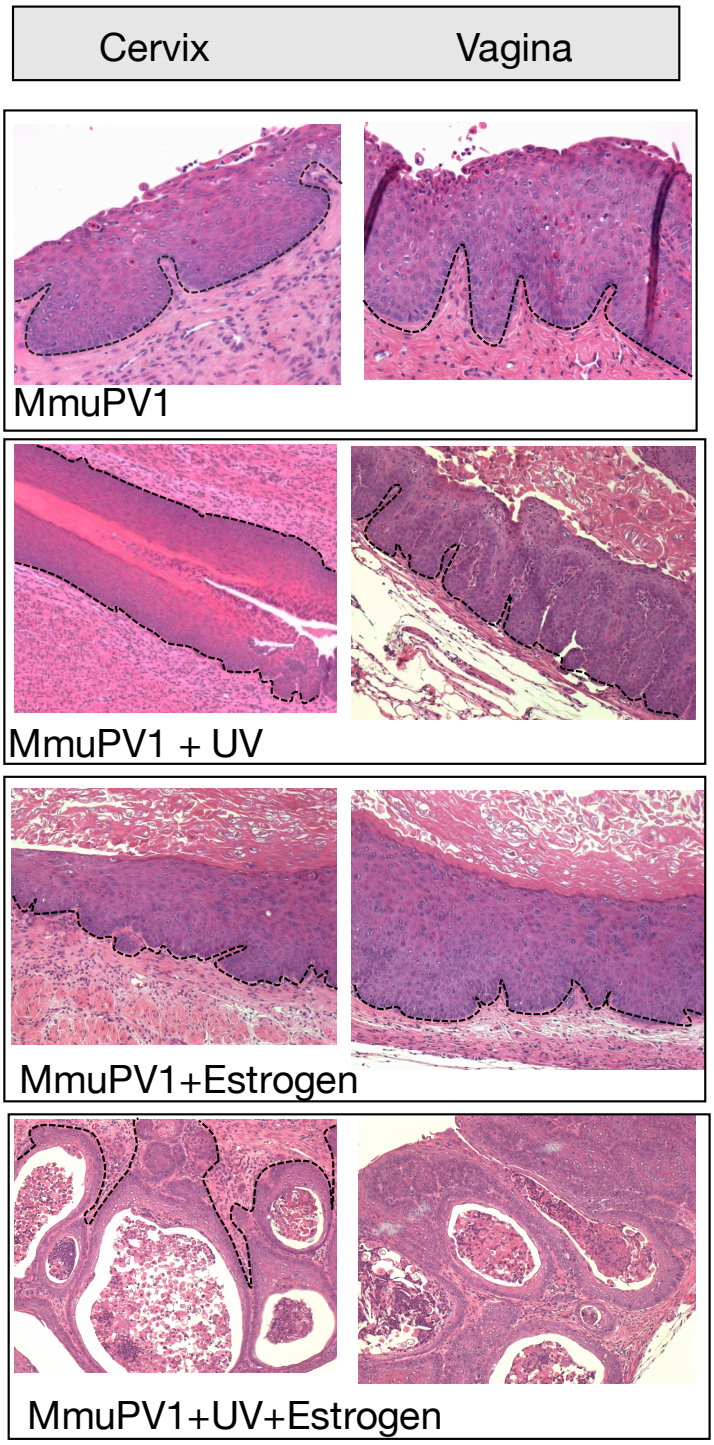

Fig. 7.3: Histopathological analysis of reproductive tracts

Representative histopathology of reproductive tracts after H&E staining.

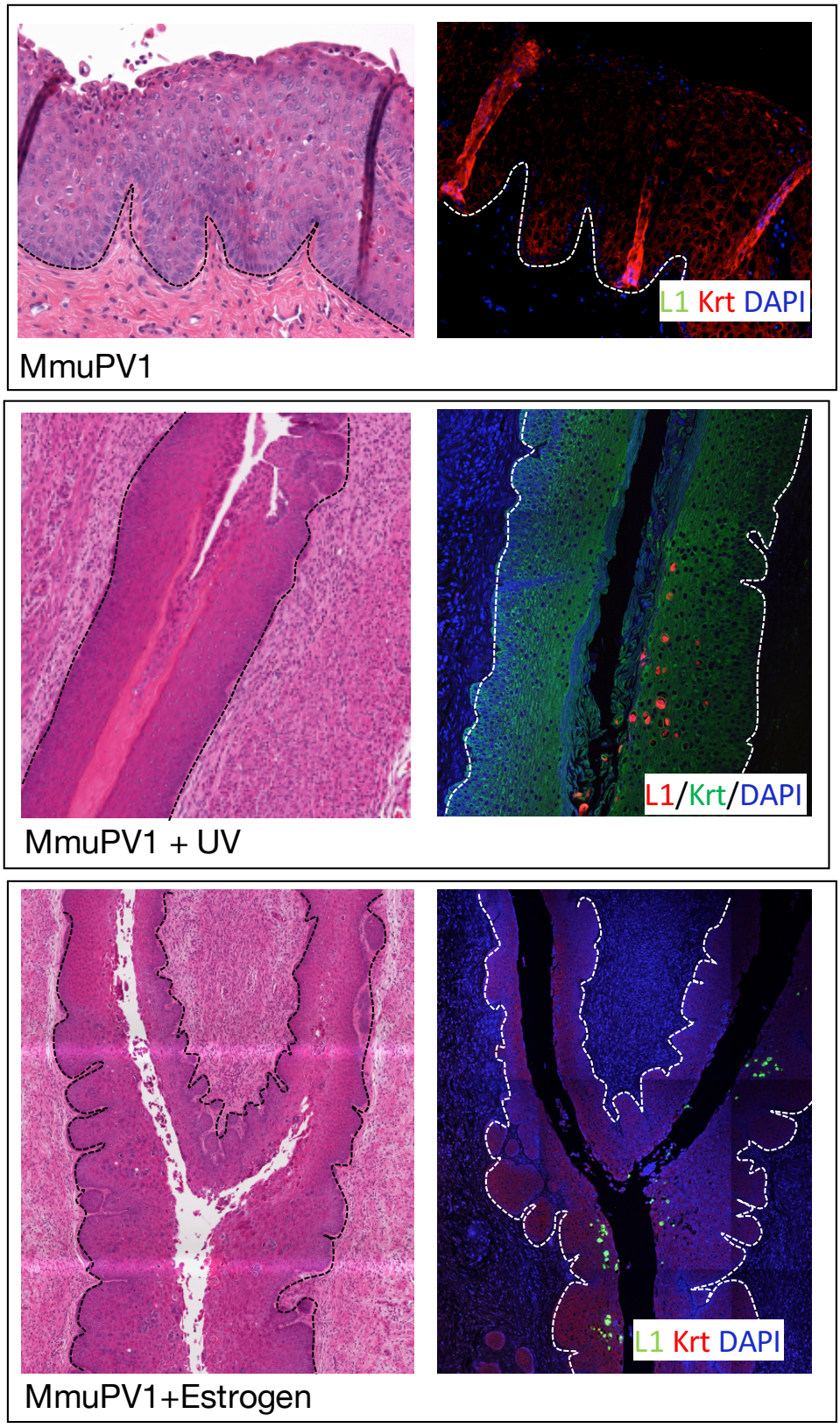

Fig. 7.4: L1 staining

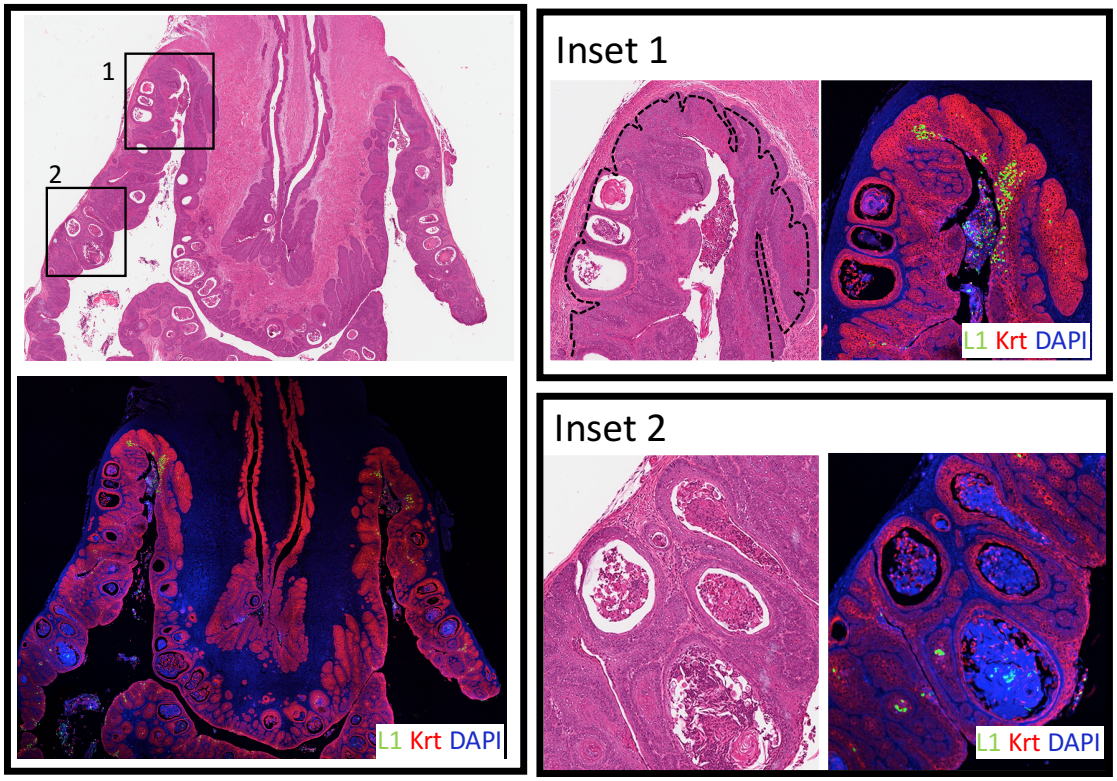

Fig. 7.5: MmuPV1 causes cancers in mice treated with UVB and estrogen

Left panel: Wide-field H&E image of cancer in cervico-vaginal tract of FVB mice infected with MmuPV1 in conjunction with UVB and estrogen and L1 (green)/Krt (red) immunofluorescence performed on serial section showing presence of L1 positive cells. Right panel: Inset 1 and Inset 2 show two enlarged areas of vaginal cancers and L1 staining.

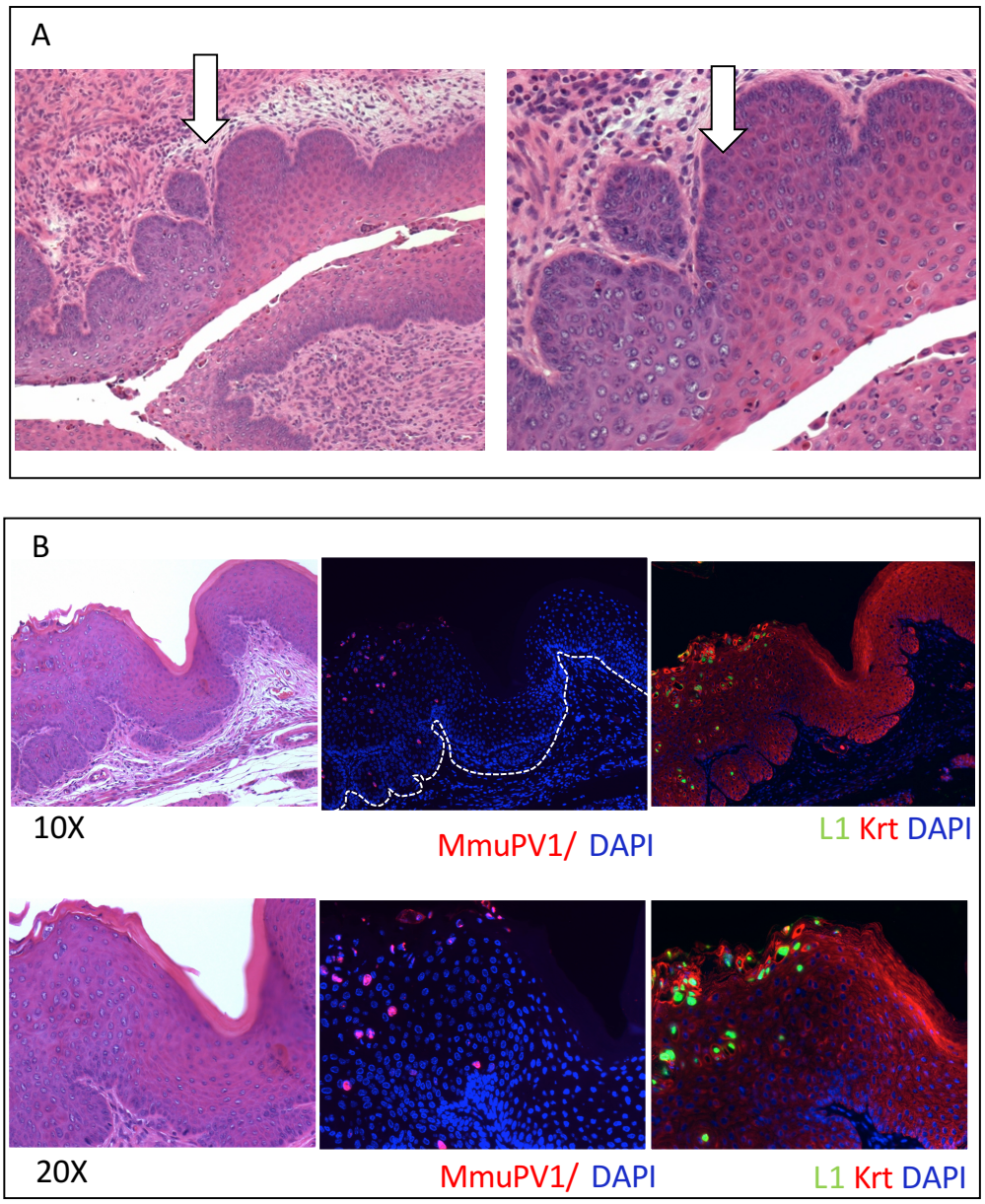

Fig. 7.6: Infection junctions seen in infected mice

In (A) Infection junctions are seen in MmuPV1-infected cervico-vaginal tracts. Prominent koilocytes are seen in areas left of arrow and relatively normal epithelia is seen on left side of arrow. As seen in B, MmuPV1 amplified DNA (FISH, middle panel) and L1 (right panel) is seen only in the infected areas of the junction.

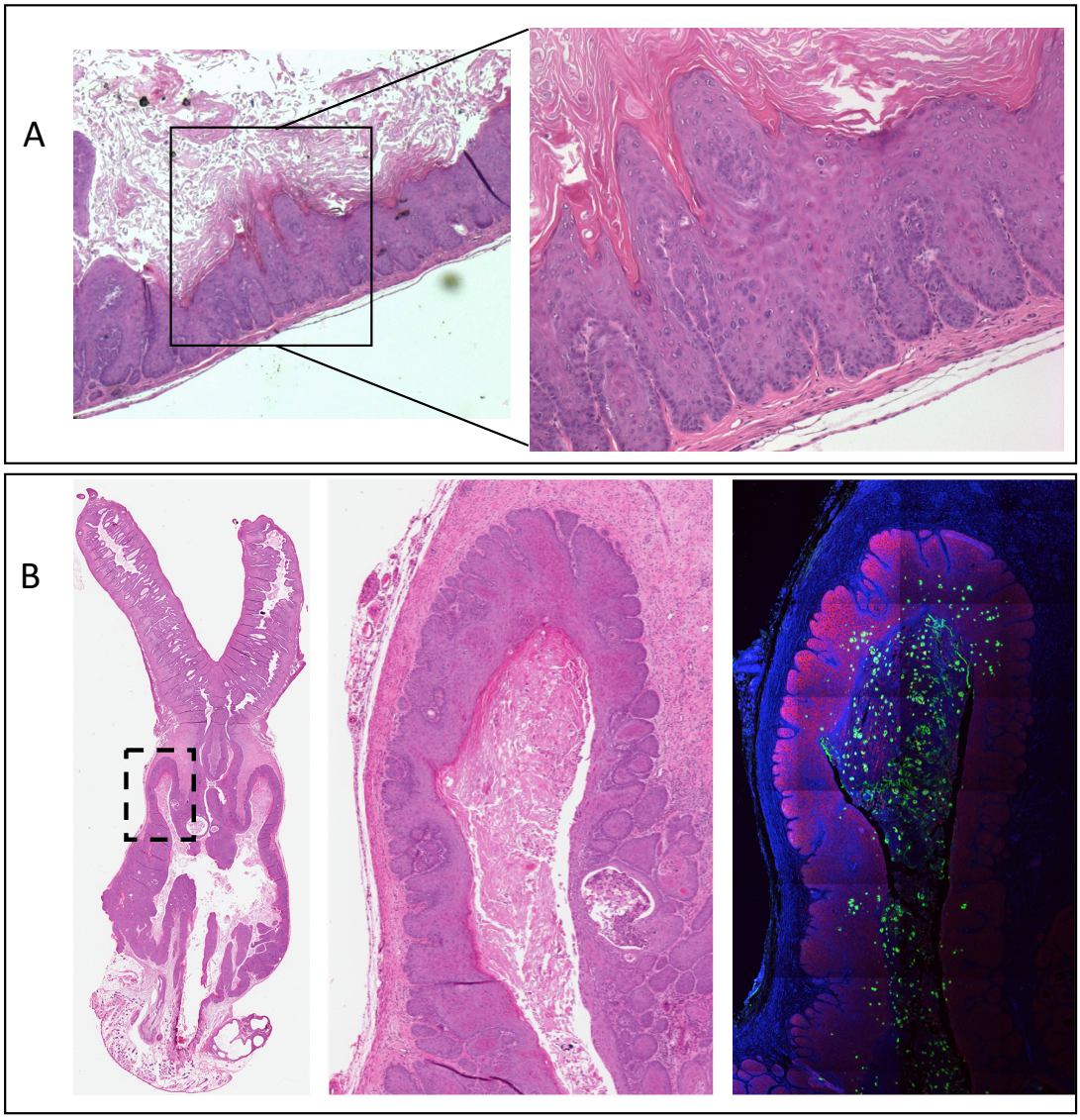

Fig. 7.7. Unusual histopathological features seen

A. Exophytic papillomas seen in vaginal tract

B. Hyperkeratinization filled with L1(green) positive cells seen in luminal space of vaginal tract.

7.3. Discussion

MmuPV1 was first isolated from a cutaneous lesion (55) and most effort so far has been directed towards studying MmuPV1-infection in the skin of mice (56, 100, 118, 127, 128, 228). Some studies demonstrated that MmuPV1 has expanded tissue tropism, which led to disease arising in mucosal tissue (oral and cervicovaginal) in immunodeficient *FoxN1*$^{nu/nu}$ mice (119, 120, 126). It is worth noting that the *FoxN1*$^{nu/nu}$ mouse, which are T-cell deficient by virtue of mutation of the FOXN1 gene, have been suggested to have a compromised epithelial barrier (363). Furthermore, the skin of *FoxN1*$^{nu/nu}$ mice has a larger than normal population of OCT4-positive dermal cells supporting a highly proliferative epithelial stem-cell niche (302). These properties of nude mice may render them more permissive to papillomavirus infections and thereby contribute to the ability of MmuPV1 to infect both cutaneous and mucosal epithelia of this mouse strain. Our findings that MmuPV1 can also infect, not only cutaneous cutaneous epithelium (citation) but also mucosal epithelium of wild type, immunocompetent FVB/N mice, indicates that the wide tropism of this virus is not a consequence of a compromise epithelial barrier, but an inherent feature of this virus.

We have found that unlike the cutaneous disease where MmuPV1 fails to cause any phenotypic disease in wild-type immunocompetent mice (118), female reproductive tracts infected with MmuPV1 only, low to mid grade precancerous lesions (Table 7.1, Fig. 7.2, Fig. 7.3, top panel). One potential explanation for this observation is that these mice have been pre-treated with Depo-provera which is a progesterone receptor agonist that can induce diestrous in mice up to 4-weeks post administration. In studies where mice were being tested for susceptibility to genital herpes simplex virus-2 (HSV-2), it

was found that Depo-provera had inhibitory effects on immune responses to HSV-2 and facilitated virus infection (364). This has also been seen in rat models in which progesterone-treated rats became heavily infected following genital exposure to *Chlamydia* associated with severe inflammation (365). As reported previously, the immune environment plays a critical role in MmuPV1 pathogenesis, at least in the skin (101, 118, 127, 128). Therefore it is possible that alteration of immune responses facilitated by treatment with Depo-provera may help in facilitating MmuPV1 infection in the reproductive tract of these mice. It is worth noting that we failed to detect any L1 positive cells in the lesions at 4-months post-infection in the absence of treatment with UVB or estrogen (Fig. 7.4, top panel), in contrast to what we observed in the female reproductive tracts of infected nude mice (Fig. 7.1) This could be a limitation in our sensitivity for detecting L1 or because the virus infection is being cleared by the immune system in these mice that would have recovered from the effects of Depo-provera treatment at that time point.

We and others have previously demonstrated that estrogen is a necessary cofactor required for cervical carcinogenesis in *K14-HPV16* transgenic mice (280, 281, 360, 361). We found that MmuPV1-infected mice treated with estrogen developed high-grade precancerous lesions (Table 7.1, Figs. 7.2 and 7.3, panel 2). Chronic estrogen administration results in persistent proliferation of epithelial cells by inducing persistent estrous phase (366). This proliferative state potentially provides a more permissive environment for MmuPV1 to establish its life cycle in actively dividing cells. Interestingly, when MmuPV1 infections were tracked over the natural estrous cycle in nude mice by qPCR, it was found that the viral copy number fluctuated during the

different phases of the estrous cycle with the highest level during the estrus phase (367). Early studies determined that estrogen is also capable of suppressing cell-mediated immune responses systemically via interacting with estrogen receptors in the thymus (368). We now know that estrogen can impact both adaptive and innate arms of the immune system [Reviewed in(369, 370)]. We have recently shown that estrogen together with expression of the HPV16 oncogenes, E6 and E7, has a profound impact on the cervical/vaginal epithelial microenvironment in HPV-transgenic mice that includes significant changes in expression of immune-related cytokines(371). Thus estrogen and papillomaviral genes together may alter the immune environment of the cervico-vaginal niche and thereby exacerbating MmuPV1-induced disease.

In the context of the MmuPV1-infection model, we have recently reported that ultraviolet radiation (UVR) makes wild-type immunocompetent mice highly susceptible to MmuPV1-induced cutaneous disease by causing systemic immunosuppression (118). A recent epidemiological study has found correlation between cervical cancer incidence and UV exposure in caucasian females (372). Based on rodent models of viral infections, UV radiation can affect both skin-associated infections, such as those caused by herpes simplex virus (HSV-1), as well as others that are systemic and are non-cutaneous [Reviewed in (173)]. For example, it was seen that rat cytomegalovirus titers in the salivary glands of UVB-irradiated rats were significantly increased as compared to non-irradiated rats. In investigating the role of UV-radiation in the context of influenza virus,, researchers found that, when BALB/c mice were infected intranasally with the mouse-adapted strain of Hong Kong Influenza A/68 (H3N2), virus-associated mortality increased in a dose-dependent manner (373). Interestingly, the authors observed that

UVR exposure did not affect virus titers in the lung suggesting that the lethal effect of influenza virus infection in mice is mediated by the host's response to infection rather than the direct cytopathic effect of viral replication. The systemic effects of UVB have also been observed in retrovirus studies where the immunosuppressive effects of murine leukemia virus were increased in mice chronically treated with low doses of UVB (374). These observations lead us to hypothesize that UVB-mediated systemic immunosuppression can affect MmuPV1-induced mucosal disease as well. Therefore we tested if UVB can act as a co-factor in MmuPV1-induced cervical disease. We found that UVB-irradiated MmuPV1-infected mice developed higher grade of cervicovaginal disease than non-treated, MmuPV1-infected mice (Table 7.1, Figs. 7.2 and 7.3).

While both estrogen and UVB increased the severity of neoplastic disease in the female reproductive tracts of MmuPV1-infected mice, neither alone were sufficient to cause malignancies to arise in these mice. However, the combination of both UVB and estrogen led to cervical and vaginal cancers in the female reproductive tracts of MmuPV1-infected mice (Table 7.1, Figs. 7.2 and 7.5). This indicates that both UVB and estrogen cooperate in increasing the severity of disease in MmuPV1-infected wild type FVB/N mice. This observation, while intriguing, is also surprising. Based on genomic, transcriptomic and proteomics analyses, MmuPV1 appears to be more similar to high-risk cutaneous papillomaviruses; most note-worthy being its lack of the E5 oncogene (56). Most-likely, the alteration of the immune environment by UVB and/or estrogen helps the virus to cause high-grade disease in the female reproductive tract. Further it is possible that MmuPV1 integrates into the host-genome leading to persistent expression of viral oncogenes as is seen for high-risk mucosal HPVs (375). There is ample evidence that

supports the role of UVB causing DNA damage that can cause mutation of host genes, in particular tumor suppressor genes [Reviewed in (376)]; however, this is thought to be restricted to UVB-exposed epithelia. It remains to be determined whether MmuPV1 is integrated into host genome in female reproductive tract infections, but preliminary analysis of RNAseq data from MmuPV1-induced skin papillomas arising in nude mice indicates that there are virus-host chimeric reads (personal communication with our collaborator Dr. Thomas Zheng, NCI) consistent with MmuPV1 integrating into the host genome in that tissue. While roles of MmuPV1 E6 and E7 still need to be explored in depth, we have reported that MmuPV1 E6 inactivates both Notch and TGF-beta signaling pathways that can be tumor suppressive in nature depending on tissue context (228). Therefore viral modulation of host-responsive genes involved in the regulation of cancer pathways may contribute to MmuPV1-induced cervical/vaginal disease.

In summary, this is the first observation of malignancy arising in the mucosal epithelia in the MmuPV1 infection model and provides opportunities, particularly in the context of immunomodulatory approaches, for furthering our ability to prevent and/or control papillomavirus-induced cancers.

Chapter 8:

Discussion and Future Directions

In my thesis studies, I have described the development and characterization of an in *vivo* infection model to study papillomavirus-associated disease in mice using the novel murine papillomavirus (MmuPV1). I have demonstrated how genetic approaches can be used to understand the effect of host biology on MmuPV1-induced disease. In this chapter I will discuss the major findings of my thesis work; in particular the effect of UVB in modulating host immune responses in facilitating the development of MmuPV1-associated disease. The MmuPV1 infection model has provided us with an unique opportunity to answer several unexplored areas of PV research. In my graduate studies, I also have pursued a number of studies resulting in preliminary data that have not been described in the prior chapters . I will discuss some of these preliminary studies and potential future directions derived therefrom.

8.1. Discussion

8.1.1. Role of T-cells in papillomavirus infection

In my studies, the initial characterization of MmuPV1 infection model was performed in *FoxN1*$^{nu/nu}$ mouse (Chapter 4). Through these studies I found that several factors influence the onset of MmuPV1-induced papillomas that include: virus dose, genetic background of mice, and site of infection. When we infected multiple other strains of mice that were either impaired in specific immune responses such as T-cells, B-cells or had intact immune systems (Fig. 4.11A, Table 4.1), we found that T-cells play a critical role in MmuPV1-induced papillomas. Other groups also reported that T-cells and their sub-populations (CD4+ and CD8+ T-cells) play critical roles in MmuPV1 infections (101, 127, 128). We found that for the C57/BL6 genetic background, loss of CD4+ as well as CD8+ T-cells are required for MmuPV1-induced papillomas. Others have shown that

both T-cell subpopulations are required for onset of disease in the BALB/c genetic background as well (127). CD8+ T-cells, specifically effector cytotoxic T lymphocytes (CTLs), play a critical role in the clearance of virally infected epithelial cells as well as regression of epithelial neoplasia [Reviewed in(132-134)]. In several well-characterized systems, CD4+ T-cells have been shown to be necessary for induction of primary CD8+ T-cell responses as well as their proliferation, activation, and differentiation into effector cytotoxic T lymphocytes. For example, in a murine model of herpes virus infection, CD4+ T cells were required for efficient local recruitment of herpes simplex virus-specific CD8+ T cells to the vaginal epithelium (135). Therefore the observation that loss of CD4+ T-cells was not sufficient to increase susceptibility to MmuPV1-induced papillomas, seen by us (chapter 4) and others (101, 127, 128)is somewhat surprising. Furthermore, it was also observed that infection sites in C57BL/6 mice saw recruitment of CD8+ T-cells even in the absence of CD4+ T-cells (128). These observations suggest that an interplay between CD4+ and CD8+ T-cells in MmuPV1 infection model is different from at least herpes viruses. Recent studies have shown that CD4+ T helper-independent $CD8^+$ CTL responses can be elicited by several other viruses as well [e.g. ectromelia virus (136), influenza virus (137), and dengue virus (138)]. Although the details of immune recognition of MmuPV1 are yet to be determined, it seems likely that T-cells control MmuPV1 infection by potentially modulating both innate and adaptive arms of the immune system. It is worth noting that increased incidence of HPV-associated papillomas is observed in T-cell-immunosuppressed patients further emphasizing the role of CD4+ and/or CD8+ T-cell responses in PV-mediated disease (139). T-cell infiltration is seen in both cutaneous and mucosal lesions

during the spontaneous regression of papillomas (140-143). When T-cell responses to five HPV16 proteins (E6, E7, E4, L1 and L2) were analyzed in women with CIN or cervical carcinoma, CD4+ and CD8+ T-cell responses changed with severity of disease suggesting that there are differences in how viral antigens are seen by the immune system during progressive disease of the cervix(144). Hence, there is a need to understand and define the role played by HPV-16 specific T-cells during the natural course of virus infection. While such a prospective study will be hard to conduct in humans, the MmuPV1-infection model provides us the opportunity to define the contribution of T-cells during the course of PV infections.

8.1.2. UVB-mediated immunosuppression is necessary for MmuPV1-dependent disease

Several groups, including us, have reported that immunocompetent, wild-type strains of mice are resistant to MmuPV1-induced skin disease (101, 118, 127, 128). We have made the novel observation that UVB-irradiated immunocompetent animals are susceptible to MmuPV1-induced papillomas (118). These studies are described in Chapters 5 and 6. Specifically, we found that when MmuPV1-infected FVB/NJ mice were exposed to a single dose of UVB (300 mJ/cm^2) twenty-four hours before or after infection, papillomas arose at approximately 50% of the infected sites (Fig. 5-1). In contrast, non-UVB-irradiated animals were resistant to MmuPV1-induced papillomatosis. The effect of UV in virus-infection models can be two pronged wherein UV can increase susceptibility to disease by: a) directly impact the activity of viruses; or b) indirectly impact the virus by causing systemic effects on the host immune system. We found that treatment of mice with UVB before or after infection are both effective in increasing

susceptibility to MmuPV1-induced disease (Fig. 5-1B). In those experiments, *FVB/N* mice were treated with UVB 24 hours before or after infection with MmuPV1. I have found this to be true also in studies where C57 BL/6 mice were treated with UVB 5 days before or after infection; both cohorts developed a similar incidence of papillomas (data not shown). Therefore our studies suggest that UVB most likely does not directly impact papillomavirus life cycle at least during establishment of viral life cycle in the host. In support of the latter hypothesis, that UV has a systemic effect on the host facilitating virus susceptibility, we found that when infection sites (ears) were shielded from UVB exposure, papillomas still arose with equal penetrance to that seen with mice whose infections sites were not shielded, demonstrating that UVB indeed has a systemic effect in increasing susceptibility to MmuPV1-induced disease (Fig. 5-7).

Besides its role as a mutagen, UV has been shown to cause local as well as systemic immunosuppression (304). These seminal studies in conjunction with the observations that the immune status plays a critical role in MmuPV1-induced pathogenesis (Chapter 4) led us to pursue studies to test the role of UVB-mediated immunosuppression in the context of MmuPV1-induced disease. When we assessed the status of immunosuppression in UVB-irradiated animals by means of contact hypersensitivity assays, we found that, similar to prior studies, UVB induces systemic immunosuppression of the host (Fig. 5-8). Furthermore, we found there to be a correlation between UVB-induced susceptibility and onset of MmuPV-1 associated disease and UVB-induced immunosuppression when CHS assay was performed at the 3 month endpoint, when we observe maximal penetrance of MmuPV1-induced papillomatosis (Fig. 5-9). This observation while valuable does not demonstrate

causality. Therefore we sought to test whether UVB mediated immunosuppression is necessary for UVB to increase susceptibility of mice to MmuPV1-induced papillomas (Chapter 6) by means of genetic approaches.

UVB mediated immunosuppression is thought to be largely T-cell mediated and several immunosuppressive populations of T-cells (e.g. Tregs) have also been identified in response to UVR (191, 192). UVR has been shown to result in altered cytokine profiles from pro-inflammatory Th1 to the immunosuppressive Th2 profile that involves upregulation of cytokines like TNF-alpha, IL-10, IL-4 and prostaglandin E2 (193, 194). While several pathways have been studied extensively in the context of UVB mediated immunosuppression, a number of studies have demonstrated that IL-10, which is an immunosuppressive cytokine, is a critical modulator of UVB induced immunosuppression. IL-10 has been shown to activate T_{regs} leading to sustained immunosuppression (322-327). A clear role of IL10 in mediating UVB-induced immunosuppression was established using *IL10*$^{-/-}$ mice (325). Therefore to address the question of necessity of UVB-induced immunosuppression in MmuPV1-induced disease we made use of the *IL10*$^{-/-}$ mice (Fig. 6-1). We found that *IL10*$^{-/-}$ mice were resistant to UVB-induced immunosuppression; in particular the mice were impaired in their effector immune response function (Fig. 6-1B). Furthermore, MmuPV1 failed to cause disease in UVB-irradiated, *IL10*$^{-/-}$ mice (Fig. 6-1C). These data support the hypothesis that UVB mediated immunosuppression is necessary to facilitate MmuPV1-induced disease.

In exploring the pathways responsible for UVB-induced immunosuppression, we also tested whether the Aryl Hydrocarbon Receptor (AhR) plays a role in UVB's effects. Several independent studies have suggested a potential link between UVB-induced

immunosuppression and the AhR pathway (331, 337, 338). AhR is a ligand-activated transcription factor that has been known to play a critical role in the metabolism of several environmental pollutants, such as dioxin and other polycyclic aromatic hydrocarbons (PAHs) and has been extensively studied by Dr. Christopher Bradfield's lab at McArdle, the lab that first cloned AhR (377). It has been shown that UVB exposure of rat and human skin to UVB induces AhR-dependent expression and activity of CYP1a, one of the best characterized, AhR-responsive genes (337, 338). Recently, it was shown that *AhR*$^{-/-}$ mice are impaired in CHS responses when treated with UVB (339). Previous studies have shown that activation of AhR causes induction of a specific population of T-cells in the spleen which in-turn produce IL-10 (336). We observed that in the skin, UVB-mediated induction of IL-10 is dependent on AhR as skin explants from *AhR*$^{-/-}$ mice were impaired in production of IL-10 upon UVB irradiation (Fig. 6-2). Importantly, UV-irradiated *AhR*$^{-/-}$ mice were resistant to MmuPV1-induced papillomas; whereas, when we performed CD4+/CD8+ T-cell depletion in *AhR*$^{-/-}$ mice, we found them to be susceptible to MmuPV1-induced papillomas (Fig. 6-3). These observations demonstrate that UVB-mediated immunosuppression via the AhR pathway is necessary for MmuPV1-induced papillomas.

In trying to test the contributions of MmuPV1 in mucosal disease, we found that the systemic effect of UVB may extend to mucosal disease as well as we found that UVB-irradiated mice infected in the vaginal tract developed higher grade disease than non-UVB irradiated mice (Chapter 7). However, exposure to UVB alone was not sufficient in causing malignancies to arise in the reproductive tract; whereas, mice that were UVB-irradiated and treated with estrogen, a known co-carcinogen in

cervical/vaginal carcinogenesis, developed MmuPV1-induced cancers. Estrogen treatment alone did not cause cervical/vaginal cancers. These results demonstrate that UVB cooperates with estrogen to cause cervical/vaginal cancers in this PV-infection model. Based on other rodent models of viral infections, UV radiation has been shown to affect both skin-associated infections, such as those caused by herpes simplex virus (HSV-1), as well as other infections that are systemic and/or non-cutaneous [Reviewed in (173)]. These observations suggest that the systemic effects of UVB in promoting MmuPV1-induced disease is not limited to cutaneous disease.

8.1.3. Implications of UVB-mediated immunosuppression in human disease

While immunosuppressive effects of UVB have been extensively characterized in mice (378), it remains to be clearly established if there is correlation between UVB exposure and immunosuppression in humans. In 1990 study performed by Yoshikawa, *et al* (379), normal, healthy human volunteers and patients with history of non-melanoma skin cancer were tested for their capacity to develop contact hypersensitivity to dinitrochlorobenzene (DNCB) following exposure of buttock skin to UVB radiation. They found that 40% of healthy volunteers failed to develop CHS responses when DNCB was painted on irradiated sites. Further, they observed that virtually all skin cancer patients that had been exposed to UVB and DNCB failed to develop CHS responses. Fair-skinned individuals who develop sunburns readily and are at a higher risk of developing skin cancer have been found to be more susceptible to local suppression of CHS responses even at suberythermal doses of UVR exposure (380). In a more recent study, association of human polymorphisms in functional variants of 10 genes involved in the response to UV radiation (IL-10, IL-4, and TNF-α among others) was analyzed in

the context of Basal Cell Carcinoma and Squamous Cell Carcinoma. These investigators observed that there was increased risk for both basal cell carcinoma (BCC) and squamous cell carcinoma (SCC) with increasing numbers of variant IL10 haplotypes, skin type and skin burns (381). The variants studied were present in the promoter region of the gene and have been correlated with an increased production of this cytokine (382). A similar result was observed in a non-Caucasian population, where patients with the low expression IL-10 promoter variants were less likely to develop skin cancer in sun-exposed areas (383). In transplant patients chemically treated to suppress immune-mediated rejection of the organ they received, there is high prevalence of skin cancers estimated at 65-250 times higher for SCCs and 10-16 times higher for BCCs when compared to normal subjects. These tumors are found to arise predominantly on sun-exposed areas of the body. Furthermore, skin cancer incidence correlates with exposure to UV before or after transplantation (384). Cutaneous HPV infections are far more common in organ transplant recipients, and have been etiologically implicated in skin cancers arising in these patients(385). Together these studies emphasize the impact of UV exposure and/or chemically induced immunosuppression and HPV infection in the development of non-melanoma associated skin cancers (NMSCC).

UV-induced immunomodulation is a critical factor affecting the health of children [Reviewed in(355)]. While in the context of squamous cell carcinoma (SCC) cumulative lifetime sun exposure is considered as an important factor, for basal cell carcinoma (BCC) it has been suggested that short-term sun exposures and sunburns, particularly during childhood pose serious risks (386). Epidemiological data obtained from migration studies support the idea that that exposure to UV in childhood has a significant influence

on subsequent NMSC development. Firstly, individuals born in northern Europe who migrated to Australia (where there is higher solar UVR) at age 10 years or older had a three-fold decreased risk of NMSC compared with those born in Australia (387). Secondly the risk of BCC decreased as age of arrival in Australia increased (386). Together these observations suggest the level exposure to the sun during childhood has an impact on the lifetime potential risk of NMSC. Besides cancer, UVR-associated systemic immune changes have also been shown to cause photosensitivity and plaque-like lesions in patients with the autoimmune disorder lupus erythematosus (388-390).

Most immune responses to infections are controlled by Th1 responses (391) and UVR exposure is known to impact antigen presentation and Th1 responses which are both required for the immune control of intracellular infections (392). Virus-infection based animal models have shown that UVR exposure has significant effects on disease outcome in these models typically associated with down-regulation of T-cell responses [Reviewed in (352)]. Results from these infection models lead to the speculation that exposure of humans to UVR can potentially make a higher proportion of infections symptomatic, increase the severity of symptoms, increase the oncogenic potential of a microorganism and/or reduce the resistance to reinfection. In case of herpes simplex virus type 1 (HSV1) UVR has been shown to be a stimulus for recrudescence by inducing the lytic phase of the virus that has established itself in the latent phase. In a controversial double blind, placebo-controlled trial individuals suffering from HSV1 recrudescence were treated with sunblock and then UV treated where lesions had occurred previously. It was found that while 71% of the subjects treated with placebo plus UVR developed HSV1 lesions whereas none of the individuals treated with sunblock, developed

recrudescence (393). In a study assessing the potential link between UVR-associated immunosuppression and HSV1 recurrence, it was found that individuals who showed suppressed contact hypersensitivity response to UV frequently developed recrudescence (394). Interestingly, for another herpes virus, varicella zoster virus (VSV) that causes chicken pox, it has been observed that chicken pox arises more in summer months than winter months (395, 396) with highest incidence of VSV coinciding with months of highest exposure to UV-radiation (397). There are multiple lines of evidence that suggest UVR could play a role in infection by cutaneous papillomaviruses. Epidemiological data demonstrates a correlation between exposure to UVR and the prevalence of cutaneous HPVs in healthy and immunosuppressed patients (163, 164). Cutaneous HPVs are more commonly found at anatomical sites exposed to sunlight, and a history of blistering sunburn is associated with prevalent and persistent cutaneous HPV infections (17, 163-165). In a case-control study, sunburn due to cutaneous sensitivity to sunlight exposure was associated with a higher seroprevalence for genus beta HPV types (166). The strongest relationship between beta-papillomaviruses and SCC comes from patients suffering from the genetic dermatological condition called Epidermodysplasia Verruciformis (EV). EV patients have been found to be prone to HPV-induced warts and skin cancers (9, 79). In a study conducted in Uganda, where sunlight exposure is extremely high, SCCs in the conjunctiva of the eye of subjects was analyzed and beta-HPVs were identified in 86% of these SCCs suggesting that HPV possibly acts as a cofactor in development of these tumors (398-400). Recently, an association between anogenital HPVs and sunlight has also been suggested based on the observation that HPV infection peaked in summer months (401, 402). Although studies performed assessing

impact of UVR on human infections are limited, it has been shown that UVR suppresses memory immune responses as assessed by delayed-type hypersensitivity (DTH) responses to Mantoux reaction using a tuberculin purified derivative (403, 404) and application of several standard multitest antigens (405). In the latter study, volunteers were found impaired in their DTH responses following exposure to sunlight (405).

Of relevance to PV infection-based diseases and other infections is the need to understand whether sun exposure can impact immune responses to vaccination. There are a very limited number of studies addressing this issue and these studies are largely based on understanding the seasonal impact on vaccine efficacy [Reviewed in (354)]. Upon use of oral poliovirus vaccine, it was found that, in the Tel-Aviv area, seroconversion rates and antibody titers were higher in children who were vaccinated in winter (UV index <3, low) versus those who were infected in summers (UV index >10)(353, 406, 407). This was also observed in the context of the administration of the live flu vaccine (408), hepatitis B vaccine (409) and more recently the measles vaccine (410). The impact of UVR, if any, on HPV-vaccines remains to be assessed but will be of pertinent relevance.

8.2. Future directions

The MmuPV1-infection model in mice is the first ever papillomavirus infection model which makes use of the laboratory strain of mice to study papillomavirus disease biology. This model provides several important research avenues (Fig. 8-1) to PV researchers that have been difficult to explore due to lack of suitable tractable *in vivo* infection models. In the Lambert lab, several lab members are now pursuing MmuPV1 studies to answer several new questions about virus biology. Describing all potential future directions is beyond the scope of this chapter, but I will describe a few potentially important new directions that maybe pursued based on some preliminary studies and/or results described in this thesis.

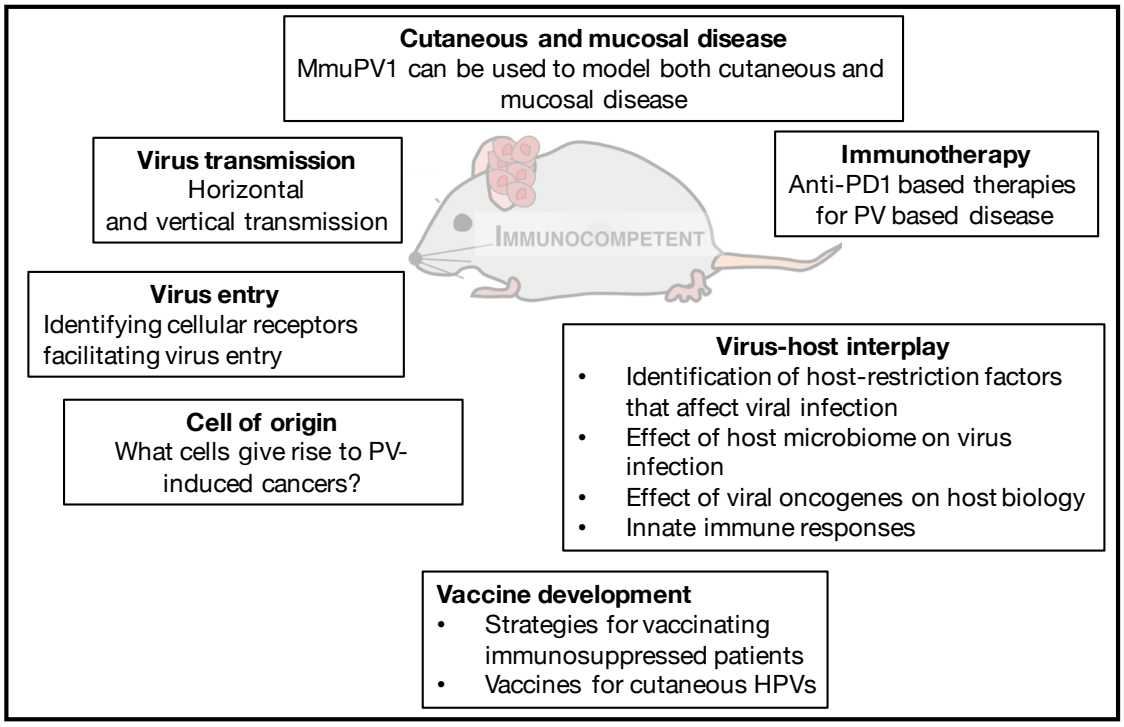

Fig. 8-1. Potential research avenues provided by MmuPV1-infection model

8.2.1. Is UVB-induced immunosuppression sufficient to account for susceptibility to MmuPV1-induced papillomas?

My thesis work has been focused to a large extent on how alterations in host-immune responses influence MmuPV1-induced disease. Some of these observations may be extrapolated to understanding contribution of host-immune responses to papillomavirus-induced disease in humans. Future work can be focused on dissecting the exact mechanisms of host-immune responses to papillomavirus-based diseases that can help us provide better health protection strategies in the context of HPV infcections and the diseases they cause. In Chapters 5-7, I have shown that UVB-modulated immunosuppression drives PV-associated disease in cutaneous as well as mucosal disease. In understanding the mechanisms responsible for UV-induced immunosuppression, I have demonstrated that UV-induced immunosuppression driven by IL-10 and AhR is necessary for the onset of MmuPV1-induced papillomas. But, my work does not answer whether IL-10 and/or AhR mediated immunosuppression is sufficient to account for susceptibility to MmuPV1-induced papillomas.

8.2.1.1. Is UVB-induced immunosuppression via IL-10 sufficient to account for susceptibility to MmuPV1-induced papillomas?

In attempting to address whether IL-10 induced immunosuppression is sufficient for MmuPV1-induced disease, I tested whether a strain of mice that over-expressed IL-10 in the epithelia was susceptible to MmuPV1-papillomas in the absence of UVB. This mouse strain (*K14vIL10*) expresses viral IL-10 (vIL-10), a product encoded by Eptein Barr Virus (EBV, human herpes virus 4) that is highly homologous to both murine and human IL-10, under the control of the keratin 14 promoter (266). Based on the observations by several

groups that IL-10 mediates suppression of a normal immune response against an incipient tumor, we hypothesized that *K14vIL10* mice, that express the viral IL-10 in stratified epithelium should be naturally susceptible to MmuPV1-induced skin papillomas. However, this was not the case (Fig. 8-2); *K14vIL10* mice did not develop any papillomas in the absence of UVB-irradiation. Furthermore, there was no statistical significance between the onsets of papillomas in UVB-irradiated *K14vIL10* versus UVB-irradiated wild-type *FVB*/N mice. This data indicates that IL10-mediated immunosuppression, in *K14vIL10* is not sufficient to account for susceptibility to MmuPV1-induced papillomas. In the original study characterizing *K14vIL10* mice it was found that these mice were impaired in delayed type hypersensitivity responses when compared to wild-type (WT) animals but not contact hypersensitivity responses. Based on the immunosuppressive role of IL10, the authors predicted that *K14vIL10* mice would be more prone to tumors when chronically UV irradiated when compared to WT mice. Surprisingly, the authors found that *K14vIL10* mice developed significantly fewer tumors than WT mice (266). This led to the speculation by the authors that perhaps continual production of vIL-10 in the transgenic mice induces receptor modulation or other downstream events that result in a different response or that the concentration of vIL-10 produced *in vivo* is not high enough to cause sufficient immunosuppression. To address the latter question, a simple approach maybe to inject recombinant IL-10 cytokine in mice and then infect with MmuPV1. The caveat to this approach is the low half life of the cytokine, lack of pharmokinetic information about IL-10 *in vivo*, and that we don't know how long these animals should be treated with IL-10.

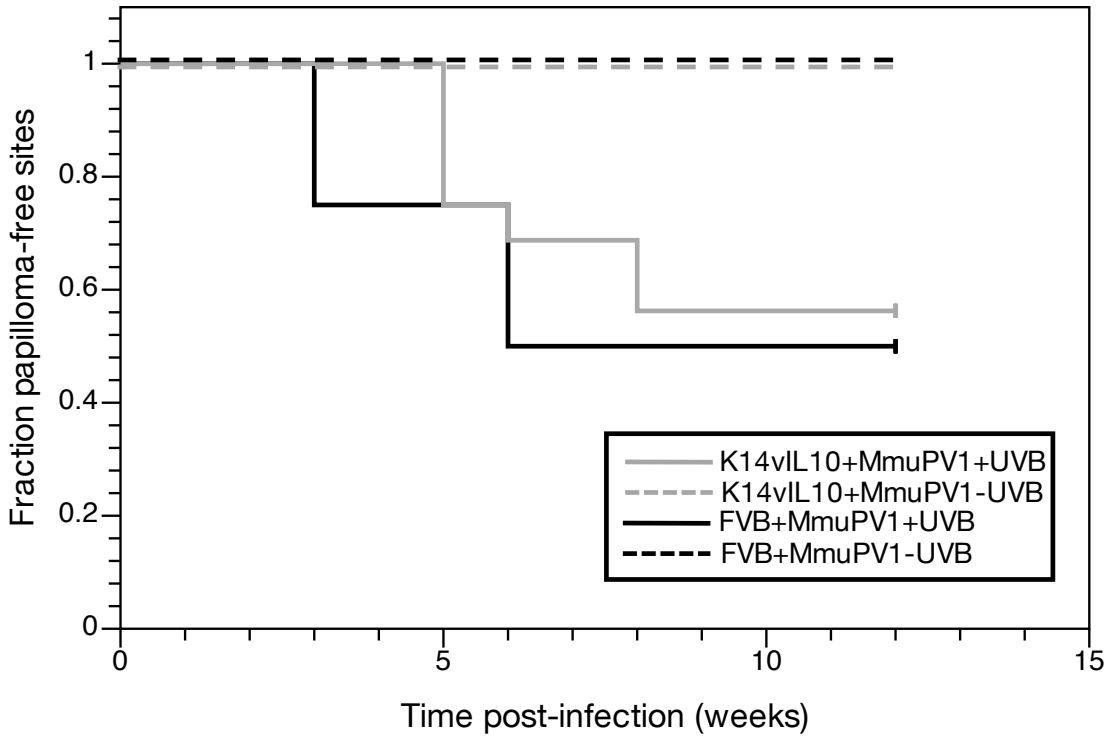

Fig. 8-2. Over-expression of IL-10 in epithelia is not sufficient for MmuPV1-induced papillomas

K14vIL10 (n=16 ear sites/group) mice were infected with MmuPV1 at 10^8 VGE with (grey) or without (grey-dashed) UVB irradiation (300mJ/cm^2). In parallel FVB wild-type mice (n=16 sites/group) were infected with MmuPV1 as well followed by UVB irradiation. Papilloma onset was monitored and Kaplan-Myer analysis was performed. Neither K14vIL10 nor FVB mice developed any papillomas in the absence of UVB. There was no statistical difference between onset of papillomas in UVB-irradiated groups.

In the context of UVB treated mice, it is possible that the IL-10 that is responsible for mediating the increased susceptibility to MmuPV1-induced disease is not derived from the epithelia. Several cells in the skin have been argued to be responsible for production UVB-induced IL-10 [Reviewed in(411)], including but not limited to keratinocytes (340, 412), tissue-resident T-cells, as well as mast cells (413). Recently, it was demonstrated that skin-infiltrating macrophages that migrate to draining lymph nodes produce IL-10 upon UV exposure. Furthermore, IL-10 derived from these macrophages was found to be immunosuppressive suggesting that macrophages may be key in inducing UV-induced immunosuppression (328). Therefore I propose testing the role of macrophage-derived IL-10 in the context of MmuPV1-induced disease. Recently, a bi-transgenic mice *(tetO)7-CMV- huIL-10* that expressed human-IL-10 under the control of tetracycline response element have been described (414). These mice, which we have recently obtained, provide us the opportunity to over-express IL-10 when crossed to an transgenic strain expressing reverse tetracycline-controlled transactivator (rtTA) from an appropriate cell type-specific promoter. In context of testing the role of macrophage-derived IL-10, I propose crossing these mice to *CD68-rtTA-tet-GFP* mice that express rtTA under the hCD68 promoter for macrophage-specific gene induction (415). The resultant offspring of this cross, when put on a doxycycline diet (416) will over-express IL-10 in macrophages and can then be used to determine whether macrophage-derived IL-10 is sufficient to increase susceptibility to MmuPV1-induced disease. Based on conflicting reports suggesting multiple sources of IL-10 in the skin in response to UVB, a potential pitfall of this approach is that macrophage-derived IL-10 may not be sufficient for MmuPV1-induced papillomas. Further, the source of IL-10 may

be different during onset versus persistence of the disease. Therefore it may be valuable to first identify the cells producing IL-10 in this infection model. In this context, I propose infecting IL10-GFP knock-in reporter mice [*Il10*^{tm1Flv}/J mice, known as *Tiger* mice (417)] with MmuPV1-followed by UVB-irradiation and harvesting tissue at different time points post-infection (e.g. immediately after UVB-irradiation, at onset of papilloma, during growth phase of papilloma). The GFP positive IL-10 expressing cells could then be sorted via FACS and analyzed for cell-type specific markers to identify the cell types expressing IL-10. Then, the genetic approach described above using *(tetO)7-CMV- huIL-10* mice could be used with the appropriate rtTA transgenic mice to determine which cell type(s) expressing IL10 is critical to induce systemic immunosuppression that makes mice susceptible to MmuPV1-induced disease.

8.2.1.2. Is UVB-induced immunosuppression via AhR sufficient to account for susceptibility to MmuPV1-induced papillomas?

To address the question whether UVB-induced immunosuppression via AhR is sufficient to account for susceptibility to MmuPV1-induced papillomas; we can activate the AhR pathways by means of known AhR agonists. One simple approach could be to feed mice a diet rich in Indole-3- carbinol (I3C), which is a known AhR ligand (418). This approach has been described recently to activate the AhR pathway in mice as well (419). Mice on an I3C diet show increased levels of IL-10 (420) confirming that the AhR pathway mediating UVB-induced immunosuppression is indeed upstream of IL-10 (Chapter 6). Since the role of I3C diet has not been tested in the context of immunosuppression, mice kept on I3C diet should be assessed for CHS responses and then infected with MmuPV1. If AhR-mediated immunosuppression is sufficient to

account for susceptibility to MmuPV1-papillomas; mice on I3C diet will be susceptible to MmuPV1-infection.

8.2.2. Effect of viral genes on host immunity

In my studies I have focused largely on the role of immunosuppression in the onset of disease. As described in Chapter 5, we learnt that there was a correlation between UVB-induced immunosuppression and onset of papillomavirus disease. Following the publication of this work (118), we also performed CHS assays at 6-months post-infection to test whether mice retain immunosuppression. For this purpose we infected mice with MmuPV1 in the right ear and exposed them to a single dose of UVB (300 mJ/cm^2) 24 hrs post-infection consistent with my prior studies. As described in Chapter 5, MmuPV1-induced warts arising on UVB-irradiated FVB mice follow different growth profiles, i.e. papillomas that arise can (i) persist and increase in size, (ii) partially regress and (iii) completely regress. Therefore, sizes of papillomas were monitored by measuring sizes of warts every 2-weeks, post papilloma-incidence. At 6-months post-infection we performed CHS assay on all mice by sensitizing mice (with 0.5 mg of DNCB) on their shaved backs and then challenging them (with 0.2 mg DNCB) on the uninfected, left ear five days post-sensitizing and measured swelling up to 96 hours (Fig. 8-3). We found that at six-months post UVB irradiation there was no significant difference between CHS responses between control group (animals not treated with UVB) and UVB-irradiated uninfected mice (*P=0*.39, Wilcoxon rank-sum, *two-sided*). All MmuPV1-infected mice, irrespective of disease status developed high CHS responses at 6 months post-infection, indicating that UVB-induced immunosuppression is lost at 6-months post-infection.

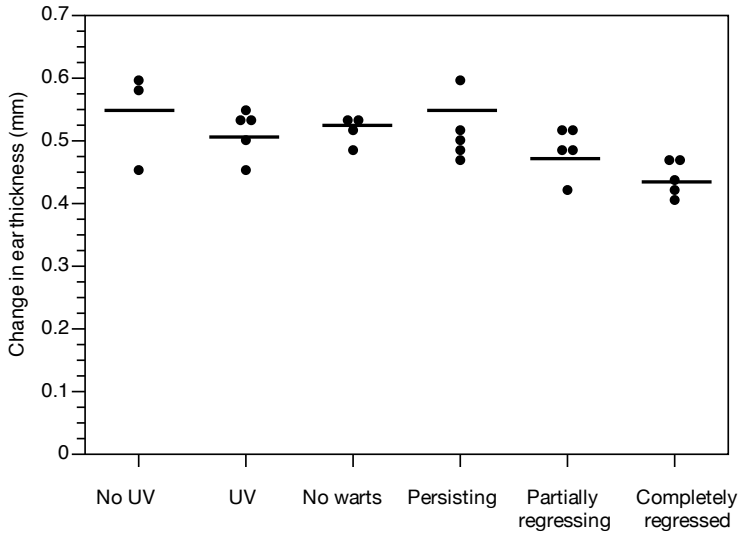

Fig 8-3. Immune suppression in UVB-irradiated mice at 6 months post-infection. Mice were either infected with MmuPV1 or vehicle followed by UVB irradiation (300mJ/cm^2) in the right ear. Papilloma sizes were measured leading to identification of persisting vs partially regressing papillomas. At 6 months post-infection, mice were sensitized with DNCB and were challenged DNCB in the left ear 5 days following infection. Ear swelling was measured by means of a micrometer screw gauge. Ear thickness is reported as the average of the difference between ear thickness 0 hrs post challenge and 72 hrs post challenge. Ear thickness for each mouse is shown as a dot plot. The black lines represent the mean reading for each group. Wilcoxon rank-sum test was used to analyze difference between several groups. There was no significant difference between CHS responses in any of the comparisons made.

The observation that immunosuppression is lost in groups of mice where papillomas are partially-regressing or have regressed completely is not entirely surprising as reversal of immune suppression most likely allows effector immune responses to kick in and contribute to papilloma-regression. However, the observation that papillomas can persist and grow in the absence of sustained immune suppression is surprising. This is also the time point in which we have seen MmuPV1-associated SCCs develop in mice. This would suggest that the virus has developed mechanisms to evade effective cellular immune responses. Several potential mechanisms of immune escape have been proposed for papillomaviruses [Reviewed in (421-424)]. First, papillomaviruses may limit production of viral proteins to evade immunological recognition. For example, E6 and E7 are expressed in low levels in basal epithelia, potentially limiting an effective immune response against the cells in which the virus is actively replicating. Papillomaviruses delay expression of late genes until the terminally differentiating layer of the epithelia (425) and it has been shown that the delayed expression of capsid-encoding genes may be due to a pattern of codon usage that inhibits their expression in basal epithelial cells (426). This can also help the virus evade immune recognition. Second, viral oncogenes may modulate immune responses by directly interacting with immune molecules.

We recently performed RNA-seq analysis in collaboration with Dr. Thomas Zheng's lab (NCI) on MmuPV1-induced papillomas arising in *FoxN1*$^{nu/nu}$ mice (Fig. 8-4) and identified 1238 genes to be significantly down-regulated and 1062 genes to be significantly up-regulated (Fig. 8-4A) in MmuPV1-induced papilloma tissue versus control uninfected tissue. Hierarchical clustering of RNAseq genes showed that papillomas clustered together separately from the controls (Fig. 8-4 B) suggesting that a

distinct set of genes is deregulated in the papillomas when compared to the control. Gene ontology analysis of the genes found to be significantly up-regulated in the papillomas (Fig. 8-4 C) showed that several of the up-regulated genes affected by MmuPV1 are associated with keratinization and epithelial differentiation. In particular we observed that family of keratin (Krt) proteins called "stress keratins" – Krt6a, Krt6b, Krt16 and Krt17 were found to be among the top 20 genes up-regulated in MmuPV1 induced papillomas (Fig. 8-4D). Keratinocytes play an important role in sensing epidermal barrier challenges and produce the first signals, known as damage-associated molecular patterns (DAMPs) that include antimicrobial peptides, cytokines and chemokines to initiate the inflammatory response in the event of a barrier breach (427-429). Several of these DAMPs that are secreted from keratinocytes and act by directly attacking invading pathogens, attracting and activating a wide range of immune cells (e.g., dendritic cells, neutrophils, macrophages, T-cells) and modulating cytokine production [reviewed in (427)]. Stressed keratinocytes rapidly induce de novo transcription of keratins 6, 16, and 17, whose normal expression pattern in stratified epithelia is restricted to the epidermis of glabrous skin, the oral mucosa, and several appendages (430).

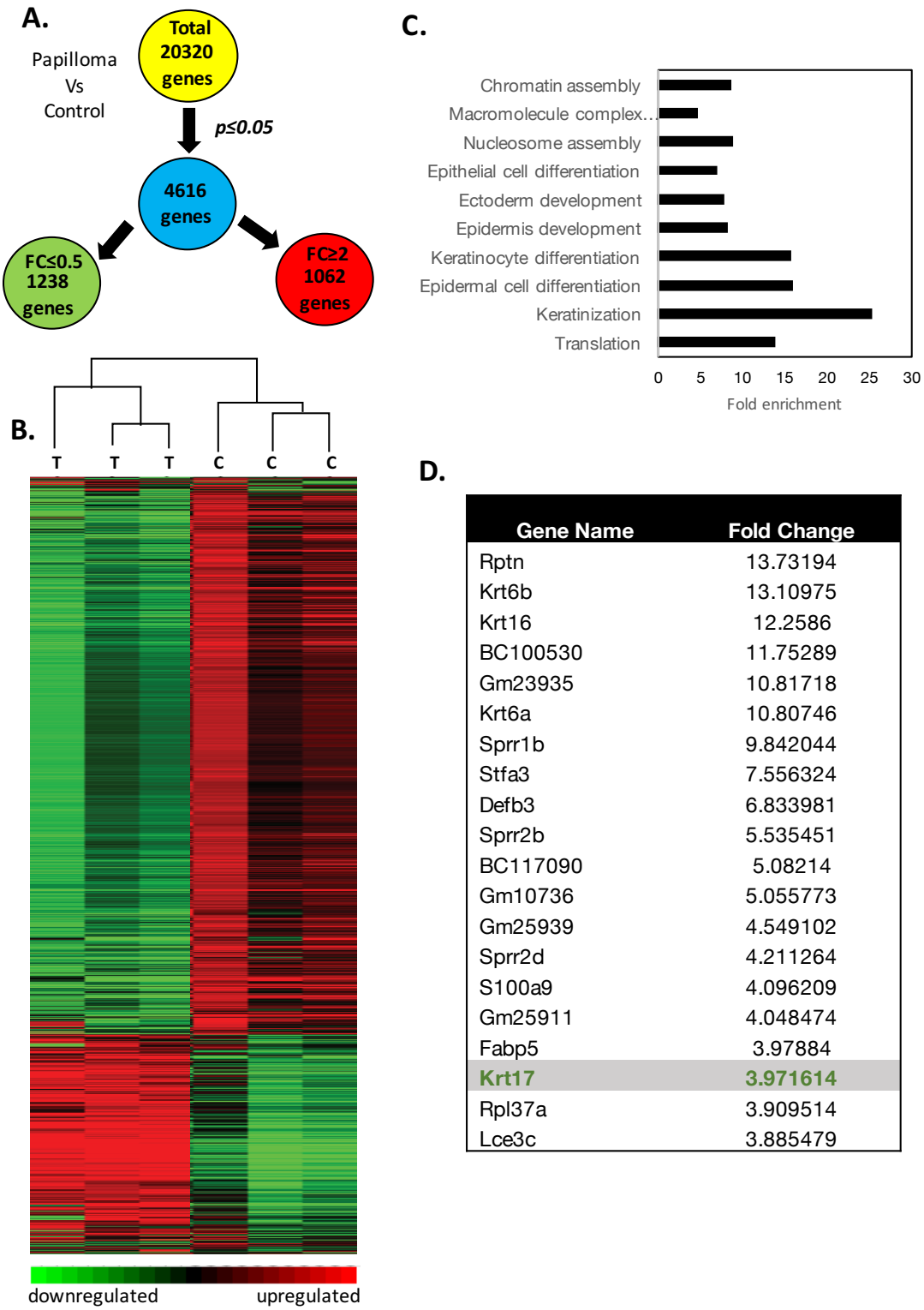

D.

Gene Name	Fold Change
Rptn	13.73194
Krt6b	13.10975
Krt16	12.2586
BC100530	11.75289
Gm23935	10.81718
Krt6a	10.80746
Sprr1b	9.842044
Stfa3	7.556324
Defb3	6.833981
Sprr2b	5.535451
BC117090	5.08214
Gm10736	5.055773
Gm25939	4.549102
Sprr2d	4.211264
S100a9	4.096209
Gm25911	4.048474
Fabp5	3.97884
Krt17	**3.971614**
Rpl37a	3.909514
Lce3c	3.885479

Fig. 8-4. RNA-seq analysis of MmuPV1-induced papillomas

Fig. 8-4. RNA-seq analysis of MmuPV1-induced papillomas

A. RNAseq analysis was performed on MmuPV1-induced papillomas arising in FoxN1$^{nu/nu}$ mice in comparison with control skin harvested from uninfected nude mice. 4616 genes were found to be significantly (*P<0.05)* between the two groups of which 1238 genes were found to be significantly downregulated (green) and 1062 genes were found to be significantly upregulated.

B. When hierarchical clustering of RNAseq genes was performed it was found that papillomas clustered together separately from the controls. Shown here is hierarchical clustering for top 1000 genes from this analysis.

C. Gene Ontology analysis was performed using DAVID (103, 104) on significantly upregulated genes (*P<0.05; fold-change >=2)*. Top 10 pathways found to be upregulated with their enrichment scores are shown.

D. Table depicting fold changes of top 20 upregulated genes is shown. Stress keratins – Krt6a, Krt6b, Krt16 and Krt17 were found to be among the top upregulated genes.

Beside their mechanical properties (431), these keratins have specialized functions in the progression of inflammation and wound healing. Krt6 impacts cell migration by interacting with Src kinase (432, 433), whereas Krt17 promotes keratinocyte survival, growth (434), and a Th1/Th17-dominated immune environment contributing to the development of basaloid skin tumors (435). Krt17 is found to be frequently up-regulated in several cancers and is often associated with a poor prognosis (436-440). It was also observed that in mouse models for skin SCC or BCC, the genetic loss of *Krt17* attenuates tumorigenesis, in part through polarization of inflammatory cytokines from a Th1/Th17- to a Th2-dominated profile leading to decreased recruitment of inflammatory and effector immune cell to sites of tumor formation (435). In a report published by Dr. Pierre Coulombe's lab it was found that in K14HPV16$^{tg/+}$ mice crossed with *Krt17*$^{-/-}$ mice, onset of cervical lesions was delayed and closely paralleled by marked reductions in hyperplasia, dysplasia and vascularization (441).

When we performed immunofluorescence analysis of Krt17 in MmuPV1-induced papillomas, we found Krt17 to be highly upregulated in papillomas arising in immunodeficient as well as UV-irradiated immunocompetent mice that were infected with MmuPV1 (Fig. 8-5A). Therefore we hypothesized that loss of Krt17 will attenuate MmuPV1-induced papilloma formation in UV-irradiated immunocompetent mice. We were provided with *Krt17*$^{-/-}$ mice by Dr. Pierre Coulombe's lab (Johns Hopkins). As seen previously (265), *Krt17*$^{-/-}$ mice showed alopecia at weaning age (21 days) which was reversed in adult mice (Fig. 8.5B). When we infected *Krt17*$^{-/-}$ mice with MmuPV1 followed by UV-irradiation we did not see development of any papillomas in these mice (Fig. 8.5C) suggesting that Krt17 is important for onset of MmuPV1-induced papillomas.

As described earlier, Krt17 is known to be involved in the formation and maintenance of various skin appendages, specifically in determining shape and orientation of hair and is therefore thought to be a potential marker of stem cells but these properties are yet to be fully analyzed (442). This raises the possibility that Krt17 positive epithelial cells maybe required for successful MmuPV1 infection, as epithelial stem cells have been thought to be potential cells of infection for papillomaviruses. Therefore we are currently in the process of performing T-cell depletion in Krt17$^{-/-}$ mice and then test if they are susceptible to MmuPV1 infections.

Based on observations made in cancer models in the context of loss of Krt17 (435, 441), it is likely that Krt17 could play a different role in onset versus progression of disease. It has been shown that loss of Krt17 plays a role in delaying SCCs and BCCs by causing cytokine polarization switch from Th1 to Th2-dominated profile during lesion progression (435, 441). Interestingly, UVB is also known to promote a Th2 dominant environment that contributes to its immunosuppressive environment (443). Hence one could speculate that the Th1 to Th2 switch caused by Krt17 may contribute to long-term persistence of MmuPV1-induced warts even in the absence of immunosuppression (Fig. 8-3). I propose that Th1/Th2 profiles of MmuPV1-induced warts be determined at 3 months and 6 months post-infection using qRT-PCR to evaluate expression of genes associated with Th1 (e.g. CXCL5, CXCR2, TNFa) and Th2 (e.g. IL4, IL20, CCR4) as described previously (441). This will help us determine if a localized cytokine polarization has occurred which is enabling the papillomas to persist in the absence of UV-dependent immunosuppression. To test the contribution of Krt17 in persistence of MmuPV1-induced disease, I propose generating a Krt17 conditional knockout model.

Here a mouse carrying Krt17 floxed gene may be mated with a tamoxifen inducible Cre to turn off expression of Krt17 in persisting papillomas at 3-6 months post-infection. I predict that turning Krt17 expression off will cause attenuation of papilloma formation at later stages in conjunction with a Th1/Th2 polarization switch. Recently, when the keratinocyte transcriptome of K14E7 mouse skin was analyzed, stress keratin genes were found to be significantly altered in the K14E7 mouse model over time (444) suggesting that perhaps HPV16 E7 is responsible for Krt17 upregulation. It remains to be tested whether MmuPV1 oncogenes E6 and/or E7 are responsible for Krt17 upregulation. These functions can be further teased apart by transducing mouse keratinocyte cell lines with MmuPV1 E6 and/or E7 and looking for Krt17 upregulation.

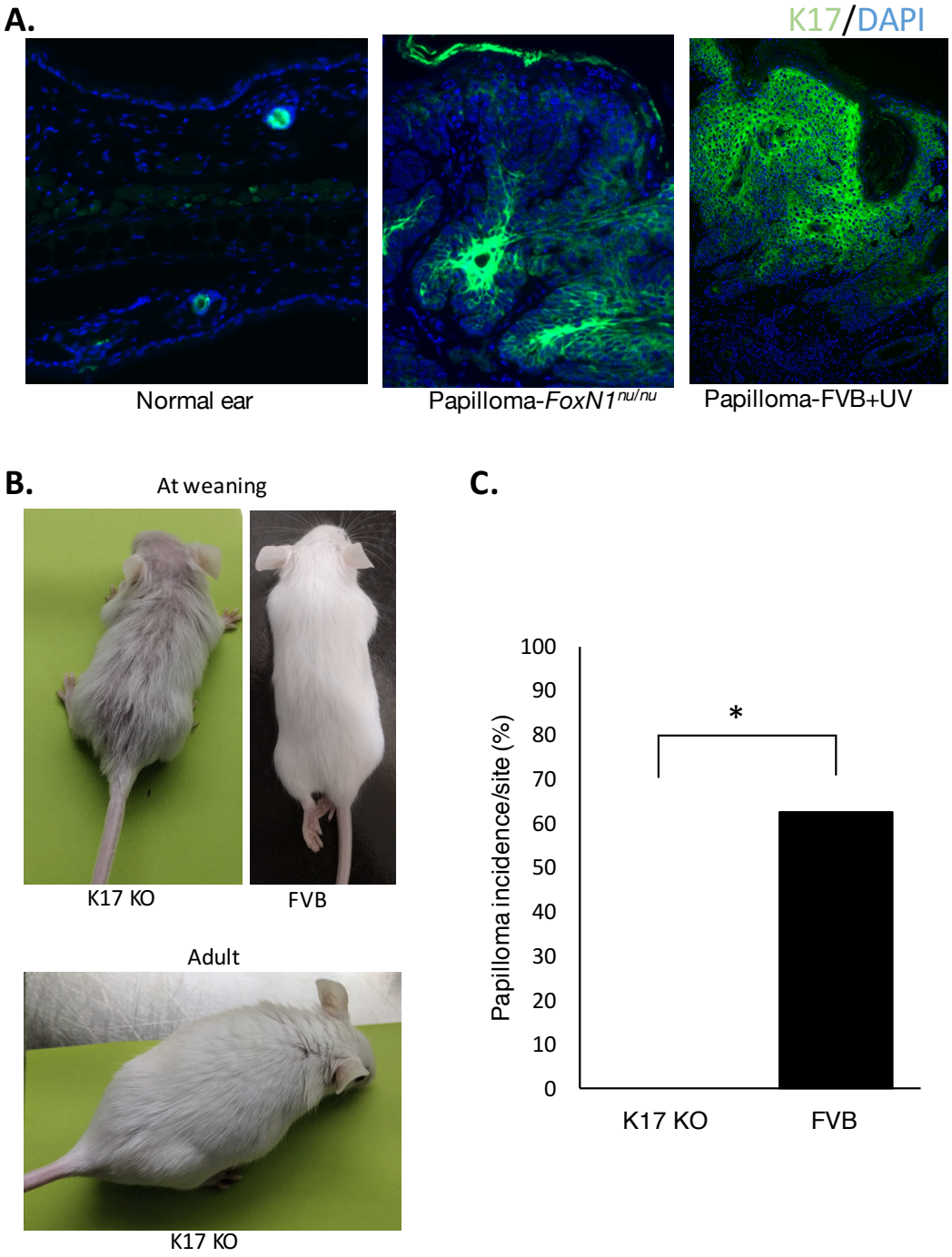

Fig. 8-5. K17 null mice are resistant to MmuPV1-induced papillomas

Fig. 8-5. K17 null mice are resistant to MmuPV1-induced papillomas

A. Krt17 staining (green) was performed on uninfected ear skin harvested from FVB mice (left), papillomas arising in nude mice at 3 months post-infection (middle), and papillomas arising in UVB-irradiated FVB at 3 months post- infection (right). Tissue was counterstained with DAPI (blue).

B. Phenotypes of K17 KO mice. At wean age K17 KO mice show alopecia (top left) in comparison with WT FVB mice (top right) that have normal hair growth. This phenotype is reversed in adult (6 weeks old) K17 KO mice.

C. K17 KO mice (n=24 sites) and FVB mice (n=16 sites) were infected with 10^8 VGE dose MmuPV1 followed by UVB irradiation (300mJ/cm^2) 24 hours post- infection. At 16 weeks post-infection, 62.5% of infected sites in FVB mice developed papillomas whereas no papillomas were seen in K17 KO mice.

VIII. References

1. **Uberoi A, Lambert PF.** 2017. Rodent Papillomaviruses. Viruses **9**.
2. **Shope RE, Hurst EW.** 1933. Infectious Papillomatosis of Rabbits : With a Note on the Histopathology. J Exp Med **58:**607-624.
3. **Boshart M, Gissmann L, Ikenberg H, Kleinheinz A, Scheurlen W, zur Hausen H.** 1984. A new type of papillomavirus DNA, its presence in genital cancer biopsies and in cell lines derived from cervical cancer. EMBO J **3:**1151-1157.
4. **Durst M, Gissmann L, Ikenberg H, zur Hausen H.** 1983. A papillomavirus DNA from a cervical carcinoma and its prevalence in cancer biopsy samples from different geographic regions. Proc Natl Acad Sci U S A **80:**3812-3815.
5. **DiMaio D.** 2015. Nuns, warts, viruses, and cancer. Yale J Biol Med **88:**127-129.
6. **Van Doorslaer K, Li Z, Xirasagar S, Maes P, Kaminsky D, Liou D, Sun Q, Kaur R, Huyen Y, McBride AA.** 2017. The Papillomavirus Episteme: a major update to the papillomavirus sequence database. Nucleic Acids Res **45:**D499-D506.
7. **McLaughlin-Drubin ME, Meyers J, Munger K.** 2012. Cancer associated human papillomaviruses. Curr Opin Virol **2:**459-466.
8. **Jablonska S, Majewski S, Obalek S, Orth G.** 1997. Cutaneous warts. Clin Dermatol **15:**309-319.
9. **Jablonska S, Orth G, Obalek S, Croissant O.** 1985. Cutaneous warts. Clinical, histologic, and virologic correlations. Clin Dermatol **3:**71-82.
10. **Tschandl P, Rosendahl C, Kittler H.** 2014. Cutaneous human papillomavirus infection: manifestations and diagnosis. Curr Probl Dermatol **45:**92-97.
11. **Lebwohl MG, Rosen T, Stockfleth E.** 2010. The role of human papillomavirus in common skin conditions: current viewpoints and therapeutic options. Cutis **86:**suppl 1-11; quiz suppl 12.

12. **Mammas IN, Spandidos DA, Sourvinos G.** 2014. Genomic diversity of human papillomaviruses (HPV) and clinical implications: an overview in adulthood and childhood. Infect Genet Evol **21:**220-226.

13. **van Haalen FM, Bruggink SC, Gussekloo J, Assendelft WJ, Eekhof JA.** 2009. Warts in primary schoolchildren: prevalence and relation with environmental factors. Br J Dermatol **161:**148-152.

14. **Akgul B, Cooke JC, Storey A.** 2006. HPV-associated skin disease. J Pathol **208:**165-175.

15. **Astori G, Lavergne D, Benton C, Hockmayr B, Egawa K, Garbe C, de Villiers EM.** 1998. Human papillomaviruses are commonly found in normal skin of immunocompetent hosts. J Invest Dermatol **110:**752-755.

16. **Gassenmaier A, Fuchs P, Schell H, Pfister H.** 1986. Papillomavirus DNA in warts of immunosuppressed renal allograft recipients. Arch Dermatol Res **278:**219-223.

17. **Antonsson A, Forslund O, Ekberg H, Sterner G, Hansson BG.** 2000. The ubiquity and impressive genomic diversity of human skin papillomaviruses suggest a commensalic nature of these viruses. J Virol **74:**11636-11641.

18. **Howley PM, Pfister HJ.** 2015. Beta genus papillomaviruses and skin cancer. Virology **479-480:**290-296.

19. **Connolly K, Manders P, Earls P, Epstein RJ.** 2014. Papillomavirus-associated squamous skin cancers following transplant immunosuppression: one Notch closer to control. Cancer Treat Rev **40:**205-214.

20. **Meyers C, Laimins LA.** 1994. In vitro systems for the study and propagation of human papillomaviruses. Curr Top Microbiol Immunol **186:**199-215.

21. **Christensen ND, Budgeon LR, Cladel NM, Hu J.** 2016. Recent advances in preclinical model systems for papillomaviruses. Virus Res doi:10.1016/j.virusres.2016.12.004.

22. **Gil da Costa RM, Peleteiro MC, Pires MA, DiMaio D.** 2016. An Update on Canine, Feline and Bovine Papillomaviruses. Transbound Emerg Dis doi:10.1111/tbed.12555.

23. **Doorbar J.** 2016. Model systems of human papillomavirus-associated disease. J Pathol **238:**166-179.

24. **Rector A, Van Ranst M.** 2013. Animal papillomaviruses. Virology **445:**213-223.

25. **Peh WL, Middleton K, Christensen N, Nicholls P, Egawa K, Sotlar K, Brandsma J, Percival A, Lewis J, Liu WJ, Doorbar J.** 2002. Life cycle heterogeneity in animal models of human papillomavirus-associated disease. J Virol **76:**10401-10416.

26. **Campo MS.** 2002. Animal models of papillomavirus pathogenesis. Virus Res **89:**249-261.

27. **Munday JS, Kiupel M.** 2010. Papillomavirus-associated cutaneous neoplasia in mammals. Vet Pathol **47:**254-264.

28. **Chen EY, Howley PM, Levinson AD, Seeburg PH.** 1982. The primary structure and genetic organization of the bovine papillomavirus type 1 genome. Nature **299:**529-534.

29. **Lancaster WD, Olson C, Meinke W.** 1976. Quantitation of bovine papilloma viral DNA in viral-induced tumors. J Virol **17:**824-831.

30. **Olson C.** 1963. Cutaneous Papillomatosis in Cattle and Other Animals. Ann N Y Acad Sci **108:**1042-1056.

31. **Nasir L, Campo MS.** 2008. Bovine papillomaviruses: their role in the aetiology of cutaneous tumours of bovids and equids. Vet Dermatol **19:**243-254.

32. **DiMaio D, Petti LM.** 2013. The E5 proteins. Virology **445:**99-114.

33. **Munday JS.** 2014. Bovine and human papillomaviruses: a comparative review. Vet Pathol **51:**1063-1075.

34. **Venuti A, Paolini F, Nasir L, Corteggio A, Roperto S, Campo MS, Borzacchiello G.** 2011. Papillomavirus E5: the smallest oncoprotein with many functions. Mol Cancer **10:**140.

35. **Lange CE, Favrot C.** 2011. Canine papillomaviruses. Vet Clin North Am Small Anim Pract **41:**1183-1195.

36. **Nicholls PK, Stanley MA.** 1999. Canine papillomavirus--A centenary review. J Comp Pathol **120:**219-233.

37. **Stanley MA.** 2003. Progress in prophylactic and therapeutic vaccines for human papillomavirus infection. Expert Rev Vaccines **2:**381-389.

38. **Frazer IH.** 1996. The role of vaccines in the control of STDs: HPV vaccines. Genitourin Med **72:**398-403.

39. **Nicholls PK, Stanley MA.** 2000. The immunology of animal papillomaviruses. Vet Immunol Immunopathol **73:**101-127.

40. **Frazer IH.** 2014. Development and implementation of papillomavirus prophylactic vaccines. J Immunol **192:**4007-4011.

41. **Rous P, Kidd JG.** 1938. The Carcinogenic Effect of a Papilloma Virus on the Tarred Skin of Rabbits : I. Description of the Phenomenon. J Exp Med **67:**399-428.

42. **Kerr PJ, Donnelly TM.** 2013. Viral infections of rabbits. Vet Clin North Am Exot Anim Pract **16:**437-468.

43. **Christensen ND.** 2005. Cottontail rabbit papillomavirus (CRPV) model system to test antiviral and immunotherapeutic strategies. Antivir Chem Chemother **16:**355-362.

44. **Breitburd F, Salmon J, Orth G.** 1997. The rabbit viral skin papillomas and carcinomas: a model for the immunogenetics of HPV-associated carcinogenesis. Clin Dermatol **15:**237-247.

45. **Peng X, Knouse JA, Hernon KM.** 2015. Rabbit Models for Studying Human Infectious Diseases. Comp Med **65:**499-507.

46. **Doorbar J.** 2005. The papillomavirus life cycle. J Clin Virol **32 Suppl 1:**S7-15.

47. **zur Hausen H, de Villiers EM.** 2014. Cancer "causation" by infections--individual contributions and synergistic networks. Semin Oncol **41:**860-875.

48. **Schulz E, Gottschling M, Ulrich RG, Richter D, Stockfleth E, Nindl I.** 2012. Isolation of three novel rat and mouse papillomaviruses and their genomic characterization. PLoS One **7:**e47164.

49. **Rogovskyy AS, Chen Z, Burk RD, Bankhead T.** 2014. Characterization of the North American beaver (Castor canadensis) papillomavirus genome. Vet Microbiol **168:**214-220.

50. **Rector A, Tachezy R, Van Doorslaer K, MacNamara T, Burk RD, Sundberg JP, Van Ranst M.** 2005. Isolation and cloning of a papillomavirus from a North American porcupine by using multiply primed rolling-circle amplification: the Erethizon dorsatum papillomavirus type 1. Virology **331:**449-456.

51. **Iwasaki T, Maeda H, Kameyama Y, Moriyama M, Kanai S, Kurata T.** 1997. Presence of a novel hamster oral papillomavirus in dysplastic lesions of hamster lingual mucosa induced by application of dimethylbenzanthracene and excisional wounding: molecular cloning and complete nucleotide sequence. J Gen Virol **78 (Pt 5):**1087-1093.

52. **Nafz J, Schafer K, Chen SF, Bravo IG, Ibberson M, Nindl I, Stockfleth E, Rosl F.** 2008. A novel rodent papillomavirus isolated from anogenital lesions in its natural host. Virology **374:**186-197.

53. **Van Doorslaer K, Rector A, Jenson AB, Sundberg JP, Van Ranst M, Ghim SJ.** 2007. Complete genomic characterization of a murine papillomavirus isolated from papillomatous lesions of a European harvest mouse (Micromys minutus). J Gen Virol **88:**1484-1488.

54. **Sundberg JP, O'Banion MK, Shima A, Knupp C, Reichmann ME.** 1988. Papillomas and carcinomas associated with a papillomavirus in European harvest mice (Micromys minutus). Vet Pathol **25:**356-361.

55. **Ingle A, Ghim S, Joh J, Chepkoech I, Bennett Jenson A, Sundberg JP.** 2011. Novel laboratory mouse papillomavirus (MusPV) infection. Vet Pathol **48:**500-505.

56. **Joh J, Jenson AB, Proctor M, Ingle A, Silva KA, Potter CS, Sundberg JP, Ghim SJ.** 2012. Molecular diagnosis of a laboratory mouse papillomavirus (MusPV). Exp Mol Pathol **93:**416-421.

57. **Tan CH, Tachezy R, Van Ranst M, Chan SY, Bernard HU, Burk RD.** 1994. The Mastomys natalensis papillomavirus: nucleotide sequence, genome organization, and phylogenetic relationship of a rodent papillomavirus involved in tumorigenesis of cutaneous epithelia. Virology **198:**534-541.

58. **Amtmann E, Volm M, Wayss K.** 1984. Tumour induction in the rodent Mastomys natalensis by activation of endogenous papilloma virus genomes. Nature **308:**291-292.

59. **Kocjan BJ, Hosnjak L, Racnik J, Zadravec M, Poljak M.** 2014. Complete Genome Sequence of Phodopus sungorus Papillomavirus Type 1 (PsPV1), a Novel Member of the Pipapillomavirus Genus, Isolated from a Siberian Hamster. Genome Announc **2**.

60. **Joh J, Jenson AB, King W, Proctor M, Ingle A, Sundberg JP, Ghim SJ.** 2011. Genomic analysis of the first laboratory-mouse papillomavirus. J Gen Virol **92:**692-698.

61. **Stevens H, Rector A, Van Ranst M.** 2010. Multiply primed rolling-circle amplification method for the amplification of circular DNA viruses. Cold Spring Harb Protoc **2010:**pdb prot5415.

62. **Rector A, Tachezy R, Van Ranst M.** 2004. A sequence-independent strategy for detection and cloning of circular DNA virus genomes by using multiply primed rolling-circle amplification. J Virol **78:**4993-4998.

63. **Hu J, Cladel NM, Budgeon LR, Balogh KK, Christensen ND.** 2017. The Mouse Papillomavirus Infection Model. Viruses **9**.

64. **Zheng ZM, Baker CC.** 2006. Papillomavirus genome structure, expression, and post-transcriptional regulation. Front Biosci **11:**2286-2302.

65. **Doorbar J.** 2007. Papillomavirus life cycle organization and biomarker selection. Dis Markers **23:**297-313.

66. **Doorbar J, Quint W, Banks L, Bravo IG, Stoler M, Broker TR, Stanley MA.** 2012. The biology and life-cycle of human papillomaviruses. Vaccine **30 Suppl 5:**F55-70.

67. **Howley PM.** 2006. Warts, cancer and ubiquitylation: lessons from the papillomaviruses. Trans Am Clin Climatol Assoc **117:**113-126; discussion 126-117.

68. **Bernard HU.** 1994. Coevolution of papillomaviruses with human populations. Trends Microbiol **2:**140-143.

69. **Garcia-Vallve S, Alonso A, Bravo IG.** 2005. Papillomaviruses: different genes have different histories. Trends Microbiol **13:**514-521.

70. **Gottschling M, Goker M, Stamatakis A, Bininda-Emonds OR, Nindl I, Bravo IG.** 2011. Quantifying the phylodynamic forces driving papillomavirus evolution. Mol Biol Evol **28:**2101-2113.

71. **Schulz E, Gottschling M, Wibbelt G, Stockfleth E, Nindl I.** 2009. Isolation and genomic characterization of the first Norway rat (Rattus norvegicus) papillomavirus and its phylogenetic position within Pipapillomavirus, primarily infecting rodents. J Gen Virol **90:**2609-2614.

72. **Egawa N, Egawa K, Griffin H, Doorbar J.** 2015. Human Papillomaviruses; Epithelial Tropisms, and the Development of Neoplasia. Viruses **7:**3863-3890.

73. **de Villiers EM, Fauquet C, Broker TR, Bernard HU, zur Hausen H.** 2004. Classification of papillomaviruses. Virology **324:**17-27.

74. **Kumar S, Stecher G, Tamura K.** 2016. MEGA7: Molecular Evolutionary Genetics Analysis Version 7.0 for Bigger Datasets. Mol Biol Evol **33:**1870-1874.

75. **de Villiers EM.** 2013. Cross-roads in the classification of papillomaviruses. Virology **445:**2-10.

76. **Bergvall M, Melendy T, Archambault J.** 2013. The E1 proteins. Virology **445:**35-56.

77. **McBride AA.** 2013. The papillomavirus E2 proteins. Virology **445:**57-79.

78. **Doorbar J.** 2013. The E4 protein; structure, function and patterns of expression. Virology **445:**80-98.

79. **Orth G.** 2008. Host defenses against human papillomaviruses: lessons from epidermodysplasia verruciformis. Current topics in microbiology and immunology **321:**59-83.

80. **Garcia-Vallve S, Alonso A, Bravo IG.** 2005. Papillomaviruses: different genes have different histories. Trends in microbiology **13:**514-521.

81. **Roman A, Munger K.** 2013. The papillomavirus E7 proteins. Virology **445:**138-168.

82. **Vande Pol SB, Klingelhutz AJ.** 2013. Papillomavirus E6 oncoproteins. Virology **445:**115-137.

83. **Rudolph R, Hundeiker M.** 1975. ["Keratoacanthomas" in mastomys natalensis (author's transl)]. Arch Dermatol Res **254:**239-243.

84. **Rudolph R, Thiel W.** 1976. [Pathological anatomy and histology of spontaneous, epithelial skin tumors in Mastomys natalensis]. Zentralbl Veterinarmed A **23:**429-441.

85. **Muller H, Gissmann L.** 1978. Mastomys natalensis papilloma virus (MnPV), the causative agent of epithelial proliferations: characterization of the virus particle. J Gen Virol **41:**315-323.

86. **Reinacher M, Muller H, Thiel W, Rudolph RL.** 1978. Localization of papillomavirus and virus-specific antigens in the skin of tumor-bearing Mastomys natalensis (GRA Giessen). Med Microbiol Immunol **165:**93-99.

87. **Rudolph RL.** 1980. [Neoplasms of the skin in a wild-colored inbred strain of Mastomys natalensis (WSA Giessen)]. Vet Pathol **17:**600-613.

88. **Kruppa TF, Iglauer F, Ihnen E, Miller K, Kunstyr I.** 1990. Mastomys natalensis or Mastomys coucha. Correct species designation in animal experiments. Trop Med Parasitol **41:**219-220.

89. **Schafer K, Neumann J, Waterboer T, Rosl F.** 2011. Serological markers for papillomavirus infection and skin tumour development in the rodent model Mastomys coucha. J Gen Virol **92:**383-394.

90. **Vinzon SE, Braspenning-Wesch I, Muller M, Geissler EK, Nindl I, Grone HJ, Schafer K, Rosl F.** 2014. Protective vaccination against papillomavirus-induced skin tumors under immunocompetent and immunosuppressive conditions: a preclinical study using a natural outbred animal model. PLoS Pathog **10:**e1003924.

91. **Nafz J, Kohler A, Ohnesorge M, Nindl I, Stockfleth E, Rosl F.** 2007. Persistence of Mastomys natalensis papillomavirus in multiple organs identifies novel targets for infection. J Gen Virol **88:**2670-2678.

92. **Blanpain C, Fuchs E.** 2006. Epidermal stem cells of the skin. Annu Rev Cell Dev Biol **22:**339-373.

93. **Schmitt A, Rochat A, Zeltner R, Borenstein L, Barrandon Y, Wettstein FO, Iftner T.** 1996. The primary target cells of the high-risk cottontail rabbit papillomavirus colocalize with hair follicle stem cells. J Virol **70:**1912-1922.

94. **Maglennon GA, Doorbar J.** 2012. The biology of papillomavirus latency. Open Virol J **6:**190-197.

95. **Siegsmund M, Wayss K, Amtmann E.** 1991. Activation of latent papillomavirus genomes by chronic mechanical irritation. J Gen Virol **72 (Pt 11):**2787-2789.

96. **Wayss K, Reyes-Mayes D, Volm M.** 1981. Chemical carcinogenesis by the two-stage protocol in the skin Mastomys natalensis (Muridae) using topical initiation with 7,12-dimethylbenz(a)anthracene and topical promotion with 12-0-tetradecanoylphorbol-13-acetate. Virchows Arch B Cell Pathol Incl Mol Pathol **38:**13-21.

97. **Helfrich I, Chen M, Schmidt R, Furstenberger G, Kopp-Schneider A, Trick D, Grone HJ, Zur Hausen H, Rosl F.** 2004. Increased incidence of squamous cell carcinomas in Mastomys natalensis papillomavirus E6 transgenic mice during two-stage skin carcinogenesis. J Virol **78:**4797-4805.

98. **Hasche D, Stephan S, Savelyeva L, Westermann F, Rosl F, Vinzon SE.** 2016. Establishment of an Immortalized Skin Keratinocyte Cell Line Derived from the Animal Model Mastomys coucha. PLoS One **11:**e0161283.

99. **Salvermoser M, Chotewutmontri S, Braspenning-Wesch I, Hasche D, Rosl F, Vinzon SE.** 2016. Transcriptome analysis of Mastomys natalensis papillomavirus in productive lesions after natural infection. J Gen Virol **97:**1658-1669.

100. **Handisurya A, Day PM, Thompson CD, Buck CB, Pang YY, Lowy DR, Schiller JT.** 2013. Characterization of Mus musculus papillomavirus 1 infection in situ reveals an unusual pattern of late gene expression and capsid protein localization. J Virol **87:**13214-13225.

101. **Sundberg JP, Stearns TM, Joh J, Proctor M, Ingle A, Silva KA, Dadras SS, Jenson AB, Ghim SJ.** 2014. Immune status, strain background, and anatomic site of inoculation affect mouse papillomavirus (MmuPV1) induction of exophytic papillomas or endophytic trichoblastomas. PLoS One **9:**e113582.

102. **Florin L, Sapp C, Streeck RE, Sapp M.** 2002. Assembly and translocation of papillomavirus capsid proteins. J Virol **76:**10009-10014.

103. **Egawa K, Iftner A, Doorbar J, Honda Y, Iftner T.** 2000. Synthesis of viral DNA and late capsid protein L1 in parabasal spinous cell layers of naturally occurring benign warts infected with human papillomavirus type 1. Virology **268:**281-293.

104. **Xue XY, Majerciak V, Uberoi A, Kim BH, Gotte D, Chen X, Cam M, Lambert PF, Zheng ZM.** 2017. The full transcription map of mouse papillomavirus type 1 (MmuPV1) PLoS Pathog **Accepted**.

105. **Cladel NM, Budgeon LR, Cooper TK, Balogh KK, Christensen ND, Myers R, Majerciak V, Gotte D, Zheng ZM, Hu J.** 2017. Mouse papillomavirus infections spread to cutaneous sites with progression to malignancy. J Gen Virol doi:10.1099/jgv.0.000926.

106. **Nicholls PK, Doorbar J, Moore RA, Peh W, Anderson DM, Stanley MA.** 2001. Detection of viral DNA and E4 protein in basal keratinocytes of experimental canine oral papillomavirus lesions. Virology **284:**82-98.

107. **Boxman IL, Berkhout RJ, Mulder LH, Wolkers MC, Bouwes Bavinck JN, Vermeer BJ, ter Schegget J.** 1997. Detection of human papillomavirus DNA in plucked hairs from renal transplant recipients and healthy volunteers. J Invest Dermatol **108:**712-715.

108. **Buck CB, Day PM, Trus BL.** 2013. The papillomavirus major capsid protein L1. Virology **445:**169-174.

109. **Wang JW, Roden RB.** 2013. L2, the minor capsid protein of papillomavirus. Virology **445:**175-186.

110. **Handisurya A, Day PM, Thompson CD, Buck CB, Kwak K, Roden RB, Lowy DR, Schiller JT.** 2012. Murine skin and vaginal mucosa are similarly susceptible to infection by pseudovirions of different papillomavirus classifications and species. Virology **433:**385-394.

111. **Day PM, Thompson CD, Lowy DR, Schiller JT.** 2015. The HPV16 and MusPV1 papillomaviruses initially interact with distinct host components on the basement membrane. Virology **481:**79-94.

112. **Sapp M, Day PM.** 2009. Structure, attachment and entry of polyoma- and papillomaviruses. Virology **384:**400-409.

113. **Surviladze Z, Dziduszko A, Ozbun MA.** 2012. Essential roles for soluble virion-associated heparan sulfonated proteoglycans and growth factors in human papillomavirus infections. PLoS Pathog **8:**e1002519.

114. **Spoden G, Kuhling L, Cordes N, Frenzel B, Sapp M, Boller K, Florin L, Schelhaas M.** 2013. Human papillomavirus types 16, 18, and 31 share similar endocytic requirements for entry. J Virol **87:**7765-7773.

115. **Flanagan SP.** 1966. 'Nude', a new hairless gene with pleiotropic effects in the mouse. Genet Res **8:**295-309.

116. **Pantelouris EM.** 1968. Absence of thymus in a mouse mutant. Nature **217:**370-371.

117. **Quigley DA, Kandyba E, Huang P, Halliwill KD, Sjolund J, Pelorosso F, Wong CE, Hirst GL, Wu D, Delrosario R, Kumar A, Balmain A.** 2016. Gene Expression Architecture of Mouse Dorsal and Tail Skin Reveals Functional Differences in Inflammation and Cancer. Cell Rep **16:**1153-1165.

118. **Uberoi A, Yoshida S, Frazer IH, Pitot HC, Lambert PF.** 2016. Role of Ultraviolet Radiation in Papillomavirus-Induced Disease. PLoS Pathog **12:**e1005664.

119. **Cladel NM, Budgeon LR, Balogh KK, Cooper TK, Hu J, Christensen ND.** 2015. A novel pre-clinical murine model to study the life cycle and progression of cervical and anal papillomavirus infections. PLoS One **10:**e0120128.

120. **Cladel NM, Budgeon LR, Cooper TK, Balogh KK, Hu J, Christensen ND.** 2013. Secondary infections, expanded tissue tropism, and evidence for malignant potential in immunocompromised mice infected with Mus musculus papillomavirus 1 DNA and virus. J Virol **87:**9391-9395.

121. **Bosma M, Schuler W, Bosma G.** 1988. The scid mouse mutant. Curr Top Microbiol Immunol **137:**197-202.

122. **Blunt T, Finnie NJ, Taccioli GE, Smith GC, Demengeot J, Gottlieb TM, Mizuta R, Varghese AJ, Alt FW, Jeggo PA, Jackson SP.** 1995. Defective DNA-dependent protein kinase activity is linked to V(D)J recombination and DNA repair defects associated with the murine scid mutation. Cell **80:**813-823.

123. **Christianson SW, Shultz LD, Leiter EH.** 1993. Adoptive transfer of diabetes into immunodeficient NOD-scid/scid mice. Relative contributions of CD4+ and CD8+ T-cells from diabetic versus prediabetic NOD.NON-Thy-1a donors. Diabetes **42:**44-55.

124. **Nonoyama S, Smith FO, Bernstein ID, Ochs HD.** 1993. Strain-dependent leakiness of mice with severe combined immune deficiency. J Immunol **150:**3817-3824.

125. **Shultz LD, Schweitzer PA, Christianson SW, Gott B, Schweitzer IB, Tennent B, McKenna S, Mobraaten L, Rajan TV, Greiner DL, et al.** 1995. Multiple defects in innate and adaptive immunologic function in NOD/LtSz-scid mice. J Immunol **154:**180-191.

126. **Cladel NM, Budgeon LR, Balogh KK, Cooper TK, Hu J, Christensen ND.** 2016. Mouse papillomavirus MmuPV1 infects oral mucosa and preferentially targets the base of the tongue. Virology **488:**73-80.

127. **Wang JW, Jiang R, Peng S, Chang YN, Hung CF, Roden RB.** 2015. Immunologic Control of Mus musculus Papillomavirus Type 1. PLoS Pathog **11:**e1005243.

128. **Handisurya A, Day PM, Thompson CD, Bonelli M, Lowy DR, Schiller JT.** 2014. Strain-specific properties and T cells regulate the susceptibility to papilloma induction by Mus musculus papillomavirus 1. PLoS Pathog **10:**e1004314.

129. **Nesnow S, Bergman H, Slaga TJ.** 1986. Comparison of the tumorigenic response of SENCAR and C57BL/6 mice to benzo(a)pyrene and the inter-experimental variability over a three-year period. Environ Health Perspect **68:**19-25.

130. **Slaga TJ.** 1986. SENCAR mouse skin tumorigenesis model versus other strains and stocks of mice. Environ Health Perspect **68:**27-32.

131. **Joh J, Chilton PM, Wilcher SA, Zahin M, Park J, Proctor ML, Ghim SJ, Jenson AB.** 2017. T cell-mediated antitumor immune response eliminates skin tumors induced by mouse papillomavirus, MmuPV1. Exp Mol Pathol **103:**181-190.

132. **Williams MA, Bevan MJ.** 2007. Effector and memory CTL differentiation. Annu Rev Immunol **25:**171-192.

133. **Wherry EJ, Ahmed R.** 2004. Memory CD8 T-cell differentiation during viral infection. J Virol **78:**5535-5545.

134. **Whitmire JK.** 2011. Induction and function of virus-specific CD4+ T cell responses. Virology **411:**216-228.

135. **Nakanishi Y, Lu B, Gerard C, Iwasaki A.** 2009. CD8(+) T lymphocyte mobilization to virus-infected tissue requires CD4(+) T-cell help. Nature **462:**510-513.

136. **Buller RM, Holmes KL, Hugin A, Frederickson TN, Morse HC, 3rd.** 1987. Induction of cytotoxic T-cell responses in vivo in the absence of CD4 helper cells. Nature **328:**77-79.

137. **Ruedl C, Kopf M, Bachmann MF.** 1999. CD8(+) T cells mediate CD40-independent maturation of dendritic cells in vivo. J Exp Med **189:**1875-1884.

138. **Yauch LE, Prestwood TR, May MM, Morar MM, Zellweger RM, Peters B, Sette A, Shresta S.** 2010. CD4+ T cells are not required for the induction of dengue virus-specific CD8+ T cell or antibody responses but contribute to protection after vaccination. J Immunol **185:**5405-5416.

139. **Wieland U, Kreuter A, Pfister H.** 2014. Human papillomavirus and immunosuppression. Curr Probl Dermatol **45:**154-165.

140. **Berman A, Winkelmann RK.** 1980. Involuting common warts. Clinical and histopathologic findings. J Am Acad Dermatol **3:**356-362.

141. **Iwatsuki K, Tagami H, Takigawa M, Yamada M.** 1986. Plane warts under spontaneous regression. Immunopathologic study on cellular constituents leading to the inflammatory reaction. Arch Dermatol **122:**655-659.

142. **Thivolet J, Viac J, Staquet MJ.** 1982. Cell-mediated immunity in wart infection. Int J Dermatol **21:**94-98.

143. **Coleman N, Stanley MA.** 1994. Analysis of HLA-DR expression on keratinocytes in cervical neoplasia. Int J Cancer **56:**314-319.

144. **Steele JC, Mann CH, Rookes S, Rollason T, Murphy D, Freeth MG, Gallimore PH, Roberts S.** 2005. T-cell responses to human papillomavirus type 16 among women with different grades of cervical neoplasia. Br J Cancer **93:**248-259.

145. **Stanley MA.** 2012. Epithelial cell responses to infection with human papillomavirus. Clin Microbiol Rev **25:**215-222.

146. **Amador-Molina A, Hernandez-Valencia JF, Lamoyi E, Contreras-Paredes A, Lizano M.** 2013. Role of innate immunity against human papillomavirus (HPV) infections and effect of adjuvants in promoting specific immune response. Viruses **5:**2624-2642.

147. **Yan N, Chen ZJ.** 2012. Intrinsic antiviral immunity. Nat Immunol **13:**214-222.

148. **Stepp WH, Meyers JM, McBride AA.** 2013. Sp100 provides intrinsic immunity against human papillomavirus infection. MBio **4:**e00845-00813.

149. **Lazarczyk M, Pons C, Mendoza JA, Cassonnet P, Jacob Y, Favre M.** 2008. Regulation of cellular zinc balance as a potential mechanism of EVER-mediated protection against pathogenesis by cutaneous oncogenic human papillomaviruses. J Exp Med **205:**35-42.

150. **Gunasekharan V, Laimins LA.** 2013. Human papillomaviruses modulate microRNA 145 expression to directly control genome amplification. J Virol **87:**6037-6043.

151. **Saikia P, Fensterl V, Sen GC.** 2010. The inhibitory action of P56 on select functions of E1 mediates interferon's effect on human papillomavirus DNA replication. J Virol **84:**13036-13039.

152. **Lo Cigno I, De Andrea M, Borgogna C, Albertini S, Landini MM, Peretti A, Johnson KE, Chandran B, Landolfo S, Gariglio M.** 2015. The Nuclear DNA Sensor IFI16 Acts as a Restriction Factor for Human Papillomavirus Replication through Epigenetic Modifications of the Viral Promoters. J Virol **89:**7506-7520.

153. **Porter SS, Stepp WH, Stamos JD, McBride AA.** 2017. Host cell restriction factors that limit transcription and replication of human papillomavirus. Virus Res **231:**10-20.

154. **Warren CJ, Westrich JA, Doorslaer KV, Pyeon D.** 2017. Roles of APOBEC3A and APOBEC3B in Human Papillomavirus Infection and Disease Progression. Viruses **9**.

155. **Vartanian JP, Guetard D, Henry M, Wain-Hobson S.** 2008. Evidence for editing of human papillomavirus DNA by APOBEC3 in benign and precancerous lesions. Science **320:**230-233.

156. **Warren CJ, Xu T, Guo K, Griffin LM, Westrich JA, Lee D, Lambert PF, Santiago ML, Pyeon D.** 2015. APOBEC3A functions as a restriction factor of human papillomavirus. J Virol **89:**688-702.

157. **Mirabello L, Yeager M, Yu K, Clifford GM, Xiao Y, Zhu B, Cullen M, Boland JF, Wentzensen N, Nelson CW, Raine-Bennett T, Chen Z, Bass S, Song L, Yang Q, Steinberg M, Burdett L, Dean M, Roberson D, Mitchell J, Lorey T, Franceschi S, Castle PE, Walker J, Zuna R, Kreimer AR, Beachler DC, Hildesheim A, Gonzalez P, Porras C, Burk RD, Schiffman M.** 2017. HPV16 E7 Genetic Conservation Is Critical to Carcinogenesis. Cell **170:**1164-1174 e1166.

158. **Randelia HP, Sanghvi L.** 1961. 'Bare', a new hairless mutant in the mouse—genetics and histology. Genetical Research **2:**283-289.

159. **Bhisey RA, Veturkar PL, Borges A.** 1987. Comparison of sensitivity of Swiss albino and hairless Swiss bare mice to two stage skin tumorigenesis. Indian J Exp Biol **25:**90-96.

160. **Bhisey RA, Veturkar PL, Jeyapaul J, Borges A.** 1988. Effects of TPA dose variation and mezerein on skin tumorigenesis by initiation promotion protocol in S/RV Cri mice. Indian J Exp Biol **26:**764-767.

161. **Bhisey RA, Veturkar PL.** 1990. S/RV Cri-ba, a hairless mouse strain sensitive to skin tumorigenesis by suboptimal doses of 7,12-dimethylbenz[a]anthracene, initiation-promotion and two stage promotion protocols. Cancer Lett **52:**63-69.

162. **Benavides F, Oberyszyn TM, VanBuskirk AM, Reeve VE, Kusewitt DF.** 2009. The hairless mouse in skin research. J Dermatol Sci **53:**10-18.

163. **Chen AC, McMillan NA, Antonsson A.** 2008. Human papillomavirus type spectrum in normal skin of individuals with or without a history of frequent sun exposure. J Gen Virol **89:**2891-2897.

164. **Hampras SS, Giuliano AR, Lin HY, Fisher KJ, Abrahamsen ME, Sirak BA, Iannacone MR, Gheit T, Tommasino M, Rollison DE.** 2014. Natural history of cutaneous human papillomavirus (HPV) infection in men: the HIM study. PLoS One **9:**e104843.

165. **Iannacone MR, Michael KM, Giuliano AR, Waterboer T, Pawlita M, Rollison DE.** 2010. Risk factors for cutaneous human papillomavirus seroreactivity among patients undergoing skin cancer screening in Florida. J Infect Dis **201:**760-769.

166. **Iannacone MR, Wang W, Stockwell HG, O'Rourke K, Giuliano AR, Sondak VK, Messina JL, Roetzheim RG, Cherpelis BS, Fenske NA, Michael KM, Waterboer T, Pawlita M, Rollison DE.** 2012. Sunlight exposure and cutaneous human papillomavirus seroreactivity in basal cell and squamous cell carcinomas of the skin. J Infect Dis **206:**399-406.

167. **Tilbrook PA, Greenoak GE, Reeve VE, Canfield PJ, Gissmann L, Gallagher CH, Kulski JK.** 1989. Identification of papillomaviral DNA sequences in hairless mouse tumours induced by ultraviolet irradiation. J Gen Virol **70 (Pt 4):**1005-1009.

168. **Reeve VE, Greenoak GE, Canfield PJ, Boehm-Wilcox C, Tilbrook PA, Kulski JK, Gallagher CH.** 1989. Enhancement of u.v.-induced skin carcinogenesis in the hairless mouse by inoculation with cell-free extracts of skin tumours. Immunol Cell Biol **67 (Pt 6):**421-427.

169. **Zhang P, Nouri M, Brandsma JL, Iftner T, Steinberg BM.** 1999. Induction of E6/E7 expression in cottontail rabbit papillomavirus latency following UV activation. Virology **263:**388-394.

170. **Marcuzzi GP, Hufbauer M, Kasper HU, Weissenborn SJ, Smola S, Pfister H.** 2009. Spontaneous tumour development in human papillomavirus type 8 E6 transgenic mice and rapid induction by UV-light exposure and wounding. J Gen Virol **90:**2855-2864.

171. **Michel A, Kopp-Schneider A, Zentgraf H, Gruber AD, de Villiers EM.** 2006. E6/E7 expression of human papillomavirus type 20 (HPV-20) and HPV-27

influences proliferation and differentiation of the skin in UV-irradiated SKH-hr1 transgenic mice. J Virol **80:**11153-11164.

172. **Viarisio D, Mueller-Decker K, Kloz U, Aengeneyndt B, Kopp-Schneider A, Grone HJ, Gheit T, Flechtenmacher C, Gissmann L, Tommasino M.** 2011. E6 and E7 from beta HPV38 cooperate with ultraviolet light in the development of actinic keratosis-like lesions and squamous cell carcinoma in mice. PLoS Pathog **7:**e1002125.

173. **Norval M.** 2006. The effect of ultraviolet radiation on human viral infections. Photochem Photobiol **82:**1495-1504.

174. **Ullrich SE, Byrne SN.** 2012. The immunologic revolution: photoimmunology. J Invest Dermatol **132:**896-905.

175. **Hart PH, Gorman S, Finlay-Jones JJ.** 2011. Modulation of the immune system by UV radiation: more than just the effects of vitamin D? Nat Rev Immunol **11:**584-596.

176. **Norval M, Halliday GM.** 2011. The consequences of UV-induced immunosuppression for human health. Photochem Photobiol **87:**965-977.

177. **Schade N, Esser C, Krutmann J.** 2005. Ultraviolet B radiation-induced immunosuppression: molecular mechanisms and cellular alterations. Photochem Photobiol Sci **4:**699-708.

178. **Schwarz T.** 2010. The dark and the sunny sides of UVR-induced immunosuppression: photoimmunology revisited. J Invest Dermatol **130:**49-54.

179. **Schwarz T, Beissert S.** 2013. Milestones in photoimmunology. J Invest Dermatol **133:**E7-E10.

180. **Schwarz T, Schwarz A.** 2011. Molecular mechanisms of ultraviolet radiation-induced immunosuppression. Eur J Cell Biol **90:**560-564.

181. **Gibbs NK, Norval M.** 2013. Photoimmunosuppression: a brief overview. Photodermatol Photoimmunol Photomed **29:**57-64.

182. **Poon TS, Barnetson RS, Halliday GM.** 2005. Sunlight-induced immunosuppression in humans is initially because of UVB, then UVA, followed by interactive effects. J Invest Dermatol **125:**840-846.

183. **Byrne SN, Spinks N, Halliday GM.** 2002. Ultraviolet a irradiation of C57BL/6 mice suppresses systemic contact hypersensitivity or enhances secondary immunity depending on dose. J Invest Dermatol **119:**858-864.

184. **Kripke ML.** 1984. Immunological unresponsiveness induced by ultraviolet radiation. Immunol Rev **80:**87-102.

185. **Mottram PL, Mirisklavos A, Clunie GJ, Noonan FP.** 1988. A single dose of UV radiation suppresses delayed type hypersensitivity responses to alloantigens and prolongs heart allograft survival in mice. Immunol Cell Biol **66 (Pt 5-6):**377-385.

186. **Noonan FP, De Fabo EC, Kripke ML.** 1981. Suppression of contact hypersensitivity by UV radiation and its relationship to UV-induced suppression of tumor immunity. Photochem Photobiol **34:**683-689.

187. **De Fabo EC, Noonan FP.** 1983. Mechanism of immune suppression by ultraviolet irradiation in vivo. I. Evidence for the existence of a unique photoreceptor in skin and its role in photoimmunology. J Exp Med **158:**84-98.

188. **Walterscheid JP, Nghiem DX, Kazimi N, Nutt LK, McConkey DJ, Norval M, Ullrich SE.** 2006. Cis-urocanic acid, a sunlight-induced immunosuppressive factor, activates immune suppression via the 5-HT2A receptor. Proc Natl Acad Sci U S A **103:**17420-17425.

189. **Lee CH, Wu SB, Hong CH, Yu HS, Wei YH.** 2013. Molecular Mechanisms of UV-Induced Apoptosis and Its Effects on Skin Residential Cells: The Implication in UV-Based Phototherapy. Int J Mol Sci **14:**6414-6435.

190. **Rana S, Byrne SN, MacDonald LJ, Chan CY, Halliday GM.** 2008. Ultraviolet B suppresses immunity by inhibiting effector and memory T cells. Am J Pathol **172:**993-1004.

191. **Elmets CA, Bergstresser PR, Tigelaar RE, Wood PJ, Streilein JW.** 1983. Analysis of the mechanism of unresponsiveness produced by haptens painted on skin exposed to low dose ultraviolet radiation. J Exp Med **158:**781-794.

192. **Schwarz T.** 2008. 25 years of UV-induced immunosuppression mediated by T cells-from disregarded T suppressor cells to highly respected regulatory T cells. Photochem Photobiol **84:**10-18.

193. **Clydesdale GJ, Dandie GW, Muller HK.** 2001. Ultraviolet light induced injury: immunological and inflammatory effects. Immunol Cell Biol **79:**547-568.

194. **Ullrich SE.** 1996. Does exposure to UV radiation induce a shift to a Th-2-like immune reaction? Photochem Photobiol **64:**254-258.

195. **Chapman RS, Cooper KD, De Fabo EC, Frederick JE, Gelatt KN, Hammond SP, Hersey P, Koren HS, Ley RD, Noonan F, et al.** 1995. Solar ultraviolet radiation and the risk of infectious disease: summary of a workshop. Photochem Photobiol **61:**223-247.

196. **Patra V, Byrne SN, Wolf P.** 2016. The Skin Microbiome: Is It Affected by UV-induced Immune Suppression? Front Microbiol **7:**1235.

197. **Tseng CC, Li CS.** 2007. Inactivation of viruses on surfaces by ultraviolet germicidal irradiation. J Occup Environ Hyg **4:**400-405.

198. **Lytle CD, Knott DC.** 1982. Enhanced mutagenesis parallels enhanced reactivation of herpes virus in a human cell line. EMBO J **1:**701-703.

199. **Cornelis JJ, Su ZZ, Rommelaere J.** 1982. Direct and indirect effects of ultraviolet light on the mutagenesis of parvovirus H-1 in human cells. EMBO J **1:**693-699.

200. **Chodosh LA.** 2001. UV crosslinking of proteins to nucleic acids. Curr Protoc Mol Biol **Chapter 12:**Unit 12 15.

201. **Rainbow AJ, Castillo JE.** 1992. Homologous recombination of adenovirus DNA in mammalian cells: enhanced recombination following UV-irradiation of the virus. Mutat Res **274:**201-210.

202. **Dasgupta UB, Summers WC.** 1980. Genetic recombination of herpes simplex virus, the role of the host cell and UV-irradiation of the virus. Mol Gen Genet **178:**617-623.

203. **Stein B, Kramer M, Rahmsdorf HJ, Ponta H, Herrlich P.** 1989. UV-induced transcription from the human immunodeficiency virus type 1 (HIV-1) long terminal repeat and UV-induced secretion of an extracellular factor that induces HIV-1 transcription in nonirradiated cells. J Virol **63:**4540-4544.

204. **Loiacono CM, Taus NS, Mitchell WJ.** 2003. The herpes simplex virus type 1 ICP0 promoter is activated by viral reactivation stimuli in trigeminal ganglia neurons of transgenic mice. J Neurovirol **9:**336-345.

205. **Jackson S, Harwood C, Thomas M, Banks L, Storey A.** 2000. Role of Bak in UV-induced apoptosis in skin cancer and abrogation by HPV E6 proteins. Genes Dev **14:**3065-3073.

206. **Underbrink MP, Howie HL, Bedard KM, Koop JI, Galloway DA.** 2008. E6 proteins from multiple human betapapillomavirus types degrade Bak and protect keratinocytes from apoptosis after UVB irradiation. J Virol **82:**10408-10417.

207. **Giampieri S, Garcia-Escudero R, Green J, Storey A.** 2004. Human papillomavirus type 77 E6 protein selectively inhibits p53-dependent transcription of proapoptotic genes following UV-B irradiation. Oncogene **23:**5864-5870.

208. **Maglennon GA, McIntosh PB, Doorbar J.** 2014. Immunosuppression facilitates the reactivation of latent papillomavirus infections. J Virol **88:**710-716.

209. **O'Banion MK, Reichmann ME, Sundberg JP.** 1988. Cloning and characterization of a papillomavirus associated with papillomas and carcinomas in the European harvest mouse (Micromys minutus). J Virol **62:**226-233.

210. **Nafz J, Ohnesorge M, Stockfleth E, Rosl F, Nindl I.** 2007. Imiquimod treatment of papilloma virus and DMBA /TPA-induced cutaneous skin cancer in Mastomys coucha: an unique animal model system useful for preclinical studies. Br J Dermatol **157 Suppl 2:**14-17.

211. **Garland SM, Brotherton JML, Moscicki AB, Kaufmann AM, Stanley M, Bhatla N, Sankaranarayanan R, de Sanjosé S, Palefsky JM.** 2017. HPV vaccination of immunocompromised hosts. Papillomavirus Research **4:**35-38.

212. **Jiang RT, Wang JW, Peng S, Huang TC, Wang C, Cannella F, Chang YN, Viscidi RP, Best SRA, Hung CF, Roden RBS.** 2017. Spontaneous and Vaccine-Induced Clearance of Mus Musculus Papillomavirus 1 Infection. J Virol **91**.

213. **Wang X, Meyers C, Wang HK, Chow LT, Zheng ZM.** 2011. Construction of a full transcription map of human papillomavirus type 18 during productive viral infection. J Virol **85:**8080-8092.

214. **Ozbun MA, Meyers C.** 1997. Characterization of late gene transcripts expressed during vegetative replication of human papillomavirus type 31b. J Virol **71:**5161-5172.

215. **Grassmann K, Rapp B, Maschek H, Petry KU, Iftner T.** 1996. Identification of a differentiation-inducible promoter in the E7 open reading frame of human papillomavirus type 16 (HPV-16) in raft cultures of a new cell line containing high copy numbers of episomal HPV-16 DNA. J Virol **70:**2339-2349.

216. **Sankovski E, Mannik A, Geimanen J, Ustav E, Ustav M.** 2014. Mapping of betapapillomavirus human papillomavirus 5 transcription and characterization of viral-genome replication function. J Virol **88:**961-973.

217. **Isok-Paas H, Mannik A, Ustav E, Ustav M.** 2015. The transcription map of HPV11 in U2OS cells adequately reflects the initial and stable replication phases of the viral genome. Virol J **12:**59.

218. **Jia R, Zheng ZM.** 2009. Regulation of bovine papillomavirus type 1 gene expression by RNA processing. Front Biosci (Landmark Ed) **14:**1270-1282.

219. **Probst-Hunczek S, Jager G, Schneider M, Notz E, Stubenrauch F, Iftner T.** 2015. RNA sequencing analysis identifies novel spliced transcripts but does not indicate quantitative or qualitative changes of viral transcripts during progression of cottontail rabbit papillomavirus-induced tumours. J Gen Virol **96:**3083-3089.

220. **Palermo-Dilts DA, Broker TR, Chow LT.** 1990. Human papillomavirus type 1 produces redundant as well as polycistronic mRNAs in plantar warts. J Virol **64:**3144-3149.

221. **Lambert PF, Spalholz BA, Howley PM.** 1987. A transcriptional repressor encoded by BPV-1 shares a common carboxy-terminal domain with the E2 transactivator. Cell **50:**69-78.

222. **Lambert PF, Monk BC, Howley PM.** 1990. Phenotypic analysis of bovine papillomavirus type 1 E2 repressor mutants. J Virol **64:**950-956.

223. **Jeckel S, Loetzsch E, Huber E, Stubenrauch F, Iftner T.** 2003. Identification of the E9/E2C cDNA and functional characterization of the gene product reveal a new repressor of transcription and replication in cottontail rabbit papillomavirus. J Virol **77:**8736-8744.

224. **Chiang CM, Broker TR, Chow LT.** 1991. An E1M--E2C fusion protein encoded by human papillomavirus type 11 is asequence-specific transcription repressor. J Virol **65:**3317-3329.

225. **Lace MJ, Anson JR, Thomas GS, Turek LP, Haugen TH.** 2008. The E8--E2 gene product of human papillomavirus type 16 represses early transcription and replication but is dispensable for viral plasmid persistence in keratinocytes. J Virol **82:**10841-10853.

226. **Stubenrauch F, Hummel M, Iftner T, Laimins LA.** 2000. The E8E2C protein, a negative regulator of viral transcription and replication, is required for extrachromosomal maintenance of human papillomavirus type 31 in keratinocytes. J Virol **74:**1178-1186.

227. **Straub E, Dreer M, Fertey J, Iftner T, Stubenrauch F.** 2014. The viral E8^E2C repressor limits productive replication of human papillomavirus 16. J Virol **88:**937-947.

228. **Meyers JM, Uberoi A, Grace M, Lambert PF, Munger K.** 2017. Cutaneous HPV8 and MmuPV1 E6 Proteins Target the NOTCH and TGF-beta Tumor

Suppressors to Inhibit Differentiation and Sustain Keratinocyte Proliferation. PLoS Pathog **13:**e1006171.

229. **Zanier K, Charbonnier S, Sidi AO, McEwen AG, Ferrario MG, Poussin-Courmontagne P, Cura V, Brimer N, Babah KO, Ansari T, Muller I, Stote RH, Cavarelli J, Vande Pol S, Trave G.** 2013. Structural basis for hijacking of cellular LxxLL motifs by papillomavirus E6 oncoproteins. Science **339:**694-698.

230. **Brimer N, Lyons C, Vande Pol SB.** 2007. Association of E6AP (UBE3A) with human papillomavirus type 11 E6 protein. Virology **358:**303-310.

231. **Huibregtse JM, Scheffner M, Howley PM.** 1991. A cellular protein mediates association of p53 with the E6 oncoprotein of human papillomavirus types 16 or 18. EMBO J **10:**4129-4135.

232. **White EA, Kramer RE, Tan MJ, Hayes SD, Harper JW, Howley PM.** 2012. Comprehensive analysis of host cellular interactions with human papillomavirus E6 proteins identifies new E6 binding partners and reflects viral diversity. J Virol **86:**13174-13186.

233. **Tong X, Howley PM.** 1997. The bovine papillomavirus E6 oncoprotein interacts with paxillin and disrupts the actin cytoskeleton. Proc Natl Acad Sci U S A **94:**4412-4417.

234. **Ronco LV, Karpova AY, Vidal M, Howley PM.** 1998. Human papillomavirus 16 E6 oncoprotein binds to interferon regulatory factor-3 and inhibits its transcriptional activity. Genes Dev **12:**2061-2072.

235. **Tan MJ, White EA, Sowa ME, Harper JW, Aster JC, Howley PM.** 2012. Cutaneous beta-human papillomavirus E6 proteins bind Mastermind-like coactivators and repress Notch signaling. Proc Natl Acad Sci U S A **109:**E1473-1480.

236. **Meyers JM, Spangle JM, Munger K.** 2013. The human papillomavirus type 8 E6 protein interferes with NOTCH activation during keratinocyte differentiation. J Virol **87:**4762-4767.

237. **Martinez-Zapien D, Ruiz FX, Poirson J, Mitschler A, Ramirez J, Forster A, Cousido-Siah A, Masson M, Vande Pol S, Podjarny A, Trave G, Zanier K.** 2016. Structure of the E6/E6AP/p53 complex required for HPV-mediated degradation of p53. Nature **529:**541-545.

238. **Brimer N, Lyons C, Wallberg AE, Vande Pol SB.** 2012. Cutaneous papillomavirus E6 oncoproteins associate with MAML1 to repress transactivation and NOTCH signaling. Oncogene **31:**4639-4646.

239. **Tan MJ, White EA, Sowa ME, Harper JW, Aster JC, Howley PM.** 2012. Cutaneous beta-human papillomavirus E6 proteins bind Mastermind-like coactivators and repress Notch signaling. Proceedings of the National Academy of Sciences of the United States of America **109:**E1473-1480.

240. **Wu L, Aster JC, Blacklow SC, Lake R, Artavanis-Tsakonas S, Griffin JD.** 2000. MAML1, a human homologue of Drosophila mastermind, is a transcriptional co-activator for NOTCH receptors. Nature genetics **26:**484-489.

241. **Meyers JM, Spangle JM, Munger K.** 2013. The human papillomavirus type 8 E6 protein interferes with NOTCH activation during keratinocyte differentiation. Journal of virology **87:**4762-4767.

242. **Wang J, Zhou D, Prabhu A, Schlegel R, Yuan H.** 2010. The canine papillomavirus and gamma HPV E7 proteins use an alternative domain to bind and destabilize the retinoblastoma protein. PLoS Pathog **6:**e1001089.

243. **Pim D, Bergant M, Boon SS, Ganti K, Kranjec C, Massimi P, Subbaiah VK, Thomas M, Tomaic V, Banks L.** 2012. Human papillomaviruses and the specificity of PDZ domain targeting. FEBS J **279:**3530-3537.

244. **McLaughlin-Drubin ME, Munger K.** 2009. The human papillomavirus E7 oncoprotein. Virology **384:**335-344.

245. **Halbert CL, Demers GW, Galloway DA.** 1992. The E6 and E7 genes of human papillomavirus type 6 have weak immortalizing activity in human epithelial cells. Journal of virology **66:**2125-2134.

246. **Chan HM, Smith L, La Thangue NB.** 2001. Role of LXCXE motif-dependent interactions in the activity of the retinoblastoma protein. Oncogene **20:**6152-6163.

247. **Narechania A, Terai M, Chen Z, DeSalle R, Burk RD.** 2004. Lack of the canonical pRB-binding domain in the E7 ORF of artiodactyl papillomaviruses is associated with the development of fibropapillomas. The Journal of general virology **85:**1243-1250.

248. **Van Bressem MF, Cassonnet P, Rector A, Desaintes C, Van Waerebeek K, Alfaro-Shigueto J, Van Ranst M, Orth G.** 2007. Genital warts in Burmeister's porpoises: characterization of Phocoena spinipinnis papillomavirus type 1 (PsPV-1) and evidence for a second, distantly related PsPV. The Journal of general virology **88:**1928-1933.

249. **Stevens H, Rector A, Van Der Kroght K, Van Ranst M.** 2008. Isolation and cloning of two variant papillomaviruses from domestic pigs: Sus scrofa papillomaviruses type 1 variants a and b. The Journal of general virology **89:**2475-2481.

250. **Stevens H, Rector A, Bertelsen MF, Leifsson PS, Van Ranst M.** 2008. Novel papillomavirus isolated from the oral mucosa of a polar bear does not cluster with other papillomaviruses of carnivores. Veterinary microbiology **129:**108-116.

251. **Munger K, Basile JR, Duensing S, Eichten A, Gonzalez SL, Grace M, Zacny VL.** 2001. Biological activities and molecular targets of the human papillomavirus E7 oncoprotein. Oncogene **20:**7888-7898.

252. **White EA, Munger K, Howley PM.** 2016. High-Risk Human Papillomavirus E7 Proteins Target PTPN14 for Degradation. MBio **7**.

253. **Uberoi A, Yoshida S, Lambert PF.** 2017. Development of an in vivo infection model to study Mouse papillomavirus-1 (MmuPV1). Journal of Virological Methods.

254. **Segre JA, Nemhauser JL, Taylor BA, Nadeau JH, Lander ES.** 1995. Positional cloning of the nude locus: genetic, physical, and transcription maps of the region and mutations in the mouse and rat. Genomics **28:**549-559.

255. **Shultz LD, Brehm MA, Garcia-Martinez JV, Greiner DL.** 2012. Humanized mice for immune system investigation: progress, promise and challenges. Nat Rev Immunol **12:**786-798.

256. **Cao X, Shores EW, Hu-Li J, Anver MR, Kelsall BL, Russell SM, Drago J, Noguchi M, Grinberg A, Bloom ET, et al.** 1995. Defective lymphoid development in mice lacking expression of the common cytokine receptor gamma chain. Immunity **2:**223-238.

257. **Kitamura D, Roes J, Kuhn R, Rajewsky K.** 1991. A B cell-deficient mouse by targeted disruption of the membrane exon of the immunoglobulin mu chain gene. Nature **350:**423-426.

258. **Rahemtulla A, Fung-Leung WP, Schilham MW, Kundig TM, Sambhara SR, Narendran A, Arabian A, Wakeham A, Paige CJ, Zinkernagel RM, et al.** 1991. Normal development and function of CD8+ cells but markedly decreased helper cell activity in mice lacking CD4. Nature **353:**180-184.

259. **Fung-Leung WP, Schilham MW, Rahemtulla A, Kundig TM, Vollenweider M, Potter J, van Ewijk W, Mak TW.** 1991. CD8 is needed for development of cytotoxic T cells but not helper T cells. Cell **65:**443-449.

260. **Black BL, Croom J, Eisen EJ, Petro AE, Edwards CL, Surwit RS.** 1998. Differential effects of fat and sucrose on body composition in A/J and C57BL/6 mice. Metabolism **47:**1354-1359.

261. **Potter M.** 1985. History of the BALB/c family. Curr Top Microbiol Immunol **122:**1-5.

262. **Mahler JF, Stokes W, Mann PC, Takaoka M, Maronpot RR.** 1996. Spontaneous lesions in aging FVB/N mice. Toxicol Pathol **24:**710-716.

263. **Lahvis GP, Bradfield CA.** 1998. Ahr null alleles: distinctive or different? Biochem Pharmacol **56:**781-787.

264. **Kuhn R, Lohler J, Rennick D, Rajewsky K, Muller W.** 1993. Interleukin-10-deficient mice develop chronic enterocolitis. Cell **75:**263-274.

265. **McGowan KM, Tong X, Colucci-Guyon E, Langa F, Babinet C, Coulombe PA.** 2002. Keratin 17 null mice exhibit age- and strain-dependent alopecia. Genes Dev **16:**1412-1422.

266. **Ding W, Beissert S, Deng L, Miranda E, Cassetty C, Seiffert K, Campton KL, Yan Z, Murphy GF, Bluestone JA, Granstein RD.** 2003. Altered cutaneous immune parameters in transgenic mice overexpressing viral IL-10 in the epidermis. J Clin Invest **111:**1923-1931.

267. **Mahajan VS, Demissie E, Mattoo H, Viswanadham V, Varki A, Morris R, Pillai S.** 2016. Striking Immune Phenotypes in Gene-Targeted Mice Are Driven by a Copy-Number Variant Originating from a Commercially Available C57BL/6 Strain. Cell Rep **15:**1901-1909.

268. **Afaq F, Syed DN, Malik A, Hadi N, Sarfaraz S, Kweon MH, Khan N, Zaid MA, Mukhtar H.** 2007. Delphinidin, an anthocyanidin in pigmented fruits and vegetables, protects human HaCaT keratinocytes and mouse skin against UVB-mediated oxidative stress and apoptosis. J Invest Dermatol **127:**222-232.

269. **Calvo-Castro L, Syed DN, Chamcheu JC, Vilela FM, Perez AM, Vaillant F, Rojas M, Mukhtar H.** 2013. Protective effect of tropical highland blackberry juice (Rubus adenotrichos Schltdl.) against UVB-mediated damage in human epidermal keratinocytes and in a reconstituted skin equivalent model. Photochem Photobiol **89:**1199-1207.

270. **Schowalter RM, Pastrana DV, Pumphrey KA, Moyer AL, Buck CB.** 2010. Merkel cell polyomavirus and two previously unknown polyomaviruses are chronically shed from human skin. Cell Host Microbe **7:**509-515.

271. **Stack EC, Wang C, Roman KA, Hoyt CC.** 2014. Multiplexed immunohistochemistry, imaging, and quantitation: a review, with an assessment of Tyramide signal amplification, multispectral imaging and multiplex analysis. Methods **70:**46-58.

272. **Adams JC.** 1992. Biotin amplification of biotin and horseradish peroxidase signals in histochemical stains. J Histochem Cytochem **40:**1457-1463.

273. **Bobrow MN, Litt GJ, Shaughnessy KJ, Mayer PC, Conlon J.** 1992. The use of catalyzed reporter deposition as a means of signal amplification in a variety of formats. J Immunol Methods **150:**145-149.

274. **Shindler KS, Roth KA.** 1996. Double immunofluorescent staining using two unconjugated primary antisera raised in the same species. J Histochem Cytochem **44:**1331-1335.

275. **Hopman AH, Ramaekers FC, Speel EJ.** 1998. Rapid synthesis of biotin-, digoxigenin-, trinitrophenyl-, and fluorochrome-labeled tyramides and their application for In situ hybridization using CARD amplification. J Histochem Cytochem **46:**771-777.

276. **Dunn LA, Evander M, Tindle RW, Bulloch AL, de Kluyver RL, Fernando GJ, Lambert PF, Frazer IH.** 1997. Presentation of the HPV16E7 protein by skin grafts is insufficient to allow graft rejection in an E7-primed animal. Virology **235:**94-103.

277. **Gosmann C, Mattarollo SR, Bridge JA, Frazer IH, Blumenthal A.** 2014. IL-17 suppresses immune effector functions in human papillomavirus-associated epithelial hyperplasia. J Immunol **193:**2248-2257.

278. **Roberts JN, Buck CB, Thompson CD, Kines R, Bernardo M, Choyke PL, Lowy DR, Schiller JT.** 2007. Genital transmission of HPV in a mouse model is potentiated by nonoxynol-9 and inhibited by carrageenan. Nat Med **13:**857-861.

279. **Huang HS, Buck CB, Lambert PF.** 2010. Inhibition of gamma secretase blocks HPV infection. Virology **407:**391-396.

280. **Brake T, Lambert PF.** 2005. Estrogen contributes to the onset, persistence, and malignant progression of cervical cancer in a human papillomavirus-transgenic mouse model. Proc Natl Acad Sci U S A **102:**2490-2495.

281. **Riley RR, Duensing S, Brake T, Munger K, Lambert PF, Arbeit JM.** 2003. Dissection of human papillomavirus E6 and E7 function in transgenic mouse models of cervical carcinogenesis. Cancer Res **63:**4862-4871.

282. **Hennings H, Glick AB, Lowry DT, Krsmanovic LS, Sly LM, Yuspa SH.** 1993. FVB/N mice: an inbred strain sensitive to the chemical induction of squamous cell carcinomas in the skin. Carcinogenesis **14:**2353-2358.

283. **Baron BW, Langan G, Huo D, Baron JM, Montag A.** 2005. Squamous cell carcinomas of the skin at ear tag sites in aged FVB/N mice. Comp Med **55:**231-235.

284. **Kitagaki M, Hirota M.** 2007. Auricular chondritis caused by metal ear tagging in C57BL/6 mice. Vet Pathol **44:**458-466.

285. **Cladel NM, Hu J, Balogh KK, Christensen ND.** 2010. Differences in methodology, but not differences in viral strain, account for variable experimental outcomes in laboratories utilizing the cottontail rabbit papillomavirus model. J Virol Methods **165:**36-41.

286. **Cladel NM, Hu J, Balogh K, Mejia A, Christensen ND.** 2008. Wounding prior to challenge substantially improves infectivity of cottontail rabbit papillomavirus and allows for standardization of infection. J Virol Methods **148:**34-39.

287. **Reuter JD, Gomez D, Brandsma JL, Rose JK, Roberts A.** 2001. Optimization of cottontail rabbit papilloma virus challenge technique. J Virol Methods **98:**127-134.

288. **Xue XY, Majerciak V, Uberoi A, Kim BH, Gotte D, Chen X, Cam M, Lambert PF, Zheng ZM.** 2017. The full transcription map of mouse papillomavirus type 1 (MmuPV1) in mouse wart tissues. PLoS Pathog **13:**e1006715.

289. **Johnson KM, Kines RC, Roberts JN, Lowy DR, Schiller JT, Day PM.** 2009. Role of heparan sulfate in attachment to and infection of the murine female genital tract by human papillomavirus. Journal of virology **83:**2067-2074.

290. **Pyeon D, Lambert PF, Ahlquist P.** 2005. Production of infectious human papillomavirus independently of viral replication and epithelial cell differentiation. Proceedings of the National Academy of Sciences of the United States of America **102:**9311-9316.

291. **Hohl D.** 1990. Cornified cell envelope. Dermatologica **180:**201-211.

292. **Sugamura K, Asao H, Kondo M, Tanaka N, Ishii N, Ohbo K, Nakamura M, Takeshita T.** 1996. The interleukin-2 receptor gamma chain: its role in the multiple cytokine receptor complexes and T cell development in XSCID. Annu Rev Immunol **14:**179-205.

293. **DiSanto JP, Muller W, Guy-Grand D, Fischer A, Rajewsky K.** 1995. Lymphoid development in mice with a targeted deletion of the interleukin 2 receptor gamma chain. Proc Natl Acad Sci U S A **92:**377-381.

294. **Nakajima H, Shores EW, Noguchi M, Leonard WJ.** 1997. The common cytokine receptor gamma chain plays an essential role in regulating lymphoid homeostasis. J Exp Med **185:**189-195.

295. **Ito R, Katano I, Ida-Tanaka M, Kamisako T, Kawai K, Suemizu H, Aiso S, Ito M.** 2012. Efficient xenoengraftment in severe immunodeficient NOD/Shi-scid IL2rgammanull mice is attributed to a lack of CD11c+B220+CD122+ cells. J Immunol **189:**4313-4320.

296. **Nakajima H, Leonard WJ.** 1997. Impaired peripheral deletion of activated T cells in mice lacking the common cytokine receptor gamma-chain: defective Fas ligand expression in gamma-chain-deficient mice. J Immunol **159:**4737-4744.

297. **Rice AD, Adams MM, Lindsey SF, Swetnam DM, Manning BR, Smith AJ, Burrage AM, Wallace G, MacNeill AL, Moyer RW.** 2014. Protective properties of vaccinia virus-based vaccines: skin scarification promotes a nonspecific immune response that protects against orthopoxvirus disease. J Virol **88:**7753-7763.

298. **Amella CA, Lofgren LA, Ronn AM, Nouri M, Shikowitz MJ, Steinberg BM.** 1994. Latent infection induced with cottontail rabbit papillomavirus. A model for human papillomavirus latency. Am J Pathol **144:**1167-1171.

299. **Maglennon GA, McIntosh P, Doorbar J.** 2011. Persistence of viral DNA in the epithelial basal layer suggests a model for papillomavirus latency following immune regression. Virology **414:**153-163.

300. **Dohmae K, Okabe M, Nishimune Y.** 1994. Experimental transmission of hantavirus infection in laboratory rats. J Infect Dis **170:**1589-1592.

301. **Grabowska AI, Wilanowski T.** 2017. FOXN1 Transcription Factor in Epithelial Growth and Wound Healing. Mol Cell Biol **37**.

302. **Bohr S, Patel SJ, Vasko R, Shen K, Huang G, Yarmush ML, Berthiaume F.** 2013. Highly upregulated Lhx2 in the Foxn1-/- nude mouse phenotype reflects a dysregulated and expanded epidermal stem cell niche. PLoS One **8:**e64223.

303. **Chan SY, Delius H, Halpern AL, Bernard HU.** 1995. Analysis of genomic sequences of 95 papillomavirus types: uniting typing, phylogeny, and taxonomy. J Virol **69:**3074-3083.

304. **Kripke ML.** 2013. Reflections on the field of photoimmunology. J Invest Dermatol **133:**27-30.

305. **Fisher MS, Kripke ML.** 1977. Systemic alteration induced in mice by ultraviolet light irradiation and its relationship to ultraviolet carcinogenesis. Proc Natl Acad Sci U S A **74:**1688-1692.

306. **DeFabo EC, Kripke ML.** 1979. Dose-response characteristics of immunologic unresponsiveness to UV-induced tumors produced by UV irradiation of mice. Photochem Photobiol **30:**385-390.

307. **De Fabo EC, Kripke ML.** 1980. Wavelength dependence and dose-rate independence of UV radiation-induced immunologic unresponsiveness of mice to a UV-induced fibrosarcoma. Photochem Photobiol **32:**183-188.

308. **Schwarz A, Schwarz T.** 2002. Molecular determinants of UV-induced immunosuppression. Exp Dermatol **11 Suppl 1:**9-12.

309. **Kripke ML, Thorn RM, Lill PH, Civin CI, Pazmino NH, Fisher MS.** 1979. Further characterization of immunological unresponsiveness induced in mice by ultraviolet radiation. Growth and induction of nonultraviolet-induced tumors in ultraviolet-irradiated mice. Transplantation **28:**212-217.

310. **Kripke ML, Cox PA, Alas LG, Yarosh DB.** 1992. Pyrimidine dimers in DNA initiate systemic immunosuppression in UV-irradiated mice. Proc Natl Acad Sci U S A **89:**7516-7520.

311. **Frazer IH, Leippe DM, Dunn LA, Liem A, Tindle RW, Fernando GJ, Phelps WC, Lambert PF.** 1995. Immunological responses in human papillomavirus 16 E6/E7-transgenic mice to E7 protein correlate with the presence of skin disease. Cancer Res **55:**2635-2639.

312. **Forslund O, Lindelof B, Hradil E, Nordin P, Stenquist B, Kirnbauer R, Slupetzky K, Dillner J.** 2004. High prevalence of cutaneous human papillomavirus DNA on the top of skin tumors but not in "Stripped" biopsies from the same tumors. J Invest Dermatol **123:**388-394.

313. **Hufbauer M, Lazic D, Akgul B, Brandsma JL, Pfister H, Weissenborn SJ.** 2010. Enhanced human papillomavirus type 8 oncogene expression levels are crucial for skin tumorigenesis in transgenic mice. Virology **403:**128-136.

314. **Herber R, Liem A, Pitot H, Lambert PF.** 1996. Squamous epithelial hyperplasia and carcinoma in mice transgenic for the human papillomavirus type 16 E7 oncogene. J Virol **70:**1873-1881.

315. **Song S, Pitot HC, Lambert PF.** 1999. The human papillomavirus type 16 E6 gene alone is sufficient to induce carcinomas in transgenic animals. J Virol **73:**5887-5893.

316. **Dong W, Kloz U, Accardi R, Caldeira S, Tong WM, Wang ZQ, Jansen L, Durst M, Sylla BS, Gissmann L, Tommasino M.** 2005. Skin hyperproliferation and susceptibility to chemical carcinogenesis in transgenic mice expressing E6 and E7 of human papillomavirus type 38. J Virol **79:**14899-14908.

317. **Paiva I, Gil da Costa RM, Ribeiro J, Sousa H, Bastos M, Faustino-Rocha A, Lopes C, Oliveira PA, Medeiros R.** 2015. A role for microRNA-155 expression in microenvironment associated to HPV-induced carcinogenesis in K14-HPV16 transgenic mice. PLoS One **10:**e0116868.

318. **Hashimoto Y, Arai I, Nakanishi Y, Sakurai T, Nakamura A, Nakaike S.** 2004. Scratching of their skin by NC/Nga mice leads to development of dermatitis. Life Sci **76:**783-794.

319. **Streilein JW, Bergstresser PR.** 1988. Genetic basis of ultraviolet-B effects on contact hypersensitivity. Immunogenetics **27:**252-258.

320. **de Gruijl FR.** 2008. UV-induced immunosuppression in the balance. Photochem Photobiol **84:**2-9.

321. **Schwarz T.** 2005. Mechanisms of UV-induced immunosuppression. Keio J Med **54:**165-171.

322. **Maeda A, Beissert S, Schwarz T, Schwarz A.** 2008. Phenotypic and functional characterization of ultraviolet radiation-induced regulatory T cells. J Immunol **180:**3065-3071.

323. **Schwarz A, Maeda A, Wild MK, Kernebeck K, Gross N, Aragane Y, Beissert S, Vestweber D, Schwarz T.** 2004. Ultraviolet radiation-induced regulatory T cells not only inhibit the induction but can suppress the effector phase of contact hypersensitivity. J Immunol **172:**1036-1043.

324. **Schwarz A, Beissert S, Grosse-Heitmeyer K, Gunzer M, Bluestone JA, Grabbe S, Schwarz T.** 2000. Evidence for functional relevance of CTLA-4 in ultraviolet-radiation-induced tolerance. J Immunol **165:**1824-1831.

325. **Loser K, Apelt J, Voskort M, Mohaupt M, Balkow S, Schwarz T, Grabbe S, Beissert S.** 2007. IL-10 controls ultraviolet-induced carcinogenesis in mice. J Immunol **179:**365-371.

326. **Beissert S, Hosoi J, Kuhn R, Rajewsky K, Muller W, Granstein RD.** 1996. Impaired immunosuppressive response to ultraviolet radiation in interleukin-10-deficient mice. J Invest Dermatol **107:**553-557.

327. **Ullrich SE.** 1994. Mechanism involved in the systemic suppression of antigen-presenting cell function by UV irradiation. Keratinocyte-derived IL-10 modulates antigen-presenting cell function of splenic adherent cells. J Immunol **152:**3410-3416.

328. **Toichi E, Lu KQ, Swick AR, McCormick TS, Cooper KD.** 2008. Skin-infiltrating monocytes/macrophages migrate to draining lymph nodes and produce IL-10 after contact sensitizer exposure to UV-irradiated skin. J Invest Dermatol **128:**2705-2715.

329. **Nasti TH, Iqbal O, Tamimi IA, Geise JT, Katiyar SK, Yusuf N.** 2011. Differential roles of T-cell subsets in regulation of ultraviolet radiation induced cutaneous photocarcinogenesis. Photochem Photobiol **87:**387-398.

330. **Yoshiki R, Kabashima K, Sakabe J, Sugita K, Bito T, Nakamura M, Malissen B, Tokura Y.** 2010. The mandatory role of IL-10-producing and OX40 ligand-expressing mature Langerhans cells in local UVB-induced immunosuppression. J Immunol **184:**5670-5677.

331. **Fritsche E, Schafer C, Calles C, Bernsmann T, Bernshausen T, Wurm M, Hubenthal U, Cline JE, Hajimiragha H, Schroeder P, Klotz LO, Rannug A, Furst P, Hanenberg H, Abel J, Krutmann J.** 2007. Lightening up the UV response by identification of the arylhydrocarbon receptor as a cytoplasmatic target for ultraviolet B radiation. Proc Natl Acad Sci U S A **104:**8851-8856.

332. **Agostinis P, Garmyn M, Van Laethem A.** 2007. The Aryl hydrocarbon receptor: an illuminating effector of the UVB response. Sci STKE **2007:**pe49.

333. **McIntosh BE, Hogenesch JB, Bradfield CA.** 2010. Mammalian Per-Arnt-Sim proteins in environmental adaptation. Annu Rev Physiol **72:**625-645.

334. **Stejskalova L, Dvorak Z, Pavek P.** 2011. Endogenous and exogenous ligands of aryl hydrocarbon receptor: current state of art. Curr Drug Metab **12:**198-212.

335. **Stevens EA, Mezrich JD, Bradfield CA.** 2009. The aryl hydrocarbon receptor: a perspective on potential roles in the immune system. Immunology **127:**299-311.

336. **Gandhi R, Kumar D, Burns EJ, Nadeau M, Dake B, Laroni A, Kozoriz D, Weiner HL, Quintana FJ.** 2010. Activation of the aryl hydrocarbon receptor induces human type 1 regulatory T cell-like and Foxp3(+) regulatory T cells. Nat Immunol **11:**846-853.

337. **Katiyar SK, Matsui MS, Mukhtar H.** 2000. Ultraviolet-B exposure of human skin induces cytochromes P450 1A1 and 1B1. J Invest Dermatol **114:**328-333.

338. **Mukhtar H, DelTito BJ, Jr., Matgouranis PM, Das M, Asokan P, Bickers DR.** 1986. Additive effects of ultraviolet B and crude coal tar on cutaneous carcinogen metabolism: possible relevance to the tumorigenicity of the Goeckerman regimen. J Invest Dermatol **87:**348-353.

339. **Navid F, Bruhs A, Schuller W, Fritsche E, Krutmann J, Schwarz T, Schwarz A.** 2013. The Aryl hydrocarbon receptor is involved in UVR-induced immunosuppression. J Invest Dermatol **133:**2763-2770.

340. **Nishigori C, Yarosh DB, Ullrich SE, Vink AA, Bucana CD, Roza L, Kripke ML.** 1996. Evidence that DNA damage triggers interleukin 10 cytokine production in UV-irradiated murine keratinocytes. Proc Natl Acad Sci U S A **93:**10354-10359.

341. **Rivas JM, Ullrich SE.** 1994. The role of IL-4, IL-10, and TNF-alpha in the immune suppression induced by ultraviolet radiation. J Leukoc Biol **56:**769-775.

342. **Schwarz A, Grabbe S, Riemann H, Aragane Y, Simon M, Manon S, Andrade S, Luger TA, Zlotnik A, Schwarz T.** 1994. In vivo effects of interleukin-10 on contact hypersensitivity and delayed-type hypersensitivity reactions. J Invest Dermatol **103:**211-216.

343. **Apetoh L, Quintana FJ, Pot C, Joller N, Xiao S, Kumar D, Burns EJ, Sherr DH, Weiner HL, Kuchroo VK.** 2010. The aryl hydrocarbon receptor interacts with c-Maf to promote the differentiation of type 1 regulatory T cells induced by IL-27. Nat Immunol **11:**854-861.

344. **van den Bogaard EH, Bergboer JG, Vonk-Bergers M, van Vlijmen-Willems IM, Hato SV, van der Valk PG, Schroder JM, Joosten I, Zeeuwen PL, Schalkwijk J.** 2013. Coal tar induces AHR-dependent skin barrier repair in atopic dermatitis. J Clin Invest **123:**917-927.

345. **Fernandez-Salguero PM, Ward JM, Sundberg JP, Gonzalez FJ.** 1997. Lesions of aryl-hydrocarbon receptor-deficient mice. Vet Pathol **34:**605-614.

346. **van den Bogaard EH, Podolsky MA, Smits JP, Cui X, John C, Gowda K, Desai D, Amin SG, Schalkwijk J, Perdew GH, Glick AB.** 2015. Genetic and pharmacological analysis identifies a physiological role for the AHR in epidermal differentiation. J Invest Dermatol **135:**1320-1328.

347. **Anna B, Blazej Z, Jacqueline G, Andrew CJ, Jeffrey R, Andrzej S.** 2007. Mechanism of UV-related carcinogenesis and its contribution to nevi/melanoma. Expert Rev Dermatol **2:**451-469.

348. **Leiter U, Garbe C.** 2008. Epidemiology of melanoma and nonmelanoma skin cancer--the role of sunlight. Adv Exp Med Biol **624:**89-103.

349. **Diffey BL.** 2002. What is light? Photodermatol Photoimmunol Photomed **18:**68-74.

350. **Halliday GM, Damian DL, Rana S, Byrne SN.** 2012. The suppressive effects of ultraviolet radiation on immunity in the skin and internal organs: implications for autoimmunity. J Dermatol Sci **66:**176-182.

351. **Norval M, el-Ghorr A, Garssen J, Van Loveren H.** 1994. The effects of ultraviolet light irradiation on viral infections. Br J Dermatol **130:**693-700.

352. **Norval M, Garssen J, Van Loveren H, el-Ghorr AA.** 1999. UV-induced changes in the immune response to microbial infections in human subjects and animal models. J Epidemiol **9:**S84-92.

353. **Termorshuizen F, Garssen J, Norval M, Koulu L, Laihia J, Leino L, Jansen CT, De Gruijl F, Gibbs NK, De Simone C, Van Loveren H.** 2002. A review of studies on the effects of ultraviolet irradiation on the resistance to infections: evidence from rodent infection models and verification by experimental and observational human studies. Int Immunopharmacol **2:**263-275.

354. **Norval M, Woods GM.** 2011. UV-induced immunosuppression and the efficacy of vaccination. Photochem Photobiol Sci **10:**1267-1274.

355. **Norval M.** 2011. The challenges of UV-induced immunomodulation for children's health. Prog Biophys Mol Biol **107:**323-332.

356. **Slobedman B, Barry PA, Spencer JV, Avdic S, Abendroth A.** 2009. Virus-encoded homologs of cellular interleukin-10 and their control of host immune function. J Virol **83:**9618-9629.

357. **Bermudez-Morales VH, Gutierrez LX, Alcocer-Gonzalez JM, Burguete A, Madrid-Marina V.** 2008. Correlation between IL-10 gene expression and HPV infection in cervical cancer: a mechanism for immune response escape. Cancer Invest **26:**1037-1043.

358. **Nguyen NT, Hanieh H, Nakahama T, Kishimoto T.** 2013. The roles of aryl hydrocarbon receptor in immune responses. Int Immunol **25:**335-343.

359. **Wolf P, Nghiem DX, Walterscheid JP, Byrne S, Matsumura Y, Matsumura Y, Bucana C, Ananthaswamy HN, Ullrich SE.** 2006. Platelet-activating factor is crucial in psoralen and ultraviolet A-induced immune suppression, inflammation, and apoptosis. Am J Pathol **169:**795-805.

360. **Chung SH, Wiedmeyer K, Shai A, Korach KS, Lambert PF.** 2008. Requirement for estrogen receptor alpha in a mouse model for human papillomavirus-associated cervical cancer. Cancer Res **68:**9928-9934.

361. **Arbeit JM, Howley PM, Hanahan D.** 1996. Chronic estrogen-induced cervical and vaginal squamous carcinogenesis in human papillomavirus type 16 transgenic mice. Proc Natl Acad Sci U S A **93:**2930-2935.

362. **Ward BE, Saleh AM, Williams JV, Zitz JC, Crum CP.** 1992. Papillary immature metaplasia of the cervix: a distinct subset of exophytic cervical condyloma associated with HPV-6/11 nucleic acids. Mod Pathol **5:**391-395.

363. **Baxter RM, Brissette JL.** 2002. Role of the nude gene in epithelial terminal differentiation. J Invest Dermatol **118:**303-309.

364. **Kaushic C, Ashkar AA, Reid LA, Rosenthal KL.** 2003. Progesterone increases susceptibility and decreases immune responses to genital herpes infection. J Virol **77:**4558-4565.

365. **Kaushic C, Zhou F, Murdin AD, Wira CR.** 2000. Effects of estradiol and progesterone on susceptibility and early immune responses to Chlamydia

trachomatis infection in the female reproductive tract. Infect Immun **68:**4207-4216.

366. **Quarmby VE, Korach KS.** 1984. The influence of 17 beta-estradiol on patterns of cell division in the uterus. Endocrinology **114:**694-702.

367. **Hu J, Budgeon LR, Cladel NM, Balogh K, Myers R, Cooper TK, Christensen ND.** 2015. Tracking vaginal, anal and oral infection in a mouse papillomavirus infection model. J Gen Virol **96:**3554-3565.

368. **Luster MI, Hayes HT, Korach K, Tucker AN, Dean JH, Greenlee WF, Boorman GA.** 1984. Estrogen immunosuppression is regulated through estrogenic responses in the thymus. J Immunol **133:**110-116.

369. **Kovats S.** 2015. Estrogen receptors regulate innate immune cells and signaling pathways. Cell Immunol **294:**63-69.

370. **Khan D, Ansar Ahmed S.** 2015. The Immune System Is a Natural Target for Estrogen Action: Opposing Effects of Estrogen in Two Prototypical Autoimmune Diseases. Front Immunol **6:**635.

371. **Spurgeon ME, den Boon JA, Horswill M, Barthakur S, Forouzan O, Rader JS, Beebe DJ, Roopra A, Ahlquist P, Lambert PF.** 2017. Human papillomavirus oncogenes reprogram the cervical cancer microenvironment independently of and synergistically with estrogen. Proceedings of the National Academy of Sciences **114:**E9076-E9085.

372. **Godar DE, Tang R, Merrill SJ.** 2014. Pharyngeal and cervical cancer incidences significantly correlate with personal UV doses among whites in the United States. Anticancer Res **34:**4993-4999.

373. **Ryan LK, Neldon DL, Bishop LR, Gilmour MI, Daniels MJ, Sailstad DM, Selgrade MJ.** 2000. Exposure to ultraviolet radiation enhances mortality and pathology associated with influenza virus infection in mice. Photochem Photobiol **72:**497-507.

374. **Brozek CM, Shopp GM, Ryan SL, Gillespie PM, Kusewitt DF, Rajagopalan MS, Ley KD, Ley RD.** 1992. In vivo exposure to ultraviolet radiation enhances

pathogenic effects of murine leukemia virus, LP-BM5, in murine acquired immunodeficiency syndrome. Photochem Photobiol **56:**287-295.

375. **McBride AA, Warburton A.** 2017. The role of integration in oncogenic progression of HPV-associated cancers. PLoS Pathog **13:**e1006211.

376. **de Gruijl FR, van Kranen HJ, Mullenders LH.** 2001. UV-induced DNA damage, repair, mutations and oncogenic pathways in skin cancer. J Photochem Photobiol B **63:**19-27.

377. **Dolwick KM, Schmidt JV, Carver LA, Swanson HI, Bradfield CA.** 1993. Cloning and expression of a human Ah receptor cDNA. Mol Pharmacol **44:**911-917.

378. **Noonan FP, Hoffman HA.** 1994. Susceptibility to immunosuppression by ultraviolet B radiation in the mouse. Immunogenetics **39:**29-39.

379. **Yoshikawa T, Rae V, Bruins-Slot W, Van den Berg JW, Taylor JR, Streilein JW.** 1990. Susceptibility to effects of UVB radiation on induction of contact hypersensitivity as a risk factor for skin cancer in humans. J Invest Dermatol **95:**530-536.

380. **Kelly DA, Young AR, McGregor JM, Seed PT, Potten CS, Walker SL.** 2000. Sensitivity to sunburn is associated with susceptibility to ultraviolet radiation-induced suppression of cutaneous cell-mediated immunity. J Exp Med **191:**561-566.

381. **Welsh MM, Karagas MR, Kuriger JK, Houseman A, Spencer SK, Perry AE, Nelson HH.** 2011. Genetic determinants of UV-susceptibility in non-melanoma skin cancer. PLoS One **6:**e20019.

382. **Alamartine E, Berthoux P, Mariat C, Cambazard F, Berthoux F.** 2003. Interleukin-10 promoter polymorphisms and susceptibility to skin squamous cell carcinoma after renal transplantation. J Invest Dermatol **120:**99-103.

383. **Nagano T, Kunisada M, Yu X, Masaki T, Nishigori C.** 2008. Involvement of interleukin-10 promoter polymorphisms in nonmelanoma skin cancers-a case study in non-Caucasian skin cancer patients. Photochem Photobiol **84:**63-66.

384. **Ho WL, Murphy GM.** 2008. Update on the pathogenesis of post-transplant skin cancer in renal transplant recipients. Br J Dermatol **158:**217-224.

385. **Proby CM, Harwood CA, Neale RE, Green AC, Euvrard S, Naldi L, Tessari G, Feltkamp MC, de Koning MN, Quint WG, Waterboer T, Pawlita M, Weissenborn S, Wieland U, Pfister H, Stockfleth E, Nindl I, Abeni D, Schegget JT, Bouwes Bavinck JN, group E-H-U-C.** 2011. A case-control study of betapapillomavirus infection and cutaneous squamous cell carcinoma in organ transplant recipients. Am J Transplant **11:**1498-1508.

386. **Rosso S, Zanetti R, Martinez C, Tormo MJ, Schraub S, Sancho-Garnier H, Franceschi S, Gafa L, Perea E, Navarro C, Laurent R, Schrameck C, Talamini R, Tumino R, Wechsler J.** 1996. The multicentre south European study 'Helios'. II: Different sun exposure patterns in the aetiology of basal cell and squamous cell carcinomas of the skin. Br J Cancer **73:**1447-1454.

387. **Armstrong BK, Kricker A.** 2001. The epidemiology of UV induced skin cancer. J Photochem Photobiol B **63:**8-18.

388. **Kuhn A, Wenzel J, Weyd H.** 2014. Photosensitivity, apoptosis, and cytokines in the pathogenesis of lupus erythematosus: a critical review. Clin Rev Allergy Immunol **47:**148-162.

389. **Kuhn A, Beissert S.** 2005. Photosensitivity in lupus erythematosus. Autoimmunity **38:**519-529.

390. **Lehmann P, Holzle E, Kind P, Goerz G, Plewig G.** 1990. Experimental reproduction of skin lesions in lupus erythematosus by UVA and UVB radiation. J Am Acad Dermatol **22:**181-187.

391. **Infante-Duarte C, Kamradt T.** 1999. Th1/Th2 balance in infection. Springer Semin Immunopathol **21:**317-338.

392. **Ullrich SE.** 1995. Modulation of immunity by ultraviolet radiation: key effects on antigen presentation. J Invest Dermatol **105:**30S-36S.

393. **Rooney JF, Bryson Y, Mannix ML, Dillon M, Wohlenberg CR, Banks S, Wallington CJ, Notkins AL, Straus SE.** 1991. Prevention of ultraviolet-light-induced herpes labialis by sunscreen. Lancet **338:**1419-1422.

394. **Taylor JR, Schmieder GJ, Shimizu T, Tie C, Streilein JW.** 1994. Interrelationship between ultraviolet light and recurrent herpes simplex infections in man. J Dermatol Sci **8:**224-232.

395. **Gallerani M, Manfredini R.** 2000. Seasonal variation in herpes zoster infection. Br J Dermatol **142:**588-589.

396. **Zak-Prelich M, Borkowski JL, Alexander F, Norval M.** 2002. The role of solar ultraviolet irradiation in zoster. Epidemiol Infect **129:**593-597.

397. **Zak-Prelich M, McKenzie RC, Sysa-Jedrzejowska A, Norval M.** 2003. Local immune responses and systemic cytokine responses in zoster: relationship to the development of postherpetic neuralgia. Clin Exp Immunol **131:**318-323.

398. **Ateenyi-Agaba C, Weiderpass E, Tommasino M, Smet A, Arslan A, Dai M, Katongole-Mbidde E, Hainaut P, Snijders PJ, Franceschi S.** 2006. Papillomavirus infection in the conjunctiva of individuals with and without AIDS: an autopsy series from Uganda. Cancer Lett **239:**98-102.

399. **Ateenyi-Agaba C, Dai M, Le Calvez F, Katongole-Mbidde E, Smet A, Tommasino M, Franceschi S, Hainaut P, Weiderpass E.** 2004. TP53 mutations in squamous-cell carcinomas of the conjunctiva: evidence for UV-induced mutagenesis. Mutagenesis **19:**399-401.

400. **Ateenyi-Agaba C, Weiderpass E, Smet A, Dong W, Dai M, Kahwa B, Wabinga H, Katongole-Mbidde E, Franceschi S, Tommasino M.** 2004. Epidermodysplasia verruciformis human papillomavirus types and carcinoma of the conjunctiva: a pilot study. Br J Cancer **90:**1777-1779.

401. **Hrushesky WJ, Sothern RB, Rietveld WJ, Du-Quiton J, Boon ME.** 2006. Sun exposure, sexual behavior and uterine cervical human papilloma virus. Int J Biometeorol **50:**167-173.

402. **Hrushesky WJ, Sothern RB, Rietveld WJ, Du Quiton J, Boon ME.** 2005. Season, sun, sex, and cervical cancer. Cancer Epidemiol Biomarkers Prev **14:**1940-1947.

403. **Howes RA, Halliday GM, Damian DL.** 2006. Effect of topical melatonin on ultraviolet radiation-induced suppression of Mantoux reactions in humans. Photodermatol Photoimmunol Photomed **22:**267-269.

404. **Damian DL, Halliday GM, Taylor CA, Barnetson RS.** 1998. Ultraviolet radiation induced suppression of Mantoux reactions in humans. J Invest Dermatol **110:**824-827.

405. **Moyal DD, Fourtanier AM.** 2001. Broad-spectrum sunscreens provide better protection from the suppression of the elicitation phase of delayed-type hypersensitivity response in humans. J Invest Dermatol **117:**1186-1192.

406. **John TJ, Jayabal P.** 1972. Oral polio vaccination of children in the tropics. I. The poor seroconversion rates and the absence of viral interference. Am J Epidemiol **96:**263-269.

407. **Swartz TA, Skalska P, Gerichter CG, Cockburn WC.** 1972. Routine administration of oral polio vaccine in a subtropical area. Factors possibly influencing sero-conversion rates. J Hyg (Lond) **70:**719-726.

408. **Zykov MP, Sosunov AV.** 1987. Vaccination activity of live influenza vaccine in different seasons of the year. J Hyg Epidemiol Microbiol Immunol **31:**453-459.

409. **Sleijffers A, Garssen J, de Gruijl FR, Boland GJ, van Hattum J, van Vloten WA, van Loveren H.** 2001. Influence of ultraviolet B exposure on immune responses following hepatitis B vaccination in human volunteers. J Invest Dermatol **117:**1144-1150.

410. **Linder N, Abudi Y, Abdalla W, Badir M, Amitai Y, Samuels J, Mendelson E, Levy I.** 2011. Effect of season of inoculation on immune response to rubella vaccine in children. J Trop Pediatr **57:**299-302.

411. **Moore KW, de Waal Malefyt R, Coffman RL, O'Garra A.** 2001. Interleukin-10 and the interleukin-10 receptor. Annu Rev Immunol **19:**683-765.

412. **Enk CD, Sredni D, Blauvelt A, Katz SI.** 1995. Induction of IL-10 gene expression in human keratinocytes by UVB exposure in vivo and in vitro. J Immunol **154:**4851-4856.

413. **Grimbaldeston MA, Nakae S, Kalesnikoff J, Tsai M, Galli SJ.** 2007. Mast cell-derived interleukin 10 limits skin pathology in contact dermatitis and chronic irradiation with ultraviolet B. Nat Immunol **8:**1095-1104.

414. **Spight D, Zhao B, Haas M, Wert S, Denenberg A, Shanley TP.** 2005. Immunoregulatory effects of regulated, lung-targeted expression of IL-10 in vivo. Am J Physiol Lung Cell Mol Physiol **288:**L251-265.

415. **Pillai MM, Hayes B, Torok-Storb B.** 2009. Inducible transgenes under the control of the hCD68 promoter identifies mouse macrophages with a distribution that differs from the F4/80 - and CSF-1R-expressing populations. Exp Hematol **37:**1387-1392.

416. **Kistner A, Gossen M, Zimmermann F, Jerecic J, Ullmer C, Lubbert H, Bujard H.** 1996. Doxycycline-mediated quantitative and tissue-specific control of gene expression in transgenic mice. Proc Natl Acad Sci U S A **93:**10933-10938.

417. **Kamanaka M, Kim ST, Wan YY, Sutterwala FS, Lara-Tejero M, Galan JE, Harhaj E, Flavell RA.** 2006. Expression of interleukin-10 in intestinal lymphocytes detected by an interleukin-10 reporter knockin tiger mouse. Immunity **25:**941-952.

418. **Bradfield CA, Bjeldanes LF.** 1984. Effect of dietary indole-3-carbinol on intestinal and hepatic monooxygenase, glutathione S-transferase and epoxide hydrolase activities in the rat. Food Chem Toxicol **22:**977-982.

419. **Diaz-Diaz CJ, Ronnekleiv-Kelly SM, Nukaya M, Geiger PG, Balbo S, Dator R, Megna BW, Carney PR, Bradfield CA, Kennedy GD.** 2016. The Aryl Hydrocarbon Receptor is a Repressor of Inflammation-associated Colorectal Tumorigenesis in Mouse. Ann Surg **264:**429-436.

420. **Benson JM, Shepherd DM.** 2011. Dietary ligands of the aryl hydrocarbon receptor induce anti-inflammatory and immunoregulatory effects on murine dendritic cells. Toxicol Sci **124:**327-338.

421. **Bhat P, Mattarollo SR, Gosmann C, Frazer IH, Leggatt GR.** 2011. Regulation of immune responses to HPV infection and during HPV-directed immunotherapy. Immunol Rev **239:**85-98.

422. **Frazer IH, Thomas R, Zhou J, Leggatt GR, Dunn L, McMillan N, Tindle RW, Filgueira L, Manders P, Barnard P, Sharkey M.** 1999. Potential strategies utilised by papillomavirus to evade host immunity. Immunol Rev **168:**131-142.

423. **Kanodia S, Fahey LM, Kast WM.** 2007. Mechanisms used by human papillomaviruses to escape the host immune response. Curr Cancer Drug Targets **7:**79-89.

424. **Tindle RW.** 2002. Immune evasion in human papillomavirus-associated cervical cancer. Nat Rev Cancer **2:**59-65.

425. **Schwartz S.** 2000. Regulation of human papillomavirus late gene expression. Ups J Med Sci **105:**171-192.

426. **Zhou J, Liu WJ, Peng SW, Sun XY, Frazer I.** 1999. Papillomavirus capsid protein expression level depends on the match between codon usage and tRNA availability. J Virol **73:**4972-4982.

427. **Bianchi ME.** 2007. DAMPs, PAMPs and alarmins: all we need to know about danger. J Leukoc Biol **81:**1-5.

428. **Oppenheim JJ, Yang D.** 2005. Alarmins: chemotactic activators of immune responses. Curr Opin Immunol **17:**359-365.

429. **Lai Y, Gallo RL.** 2009. AMPed up immunity: how antimicrobial peptides have multiple roles in immune defense. Trends Immunol **30:**131-141.

430. **DePianto D, Coulombe PA.** 2004. Intermediate filaments and tissue repair. Exp Cell Res **301:**68-76.

431. **Coulombe PA, Omary MB.** 2002. 'Hard' and 'soft' principles defining the structure, function and regulation of keratin intermediate filaments. Curr Opin Cell Biol **14:**110-122.

432. **Kim S, Wong P, Coulombe PA.** 2006. A keratin cytoskeletal protein regulates protein synthesis and epithelial cell growth. Nature **441:**362-365.

433. **Rotty JD, Coulombe PA.** 2012. A wound-induced keratin inhibits Src activity during keratinocyte migration and tissue repair. J Cell Biol **197:**381-389.

434. **Tong X, Coulombe PA.** 2006. Keratin 17 modulates hair follicle cycling in a TNFalpha-dependent fashion. Genes Dev **20:**1353-1364.

435. **Depianto D, Kerns ML, Dlugosz AA, Coulombe PA.** 2010. Keratin 17 promotes epithelial proliferation and tumor growth by polarizing the immune response in skin. Nat Genet **42:**910-914.

436. **van de Rijn M, Perou CM, Tibshirani R, Haas P, Kallioniemi O, Kononen J, Torhorst J, Sauter G, Zuber M, Kochli OR, Mross F, Dieterich H, Seitz R, Ross D, Botstein D, Brown P.** 2002. Expression of cytokeratins 17 and 5 identifies a group of breast carcinomas with poor clinical outcome. Am J Pathol **161:**1991-1996.

437. **Wang YF, Lang HY, Yuan J, Wang J, Wang R, Zhang XH, Zhang J, Zhao T, Li YR, Liu JY, Zeng LH, Guo GZ.** 2013. Overexpression of keratin 17 is associated with poor prognosis in epithelial ovarian cancer. Tumour Biol **34:**1685-1689.

438. **Escobar-Hoyos LF, Yang J, Zhu J, Cavallo JA, Zhai H, Burke S, Koller A, Chen EI, Shroyer KR.** 2014. Keratin 17 in premalignant and malignant squamous lesions of the cervix: proteomic discovery and immunohistochemical validation as a diagnostic and prognostic biomarker. Mod Pathol **27:**621-630.

439. **Cohen-Kerem R, Madah W, Sabo E, Rahat MA, Greenberg E, Elmalah I.** 2004. Cytokeratin-17 as a potential marker for squamous cell carcinoma of the larynx. Ann Otol Rhinol Laryngol **113:**821-827.

440. **Ide M, Kato T, Ogata K, Mochiki E, Kuwano H, Oyama T.** 2012. Keratin 17 expression correlates with tumor progression and poor prognosis in gastric adenocarcinoma. Ann Surg Oncol **19:**3506-3514.

441. **Hobbs RP, Batazzi AS, Han MC, Coulombe PA.** 2016. Loss of Keratin 17 induces tissue-specific cytokine polarization and cellular differentiation in HPV16-driven cervical tumorigenesis in vivo. Oncogene **35:**5653-5662.

442. **Larouche D, Tong X, Fradette J, Coulombe PA, Germain L.** 2008. Vibrissa hair bulge houses two populations of skin epithelial stem cells distinct by their keratin profile. FASEB J **22:**1404-1415.

443. **Garssen J, Vandebriel RJ, De Gruijl FR, Wolvers DA, Van Dijk M, Fluitman A, Van Loveren H.** 1999. UVB exposure-induced systemic modulation of Th1- and Th2-mediated immune responses. Immunology **97:**506-514.

444. **Zhussupbekova S, Sinha R, Kuo P, Lambert PF, Frazer IH, Tuong ZK.** 2016. A Mouse Model of Hyperproliferative Human Epithelium Validated by Keratin Profiling Shows an Aberrant Cytoskeletal Response to Injury. EBioMedicine **9:**314-323.